Understanding The Molecular Basis Of Ras-Association Domain Family Member 7 (Rassf7) Function

Gulsen, Tulay

Award date:
2015

Awarding institution:
University of Bath

UNDERSTANDING THE MOLECULAR BASIS OF RAS-ASSOCIATION DOMAIN FAMILY MEMBER 7 (RASSF7) FUNCTION

Tülay Gülşen

A thesis submitted for the degree of Doctor of Philosophy

University of Bath

Department of Biology and Biochemistry

April 2015

Table of Contents

Abstract

RASSF7 protein localises to the centrosome and plays a key role in mitosis. Its expression is also increased in a range of tumour types. However, little is known about the molecular basis of RASSF7's function and it is not clear if it acts as an oncogene in the cancers where its levels are elevated. This thesis carries out the first analysis of the domains of rassf7, focusing on which of them are responsible for its localisation.

Constructs were generated to allow the expression of a series of truncated versions of rassf7 and the localisation of these proteins were analysed. This was carried out in *Xenopus* embryos and my data shows that the coiled-coil domain of rassf7 is required and sufficient to direct its centrosomal localisation. Surprisingly, removal of the extreme C-terminus of the protein caused rassf7 to accumulate at the centrosome and drive centrosome and mitotic defects, and ultimately cell death. Interestingly, analysis of a database of tumour sequences identified a mutation in RASSF7, which would cause a similar C-terminal truncation of the protein. Based on my data, this truncated protein might drive centrosomal defects and we propose the hypothesis that truncated RASSF7 could act as an oncogene in a small subset of tumours with such mutations.

Finally, studies in *Xenopus* showed the first evidence that RASSF7 can localise at the tight junctions. The coiled-coil domain was found to be required for driving the tight junctional localisation of rassf7. This data suggests a new function for rassf7 at the junctions that will be an interesting avenue for future work.

List of Figures

List of Tables

Abbreviations

APC/c	Anaphase promoting complex/cyclosome
ASPP	Ankyrin-repeat, SH3 domain, and proline-rich region containing protein
ATM	Aurothiomalate
ATP	Adenosine 5'-triphosphate
bp	Base pairs
BRCA1	Breast cancer 1
BSA	Bovine serum albumin
Bub	Budding uninhibited by benzimidazole
BubR1	Bub related protein 1
°C	Degress Celcius
Cdc20	Cell division cycle 20
CDK	Cyclin-dependent kinase
cDNA	Complementary DNA
CENP-A	Centromere protein A
Cep192	Centromere protein 192
C-Nap1	Centrosomal Nek2 associated protein 1
CP110	Centrosomal protein 110
DAPI	4',6'-diamidino-2-phenylindole
ddH_2O	Double distilled water
DMEM	Dulbecco's modified Eagle's medium

DMSO	Dimethyl sulfoxide
DNA	Deoxyribonucleic acid
EDTA	Diaminoethanetetra-acetic acid disodium salt
FBS	Fetal Bovine serum
GFP	Green fluorescent protein
GTP	Guanosine triphosphate
HA	Haemagglutinin
HCG	Human chorionic gonadotrophin
HTLS	Heat-treated lamb serum
IHC	Immunohistochemistry
INCENP	Inner centromere protein
ISH	In *situ* hybridisation
JNK	c-Jun-NH2-kinase
kb	Kilo base
KD	Knockdown
LB	Luria-Bertani
MCAK	Mitotic centromere-associated kinesin
MDCK	Madin-Darby Canine Kidney Cells
MKK7	MAP kinase kinase 7
MPM	Mitotic phosphoprotein monoclonal antibody
mg	Milligram

ml	Milliltre
mM	Milimolar
MMR	Marc's Modified Ringer's
Mps1	Monopolar spindle 1
mRNA	Messenger ribonucleic acid
MST	Mammalian sterile20-like
MTOC	Microtubule organising centre
n	population size
NEDD1	Neural precursor cell expressed, developmentally down-regulated 1
NEK	NIMA related kinase
NCBI	National centre for Biotechnology information
ng	Nanogram
NGS	Normal goat serum
NIMA	Never in mitosis A
p	Probability value
PBS	Phosphate buffered saline
PB1	Polo Box domain 1
PCM	Pericentriolar material
PCR	Polymerase chain reaction
PFA	Paraformaldehyde
PKA	Protein kinase A

PLK	Polo-like kinase
PMSG	Pregnant mare serum gonadotrophin
PP1	Protein phosphatase 1
RA	Ras association
RASSF	Ras association domain family
RASSF7	Refers to Human RASSF7
rassf7	Refers to *Xenopus* RASSF7
RT	Room temprature
SAS	Spindle assembly abnormal protein
TPX-2	Targeting protein for Xklp2
U	Units of enzyme
USP33	Ubiquitin specific peptidase 33
UV	Ultraviolet
WT	Wild type
ZO-1	Zonula Occludens-1
µl	Microlitre
µm	Micrometre
µg	Microgram
µM	Micromolar

Acknowledgements

First and foremost, I would like to express my special appreciation and thanks to my supervisor, Dr Andrew Chalmers. You have been a tremendous supervisor for me and I don't think my English or my Turkish is enough to explain how grateful I am. Most importantly, you have been encouraging; with a constant smile on your face, and you have had confidence in me, which I didn't have most of the time. I would not have achieved this without your support, guidance and patience. I would also like to thank my second supervisor, Dr Paul Whitley, for his valuable help and advice.

Many thanks also go to Prof David Tosh, Prof Will Wood, Dr Rob Williams, Dr Julien Licchesi and Dr Momna Hejmadi for many helpful discussions and advice about the project but most importantly their friendly faces made my PhD an enjoyable experience.

I would like to thank all members past and present of the Chalmers, Whitley, Wood, Licchesi and Williams labs. My special thanks go to Carla, Gail, Tori, Natalie and Duygu with whom I have found lifelong friends and I am so lucky to have you in my life. I would also like to thank Ben, Chris and Omar for their useful comments and making the write-up room a friendly place. I would also like to thank Emilia for being a surrogate mum and not letting me feel alone.

Many thanks go to my project students, Charlotte, RP and Irene for their contribution to the project. I am also very grateful to Dr Adrian Rogers for his valuable technical assistance with the confocal microscopy.

I could not have completed my PhD without the support from all my family and I would like to express my feelings in Turkish:

Annem Hatice Gulsen'e; sen olmadan asla basaramazdim, bu kitabin icinde yazanlardan fazla birsey anlamayacak olsan da bu tez benim oldugu kadar senin eserin, hatta benden cok senin. Senin kadar mukemmel bir anneye sahip oldugum icin dunyanin en sansli kiziyim. Babam Kemal Gulsen'e; bu bursu kazandigimda en cok sen cesaretlendirdin beni ve gurur duydun benimle simdi ve her zaman sen benim gururumsun, babamsin, iyi ki varsin. Ayrica abim Firat ve esi Goknur'a yanimda olduklari icin cok tesekkur ederim. Ve yegenim Deniz Mayis'a, gulucukleri ve sesiyle nese kaynagim oldu. Burada yazmaya firsatim olmadigi butun aileme, ozellikle Songul Teyzem'e, kuzenim Derya'ya ve ailemin bi parcasi olan Sultan'a cok tesekkur ederim.

Finally I would like to thank to triple B, for making it almost impossible to have a PhD, but now I know for sure it would only be impossible without him and his support.

1 Introduction

Mitosis is a spectacular part of the cell cycle and it is over one hundred years since errors in this process were first linked to the origin of some cancers (Boveri, 1902). This thesis will test the hypothesis that the centrosomal protein RASSF7 is a new mitotic regulator with a potential role in promoting cancer formation. Therefore, this introduction will focus on three areas: mitosis, the role and structure of the centrosome and the RASSF family of proteins.

1.1 A general overview of the cell cycle and mitosis

That 'Cells originate from cells' is a basic principle of cell biology, which was coined by Rudolf Virchow in 1858 (Virchow 1858). He determined that all cells originate from pre-existing cells and that cell division is the way multicellular organisms increase in size and complexity. However, the mechanisms controlling normal cell division are still not completely understood and even less is known about how uncontrolled cell division can lead to cancer. The cell cycle is the process by which mother cells divide to give two daughter cells, it consists of a series of events that ensure correct transmission of the genetic material from one generation of cells to the next (Salaun et al., 2008).

.

In eukaryotes, the cell cycle consists of two separate phases: interphase and mitosis (Zucca and Nigg, 1995). Interphase is further divided into three phases: S-phase for DNA Synthesis during which centrosome duplication occurs is bracketed by two Gap-phases, G1 and G2 (Vermeulen et al., 2003) (Figure 1.1). The cell cycle contains three cell cycle checkpoints: G1-S, G2-M and the

spindle assembly (Lukas et al., 2004). These checkpoints consist of regulatory pathw ays that control the order and timing of cell cycle transitions and regulate crucial events such as DNA replication and chromosome segregation (Elledge, 1996). Additionally, DNA damage causes checkpoints to arrest the cell cycle thereby providing time for repair including transcription of DNA repair (Kastan and Bartek, 2004). This section w ill focus on the mitosis phase of the cell cycle as the w ork reported here w as mainly related to this phase.

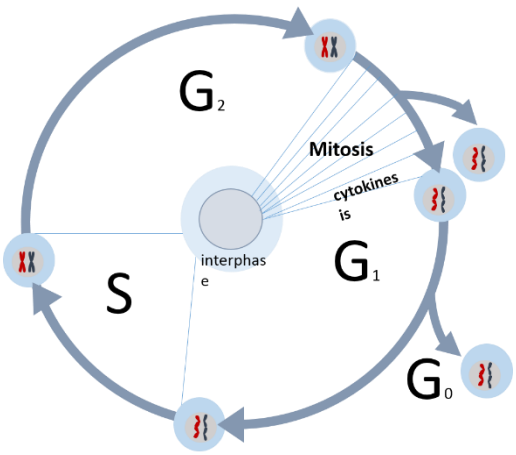

Figure 1.1: **Schematic diagram of the mammalian cell cycle.** During G1 (Gap phase 1) metabolic changes prepare the cell for division; cellular contents, excluding the chromosomes are duplicated. During S phase (stands for DNA synthesis) genetic material is duplicated. At G2 (Gap Phase 2) the cell double checks the duplicated chromosomes for errors and makes any necessary repairs. During M phase (division phase) a nuclear division (mitosis) is followed by a cell division (cytokinesis). Figure adapted from http://www2.le.ac.uk/departments/genetics/vgec/schoolscolleges/topics/cellcycle-mitosis-meiosis.

Mitosis is the fundamental biological process that generates two genetically identical daughter cells from a single mother cell. More specifically, it is the stage in the cell cycle whereby duplicated copies of the chromosomal genetic material (condensed as sister chromatids) are equally segregated into two dividing cells. This phase comprises reorganization of cellular architecture, including the assembly of the mitotic spindle and the formation of an actomyosin-based contractile ring. The orchestration of events in M phase in time and space require accurate regulation since in mammals for example the failure of faithful chromosome segregation could cause severe defects such as spontaneous abortions, birth defects and cancer (Barr et al., 2004). Thus, mitosis is crucial for the proliferation, propagation and development of uni-cellular and multi-cellular organisms.

1.1.1 Mitotic stages

Due to the fundamental requirement of mitosis, cells segregate their chromosomes with incredibly high fidelity (Kops, 2009). This segregation occurs in a specific order in stages classified as prophase, prometaphase, metaphase, anaphase, telophase and cytokinesis. These mitotic stages are shown schematically in Figure 1.2A and in confocal images in Figure 1.2B.

During prophase, the chromatin starts to condense to form well-defined-chromosomes, in a process termed condensation, through the action of condensins (Strunnikov, 2003). Chromosomes, which consist of a pair of sister chromatids, are held together through the action of cohesins in a structure known as the centromere (Belmont, 2006; Michaelis et al., 1997). Cohesins are

added to chromosomes in S phase and resolved in two steps: first they are removed from chromosome arms during prophase, when the centrosomes are already duplicated, and subsequently removed from the centromere at the metaphase-to-anaphase transition (Waizenegger et al., 2000).

Centrosome maturation occurs during prophase and duplicated centrosomes then separate and begin to migrate within the nucleus to form two groups at opposite poles (Salaun et al., 2008). Another important event during prophase is the start of the formation of the mitotic spindle. This event is concomitant with the movement of the centrosomes, also referred to as spindle poles, to opposite ends of the cell. During prophase the mitotic spindle forms and by its conclusion the nuclear membrane starts to breakdown, which marks the beginning of prometaphase.

A)

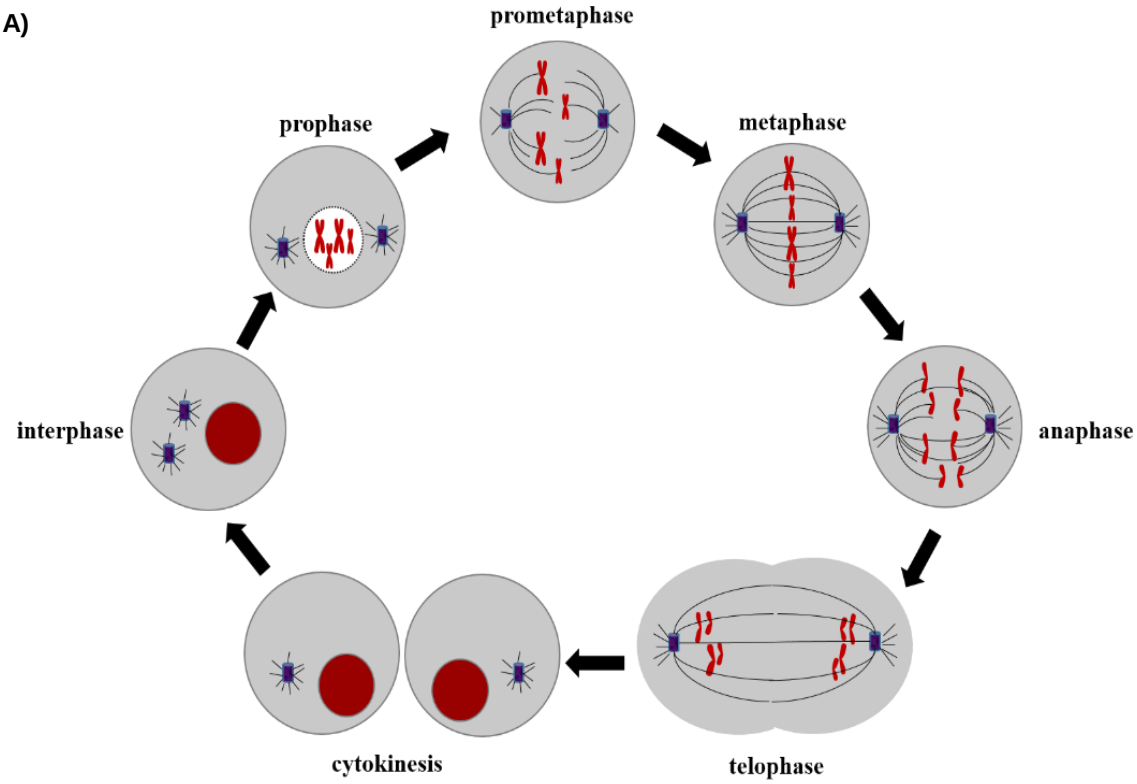
prometaphase
prophase
metaphase
interphase
anaphase
cytokinesis
telophase

B)

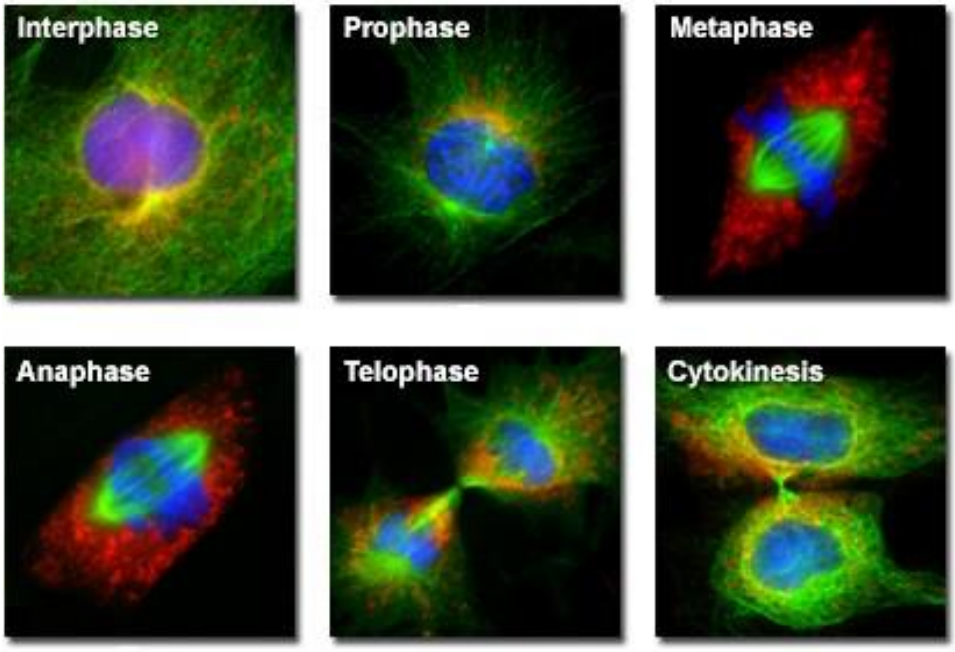
Interphase
Prophase
Metaphase
Anaphase
Telophase
Cytokinesis

Figure 1.2. The different phases of mitosis. (A) An overview of the events that occur during mitosis. Following DNA and centrosome replication at interphase, the dividing cell progresses into prophase where the nuclear chromatin condenses to form chromosomes, each consisting of two sister chromatids bound at their centromeres. Simultaneously, centrosomes, duplicated during interphase, mature and migrate to opposite poles of the nucleus, producing a bipolar mitotic spindle. At prometaphase, the nuclear envelop breaks down, allowing sister chromatids to interact and attach to opposite spindle poles via centromeric structures called kinetochores. Subsequent re-arrangement of the mitotic spindle allows chromosomes to align or congress in a linear fashion at metaphase. This is followed by the segregation of sister chromatids towards each centrosome during anaphase, resulting in two copies of the karyotype at opposite sides of the cell. Following contraction at the cell equator and subsequent cytokinesis, the result yields two genetically identical daughter cells, each with a centrosome. Illustration was adapted from (Salaun et al., 2008). **(B)** Immunoflouorescent images of mitosis in rat kangaroo epithelial kidney cells, representing five different mitotic stages as well as the interphase. The DNA is shown in blue, mitochondria is shown in red and microtubules are shown in green. Micrographs from micro.magnet.fsu.edu.

In prometaphase, the nuclear membrane is broken down, the microtubules originating from centrosomes reach the chromosomes, the chromosomes, led by their centromeres become thicker and migrate to the equatorial plane that bisects the cell and lies perpendicular to the axis specified by the centrosomes (Sikirzhytski et al., 2014). This arrangement of the mitotic spindle forms what is called the 'metaphase plate'. The kinetochore, a structure associated with the centromere of each chromosome, provides an anchor for the binding of spindle fibres.

Microtubules are highly dynamic polymers and they probe the cytoplasm with their plus-ends to capture chromosomes (Hayden et al., 1990; Holy and Leibler, 1994; Jemseena and Gopalakrishnan, 2013). Centrosomes nucleate asters of microtubules that search for and attach to the chromosomes. Further

microtubules, similarly nucleated by the chromosomes, assist assembly of a bipolar spindle. The centromeres and their associated kinetochores are therefore important for microtubule nucleation, in a process regulated by the metaphase spindle assembly checkpoint.

During metaphase, chromosomes reach their maximum condensation state to form the metaphase plate. Each chromosome consists of two sister chromatids held together by specialised proteins known as cohesins. There are several necessary preconditions for the subsequent correct segregation of the duplicated DNA into each daughter cell. First, each pair of chromatid kinetochores must attach one kinetochore to a centrosomally nucleated microtubule array; the same process occurs at the other pole of the cell. (Inoue and Salmon, 1995). Secondly, the dynamic instability of the microtubules regulates the formation of a bipolar spindle such that at the completion of metaphase, the spindle is subject to tension and every chromosomes kinetochore is aligned on the metaphase plate and attached to both centrosomes. Metaphase continues until each of the conditions described above are fully complete resulting in exit from spindle assembly checkpoint (Salaun et al., 2008).

Anaphase is initiated following this check point exit (de Gramont and Cohen-Fix, 2005). Anaphase comprises an initial phase during which sister chromatids are pulled in opposite directions towards their respective mitotic poles (Anaphase A), and a subsequent stage (Anaphase B) when further separation of the sister chromatids occurs. To allow this to occur, the cohesins that remained associated with the sister chromatids are degraded, enabling the tension within the spindle to pull each sister chromatid toward the poles,

resulting in the division of the genetic information between two identical sets of chromosomes.

While the chromosomes are undergoing their spindle-mediated movement to the poles, numerous kinetochore associated proteins detach, remain at the centre of cell, and participate in the assembly of the central spindle. Subsequently, a structure known as a 'contractile actin ring' forms below the plasma membrane in close proximity to the central spindle. These produce two cells attached at the midbody by contraction of the plasma membrane toward the equator of the cell (Barr and Gruneberg, 2007). This stage is known as telophase, and is followed by cytokinesis, which completes cell division.

Cytokinesis (division of cytoplasm) the final cellular division to form two new cells is arguably the least well understood event of mitosis . To separate the two daughter cells, the midbody breaks and the cleavage furrow appears at the cell surface, and completely divides the cell in two by progressively becoming deeper and spreading around the circumference of the cell. To avoid the cell leaking its contents, the plasma membrane is rapidly repaired by recruiting Golgi-derived membrane vesicles that also contain proteins essential for cytokinesis (Salaun et al., 2008).

1.1.2 Mitotic proteins

One remaining and key question is what regulates the cell cycle? The transition between different phases of the cell cycle depends on various regulatory proteins including ubiquitins, kinases, phosphatases and scaffolding proteins.

Dynamic control of protein phosphorylation plays a crucial role for the regulation of multiple cellular processes including mitosis and cytokinesis. Recent studies

have also emphasised the importance of protein phosphatases in spatial and temporal control of protein activity (Barr et al., 2011; Chen et al., 2007; Gharbi-Ayachi et al., 2010; Kitajima et al., 2006; Mochida et al., 2009; Mochida et al., 2010; Riedel et al., 2006; Zeng et al., 2010). It is this balance of kinase and phosphatase activity that orchestrates the changes seen during cell division (Figure 1.3) Interference with either type of activity will alter the amount and half-life of substrate phosphorylation (Heinrich et al., 2002), and thus disturb orderly mitotic progression (Figure 1.4).

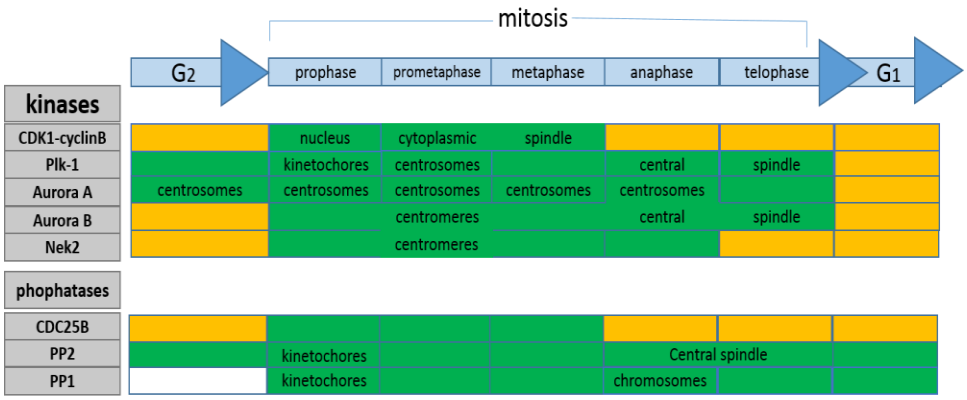

Figure 1.3: Localisation and activation of mitotic kinases and phosphatases during the cell cycle. The green bar indicates high activity of kinases or phosphatases during specific phases of the cell cycle and where applicable, subcellular localisation of kinase/phosphatase is shown. The yellow bars indicate inactive forms of the kinase/phosphatases during cell cycle stages. The white bar indicates unknown activity. Figure adapted from (Wurzenberger and Gerlich, 2011).

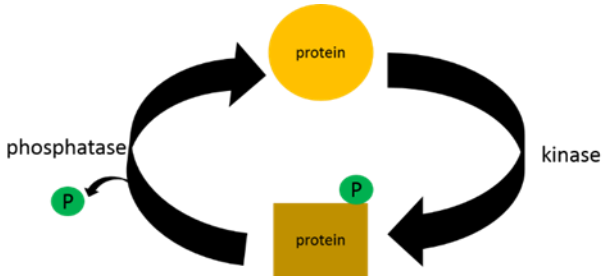

Figure 1.4: Kinase-phosphatase cycle. Simultaneous activity of a kinase and a phosphatase. A protein kinase adds a phosphate group (P) to the protein, known as phosphorylation. Adding the P (phosphorylation) alters the biological properties of the protein. A protein phosphatase removes P from the protein. The relative balance of kinase/phosphatase activity determines the amount of phosphorylated protein, which is present. Figure adapted from (Fisher et al., 2012).

This section will focus on kinases, as they are well studied and linked to subsequent experiments. The protein kinases described below are all involved in the regulation of multiple events during mitotic progression and cytokinesis. Protein phosphorylation is carried out by a series of conserved serine/threonine protein kinases of the Cdk, Polo, Aurora and Nek families. These protein kinases have well-established roles in phosphorylating key mitotic substrates (Barr et al., 2004; Lindqvist et al., 2009; Nigg, 2001; O'Farrell, 2001; Ruchaud et al., 2007; Salaun et al., 2008). Therefore, without the dynamic control of protein phosphorylation correct mitosis cannot occur.

1.1.2.1 The cyclin-dependent kinases

In mammalian cells, protein kinases such as Cdk, Plk, Aurora and Nek play a key role in driving cell division.

Cyclin-dependent kinases (Cdks) were first discovered by combining the results of genetic and biochemical studies. For example, a seminal study of the yeast cell cycle by Nurse (1975) identified genes responsible of the regulation of cell size during nuclear division (Nurse, 1975). Similarly, biochemical experiments conducted on amphibian oocytes (Masui and Markert, 1971; Smith and Ecker, 1971) led to the identification of maturating-promoting factor (MPF), a factor facilitating entry into mitosis. Lohka and co-workers used *Xenopus* oocytes to purify MPF from a structure known as the centromere (Lohka et al., 1988), which was subsequently found to be composed of Cdk1 (Arion et al., 1988; Dunphy et al., 1988; Gautier et al., 1988; Labbe et al., 1988).

Cdks regulate key events including commitment to the cell cycle, DNA synthesis and the triggering of mitosis (Malumbres, 2011). Cdks are a family of serine/threonine kinases that promote progression through the cell cycle by phosphorylating many target proteins (Chee and Haase, 2010). Cdk activity is controlled by protein-protein interactions and reversible phosphorylation (Morgan, 1995). Cdks need to bind cyclins to become active (Nigg, 1995).

Approximately twelve human Cdks have been described; the first, Cdk1 (or cdc2), was considered responsible for all cell cycle transitions and was therefore termed the 'cell cycle master kinase' (Fisher and Nurse, 1996). However, this was only true for yeast where Cdk1 kinase activity was demonstrated essential for transition between G1/S and G2/M (Durkacz et al., 1986). In contrast, in mammalian cells Cdk1 activity is only required for G2/M

transition (Draetta and Beach, 1988). Cdk1 activation is dependent of binding both cyclin A and cyclin B (Draetta et al., 1989; Karaiskou et al., 2001). Cdk1 is the only CDK essential for cell cycle in mammals (Santamaria et al., 2007), whereas both Cdk2 and Cdk3 are dispensable (Malumbres and Barbacid, 2005; Ortega et al., 2003). Cdk7, Cdk8, Cdk9, Cdk11 and Cdc20 are known as a transcriptional subfamily and are not associated with the cell cycle in mammals (Malumbres, 2014).

Significantly, misregulation of Cdks is one of the most common changes associated with human cancer (Malumbres and Barbacid, 2007). Furthermore, the Cdks do not function alone; a number of additional kinases are required to regulate mitotic events. These are kinases of the Polo, Aurora and Nek families that are involved in the centrosome cycle and the regulation of spindle function (which will be discussed in the next section which focuses on centrosomes); the spindle assembly checkpoint is regulated by Bub1, BubR1 and Mps1 (Malumbres and Barbacid, 2007) (Figure 1.5).

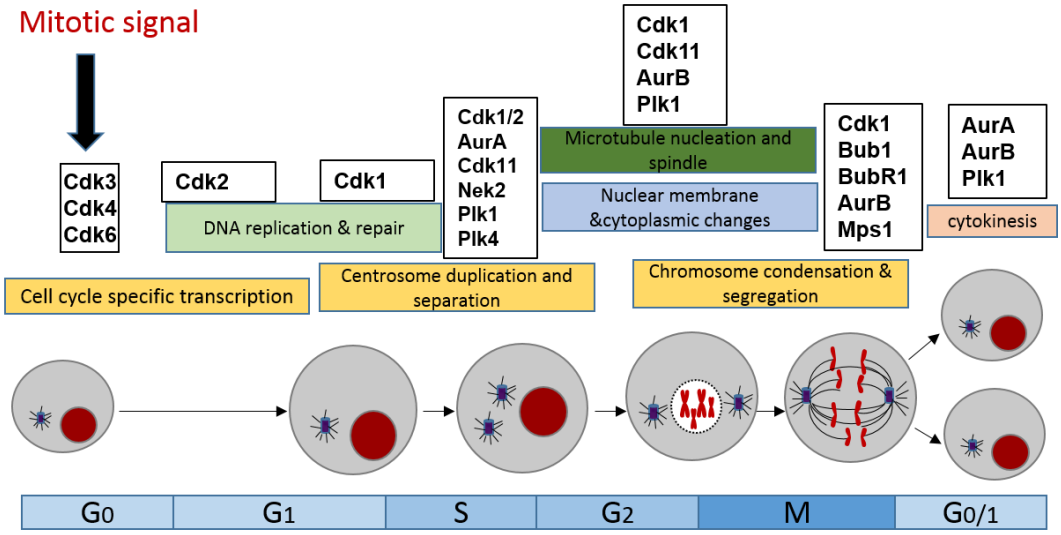

Figure 1.5: An overview of mammalian cell cycle kinases during mitosis. Drawings represent a normal cell entering mitosis and growing in size. The genome is represented in red, the microtubules are in black and centrosomes as purple small cylinders. As the cell receives the mitotic signal, Cdk3, 4 and 6 start cell cycle specific transcription Cdk2 and Cdk1 controls DNA replication and repair, respectively. Cdk1, Cdk11, Nek2, Aurora A, Plk1 and Plk4 are involved in centrosome duplication and separation. Nuclear membrane and cytoplasmic changes including microtubule nucleation and spindle formation require Cdk1, Cdk11 Aurora B and Plk1 activity whereas chromosomal changes (condensation and segregation) are controlled by Cdk1, Aurora B, Bub1, BubR1 and Mps1. Aurora A, Aurora B and Plk1 are involved in cytokinesis. Image adapted from (Malumbres, 2011).

1.1.2.2 The Polo-like kinases

The Polo-like Kinases (Plks) were first identified in a *Drosophila*-based screen to isolate mutants affecting spindle pole behaviour (Sunkel and Glover, 1988). Mammalian Plks are a family of four different proteins that regulate different aspects of the cell cycle and have different subcellular localization (Nigg, 1998), *Xenopus* expresses three Plks (Plx1-3) whereas in other species, such as *Drosophila* and yeast, have only one member (Takai et al., 2005; Takaki et al., 2008; van de Weerdt and Medema, 2006).

Plk1 is the most extensively studied mitotic kinase, whereas Plk2, Plk3 and Plk4 are more likely involved only in interphase (Nigg, 1998; van de Weerdt and Medema, 2006) although Plk4 activity is required for both centriole duplication and assembly of the mitotic spindle (Habedanck et al., 2005).

The activity and localisation of Plk1 are subject to dynamic regulation during the cell cycle, with high expression from late S-phase to G2 (Golsteyn et al., 1995; Hamanaka et al., 1995; Lee et al., 1995). Plk1 localises to both the cytoplasm and nucleus during G2 and is subject to centrosome specific targeting (Golsteyn et al., 1995; Taniguchi et al., 2002). Plk1 is found at the centrosomes and kinetochores during early mitosis (Golsteyn et al., 1995); however at the onset of anaphase Plk1 also accumulates at the spindle midzone and midbody via a carboxly-terminal domain (Polo-box domain PBD) (Takaki et al., 2008). The regulation of Plk1 kinase activity is achieved by binding of the kinase domain to the PBD domain (Archambault and Carmena, 2012; Bruinsma et al., 2012; Park et al., 2010b). New insights into this mechanism were provided by the crystal structure of the zebrafish kinase domain–PBD complex when this was bound to a PB-binding motif of *Drosophila* microtubule-associated protein 205 (Archambault et al., 2008; Xu et al., 2013). Inhibition of the kinase domain is achieved in three ways. First by reduced flexibility of the kinase domain hinge region mediated by the PBD (the site of Ser137 localisation). Second, by an interdomain linker that connects the kinase domain with the PBD and captures the T-loop (the site of Thr210 localisation). Third, autoinhibition is stabilised by binding of the PBD to Map205 which also separates the kinase from its substrates (Zitouni et al., 2014).

In vertebrate cells, various cellular processes are controlled by Plk1 and are summarised in Figure 1.6 (Petronczki et al., 2008; van de Weerdt and Medema, 2006). When Plk1 is absent, animal cells are not able to form a bipolar spindle or attach kinetochores to microtubules (van de Weerdt and Medema, 2006). Instead, cells form a monopolar spindle that is surrounded by radially arranged chromosomes (Kumagai and Dunphy, 1996; Toyoshima-Morimoto et al., 2001) causing the trapping of cells in mitosis due to activation of the spindle assembly checkpoint (Takaki et al., 2008).

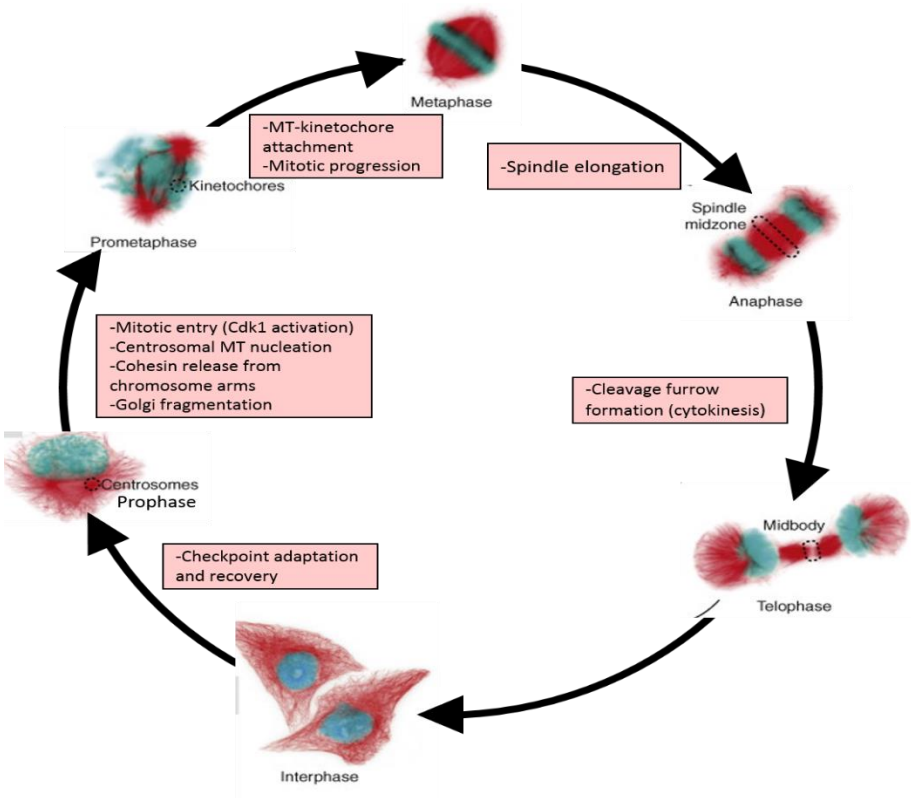

Figure 1.6: Localisation and roles of Polo-like kinase 1 during the cell cycle. Roles of Plk1 are represented in pink boxes and localisation is shown by dotted lines. Cell cycle stages are represented by immunofluorescence of cultured human cells. Microtubules are shown in red and genetic material in blue. Figure adapted and micrographs are taken from (Takaki et al., 2008).

Related to its role in cell division regulation, Plk1 also contributes to the formation and proliferation of human cancers. Overexpression Plk1 is observed in many human tumours including lymphomas, melanomas and carcinomas (Eckerdt et al., 2005; Strebhardt and Ullrich, 2006; Winkles and Alberts, 2005). Overexpression of Plk in mouse fibroblasts resulted in a block in contact inhibition enabling the formation of tumours in nude mice (Smith et al., 1997). These data suggest that Plk1 contributes to tumorigenesis. This also leads to the argument that if Plk1 enhances tumour formation, then selective inhibition of Plk1 may promote tumour regression (Archambault et al., 2015). One specific Plk1 inhibitor called BI2536 shows promise as a cytotoxic drug for the treatment of several cancers; in non-small cell lung cancer (NSCLC) this causes mitotic catastrophe due to activation of spindle assembly checkpoint (Choi et al., 2015). Therefore, Plk1 has attracted the attention as a potential target for anti-cancer therapy.

1.1.2.3 Aurora kinases

Aurora kinases are a family of serine/threonine protein kinases that regulate various cell division processes (Carmena and Earnshaw , 2003). Aurora kinase hasbeen studied in *S. cerevisae* (Chan and Botstein, 1993); however, the first aurora allele was identified among *Drosophila* mutants displaying defects in spindle-pole behaviour (Glover et al., 1995). Yeast possesses only one Aurora kinase, whilst two (A and B) are found in invertebrates such as *Drosophila* and *C. elegans*, and vertebrates, including mammals have three Aurora isoforms (A, B and C) (Adams et al., 2001a; Adams et al., 2001b; Nigg, 2001) that are

very similar in sequence (Giet and Prigent, 1999) but have district localisations and functions. Aurora A, B and C will be discussed individually below.

1.1.2.3.1 Aurora A

The defining feature of the Aurora-A subfamily is its association with both centrosomes and regions of microtubules located adjacent to the centrosome (Bettencourt-Dias et al., 2004; Glover et al., 1995; Schumacher et al., 1998). Aurora A localises to the centrosomes. The centrosomal localisation of Aurora A is dynamic and is subject to continuous exchange with a cytoplasmic pool (Berdnik and Knoblich, 2002). This was shown by photobleaching (FRAP) studies in mitotic HeLa cells which revealed that the level of Aurora A was reduced in G1 cells, by prophase it was concentrated around the centrosomes, whilst in metaphase it became associated with the microtubules near the spindle poles, had a similar distribution in anaphase before finally becoming concentrated at the midbody in cytokinesis (Carmena and Earnshaw, 2003). Activation of Aurora A is mediated by binding to its substrates such as the microtubule-associated protein TPX2 (Tsai et al., 2003). Both phosphorylation/dephosphorylation and degradation is required for the regulation of Aurora A (Carmena and Earnshaw, 2003). Phosphorylation stimulates kinase activity and *Xenopus* Aurora A contains three important phosphorylation sites for the kinase activity (Littlepage and Ruderman, 2002; Littlepage et al., 2002). Phosphorylation of Thr295 (Thr288 in human Aurora A), which resides in the activation loop and is required for kinase activity (Walter et al., 2000). The target residue is located in a protein kinase A (PKA) consensus motif ((R/K)X(T/S)(I/L/V)) (Cheeseman et al., 2002) and PKA can both

phosphorylate and activate Aurora A *in vitro* (Walter et al., 2000). Phosphorylation of Ser53 occurs during M phase and has a putative role in the regulation of Aurora A degradation (Castro et al., 2002a; Castro et al., 2002b; Honda et al., 2000). The third phosphorylation site, Ser349 is not essential for catalytic activity (Littlepage and Ruderman, 2002; Littlepage et al., 2002). In addition, the phosphatase PP1 negatively regulates the Aurora A kinase activity by regulating TPX2 activity (Eyers et al., 2003; Eyers and Maller, 2003; Tsai et al., 2003).

Aurora A phosphorylates CDC25B (cell division cycle protein 25B) and this phosphorylation contributes to G2/M transition (Dutertre et al., 2004). Aurora A activity is required for centrosome separation and maturation and requires recruitment of proteins associated with microtubule nucleation (this will be discussed in more detail in the centrosome section) (Berdnik and Knoblich, 2002; Salaun et al., 2008). The Aurora A kinase phosphorylates both motor proteins (Giet and Prigent, 1999; Giet et al., 1999) and proteins required for astral microtubule nucleation (Giet et al., 2002)(Giet et al., 2002). Aurora A plays an important role in spindle assembly in association with Ran-GTP that regulates TPX2 activity (and other centrosome associated proteins such as Numa) (Carmena and Earnshaw, 2003; Salaun et al., 2008; Tsai et al., 2003).

The Aurora A gene is located on chromosome 20q13 in a region frequently amplified in human cancers and associated with over-expression of Aurora A (Sen et al., 2002). This Aurora A over-expression/amplification is present in many cancers including breast, pancreatic, colon, ovarian, prostate, bladder and neurablastomas (Bischoff et al., 1998; Fry et al., 1998a; Tanaka et al., 1999; Zhou et al., 1998).

In vitro (in primary colorectal cancer cells and mouse NIH 3T3 cells) over-expression of Aurora A kinase causes aneuploidy and centrosome amplification that can lead to transformation of cells (Bischoff et al., 1998; Zhou et al., 1998). In summary, Aurora A is a centrosome protein whose activation is mainly regulated by phosphorylation and has a potential oncogenic role in tumours.

1.1.2.3.2 Aurora B

Human Aurora B kinase was first identified in a screen designed to detect kinases displaying over-expression in cancers (Bischoff et al., 1998). Aurora B kinases are one of the chromosomal passenger proteins required for various process during mitosis (Carmena and Earnshaw, 2003). Aurora B associates with INCENP (inner centromere protein) and INCENP/survivin/Borealin (Giet et al., 2005) which form the chromosome passenger family complex (CPC). The localisation of CPC changes during different phases of the cell cyle. In early mitosis it localises to chromosome arms, then it is detected at the inner centromeres until metaphase-anaphase transition occurs. (Adams et al., 2000). CPC proteins then relocate to the spindle midzone and to the cell cortex (Cooke et al., 1987). Aurora B and INCENP were first known to be part of the CPC complex when co-immunoprecipitated from different model systems and the study of the phenotypes derived from their knockdown showed similar defects, such as failure of chromosome segregation (Adams et al., 2000).

Activation/regulation of Aurora B is similar to Aurora A; which requires binding to some of its substrates and also phosphorylation plays an essential role for kinase activity.

Aurora B has three clear functions during mitosis. Firstly, Aurora B phosphorylates serines 10 and 28 on histone H3 and serine 7 in the centromere via histone variant CENP-A (Giet and Glover, 2001; Hsu et al., 2000; Zeitlin et al., 2001). There have been various debates about the function of these phosphorylations. One possible function for Aurora B phosphorylation is to promote chromosome condensation and cohesion (Adams et al., 2000; Goto et al., 1999; Goto et al., 2002). Another possibility is to load proteins onto the chromosomes and/or signalling in mitosis (Prigent and Dimitrov, 2003).

The second known function in mitosis for Aurora B is re-organisation of incorrect microtubule-kinetochore attachments via the spindle assembly checkpoint (SAC)(Honda et al., 2000). This is achieved via phosphorylation of mitotic centromere-associated kinesin (MCAK) by Aurora B, which then inactivates its microtubule depolymerase catalytic activity and its targeting to the kinetochores (Ohi et al., 2004). MACK also corrects the mis-attachment of the microtubules to kinetochores (Ohi et al., 2004). Aurora B has been also involved in the regulation of Ndc80/Hec1, which contributes the formation of stable kinetochore-microtubule attachments at the outer kinetochore (Nezi and Musacchio, 2009), In fact, the interaction of Ndc/Hec1 with microtubules may be affected by the phosphorylation of NDC/HEc1 by Aurora B, therefore leading to microtubule release (Cheeseman et al., 2002) Aurora B role has also been linked to the recruitment of checkpoint proteins such as Mad2 and BubR1 to kinetochores (Ditchfield et al., 2003). Besides, Aurora B can modulate BubR1 activity via phosphorylation upon entry mitosis (Ditchfield et al., 2003), therefore regulating the activity of the spindle checkpoint.

Aurora B is essential for cytokinesis, which is the third known function for the kinase. Over-expression of a catalytically inactive form of rat Aurora B leads to cytokinesis failure in a number of cell lines (Terada et al., 1998). Aurora B phosphorylates vimentin, a kinesin (ZEN-4/MKLP1) and MgcRacGAP, which are components of the cleavage furrow that are required for cytokinesis (Goto et al., 2003; Guse et al., 2005; Minoshima et al., 2003). Inactivation of Aurora B is associated with delocalization of the kinesin-like protein Pavarotti/CHO1/MKLP1/ZEN4, that is part of central spindle complex, which contributes to formation of the central spindle (Giet and Glover, 2001; Kaitna et al., 2000; Severson et al., 2000).

Aurora B has been found overexpressed in many cancers including colorectal (Katayama et al., 1999; Takahashi et al., 2000), thyroid carcinoma (Adams et al., 2000) and prostate cancer (Chieffi et al., 2006). However, amplification of the Aurora B gene has not been found in cancer and is therefore not considered an oncogene. However its over-expression does induce metastasis (Salaun et al., 2008). The functions and localisation of Aurora A and B are summarised in Figure 1.7.

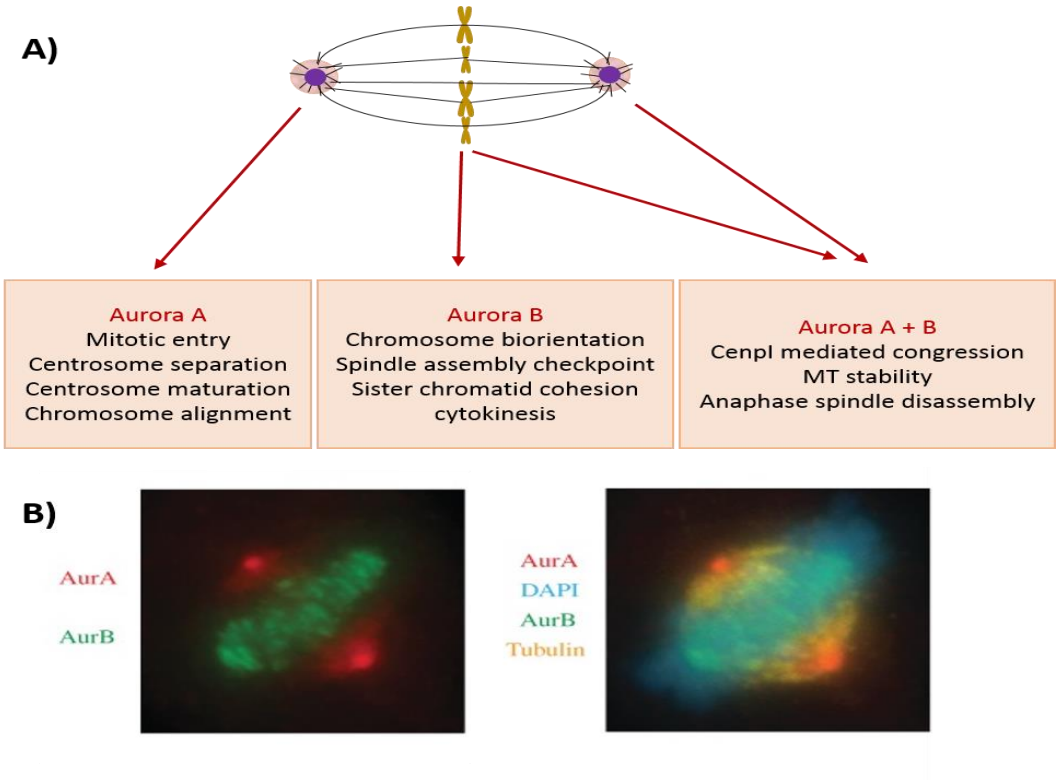

Figure 1.7: Localisation and functions of Aurora kinases. (A) Functions of Aurora kinases during mitosis are shown in the pink boxes below the illustration of the mitotic cell. Centrosomes are shown as purple circles, MTs in black and chromatids in yellow. **(B)** Localisation of Aurora kinases are shown in HeLa cells; Aurora A localises to the centrosomes whereas Aurora B localisation is centromeric. Figure adapted and micrographs are taken from (Hochegger et al., 2013).

1.1.2.3.3 Aurora C

There is little known about Aurora C Expression of Aurora C was reported in testis (Hu et al., 2000) and some human cancer cell lines (Kimura et al., 1999; Ulisse et al., 2006) with the highest level detected in the G2/M phase. Endogenous Aurora C in meiotic mouse oocytes was observed at the centromeres and the chromosome arms during prometaphase I and metaphase I; it relocalized to the midbody at telophase I and then migrated to the centromeres again in metaphase II.

As little is known about the kinase, the function and regulation of Aurora C remains unclear. It was first shown as an anaphase centrosome protein (Kimura et al., 1999), but when over-expressed, Aurora C acted like Aurora A in interphase and like Aurora B in mitosis (Dutertre et al., 2005; Sasai et al., 2004). Activation of Aurora C appears similar to other family members - it is activated by binding its substrates, especially an Aurora B substrate, INCENP (Sasai et al., 2004) suggesting that Aurora C could substitute for Aurora B. The same study also showed that in mitosis, Aurora C mimics Aurora B and rescues Aurora B deficient cells (Sasai et al., 2004).

1.1.2.4 NIMA

NIMA (Never in mitosis A) is a serine/threonine-specific protein kinase that has been implicated in controlling entry into mitosis (Doonan, 1992; Morris et al., 1988; Osmani et al., 1991). Mutations in *Aspergillus nidulans* that inactivate NIMA caused a late G2 arrest with cells containing duplicated but unseparated centrosomes (Morris et al., 1988; Osmani et al., 1991). Nek2 (NIMA related kinase-2) is the closest NIMA relative among the thirteen mammalian Nek kinases and Nek2 activity is required for mitosis (Schultz et al., 1994). Nek2 phosphorylates C-Nap1 (centrosomal Nek2-associated protein 1) and C-Nap1 phosphorylation by Nek2 is essential for centrosome separation/bipolar spindle formation (Fry, 2002; Fry et al., 1998a; Fry et al., 1998b). In *Drosophila*, Nek2 over-expression led to cytokinesis defects (Prigent et al., 2005). Related to its functions, Nek2 localises to the centrosome throughout the cell cycle as shown in HeLA cells (Andersen et al., 2003; Fry et al., 1998b; Hames and Fry, 2002). Centrosomal localisations of Nek2 homologues have been described in mouse,

Xenopus and *Drosophila* (Fry et al., 2000; Graf, 2002; Ha Kim et al., 2002; Prigent et al., 2005). Centrosomal localisation of Nek2 is associated with a motif in its C-terminal domain. This motif is also required for microtubule binding (Hames et al., 2005). In addition to centrosomal localisation, Nek2 has seen at nucleoli during interphase (Noguchi et al., 2004), on condensed chromatin in meiotic and mitoticcells (Fujioka et al., 2000; Rhee and Wolgemuth, 1997) (Ha Kim et al., 2002), and at the kinetochores (Lou et al., 2004a; Lou et al., 2004b) and midbodies (Ha Kim et al., 2002; Prigent et al., 2005) of dividing cells. Nek2 activation is promoted by trans-autophosphorylation and Nek2 inhibition is mediated by dephosphorylation by the phosphatase PP1 (Helps et al., 2000).

There is no clear evidence for Nek2 acting as an oncogene although its over-expression induces errors in centrosome organization and function (Hayward and Fry, 2006; Lingle et al., 2002).

Other members of Nek family also play roles during mitosis including Nek6, which is required for mitosis progression (shown in HeLa cells) (Belham et al., 2003; Yin et al., 2003), and Nek9 that phosphorylates and activates Nek6 and is required for spindle assembly (Roig et al., 2005).

The best-studied mitotic protein kinases have been described above; however, as demonstrated by various screens many more kinases with potential roles mitosis remain to be identified and/or characterised (Bettencourt-Dias et al., 2004; Nizard et al., 2014; Thrane et al., 2014).

1.2 The centrosome

Centrosomes play a key role in regulating mitosis and are central to the work reported in this thesis so will be considered in detail in this section.

Centrosomes were first discovered in 1887 by Theodor Boveri and Édouard Joseph Louis Marie Van Beneden while working on cell division in the egg of the roundworm *Ascaris,* which they called 'polar corpuscles' or centrosomes. Centrosomes were suspected to have a role in cell symmetry, breaking the maintenance of cell polarity as the mitotic spindle appeared to raise from two dot-like objects one at each pole of the spindle (Glover et al., 1993). However, in non-dividing cells, one single centrosome was observed next to the nucleus; as the cell started to divide, the centrosome appeared to divide and started to move apart. The identical centrosomes became the centres that organized microtubules. This separation of centrosomes occurs only once during mitosis and ensures the equal distribution of genetic material to the two daughter cells.

More than a century later after its discovery we now know that the centrosome serves as a microtubule organising centre, regulating microtubule dynamics (assembly and stability) to facilitate several microtubule-dependent processes including cell motility, cell shape and integrity, cell polarity, vesicular and molecular transport (Bornens, 2012; Kramer et al., 2004; Lukasiewicz and Lingle, 2009; Schatten, 2008). This thesis focuses on the role of the centrosomes in mitosis.

During mitosis, microtubule-organizing function of the centrosome is employed in the nucleation of a bipolar mitotic spindle, a critical requirement for chromosome biorientation and subsequent segregation (Kops, 2009). Given its

direct and/or indirect role on these processes, centrosomes play a key role in mitosis.

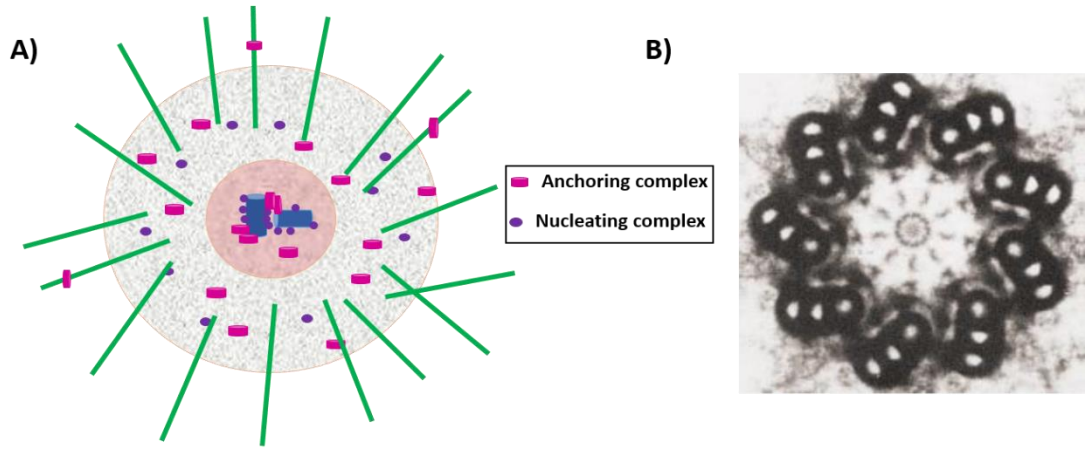

Figure 1.8: Structure of the centrosome. **(A)** Schematic diagram of a mammalian centrosome, containing two centrioles (blue cylinders) surrounded by a network of proteins embedded in the pericentriolar material (PCM, shown in grey). The nucleating (purple circles) and anchoring complexes (pink disks) contain proteins such as gamma tubulin and the others required to form the gamma tubulin ring complex that are responsible for nucleating and anchoring microtubules. Figure adapted from (Schatten, 2008). **(B)** Electron microscopy image of a centriole in an animal cell. The centriole is at the centre of the centrosome, shown as two geometric arrangements of microtubules. Each centriole has a cylindrical bundle of nine rods, each rod consists of three microtubules. Electron microscopy image is taken from (Glover et al., 1993).

Structurally, the centrosome is small, non-membranous organelle, composed of barrel-shaped microtubule macrostructures called centrioles, surrounded by a protein complex called the pericentriolar matrix (PCM) (Lukasiewicz and Lingle, 2009). An electron microscopy image showing a schematic diagram of a centrosome and the structure of a centriole are shown in Figure 1.8.

The centriole is an evolutionarily conserved macromolecular structure that is essential for the establishment of flagella, cilia and centrosomes (Goenczy, 2012). Most centrioles consists of nine triplet microtubules are elegantly arranged into a cylinder and two orthogonally organised centrioles are present

in centrosomes (Winey and O'Toole, 2014). The formation of cilia and microtubule is controlled by the distal end of the centriole (Graser et al., 2007; Ishikawa et al., 2005) . The distal end of the centriole also controls the ciliogenesis, in association with the plasma membrane. . Recruitment of pericentriolar proteins that are important for microtubule organization is regulated by the proximal end of the centriole (Luders and Stearns, 2007).

The PCM is a fibrous scaffolding matrix that contains a large number of centrosomal proteins including γ-tubulin which then forms the γ-tubulin ring complex (γ-TuRC) and initiates microtubule nucleation(Schatten, 2008). The PCM increases in amount during mitosis, providing a nucleating centre for spindle/astral microtubules and anchors signalling molecules and components of γ-TuRC, which are believed to act as a scaffold for additional proteins to bind (Figure 1.8A) (Fu et al., 2015; Lukasiewicz and Lingle, 2009). A recent study showed that in *Drosophila*, the centriole protein Asterless (Asl) is responsible for the recruitment of the essential centriole components, DSpd-2 and Cnn, to mother centrioles. This recruitment of essential proteins leads to assembly of the pericentriolar lattice which then results in the procurement of many other PCM components.(Conduit et al., 2014).

1.2.1 Centrosome proteins

A large number of proteins have been identified as centrosomal proteins, which of many have distinct functions and involvement at the centrosome but recent studies are continuing to find many more centrosomal proteins and revealing more than one function for such proteins. (Andersen et al., 2003). The classification of proteins being centrosomal changes according to the

identification method used. The centrosome is a small, non-membranous-organelle and it does not have distinct borders, therefore identification methods can be misleading as they can fail to recover essential centrosomal proteins or include those are not actual centrosomal proteins (Schatten, 2008). Furthermore, as the centrosome is a dynamic structure that changes shape and size during cell cycle, the cohort of centrosomal proteins differs according to the phase of the cell cycle. Andersen and colleagues have determined five hundred centrosomal proteins by mass spectroscopy (Andersen et al., 2003). A review by Schatten divided centrosomal proteins identified by mass spectroscopy into the two groups: structural and regulatory (Table 1.1) (Schatten, 2008).

Table 1.1: Structural and regulatory centrosomal proteins.

Structural centrosome proteins	Regulatory centrosome proteins
Alpha tubulin Beta tubulin Gamma tubulin Gamma-tubulin complex components 1-6 Centrin 2 and 3 AKAP450 Pericentrin/kendrin Ninein Pericentriolar material 1(PCM1) Ch-Tog C-Nap-1 Cep 1, 2, 110 and 250 Centriolin CPAP CLASP1 and 2 ODF2 Cenexin Lis1 Nudel EB1 centractin myomegalin	Cdc2 Cdk1 cAMP-dependent kinase II-alpha regulatory chain cAMP-dependent kinase- alpha catalytic subunit Plk1 Nek2 Sak Casein kinase I delta and epsilon isoforms PP2A PP1 alpha 14-3-3 proteins alpha and gamma isoforms Dynein heavy chain Dynein intermediate chain Dynein light chain Dynactin 1, 2 and 3 P150 glued P50 Hsp90 TCP subunits Hsp73

As seen in the table 1.1 many some of the centrosomal proteins were well known such as gamma, alpha and beta tubulins whereas some others like AKAP450, were recently added to the list. A recent study by Jakobsen et al found 126 identified and 40 new possible centrosome proteins (Jakobsen et al., 2011). This analysis also showed that 60% of centrosome proteins possess a coiled-coil domain, indicating that this domain emerges as important for centrosome assembly (Telkoparan et al., 2013). However, more work is required to elucidate the function of many of these proteins in the complex cellular processes mediated by centrosomes.

Identifying the number of centrosomal proteins is not easy as many proteins use centrosomes as a signalling platform when participating in regulatory complexes that gather and act by signalling via the microtubule network. (Godinho and Pellman, 2014). For instance, many of the mitotic kinases (Cdk, Polo, Aurora, Nek), described in the previous section, localize to the centrosome, but may not be directly involved in the structural or regulatory functions of the centrosome. These cell cycle kinases use the centrosome as a docking platform to interact with other proteins and mediate their cell-cycle specific functions (Uetake et al., 2007). Therefore, in addition to acting as the major microtubule organising centre, the centrosome acts as a signalling hub to integrate different cell cycle regulators and orchestrate the cell cycle at several stages (Kramer et al., 2004; Nigg and Raff, 2009; Raff, 2002).

Remarkably, there is an argument about whether centrosomes are essential for microtubule organization and spindle assembly since centrosomes are absent in the majority of land plants, fungi and in the female germ cells of many animal species (Nigg and Raff, 2009; Picketth.Jd, 1969). When centrosomes are absent in *Drosophila*, either naturally or due to experimental manipulation, bipolar spindles can form in the proximity of chromosomes through a centrosome-independent pathway (Kalab and Heald, 2008). This pathway can explain the interesting finding that *Drosophila* mutants lacking the centriole duplication protein DSas-4 nevertheless progressed normally through the 4–5 days of larval development and 4–5 days of pupal development without centrioles (Basto et al., 2006); however *Drosophila* mutants lacking centrioles die soon after they hatch. Although many somatic cells lacking the centrosomes can divide and retain the ability to from a mitotic spindle and progress through

mitosis, daughter cell cycles are compromised and incapable of further cell division (Hinchcliffe et al., 2001). Therefore, while alternative mechanisms exist for the organization of microtubules for spindle assembly (Kalab and Heald, 2008; Matthies et al., 1996), centrosomal activity is crucial to ensure the high fidelity of subsequent cell cycle progression in vertebrates (Hinchcliffe et al., 2001).

1.2.2 The centrosome cycle

As discussed above, during mitosis, almost all microtubule related events in animal cells, including the formation of bipolar spindle , are organised by centrosomes (Nigg, 2007). Due to the requirement of two centrosomes for the formation of bipolar spindle, the centrosome, which comprises of two centrioles and a PCM, must duplicate once prior to mitotic progression. Strict regulation of centrosome numbers is essential for effective and correct chromosome segregation. The centrosome duplication cycle requires a pre-existing centrosome (Tsou and Stearns, 2006a; Tsou and Stearns, 2006b). This canonical duplication cycle can be split into five distinctive events: centriole disengagement, centriole duplication, daughter centriole elongation, centrosome maturation and centrosome separation, as shown in Figure 1.9.

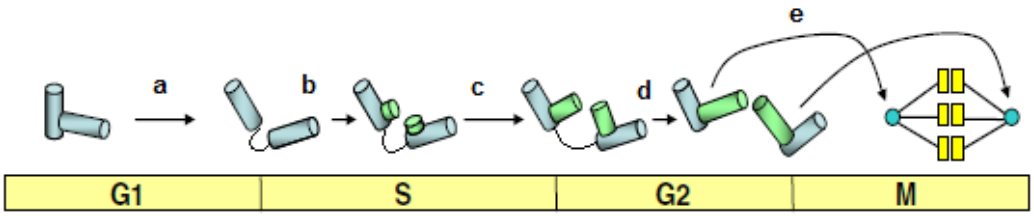

Figure 1.9: The centrosome cycle during mitosis. Five characteristic events are associated with the centrosome (centriole) cycle. a- Centriole disengagement at the end of M/G1-phase is regulated by separase, cdc20 and APC/C; b- Centriole duplication at S-phase is regulated by cdk2; c- Daughter centriole elongation during S/G2-phase is regulated by cdc25; d- Centrosome maturation at G2-phase is primarily regulated by Nek, Plk1 and Aurora A; e- Centrosome separation regulated by Plk1, Aurora A and Eg5. 'Mother' centrioles appear as blue cylinders, while daughter centrioles are green cylinders. The bipolar mitotic spindle is represented as two blue circles with emanating spindle fibres appearing as lines. Image was adapted from Fukasawa, 2011.

During first event, centriole disengagement in early G1 (at the end of M phase), tethered centrioles separate and lose their perpendicular orientation (Vidwans et al., 1999).

Like DNA replication, centriole duplication also occurs at the S phase. Cyclin-dependent kinase 2 (Cdk2) initiates centrosome duplication by phosphorylating nucleophosmin (Okuda et al., 2000). This phosphorylation leads to disassociation of nucleophosmin from the centrosome initiating centrosome disengagement and duplication (Okuda et al., 2000).

Daughter centriole elongation follows throughout S and G2 phases by the synthesis of procentrioles at the proximal ends of separated mother centrioles. (Freed et al., 1999; Lukasiewicz and Lingle, 2009; Vidwans et al., 1999)

Centrosome maturation, in which the PCM increases in size and microtubule nucleating capacity, occurs in G2 phase (Mahen and Venkitaraman, 2012).

Phosphorylation/dephosphorylation of a network of proteins is involved in the centrosome maturation and both Aurora A and Plk-1 kinases play an essential role in this maturation event (Blagden and Glover, 2003).

Centrosomes undergo separation in late G2 for subsequent migration to opposite poles and mitotic spindle assembly in prophase (Ault and Rieder, 1994).

1.2.2.1 The regulation of the centrosome cycle

All five events in the centrosome duplication cycle (described above) are regulated by a multitude of proteins, of which central mitotic kinase families, Plk, Aurora and NIMA (described above), play essential roles (Ma and Poon, 2011; Salaun et al., 2008) (Figure 1.10). This section will focus on how the centrosome cycle is regulated, with an emphasis on the protein kinases.

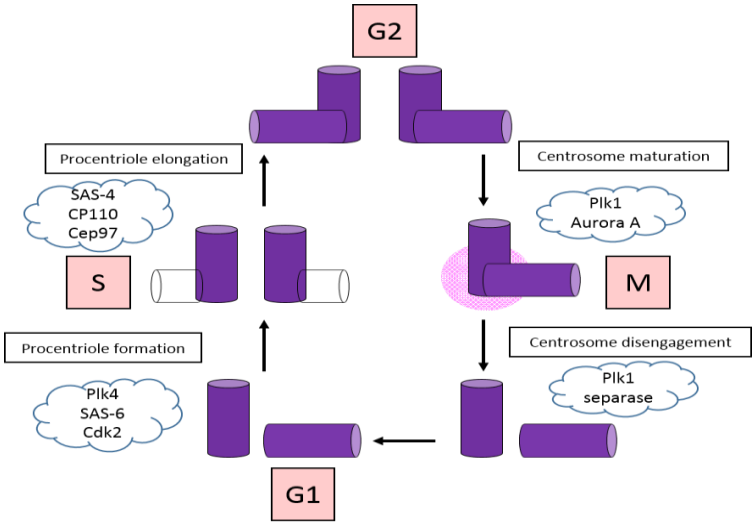

Figure 1.10: The proteins involved in the centrosome duplication cycle during mitosis. Cell cycle phases are shown in pink boxes. Centrioles are shown as purple cylinders. Plk4 is the major regulator of the centrosome duplication cycle. Oligomerization of SAS-6 and activity of Cdk2 is required for the formation of centriole nine fold symmetry. CP110, Cep97 and SAS-4 complex controls pericentriole elongation. PLk1 and Aurora A promote centrosome maturation which is followed by centrosome disengagement controlled by Plk1 and seperase activity. Image adapted from (Godinho and Pellman, 2014).

The centrosome cycle starts with the disengagement of mother and daughter centrioles. This requires Plk1 activitation in the beginning of the mitosis and separase activity after anaphase-promoting complex/cyclosome (APC/C) activity mediates securin degradation (Hatano and Sluder, 2012). Centriole disengagement was initially thought to be regulated by cell division cycle protein 20 (cdc20) and APC/C (Vidwans et al., 1999), but a more recent study showed that it relies on APC/C-Cdh1 activity (Hatano and Sluder, 2012). The same study also showed Plk1 and APC/C-Cdh1 activities can autonomously stimulate centriole disengagement in G2 arrested cells (Hatano and Sluder, 2012). Therefore, during centriole disengagement, Plk1 and APC/C–Cdh1 complexes act independently and slowly ensuring that centriole separation occurs at the right time and under the right conditions thereby avoiding the risk of multipolar spindle assembly by disengaging in a timely fashion at G2 (Hatano and Sluder, 2012).

The second event, centrosome duplication is strictly regulated and occurs contemporaneously with DNA replication. Duplication initiation requires activation of cyclin-cdk complexes; cyclin-A-cdk2 and cyclin-E-cdk2, which exchange between the nucleus and the cytoplasm to promote the initiation of centriole duplication as well as to promote DNA synthesis (Balczon, 2001; Hinchcliffe et al., 1999; Matsumoto et al., 1999; Meraldi et al., 1999).

One model suggests that the Cyclin-E-cdk2 complex regulates centrosome duplication by phosphorylating nucleophosmin (Okuda, 2002; Tokuyama et al., 2001). During G1 to S transition, Cdk2/E phosphorylates nucleophosmin, which leads removal of nucleophosmin from the centrosome. This removal is thought to be essential for centriole duplication. When a cell enters mitosis,

nucleophosmin relocates to the centrosomes and inhibits centrosome over-duplication.Therefore, it has been suggested that nucleophosmin could be controlling centrosome duplication to once per cell cycle (Okuda et al., 2000). Related to an inhibitory role in centrosome duplication, another study indicated that the centrosomal localisation of nucleophosmin depends on Ran–Crm1 (Wang et al., 2005), a nuclear-cytoplasmic shuttle complex that, when ablated, causes centrosome amplification. However, this does not explain why centrosomes cannot re-duplicate normally during S and G1, as nucleophosmin is not at the centrosomes. Therefore it is more likely that nucleophosmin acts a downstream effector of Cdc2/E complex during centrosome assembly (Tsou and Stearns, 2006a).

Cdc2/E complex also phosphorylates the centrosomal protein of 110 kDa (CP110) and this phosphorylation regulates centrosome duplication as the ablation of CP110 with siRNAs interferes with centrosome duplication in U20S cells (Chen et al., 2002).

Cyclin-E carries DNA-replication initiating factors such as Mcm5 and Orc1 onto chromatin (Geng et al., 2007), Mcm5 supresses overduplication of centrosomes at S-phase (Ferguson and Maller, 2008) and Orc1 prevents Cyclin-E-driven overduplication of centrioles (Hemerly et al., 2009). Interestingly, overexpression of Geminin, which is a DNA replication inhibitor, interferes with the centrosome duplication cycle (Tachibana et al., 2005). Therefore regulation of DNA replication and centrosome replication overlaps at a molecular level.

Polo-like kinase 4 co-operates with cyclin-cdk complexes to initiate the formation of a new centriole, and therefore plays a crucial role in the initiation of centrosome duplication (Habedanck et al., 2005). Depletion of Plk4 from

dividing cells leads to loss of centrioles, whereas overexpression of Plk4 causes establishment of several daughter centrioles (Holland et al., 2012; Holland et al., 2010). In most cells, Plk4 is a low abundance protein and capable of dimerization and transautophosphoryalation(Guderian et al., 2010). These features of Plk4 cause the recruitment of the ubiquitin ligase β-TrCP, and proteasome-mediated degradation of the protein (Cunha-Ferreira et al., 2009). This data suggests that the restriction of the new centriole formation to one per cell cycle is controlled by timely degradation of Plk-4 via ubiquitin ligases (Cunha-Ferreira et al., 2009; Rogers et al., 2009).

Essential centriole components required for centrosome duplication include δ- and ε- tubulin, Sas4, Sas6 and CP110 (Chen et al., 2002; Dutcher et al., 2002; O'Toole et al., 2003). The cell-cycle dependent expression of Sas6 and CP110 presents an important barrier to control centrosome overduplication in human cells (Chen et al., 2002; Habedanck et al., 2005; Strnad et al., 2007). In *Drosophila* and humans the centriole protein Asterless/Cep152 creates a network with Sak/Plk4 and Sas-4/CPAP complexes and the formation of this protein network is essential for centriole duplication, although its exact role in the centrosome assembly is unknown (Blachon et al., 2008; Cizmecioglu et al., 2010; Dzhindzhev et al., 2010; Hatch et al., 2010).

Centriole assembly during centrosome duplication also requires the PCM and core centrosomal components such as pericentrin. Overexpression of pericentrin increases the number of newly formed centrioles, indicating a regulatory role for the PCM cloud (Loncarek et al., 2008). Other PCM proteins essential for centrosome duplication include NEDD1, γ-tubulin and Cep192 (Haren et al., 2006a; Haren et al., 2006b; Zhu et al., 2008).

The machinery that restricts centrosome duplication to one per cell cycle still remains to be elucidated. The known proteins that associate with duplication cycle have been discussed above.

The third event, the centriole elongation, requires cdc25 (Lukasiewicz and Lingle, 2009; Vidwans et al., 1999), as shown in cdc25 mutant *Drosophila* embryos, which revealed daughter centrioles that were shorter than mother centrioles compared to wild type (Freed et al., 1999; Vidwans et al., 1999). A recent study identified that knocking down seven centrosomal proteins (FOP, CAP350, CPAP, hSAS-6, Cep170, ninein, and C-Nap1) reduced daughter centriole elongation whereas depletion of two of the centrosomal proteins (Cep97 and CP110) enhanced the elongation of centrioles (Korzeniewski et al., 2010). The same study also demonstrated that the daughter centrosome elongation is controlled by proteolysis (Korzeniewski et al., 2010).

The fourth event, centrosome maturation is controlled by a combination of three proteins: Polo-like kinase 1 (Plk1) (Lane and Nigg, 1996), Nek2 protein kinase (Prigent et al., 2005) and protein phosphatase 4 (Martin-Granados et al., 2008). The process of centrosome maturation additionally requires numerous other proteins such as Hef1 (Pugacheva and Golemis, 2005), TPX2 (De Luca et al., 2006), Bora (Hutterer et al., 2006), NDEL1 (Mori et al., 2007), and LATS2 (Toji et al., 2004). Significantly, all these proteins participate in Aurora A signalling either via recruitment of aurora A to the centrosome (De Luca et al., 2006; Hutterer et al., 2006; Pugacheva and Golemis, 2005) or as downstream effectors of Aurora A (Mori et al., 2007; Toji et al., 2004).

Aurora A localises to the centrosome after the centrosome duplication at S phase and remains at the centrosome until telophase (Gopalan et al., 1997).

Aurora A has an established role in facilitating the characteristic increase in microtubule-nucleating activity through the recruitment of complexes such as γ-TuRCs and D-TACC-Msps (Barr and Gergely, 2007; Barros et al., 2005). Indeed, in *Drosophila*, depletion of Aurora A resulted in the failure of γ-tubulin to accumulate at the centrosome; the resulting centrosomes failed to mature and separate which led to monopolar spindle formation (Berdnik and Knoblich, 2002). Formation of the bipolar spindle is very important function of the centrosome. Aurora A localises to spindle pole microtubules after nuclear envelope breakdown (Gopalan et al., 1997; Kimura et al., 1997) and operates via a Ran-regulated spindle assembly pathway (Fu et al., 2007). Ran is a small GTPase, which controls the nucleocytoplasmic transport and regulates spindle assembly by controlling the release of proteins involved in spindle assembly (Clarke and Zhang, 2001). Therefore, at the onset of mitosis, spindle assembly factors such as Tpx2 and Numa are released and allowed to localise to the centrosome by Ran (Clarke and Zhang, 2001; Gruss et al., 2001). In return, Tpx2 mediates Aurora A spindle localisation and subsequent spindle formation (Kufer et al., 2002). Intriguingly, Aurora A alone (without the centrosome) could function as microtubule-organising centre in the presence of GTP-bound Ran to induce bipolar spindle assembly (Tsai and Zheng, 2005). The mechanism responsible for driving this process is currently unknown. Thus, identification of Aurora A substrates will help to improve our understanding of Aurora A mediated spindle assembly (Barr and Gergely, 2007). For instance, one Aurora A substrate, HERP, was shown to localise at the proximal ends of mitotic spindles and ensure effective kinetochore capture by spindle microtubules (Wong and Fang, 2006).

Cyclin-cdk activity is required for centrosome maturation as well as the centrosome duplication (Saunders and Hoyt, 1992) and this activity is also regulated by Aurora A. During centrosome maturation, cyclin-B-Cdk1 is initially targeted to the centrosome by Aurora A, where Aurora A phosphorylates Cdc25 to activate cyclin-B-Cdk1 (De Souza et al., 2000; Dutertre et al., 2004). Activation of Cyclin-B-cdk1 complex is important for orchestrating timing of the mitotic entry (De Souza et al., 2000; Kramer et al., 2004).

The role of Plk1 in centrosome maturation was demonstrated in cells injected with anti-Plk1 antibodies, which resulted in mitotic arrest, monopolar spindles comprising of two un-separated centrosomes, and failure to accumulate maturation markers such as MPM-2 (mitotic phosphoprotein monoclonal antibody 2) and γ-tubulin (Lane and Nigg, 1996; Lens et al., 2010; Nigg et al., 1996). Collectively, these data establish that centrosome maturation is regulated in a complex manner and that Aurora A has a critical role.

The final event, centrosome separation, is mainly mediated by Nek2 through phosphorylation of C-Nap1 (centrosomal Nek2-associated protein 1, also called Cep250) and rootletin that are both centrosome linker components that tether mother centrioles after centriole duplication (Bahe et al., 2005; Hayward and Fry, 2006). Inactivation of Nek2 by mutation led to duplicated but un-separated centrosomes followed by cell cycle arrest in late G2 (Osmani et al., 1991).

Mutations in Aurora A caused similar phenotypes to mutants deficient for the Plk-1 and Nek2; *Drosophila* mutants were often tetraploid as a result of the inability of monopolar mitotic spindle (formed by unseparated centrosomes) to segregate chromosomes in anaphase (Glover et al., 1995). Additional matching phenotypes were seen also upon antibody-interference of motor proteins dynein

(minus-end directed) and Eg5 (plus-end directed), indicating their role in controlling the dynamic movements of centrosome separation (Lukasiewicz and Lingle, 2009; Saunders and Hoyt, 1992).

Aurora A also mediates centrosome separation (Barr and Gergely, 2007) but the molecular mechanism behind this role remains elusive although several putative roles have been suggested. One possibility is Aurora A mediates the separation via phosphorylation of the kinesin motor protein, Eg5, which can slide antiparallel microtubules and tether microtubule plus-ends (Kapitein et al., 2005). Regulation of centrosome separation by Aurora A through Eg5 was also demonstrated with orthologues in *Xenopus* (Giet et al., 1999).

In summary, as with many cell-cycle processes, the principal events of the centrosome cycle are regulated by a combination of protein phosphorylation/ dephosphorylation and stability.

1.2.3 Dysregulation of centrosomes in cancer

Centrosomes are not only key players in mitosis but are also of wider medical interest as centrosome amplification is a frequent characteristicof many cancer cells (D'Assoro et al., 2002a; D'Assoro et al., 2002b; Nigg, 2006; Pihan et al., 1998; Pihan et al., 2001) that has been associated with promoting genetic instability (Brinkley, 2001; Ghadimi et al., 2000; Lingle et al., 2002) and so therefore tumorigenesis (Figure 1.11). This hypothesis is supported by work showing that centrosome amplification can initiate tumorigenesis in *Drosophila* (Basto et al., 2008). In addition, aberrant centrosome number has been proposed to cause aneuploidy in several pre-invasive carcinomas via abnormal (multipolar) mitotic spindle assembly (Pihan et al., 2003).

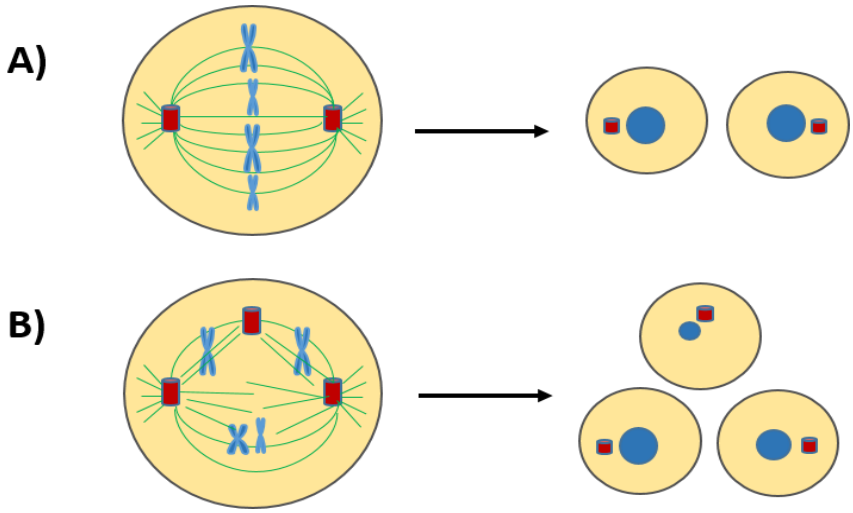

Figure 1.11: The importance of regulation of centrosome number in animal cell mitosis. (A) A mitotic mother cell with two centrosomes establishes a bipolar spindle and segregates its genetic material equally to the daughter cells. **(B)** A mitotic cell with centrosomal abnormalities such as an additional centrosome; the spindle forms abnormally, leading to missegregation of the genetic material. Centrosomes are shown in red, spindles in green and chromosomes are in blue. Figure adapted from (Raff, 2002).

1.2.3.1 Types of centrosomal defects

Centrosomal defects in human cancers are classified as numerical or structural aberrations according to their origins (Nigg, 2006). Numerical centrosome aberrations (more than 2 centrosomes per cell) such as centrosome amplifications are the most commonly identified centrosomal defects in cancer. In addition to numerical aberrations, structural centrosomal defects are also thought to occur in tumours (Fukasawa, 2011; Nigg, 2006). Structural centrosome defects can be divided into two groups: defects in either centriole structure or in the amount of PCM (Godinho and Pellman, 2014). Centriole structural defects include alterations in centriole size (increase in length and increase in the variability of centriole length). However, investigating the origins

of centriole defects is difficult due to the size of centrioles (0.2-0.5 µm long), which requires specialized fluorescence techniques or electron microscopy for effective visualisation. The increase in the amount of PCM has been also considered as a centrosome structural defect (Nigg, 2006). However, the assays commonly used to classify tumours as having 'structural' defects can be difficult to interpret (Godinho and Pellman, 2014). For instance, an increased amount of PCM can be classified as a structural defect (Nigg, 2006) although increased PCM can be either related with the increase in size (D'Assoro et al., 2002b) or can be related to supernumerary centrosomes that are clustered during interphase, which can be classified as a 'numerical defect' (D'Assoro et al., 2002a; Godinho et al., 2014; Lingle et al., 2002). Therefore, it is not trivial to determine the origin of centrosomal aberrations from fixed cell imaging and moreover studies from many primary tumours only examine PCM markers, not centriole markers (Godinho and Pellman, 2014). Thus, improved methods to categorize centrosome abnormalities are needed.

Centrosomal defects can arise via several fundamentally distinct but as yet not mutually exclusive mechanisms. These will be discussed below.

1.2.3.2 Causes of centrosome defects/amplifications

Firstly, one major cause of centrosome defects is the deregulation of the centrosome duplication cycle, which is in partly controlled by strict regulation of its own components. Deregulation of the centrosome cycle can lead to centriole overduplication (loss of cell-cycle control) or excessive centriole multiplication (loss of copy number control), which both result in formation of supernumerary centrosomes (Chan, 2011). The underlying mechanisms of such centriole

defects in cancer are still not clear. One idea is that changes in the expression (over or under expression) of genes associated with controlling the centriole structure such as Plk4, SAS-6/4, CPAP, CP110 as described above, can drive centriole defects (Brownlee and Rogers, 2013). For example, overexpression of CPAP/SAS-4 complex, increases centriole length, in several model systems including *C. elegans* (Kirkham et al., 2003), *Drosophila* (Peel et al., 2007), and proliferating human cells (Kohlmaier et al., 2009) (Schmidt et al., 2009; Tang et al., 2009). SAS-6 is also essential for the correct centrosome duplication cycle as it is involved in the establishment of the cartwheel structure that warrants the nine-fold symmetry of the centriole (Dammermann et al., 2004; Kitagawa et al., 2011; Leidel et al., 2005; Rodrigues-Martins et al., 2007; van Breugel et al., 2011).

Another important master regulator of centrosome duplication cycle is Plk4, as additional Plk4 activity leads to extra centrioles (Habedanck et al., 2005; Kleylein-Sohn et al., 2007), whereas its depletion causes a decrease in centriole number (Bettencourt-Dias et al., 2005; Habedanck et al., 2005; O'Connell et al., 2001).

Moreover, ubiquitin regulators can alter the stability of centriolar proteins and play an important role in preventing centriole overduplication (Godinho and Pellman, 2014). For example, downregulation of βTrCP causes centrosome amplification by stabilizing Plk4 (Cunha-Ferreira et al., 2009; Rogers et al., 2009; Wojcik et al., 2000), whereas overexpression of USP33 leads to increased CP100 levels and therefore centrosome amplification (Li et al., 2013a). Overexpression of PCM components, such as pericentrin (Loncarek et al., 2008) can also induce centrosome overduplication. Additionally, loss of the

tumour suppressor BRAC1 leads to centrosome amplification due to increased levels of the PCM protein, γ-tubulin (Sankaran et al., 2004; Starita et al., 2004).

Secondly, failure of cytokinesis can generate polyploid cells with supernumerary centrosomes (Meraldi et al., 2002). In this case, centrosome number in polyploid cells increases with nuclear abnormalities but do not originate from overduplication. The potential for such cells to re-enter S phase and give rise to normal progeny depends on the tetraploidy checkpoint governed by p53 function, which in such cells triggers cell cycle arrest and apoptosis (Chan, 2011; Meraldi et al., 2002).

Thirdly, centrosome amplification can be caused by errors in cell fusion (Ganem et al., 2007). For example, when cells are under the influence of fusogenic viruses, centrosome number can increase (Duelli et al., 2005; Shekhar et al., 2002).

Lastly, fragmentation of PCM can lead to disintegration of centrosomes, which blocks normal centrosome function thereby causing centrosome amplifications (Difilippantonio et al., 2009; Mikule et al., 2007).

All these studies help provide a better understanding of how the process of centrosome biogenesis is affected in tumour cells. However, there is much to investigate to understand both the origins and consequences of centrosome defects in cancer.

1.3 Introduction to the RASSF proteins

One group of proteins linked to mitosis, centrosomes and cancer is the RASSF family of proteins; therefore the next section will focus on them.

The first official member of the Ras-association domain family (RASSF) was initially identified in a yeast-two-hybrid screen as exhibiting high sequence homology to an already known Ras-effector, Nore1 (now included in the family as RASSF5) (Dammann et al., 2000). Currently the RASSF family represent a group of ten proteins that contain a Ras association (RA) domain either in their C-terminus (Classical RASSF proteins, RASSF1-6) or N-terminus (N-terminal RASSF proteins, RASSF7-10) (Sherwood et al., 2010) (Figure 1.12) in mammals and in *Xenopus*. In contrast, the *Drosophila* genome encodes two RASSF family proteins: dRASSF which is similar to human RASSF1-6; and dRASSF8, which is similar to human RASSF7 and 8 (Langton et al., 2009).

RASSF proteins are defined by the possession of a characteristic RA domain (Sherwood et al., 2010). Comparing sequences from different Ras-binding proteins identified this domain (Ponting and Benjamin, 1996). However, the name 'RA' can be misleading since this does not necessarily mean that a protein containing an RA domain will definitely bind Ras. In reality, the binding affinities of the RA domains of the RASSF family members display a great variation and some members do not bind Ras (Rodriguez-Viciana et al., 2004; Wohlgemuth et al., 2005). A conserved feature of RA domains is their is their proposed ability to form 3-dimensional 'ubiquitin fold' structure (Herrmann, 2003). It is important to study proteins with an RA domain such as RASSF family proteins to establish whether they are Ras effectors or not.

RASSF family proteins have no intrinsic enzymatic activity, but instead are thought to act as scaffolding proteins. RASSFs regulate a wide range of functions including apoptosis, autophagy, microtubule dynamics, Ras signalling, cell cycle control, epigenetic silencing, regulation of immune system and many act as tumour suppressor proteins (Avruch et al., 2009; Clark et al., 2012; Richter et al., 2009; van der Weyden and Adams, 2007; Volodko et al., 2014)

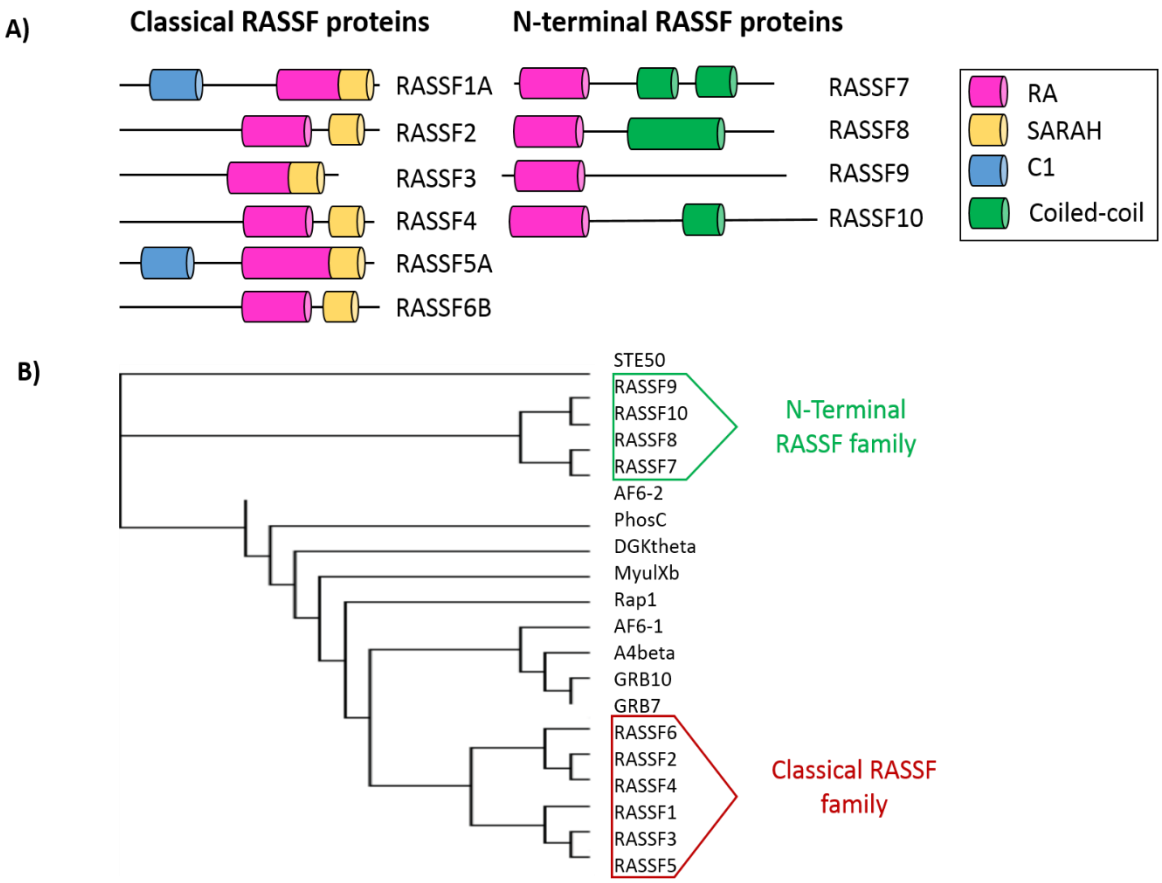

Figure 1.12: Domain architectures and differences in classical RASSF and N-terminal RASSF proteins (A) Structural differences among RASSF family proteins in domain architecture. Classical RASSF proteins have the RA domain (represented as pink cylinder) at the C-terminus end, whereas the N-terminal RASSF proteins have the RA domain at the N-terminus end. Classical family proteins contain a SARAH domain (represented as a yellow cylinder) but the N-terminal family lacks the SARAH domain whilst containing a coiled-coil domain (represented as green cylinder). **(B)** Phylogenetic differences between classical and N-terminal families. Figures adapted from (Sherwood et al., 2010).

1.3.1 The classical RASSF proteins

The classical RASSF members (RASSF1-6) share approximately 30-50% amino acid homology and contain several distinct domains including, the RA, SARAH (named after Salvador-RASSF and Hippo tumour suppressors), C1 (protein kinase C conserved region 1, only in RASSF1A, RASSF1C and RASSF5) and ATM domain (ATM-kinase phosphorylation motif, only in RASSF1A and RASSF1C) (Figure 1.12) (Richter et al., 2009; Sherwood et al., 2010). The SARAH domain is a protein-protein interaction domain, which can mediate hetero- or homodimerization of proteins with two α-helices that form a novel antiparallel helix conformation (Scheel and Hofmann, 2003). This domain is found in proteins involved in the emerging tumour suppressor pathway Hippo, which is, evolutionary conserved between *Drosophila* and mammals that regulates cell contact inhibition, organ size and tumorigenesis (Saucedo and Edgar, 2007).

The C1 domain is a diacylglycerol /phorbol ester binding (DAG) domain that facilitates the association with death receptor complexes including TNF-R1 and TRAIL (El-Kalla et al., 2010). DNA damage/repair results in the phosphorylation of the ATM motif in several RASSFs (Hamilton et al., 2009).

1.3.1.1 RASSF1

The RASSF1 gene is located at 3p21.3 within a region of common homozygous and heterozygous deletions that are frequently associated with a variety of human tumours (Dammann et al., 2000; Kok et al., 1997; Lerman et al., 2000; Sekido et al., 1998). RASSF1, which is the best-studied RASSF protein among

classical members, has 8 transcripts (A-H), resulting from alternative splicing and use of differential promoters (Volodko et al., 2014). RASSF1A and RASSF1C are the most extensively studied splice variants and they will be discussed separately below.

1.3.1.1.1 RASSF1A

RASSF1A was the first RASSF gene identified and is one of the most methylated human cancer genes and a *bona fide* tumour suppressor (Gordon and Baksh, 2011; Richter et al., 2009). It is epigenetically silenced in numerous cancers including cervical, breast, lung and prostate cancers and its loss is also considered among the earliest changes detectable in cancer (Klajic et al., 2013). Several studies have described the correlation between RASSF1A methylation and different tumour characteristics. RASSF1A promoter methylation showed an inverse correlation with K-Ras and B-Raf mutation condition in cervical tumours (Kang et al., 2007) and thyroid cancers (Brait et al., 2012; Kang et al., 2007; Nakamura et al., 2005; Xing et al., 2004a; Xing et al., 2004b). RASSF1A hypermethylation was correlated with chromosome instability in Wilms' tumours (Haruta et al., 2008) suggesting that RASSF1A has a function in controlling genomic stability.

The various domains in RASSF1A reflect the various signalling pathways that are possibly regulated by RASSF1A. For example, several studies have provided evidence that RASSF1A is a downstream effector of Ras, and interaction with Ras is achieved via its RA domain (Rodriguez-Viciana et al. 2004, Vos et al. 2000). In contrast, other data suggest that RASSF1A forms a heterodimer with RASSF5 (Nore1a), which links it to activated Ras, rather than binding directly to Ras(Ortiz-Vega et al. 2002).

The presence of the SARAH domain facilitates interaction with Mst kinases and suggests that RASSF1A is potentially a component of the tumour suppressor Hippo signalling pathway. The Hippo pathway was first discovered in *Drosophila* and is important in the regulating apoptosis and organ size (Saucedo and Edgar 2007). The proteins that are involved in Hippo pathway show very high levels of conservation and in mammals are known variously as Mst1/2 kinases, Lats1/2 (large tumour suppressor), WW45, and YAP (Yes-Activated Protein) (Saucedo and Edgar 2007). RASSF1A can associate with the MST1/2 but its exact role in regulating Hippo pathway (especially Mst kinases) is complicated. RASSF1A described to have two opposing roles on Mst1 kinase activity. RASSF1A inhibited the Mst1 kinase activity in transfected HEK293 cells (Praskova et al., 2004), whereas recombinant RASSF1A is shown to activate Mst1 activity in an in vitro kinase assay (Oh et al., 2006).

The presence of an ATM phosphorylation site in RASSF1A suggests this member of the family is a downstream effector of the ATM kinase that functions to ensure genomic stability (Hamilton et al. 2009). DNA damage activates ATM kinase which then acts by controlling the rate of cell proliferation (Shiloh 2003). RASSF1A may also participate in this process via transduction of the signal between ATM and the cell proliferation system.

RASSF1A was shown to be localised to microtubules via its C1 domain (Gordon and Baksh, 2011). The C1 domain is shown to facilitate the link between RASSF1A and death receptor complexes, such as TNF-R1 and TRAIL (El-Kalla et al., 2010). Several groups have shown the important role that RASSF1A plays in microtubule stabilisation (Dallol et al., 2004; El-Kalla et al., 2010; Liu et al., 2003; Rong et al., 2004; Vos et al., 2004). RASSF1A modulates the cell

cycle by forming a complex with microtubules (Dallol et al., 2004; El-Kalla et al., 2010; Song et al., 2004; Vos et al., 2004) and enhances microtubule polymerization (Liu et al., 2003; Vos et al., 2004). It co-immunoprecipitates with α-, β-, γ-tubulins (Dallol et al., 2004; El-Kalla et al., 2010; Rong et al., 2004; Vos et al., 2004). RASSF1A interaction with microtubules occurs through specialised microtubule associatied proteins such as MAP1B (microtubule-associated protein 1B) and MAP1S (microtubule-associated protein 1S) (Dallol et al., 2004). As these proteins bind to tubulin directly, the interaction of RASSF1A with tubulin could be indirect via MAPs (Donninger et al., 2014). The loss of RASSF1A microtubule localisation leads to inhibition of tumour suppressor properties, tubulin instability and promotes genomic instability via the loss of centrosome and mitotic spindle structures (Dallol et al., 2004; Liu et al., 2003; Vos et al., 2004). Therefore, the regulation of microtubule stability, spindle assembly and chromosome attachment by RASSF1A indicate that the tumour suppressor properties of RASSF1A are manifest through its control of cell growth, transformation, motility and invasiveness (Dallol et al., 2005; Korah et al., 2013; Vos et al., 2004).

In addition to its roles in mitosis, RASSF1A is also involved in other aspects of the cell cycle and apoptosis. RASSF1A prevents accumulation of cyclin-D1 either through JNK kinase pathway (Shivakumar et al., 2002; Whang et al., 2005) or by suppressing AP-1 activity (Song and Lim, 2004) and blocks the cell cycle at the G1/S phase (Shivakumar et al., 2002; Whang et al., 2005). RASSF1A also disrupts the MDM2-DAXX-HAUSP complex, which then leads to MDM-2 self-ubiquitination and stabilization of p53 (Song et al., 2008).

In addition to regulating microtubules and the cell cycle, RASSF1A controls at least two apoptotic pathways, Hippo (discussed above) and Bits ax (Avruch et al., 2006; Baksh et al., 2005; Donninger et al., 2011; Vos et al., 2006). RASSF1A activates Bax by direct binding to the Bax activator MOAP-1 (Baksh et al., 2005; Foley et al., 2008; Vos et al., 2006). The association with Hippo and Bax pathways prevents extreme growth and allow RASSF1A to act as a tumour suppressor.

Two studies have generated Rassf1a knockout mouse (Tommasi et al., 2005, Van Der Weyden et al., 2005). The most striking phenotype exhibited by these studies was increased susceptibility to tumour formation. The mice reportedly displayed increased prevalence of various cancers including lung adenomas, lymphomas, and breast adenocarcinoma compared with wild-type mice (Tommasi et al., 2005; van der Weyden et al., 2005).

In summary, RASSF1A is a tumour suppressor protein whose inactivation is associated with the development and formation of numerous important human tumours. However, RASSF1A can be inactivated by point mutations or gene deletions, transcriptional silencing by aberrant promoter methylation is the most common provider to loss or decrease in RASSF1A function. This epigenetic mechanism is now implicated in the inactivation of various tumour suppressors and is therefore established as a major effector to the development of a tumour. Although RASSF1A lacks obvious enzymatic activity, its possession of a Ras association (RA) domain indicates potential as an effector of the Ras oncoprotein. RASSF1A participates in the regulation of multiple apoptotic and cell cycle checkpoint pathways. Contemporary evidence supports the hypothesis that RASSF1A acts as a scaffold for assembly of multiple tumour

suppressor complexes and may additionally transmit pro-apoptotic signaling by K-Ras.

1.3.1.1.2 RASSF1C

In contrast to RASSF1A, RASSF1C does not display tumour suppressor properties and it is not silenced in tumours whilst increasing evidence suggests activity as an oncogene; overexpression of RASSF1C in breast and lung cancer cells caused enhanced cell migration/invasion (Amaar et al., 2006; Reeves et al., 2010; Volodko et al., 2014).

Other work shows that RASSF1C localises to the nucleus (in HeLa cells), but does not modulate mitosis (Kitagawa et al., 2006). Instead, RASSF1C appears to play a role in Ras-mediated cellular activities including apoptosis (Vos et al., 2000). It forms a complex with DAXX, localises to nuclear located promyelocytic leukaemia-nuclear bodies, and is degraded in response to DNA damage where upon RASSF1C is released into cytoplasm to activate the SAPK/JNK pathway (Kitagawa et al., 2006). RASSF1C may also associate and co-localise in the nucleus with the serine-proteinase inhibitor TFPI-2, which is involved in inflammation, angiogenesis and tumour growth/metastasis (Chen et al., 2012)

Both the structure and subcellular localisation of RASSF1A and RASSF1C differ and antagonism appears to exist between their physiological functions.

1.3.1.2 RASSF5

RASSF5 (also called NORE1 or RAPL) was the first member of RASSF protein family characterized (Dammann et al., 2000); the RASSF5 gene is localised at 1q32.1 (Tommasi et al., 2002). RASSF5 has three isoforms (A-C) generated via use of differential promoter and alternative splicing; among RASSF5 isoforms, RASSF5A displays 40% amino acid similarity with RASSF1A (Volodko et al., 2014).

Data obtained by several laboratories strongly suggest that RASSF5 is a tumour suppressor (Khokhlatchev et al., 2002; Moshnikova et al., 2006; Ortiz-Vega et al., 2002; Praskova et al., 2004; Vavvas et al., 1998). Most normal tissues express RASSF5, but its expression is repressed in various cancer cell lines (Hesson et al., 2003; Irimia et al., 2004; Nakamura et al., 2005). Related with its role as a tumour suppressor, in RASSF5 knockout, K-Ras transfected mouse embryonic fibroblasts developed large numbers of tumours when injected into immune compromised mice, supporting the role of RASSF5A in restricting abnormal growth (Park et al., 2010a).

The other isoform, RASSF5C, is expressed mainly in lymphoid tissues and has been implicated in T-cell receptor stimulation (Katagiri et al., 2003). It can also suppress growth in cells similar to RASSF1A (Aoyama et al., 2004). Importantly, RASSF5C participates in the regulation of cell cycle progression via p27 (Katagiri et al., 2011).

RASSF5A is a centrosomal protein able to bind microtubules, for which the RA domain is essential, and is known to be involved in cell growth regulation (Moshnikova et al., 2006). It associates with cytoskeletal proteins through its RA domain and promotes growth suppression via the ERK pathway (Moshnikova et

al., 2006). In addition, RASSF5A can interact with MST1 kinase following cell death receptor activators (TNF-α and TRAIL) and regulates apoptosis (Park et al., 2010a). RASSF5A also interacts with RASSF1A and promotes cell death (Ortiz-Vega et al., 2002). There is also evidence that RASSF5A is able to inhibit cell proliferation in a MST kinase-independent way by delaying cell cycle progression (Aoyama et al., 2004). Thus, the control of apoptosis is a key function of RASSF5.

1.3.1.3 RASSF2

The RASSF2 gene is located on chromosome 20 (locus 20p12.1) and has three different isoforms (A-C) (van der Weyden and Adams, 2007). The literature focuses on isoform A, RASSF2A, which will be referred as RASSF2. RASSF2 is a primarily nuclear protein (Cooper et al., 2008) and displays several tumour suppressor properties, including inhibition of cell growth and induction of apoptosis (Vos et al., 2003; Zhang et al., 2007). Regulation of cell growth by RASSF2 was reportedly regulated by the MAPK pathway; MAPK/ERK2 mediated phosphorylation enhances export of RASSF2 from the nucleus and a RASSF2 nuclear import mutant failed to arrest the cell cycle at G1/S phase and apoptosis (Kumari and Mahalingam, 2009; Vos et al., 2003).

Although RASSF2 binds directly to K-Ras in a GTP dependent manner via the RA domain its interaction with H-Ras is weak (Vos et al., 2003). RASSF2 also associates with MST1, engages the JNK pathway and induces apoptosis in a MST1-independent manner (Song et al., 2010).

1.3.1.4 RASSF3

The RASSF3 gene is located at 12q14.2 and is the shortest member of the classical RASSF proteins (Richter et al., 2009). It has three transcripts (A-C) resulting from alternative splicing of the exons (van der Weyden and Adams, 2007). The isoform described in the literature is RASSF3A. RASSF3 expression levels were subject to down-regulation in the majority of non-small-cell lung carcinomas, although this was not the result of DNA hypermethylation. Overexpression of RASSF3 in breast cancer cell lines inhibited the cell proliferation which suggests a protective role for RASSF3 in tumorigenesis (Jacquemart et al., 2009). A recent study showed that RASSF3 expression induces p53 stabilization by ubiquitination of MDM2 (E3 ligase for p53) (Kudo et al., 2012). Therefore it is possible to say that RASSF3 can exert potential tumour suppression properties via p53-dependent apoptosis and DNA damage mechanisms (Volodko et al., 2014). Overall, little data exists on RASSF3 indicating that more research is needed to gain a better understanding of its biological function.

1.3.1.5 RASSF4

The RASSF4 gene is located at 10q11.21 and its alternative splicing is predicted to produce numerous transcripts (A-F) (van der Weyden and Adams, 2007). The only variant described in the literature is the RASSF4A isoform and is simply referred to as RASSF4.

RASSF4 is frequently downregulated in human tumour cells and in several cancer cell lines by promoter methylation, but is extensively expressed in normal tissue (Chow et al., 2004; Eckfeld et al., 2004), suggesting a tumour

suppressor function for RASSF4. A recent paper demonstrated that RASSF4 interacts with and inhibits the tumour suppressor MST1/Hippo, indicating that RASSF4 may act as a Hippo pathway inhibitor (Crose et al., 2014). There is also evidence for RASSF4 attenuating the MAP kinase signal by suppression of ERK phosphorylation (Michifuri et al., 2013) which suggests a further possible mechanism for RASSF4-mediated tumour suppression. Similar to RASSF3, the literature on RASSF4 is limited and requires further investigation to confirm its status as a tumour suppressor.

1.3.1.6 RASSF6

The RASSF6 gene is localised at chromosome 4q13.3 and three transcripts are predicted from the RASSF6 locus (A-C) (van der Weyden and Adams, 2007). Similar to other RASSFs, RASSF6 behaves as a tumour suppressor protein (Djos et al., 2012; Hesson et al., 2009). In HeLa cells overexpression of RASSF6 induced apoptosis (Ikeda et al., 2007). RASSF6 activates Bax, induces cytochrome c release, and triggers both caspase-dependent and independent pathways of apoptosis (Ikeda et al., 2007). Moreover, RASSF6 associates with MST2 and inhibits Hippo pathway activation (Ikeda et al., 2009). RASSF6 also regulates apoptosis and the cell cycle by binding to MDM2 and facilitates its self-ubiquitination/degradation by stabilising p53 (like RASSF1A and RASSF3) (Iwasa et al., 2013). It has also been demonstrated that RASSF6 can inhibit NFκB activity (Allen et al., 2007) and possibly inflammation by respiratory syncytial virus (RVS) (Bitko et al., 2004).

In summary, the biological function of the classical RASSF proteins is too complicated to be ascribed to one process only. The members of classical

family have been associated with microtubule stability, cell cycle control and apoptosis, all of which can contribute to the tumour suppressor activity of at least some of these proteins.

1.3.2 The N-terminal RASSF proteins

The N-terminal RASSF proteins (RASSF7-10, Figure 1.12) are a recent addition to the RASSF family and thus, have been studied less extensively than some of their classical counterparts (Sherwood et al., 2010; Underhill-Day et al., 2011). The N-terminal family members have their RA domain at the opposite end (N-terminus) compared to classical members (Figure 1.12B). Additionally, unlike classical family members, the N-terminal family do not possess a SARAH domain but three (7, 8 and 10) have a coiled-coil domain, a protein-protein interaction domain that is variable and sensitive to sequence changes (Grigoryan and Keating, 2008; van der Weyden and Adams, 2007). Nevertheless, the differences between RASSF7-10 and RASSF1-6 suggest that the N-terminal RASSF proteins should not regarded as an extension of the Classical RASSF proteins, opening up the possibility of divergent roles (Sherwood et al., 2010). These will be discussed individually for each N-terminal member.

1.3.2.1 RASSF8

The RASSF8 gene is located close to KRAS2 gene on chromosome 12p11 and seven isoforms (A-G) have been predicted (van der Weyden and Adams, 2007). Both the RASSF8 and KRAS2 genes lie in a chromosomal region called Pals1 that has known sensitivity in a mouse model for lung carcinogenesis and its

association with lung adenocarcinoma risk has been shown in human homologous region (Falvella et al., 2006).

A tumour suppressor role was proposed as a result of reduced RASSF8 transcript levels in lung adenocarcinomas (Falvella et al., 2006). Overexpression of RASSF8 protein in lung cancer cell lines also inhibited anchorage-independent growth that correlates with both tumour progression and metastasis. In addition to lung adenocarcinoma, male germ cell tumours also exhibit RASSF8 transcriptional down regulation, but the mechanism behind this remains to be elucidated. Loss of RASSF8 does not appear to result from promoter methylation, except possibility in childhood leukaemia (Hesson et al., 2009).

RASSF8 may regulate cell-cell adhesion due to its localisation adjacent to the membrane at adherens junctions, specifically interacting with the components E-cadherin and β-catenin. In lung cancer cells endogenous RASSF8 localizes to AJs and binds to E-cadherin (Lock et al., 2010). Following RASSF8 depletion, E-cadherin localization is lost from discrete sites at the cell membrane and β-catenin is lost from adherens junction and accumulates in both the cytoplasm and nucleus (Lock et al., 2010). This suggests that RASSF8 depletion results in loss of both adherens junction formation and function. Lack of stabilization of β-catenin at adherens junctions allows β-catenin relocalization to the nucleus, where it is able to promote activation of the canonical Wnt signalling pathway (Brembeck et al., 2006; MacDonald et al., 2009) suggesting that RASSF8 depletion can cause increased β-catenin signalling as part of the Wnt signalling (Lock et al., 2010). Promoter activity analysis confirmed a substantial increase in NF-kB-dependent activity following RASSF8 knockdown

which suggests a role for RASSF8 in the NF-kB signalling pathway as well as in Wnt signalling (Lock et al., 2010). A recent study from *Drosophila* eye development also showed that RASSF8 is required to regulate E-cadherin and adherens junctions stability (Zaessinger et al., 2015).

Wound healing assays revealed increased cell migration in cells lacking RASSF8 expression, suggesting tumour aggressiveness may result from loss of RASSF8 (Lock et al., 2010). On the other hand, serum analysis indicated that breast cancer patients had increased mRNA levels of RASSF8 in blood plasma (Rykova et al., 2008), suggesting a tumour promoter effect of RASSF8.

1.3.2.2 RASSF9

The RASSF9 gene is located at 12q21.31 and interestingly RASSF9 is not transcribed from a CpG island region like other RASSF proteins (Richter et al., 2009). RASSF9 was first found in a yeast-two-hybrid screen searching for new partners of PAM (peptidylglycine α-amidating monooxygenase) and named as P-CIP1 (PAM COOH-terminal interactor protein 1) (Alam et al., 1996). BLAST analysis revealed that P-CIP1 has structural homology to RASSF7 and RASSF8 and was later named RASSF9 (Sherwood et al., 2010). Little is known about the expression and functional significance of RASSF9. Chen et al., characterised RASSF9 and found high levels of sequence conservation from rat to human.

RASSF9 interacted with the cytosolic domain of wild type PAM-1 and was associated with endosomes (Chen et al., 1998). A more recent study reported the predominant expression of RASSF9 in epithelial tissue (Lee et al., 2011). RASSF9 deficient mice displayed signs of senescence including increased

alopecia (hair loss), shorter life span and growth retardation suggesting a novel role for RASSF9 in maintaining epidermal homeostasis by recycling of integral proteins (Lee et al., 2011).

1.3.2.3 RASSF10

Sherwood et al. first discovered the RASSF10, because the protein was similar in sequence to RASSF9 and named it RASSF10 (Sherwood et al., 2008). The RASSF10 gene is located at 11p15.2 (Richter et al., 2009). RASSF10 is expressed in several tissues (bone marrow, thyroid, brain, prostate and caner) (Dansranjavin et al., 2012; Hesson et al., 2009; Hill et al., 2011; Schagdarsurengin et al., 2009) and hypermethylation of RASSF10 was linked to loss of gene expression in cancer cells (Dansranjavin et al., 2012; Hesson et al., 2009; Schagdarsurengin et al., 2009). In vitro analysis of RASSF10 in U87 glioma cells showed that RASS10 knockdown increased cell proliferation and survival whereas re-expression of RASSF10 blocked cell growth and colony formation, indicating a tumour suppressor function of RASSF10 (Hill et al., 2011). The tumour suppressor activity of RASSF10 was also assessed in gastric cancer cells and showed reintroduction of RASSF10 in JRST and BGC823 cell lines reduced cell viability and promoted apoptosis (Wei et al., 2013). The same study also showed that the pro-apoptotic feature of RASSF10 involves the Wnt/β-catenin signalling pathway (Wei et al., 2013). Additionally, RASSF10 has a potential role in regulation of mitotic progression related to its centrosomal localisation and localisation at microtubules (Hill et al., 2011).

The N-terminal RASSF proteins possess a different domain architecture from the classical RASSF proteins and are considered a separate family (Sherwood

et al., 2010). Although, RASSF7 and RASSF1A show similar centrosomal localization and mitotic defects when knocked down, and promoter hypermethylation occurs in both RASSF10 and members of the classical RASSF family. Although these similarities suggest that the N-terminal RASSF proteins are genuine RASSF proteins, the differences between them still outweigh the similarities reinforcing the idea that the N-terminal RASSF proteins are a separate family. Emerging evidence suggests that the N- terminal RASSF proteins could play a role in tumour formation. Further detailed study will confirm whether this new group of proteins play an important role in oncogenic progression.

1.3.2.4 RASSF7

The RASSF7 gene is located at locus 11p15.5 surrounding the HRAS1 cluster 1 (Weitzel et al., 1992). RASSF7 was originally identified as HRC1 in a study which searched for genes that are close to HRAS1 in the genome (Weitzel et al., 1992). Due to alternative splicing, RASSF7 is predicted to have three transcripts (A-C). Our laboratory identified RASSF7 in a microarray screen comparing superficial and deep cells in early *Xenopus* embryos, where it was initially called carcinoma associated protein (Chalmers et al., 2006). RASSF7 has broad expression in early *Xenopus* embryos, with high levels in neural and epidermal tissue (Sherwood et al., 2008). Studies of human cell lines and mouse embryos also showed it to be expressed in a wide range of cell and tissue types (Recino et al., 2010). Functional analysis demonstrated that RASSF7 is required for mitosis in cells from *Xenopus* embryos, where morpholino knockdown caused mitotic defects (Sherwood et al., 2008). In

human cells shRNA knockdown also caused defects in mitosis, including aberrant microtubule regrowth, a failure in chromosome congression (coming together) and reduced Aurora B activity at the kinetochores (Recino et al., 2010). An independent study showed that RASSF7 negatively regulates pro-apoptotic JNK signalling by inhibiting the activity of phosphorylated mitogen-activated protein kinase 7 (MKK7) and binds to N-Ras (Takahashi et al., 2011), but it is not currently clear whether the stress and mitotic roles are linked.

Consistent with its role in mitosis, both human and *Xenopus* studies showed that RASSF7 localises to centrosomes. The aforementioned studies were performed using fusion proteins in *Xenopus* embryos and in human cell lines by staining for endogenous RASSF7 (Recino et al., 2010; Sherwood et al., 2008). While RASSF7 localization and function in mitosis have been conclusively determined, the mechanism by which RASSF7 mediates this role has yet to be elucidated. The role of domains mediating RASSF7 localisation is not understood. Due to the lack of a catalytic domain, functional elucidation through loss-of-function analysis is limited due to the indirect downstream effects that could be elicited. Interestingly, yeast-two-hybrid studies (Morris et al., 2003; Porteous et al., 2011; Tsang et al., 2006; Yasui et al., 2007) have identified a potential RASSF7-binding partner, disrupted-in-schizophrenia 1 (DISC1), which exhibits a scaffolding function and has been associated with centrosomal function (Porteous et al., 2011). However, this interaction and functional significance requires confirmation.

In contrast to the loss of expression seen with many classical RASSF proteins, microarray studies have shown that RASSF7 expression is up-regulated in pancreatic, islet cell, endometrial, ovarian cell and thyroid cancers (Friess et al.,

2003; Li et al., 2013b; Logsdon et al., 2003; Lowe et al., 2007; Tan et al., 2009) and the increase in expression may be driven in some of these tumours by the fact that RASSF7 is up-regulated by hypoxia (Camps et al., 2008; Liang et al., 2009; Recino et al., 2010). Despite an increase in expression in many tumours it is not clear whether RASSF is acting as an oncogene and contributing to tumour formation or whether its increased expression in tumours is simply a consequence of tumour formation. To begin to understand if RASSF7 might act as an oncogene, this thesis focuses on establishing the molecular basis of RASSF7 function.

1.4 Aims of the thesis

The primary goal of the project was to investigate the molecular basis of rassf7 function, which would help to increase our understanding of how RASSF7 functions in mitosis and also establish whether increased levels are likely to promote tumour formation. In order to address this fundamental goal, the work was split into three aims:

1. Determine which domains of RASSF7 are required to localise it to the centrosome in cells from *Xenopus* embryos.
2. Investigate the effect of expression of the C-terminal truncation of raasf7 on mitosis and in centrosomes, and find out if similar truncations occur in human cancers.
3. Investigate the junctional localisation pattern of RASSF7 in *Xenopus* embryos and human cell lines.

2 Materials and Methods

2.1 Materials

Unless otherwise specified, all chemicals and general laboratory reagents were of molecular biology grade and were purchased from either Sigma-Aldrich Chemical Company or Fisher Scientific UK Ltd.

2.1.1 Reagents

The following reagents were used:

Luria Broth (LBB):

1% (w/v) Bacto™ Tryptone (BD Biosciences), 0.5% (w/v) Bacto™ Yeast Extract (BD Biosciences), 0.5% (w/v) NaCl. Autoclaved.

LB Agar Plates:

1% (w/v) Bacto™ Tryptone (BD Biosciences), 0.5% (w/v) Bacto™ Yeast Extract (BD Biosciences), 0.5% (w/v) NaCl. Autoclaved and once cooled down, 100 µg/ml ampicillin was added and poured into plastic plates. Kept at 4°C.

Phosphate Buffered Saline (PBS):

Purchased from OXID

NZY Broth:

10g NZ amine, 5g yeast extract, 5g NaCl, final volume of 1 litre with ddH_2O, pH adjusted to 7, autoclaved and stored 4°C. Prior to use 12.5mls 1M $MgCl_2$, 12.5mls 1M $MgSO_4$, 20mls 20% (w/v) glucose.

2.5% Cysteine:

2.5g/100mls dH2O, ~7 pellets NaOH, pH adjusted to 7.8-8.1

10x Marc's Modified Ringer's (MMR) solution:

2M NaCl, 0.04M KCl, 20mM $MgCl_2.6H_2O$, 4omM $CaCl_2.2H_2O$, 2mM EDTA disodium salt, 1M Hepes, pH adjusted to 7.8-8.1

10x MOPS/EGTA/Magnesium (MEM) salts:

1M MOPS 104.65g, 20mM EGTA 3.8g, 10mM Magnesium Sulphate ($MgSO_4$) 5mls of 1M, 400 mls ddH_2O, pH adjusted to 7.4 with NaOH, made up to 500ml, filter sterilized and stored at 4°C.

MOPS/EGTA/Magnesium/Formaldehyde (MEMFA) Solution:

5mls 10xMEM salts, 5mls Formaldehyde 40mls ddH_2O.

10% (w/v) Ficoll:

50g Ficoll in 500mls ddH_2O filter sterilized and stored at 4°C.

Injection Buffer:

50mls 10% Ficoll, 25mls 10xMMR, 425mls autoclaved ddh2O filter sterilized and stored at 4°C.

10x TAE (Tris-acetate-EDTA) Buffer:

48.5g Tris, 11.4mls glacial acetic acid, 20mls 0.5M EDTA (pH 8) final volume of 1 litre with ddH_2O.

Serum Gonadotrophin PhEur (PMSG):

PMSG-Intervet contains 5000 i.u. diluted in ddH_2O at concentration of 100units/ml

Human Chorionic Gonadotrophin (HCG):

(Chorulon, Intervet; 2500 i.u./cow) 1000 units/ml

10% (w/v) Benzocaine:

480mls ethanol, 20mls water, 50g benzocaine

Blocking Buffer for antibody staining:

1% BSA, 5% HTLS in PBS

Gelatin from cold water fish skin:

15% (16.67mls 45% stock, 7.5g sucrose), 20% (22mls 45% stock, 7.5g sucrose) 25% (27mls %45 stock, 7.5g sucrose).

2.1.2 Antibodies

Table 2.1 Primary antibodies used for immunofluorescence

Antibody	Species	Source	Application-Dilution
γ-tubulin	Mouse, monoclonal	Sigma T6557	IF-1:100
Active caspase 3	Rabbit	Abcam Ab13847	IF-1:100
Phospho histone H3 (Ser10)	Mouse, monoclonal	Abcam Ab14955	IF-1:500
ZO-1	Mouse	Invitrogen 33-9100	IF-1:25
RASSF7	Rabbit	Aviva System Biology ARP34390-T100	1:100
Centrin1	Rabbit	Abcam Ab11257	1:100

Table 2.2 Secondary antibodies used for immunofluorescence

Antibody	Species	Source	Application-Dilution
Mouse Alexa® Fluor 488	goat	Molecular probes A11001	IF-1:500
Mouse Alexa® Fluor 568	goat	Molecular probes A11004	IF-1:500
Rabbit Alexa® Fluor 488	goat	Molecular probes A11008	IF-1:500
Rabbit Alexa® Fluor 568	goat	Molecular probes A11011	IF-1:500

2.1.3 Primers

Table 2.3 Primers used for site directed mutagenesis and domain deletion

Construct	Forward Primer (5'-3')	Reverse Primer (3'-5')	Internal Primer No
GFP-rassf7 (RA+A+CC)	CTCAGGCAGTGTAACCTCCA ATAATTTATCCTTCAGACAGG	CCTGTCTGAAGGATAAATTA TTGGAGGTTACACTGCCTGA G	183-184
GFP-rassf7 (RA+A)	GCTTGGAGAAGAGATGTTTTA GGAGGATGAACTGCAAAGG	CCTTTGCAGTTCATCCTCCT A AAACATCTCTTCTCCAAGC	181-182
GFP-rassf7 (RA)	GAGGCGCACAGGACCATG ATTAGCTGAACGTCCATC	GATGGACGTTCAGCTAAT CATGGTCCTGTGCGCCTC	202-203
GFP-rassf7 (A+CC+B)	CTCATTCCTCGTGTTCAATAT GA GCTTAGCTGAACGTCCATCCT C	GAGGATGGACGTTCAGCTAA GCTCATATTGAACACGAGGA ATGAG	204-205
GFP-rassf7 (A+CC)	CTCAGGCAGTGTAACCTCCA ATAATTTATCCTTCAGACAGG	CCTGTCTGAAGGATAAATTA TTGGAGGTTACACTGCCTGA G	183-184
GFP-rassf7 (CC)	CCTCATTCCTCGTGTTCAATA TGT GGGAGGATGAACTGCAAAGGG	CCCTTTGCAGTTCATCCTCC CACATATTGAACACGAGGAA TGAGG	220-221
GFP-rassf7 (A)	GGAGAAGAGATGTTTTGAG AGGATGAACTGCAAAGGGC	GCCCTTTGCAGTTCATCCT CTCAAAACATCTCTTCTCC	218-219
GFP-rassf7 (CC+B)	CCTCATTCCTCGTGTTCAATT GGGAGGATGAACTGC	GCAGTTCATCCTCCCAATTG AACACGAGGAATGAGG	222-223
GFPrassf7 (B)	CCTCATTCCTCGTGTTCAATGC CAGGAATCAGGAGC	GCTCCTGATTCCTGGCATTG AACACGAGGAATGAGG	224-225

Table 2.4 Primers used for site directed mutagenesis (continued)

Construct	Forward Primer (5'-3')	Reverse Primer (3'-5')	Internal Primer No
GFP-rassf7 (S374-A)	CCCGATGAAGACCCTG CTCTTGCTGAGCCTCAC	GTGAGGCTCAGCAAGAG CAGGGTCTTCATCGGG	206-207
GFP-rassf7 (S374-D)	CCGATGAAGACCCTGA TCTTGCTGAGCCTCAC	GTGAGGCTCAGCAAGA TCAGGGTCTTCATCGG	208-209
GFP-rassf7 (S104, 105-A)	CCAGAGAGGACTTTTGTCAGG GCGGCTTTGCCCCTAAATACT CG	CGAGTATTTAGGGGCAAAGC C GCCCTGACAAAAGTCCTCTC TGG	210-211
GFP-rassf7 (S104, 105-D)	GCCCCCAGAGAGGACTTTTGT CAGGGACGACTTGCCCCTAAA TACTCG	CGAGTATTTAGGGGCAAGTC GTCCCTGACAAAAFTCCTCT CTGGGGGC	212-213
GFP-rassf7 (S/T5-A)	GGCGCGCAGGACCAACGTTAG CTGAACGTCCAGCCGCCGATA CAGG	CCTGTATCGGCGGCTGGACG TTCAGCTAAGCTTGGTCCTG CGCGCC	214-215
GFP-rassf7 (S/T5-D)	GGCGCGACGGACCAAGCTTAG CTGAACGTCCAGACGACGATA CAGGCCC	GGGCCTCTATCGTCGTCTGC ACCTTCAGCTAAGCTTGGTC CGTCGCGCC	216-217
GFP-rassf7 (RA+A+CC'+B)	GAGGAGTACACCGTGAAAATA CAGGAGCTCACTGAGCGG	CCGCTCAGTGAGCTCCTGTA TTTTCACGGTGTACTCCTC	226-227
GFP-rassf7 (RA+A+CC''+B)	GTTTTGGGAGGATGAACCGCA AAGGGAAAGGGCAG	CTGCCCTTTCCCTTTGCGGT TCATCCTCCCAAAAC	228-229
GFP-rassf7 (RA+A+CC'''+B)	GGAATCAGGAGCCCGACGAAG TGGACGAAG	CTTCGTCCACTTCGTCGGGC TCCTGATTCC	230-231

2.1.4 Plasmids

Table 2.5 Plasmids used to generate RNA for expression of GFP fusion proteins

Plasmid Name	Primers used for PCR	name of the plasmid	Internal plasmid no
GFP-rassf7 (Wild type)	-	-	301
GFP-rassf7 (RA+A+CC)	183-184	301	433
GFP-rassf7 (RA+A)	181-182	301	432
GFP-rassf7 (RA)	202-203	301	448
GFP-rassf7 (A+CC+B)	204-205	301	449
GFP-rassf7 (A+CC)	183-184	449	452
GFP-rassf7 (CC)	220-221	452	457
GFP-rassf7 (A)	218-219	449	458
GFP-rassf7 (CC+B)	222-223	449	459
GFP-rassf7 (B)	224-225	459	460
GFP-rassf7 (S374-A)	206-207	301	450
GFP-rassf7 (S374-D)	208-209	301	451
GFP-rassf7 (S104,105-A)	210-211	301	453
GFP-rassf7 (S104,105-D)	212-213	301	454
GFP-rassf7 (S/T5-A)	214-215	301	455
GFP-rassf7 (S/T5-D)	216-217	301	456
GFP-rassf7 (RA+A+CC'+B)	226-227	301	461
GFP-rassf7 (RA+A+CC''+B)	228-229	461	462
GFP-rassf7 (RA+A+CC'''+B)	230-231	462	463

2.2 Methods

2.2.1 Xenopus Methods

2.2.1.1 DNA sequences, plasmids and database/bioinformatics analysis

Xenopus RASSF7 pBlueScript SK(-) clone (X1095b08) was previously cloned into the gateway system (Life technologies, K4500-01) to generate an N-terminal GFP-rassf7 fusion pCS2 construct (Sherwood et al., 2008). A pCS2 GFP construct was also used as previously described (Chalmers et al., 2005). The sequence of the *Xenopus* RASSF7 protein was obtained from NCBI: Ras-association domain family 7 [*Xenopus laevis*] (ABR21988.1). The Simple Modular Architecture Research Tool (SMART : http://smart.embl-heidelberg.de/) was used to identify potential protein domains and this information was then used to inform design of the GFP-rassf7 truncation constructs and the coiled coil mutations which were generated as described below .

Mutations in RASSF7 from human cancer samples were identified using cBioPortal from the Cancer Genomics website (http://www.cbioportal.org/public-portal/index.do) which contained data from 89 cancer genomic studies covering a total of 20,958 tumour samples (August-Nov 2014). Sequence of the human protein was obtained from the NCBI (Ras-association domain containing protein 7 isoform 1 [Homo sapiens]:NP_003466.1) and SMART was then used to predict the effect of the mutations on the expected domains produced by human RASSF7 from these cancer samples.

2.2.1.2 Primer design and site-directed mutagenesis

The QuickChange site-directed mutagenesis kit (Agilent Technologies) was used to make plasmids coding for a series of truncated versions of GFP-rassf7 (Figure 1), by mutating the original GFP-rassf7 CS2 plasmid. Primers were designed according to the kit guidelines and PCR was carried out following the protocol supplied by the manufacturer. Following mutagenesis all constructs were sequenced to confirm the mutations were made correctly. The PCR primers were used to generate the constructs are shown in Table 2.3 and 2.4. The source plasmids used to generate the constructs and final plasmids generated are shown in Table 2.5.

Table 2.6 Cycling parameters for the QuickChange site-directed mutagenesis (Segment 2 is adjusted accordance with the type of mutation desired: Point mutations 12 cycles, single amino acid changes 16 cycles and multiple amino acid deletions/insertions 18 cycles)

Segment	Cycles	Temperature	Time
1	1	95°C	30 sec
2	12-18	95°C	30 sec
		55°C	1 min
		68°C	1 min/kb of plasmid length

2.2.1.3 Dpn1 digestion of PCR products

PCR amplification products were subsequently added with 1µl restriction enzyme Dpn 1, thoroughly mixed and incubated (at 37°C) for 1 hour to digest non-mutated parental DNA.

2.2.1.4 Transformation of competent cells

XL1-Blue supercompetent cells (Agilent Technologies) were gently thawed (from -80°C) on ice and aliquoted (50µL) into a pre-chilled 14-mL BD Falcon polypropylene round-bottom tubes, into which 1µL of Dpn I-treated DNA (per mutation) was transferred, followed by gentle mixing and incubation (at 37°C) for 1 hour. Transformation reactions were then heat-pulsed for (strictly) 45 seconds at 42°C, left on ice shortly, and added with 0.5mL pre-heated (to 42°C) NZY broth to allow expression of antibiotic resistance during 1 hour incubation at 37°C with shaking (at 225-250rpm). 250µL of the resulting transformation reactions were plated onto LB+AMP agar plates and left to colonise at 37°C overnight.

2.2.1.5 Mini-prep for sequencing

Successfully transformed colonies, selected with ampicillin resistance were subsequently used for DNA isolation with GenElute Plasmid Miniprep Kit (Sigma). Overnight cultures of two transformed colonies (per mutation) were pelleted by brief centrifugation (at ≥12,000xg for 1min) and thoroughly resuspended, followed by cell lysis for no longer than 5 minutes. Cell debris was then precipitated and pelleted by centrifugation (at ≥12,000xg for 10min). Cleared lysates (containing DNA and low density debris) were then transferred into Miniprep binding columns already-prepared (with column preparation

solution to maximise DNA binding to the column) and briefly centrifuged. Binding columns were subsequently washed and briefly centrifuged twice to remove excess ethanol. Finally, columns were transferred to a sterile collection tube, where plasmid DNA was eluted with 50µL of ddH_2O by brief centrifugation. Successful isolation and recovery of plasmid DNA was assessed by agarose gel electrophoresis (at 150 mV for 15mins).

Eluted DNA was subsequently sent for sequencing by Eurofins MWG Operon. An appropriate primer was required (to bind ~800bp upstream from the site of mutagenesis). Upon receipt of sequencing results, mutations were verified through translation with ExPASy translate tool (Artimo et al., 2012) and alignment via CLUSTAL Omega (to ensure no disruption to the rest of the amino acid sequence) (Sievers et al., 2011).

2.2.1.6 Maxiprep for plasmid isolation

Once successful mutations were detected, plasmid DNA was isolated at high yields with GenElute HP Plasmid Maxiprep Kits (Sigma) for subsequent linearization and transcription of RNA.

Overnight cultures (in 150mL LB+ media with 0.1mg/mL ampicillin) of colonies originally sequenced, were pelleted by centrifugation (at 4000xg for 10min), and thoroughly re-suspended, followed by lysis for no longer than 5 minutes. Cell lysate was then precipitated and added with 9ml of binding solution, shortly followed by filtering into prepared binding columns and centrifugation (at 3000xg for 2min). Binding columns were sequentially washed and centrifuged (at 3000xg for 2-5mins, respectively), transferred to a sterile collection tube, where plasmid DNA was eluted with 3mL of ddH_2O by centrifugation (at 3000xg

for 5min). Eluted plasmid DNA was then precipitated with 10 % (v/v) 3M NaOAc (pH 5.2) and 70%(v/v) isopropanol and pelleted (at 4000xg at 4°C for 30min). Supernatant was discarded and the DNA pellet washed with 1.5mL 70% ethanol, followed by centrifugation (as before for 10min). Finally once as much ethanol has been manually decanted, the pellet was allowed to air-dry before resuspending in 50µL of ddH_2O. The successful isolation of plasmid DNA was verified with gel electrophoresis and the yield quantified by spectrophotometric analysis.

2.2.1.7 DNA linearization and mRNA transcription

Isolated plasmid DNA (with the desired mutations) was then linearized for subsequent transcription into RNA for injection. 10µg of plasmid DNA was linearized in a 100µL reaction volume with the restriction enzyme Nsi1 in Buffer H (Agilent Technologies) overnight at 37°C. The resulting digested (linear) plasmid DNA was treated with 5µL 25mg/mL proteinase K and 6µL 10% sodium dodecyl sulphate (SDS) for 30mins to the digest proteins (including Nsi1). Linear DNA was subsequently isolated and purified by phenol chloroform extraction, followed by precipitation with 10% (v/v) 3M NaOAc (pH 5.2) and 200% (v/v) ethanol and centrifugation. Pelleted (linear) DNA was washed with 70% ethanol and re-suspended in 10µL of nuclease-free DEPC dH_2O. Again, the successful recovery of linearized DNA was assessed by agarose gel electrophoresis.

Linearized GFP-RASSF7 cDNA was transcribed into capped sense mRNA for subsequent injection using the mMessage mMachine Kit (Ambion); as per instructions, the reaction mixture [3µL nuclease-free DEPC dH_2O, 2µL 10x reaction buffer, 10µL 2x ribonucleotide (NTP/CAP) mix, 3µL of linearized

plasmid DNA and 2µL 10x enzyme (SP6 RNA polymerase) mix] was incubated at 37°C for 2hrs. Remaining linearized plasmid DNA in the resulting RNA sample was digested with 1µLTurbo DNase for 15mins and the reaction stopped with ammonium acetate (15µL in 115µL nuclease-free DEPC dH_2O). RNA was isolated and purified through phenol extraction, followed by precipitation with an equal volume of isopropanol (for 20mins at -20°C). RNA was pelleted via centrifugation (at ≥12000xg for 15mins), washed with 70% ethanol and thoroughly re-suspended in 12.5µL nuclease-free DEPC dH_2O. Isolated RNA was run on fresh agarose for verification of transcription recovery. 1µl RNA aliquots (~500ng/µL) were stored at -80°C.

2.2.1.8 Fertilisation of *Xenopus laevis* eggs

Male *X. laevis (Xenopus)* were killed by a schedule 1 method using benzocaine. Testes were harvested from the freshly killed male and used immediately, or stored for up to 1 day in L-15 medium (Sigma) at 4°C. Female *Xenopus* were injected with 50units of Pregnant Mare Serum Gonadotrophin (PMSG - Intervet®) 3 days prior to egg collection and with 500units of chorionic gonadotrophin (hCG - Intervet®) 12 hours prior to egg collection as per Home Office approved procedure. The female *Xenopus* were put into 1x MMR (Marcs Modified Ringers) to maintain the ability of the laid eggs to be fertilised and eggs were collected from this medium. The collected eggs were washed once with 0.1x MMR and fertilised with the harvested testes, in this procedure, a small piece of the testes, approximately 5mm wide was cut from a testis. It was placed into the dish containing the *Xenopus* eggs and then torn apart and wiped over the eggs. This was to release all of the sperm allowing fertilisation. The fertilised eggs were de-jellied approximately 40mins post fertilisation, 2.5% (w/v)

cysteine was added to the fertilised eggs and left for 2-3mins until the jelly could be seen to have been removed. The eggs were then washed 4 times with 0.1x MMR. Embryos were staged according to Nieuwkoop and Faber (Nieuwkoop and Faber, 1967) or by cell number. Embryos were cultured in 0.1 X MMR until the required stage or transferred to injection buffer for microinjection.

2.2.1.9 Microinjection of RNA

Glass capillary tubes (0.53" width, Drummond Scientific) were pulled using a Sutter P-97 needle puller. *Xenopus* Embryos were transferred to the injection buffer and 9.2 nl of RNA (1:1 dilution) was injected into one cell of the embryo at the two-cell stage using a Nanoject II injector (Drummand Scientific Company). The embryos were examined using a Leica M26 microscope (Deerfieled, Illinois) and any dead embryos removed. Embryos were then cultured until stage 10 or stage 30. Once at the required stage, GFP was visualised in whole embryos using a Leica MZFL III microscope (Deerfield, IL) and the embryos fixed in MEMFA (0.1 MOPS, pH 7.4, 2 2 mM EGTA, 1 mM $MgSO_4$, and 3.7% formaldehyde) for 2 hours at room temperature and where required, processed for immunofluorescence as described below.

2.2.1.10 Immunofluorescence

For antibody staining embryos were embedded in fish gelatin as described previously (Chalmers et al., 2003), except tadpole-stage (stage 30) embryos, which were incubated in 20% sucrose for 2 h, washed several times in PBS and then embedded in 15% fish gelatin for freezing. The embryos were cryosectioned and antibody stained as described (Chalmers et al., 2003). The

following antibodies were used: monoclonal anti-γ-tubulin produced in mouse clone GTU-88 (Sigma; T6557, 1 in 100), polyclonal rabbit anti-active caspase 3 (Abcam; ab13847, 1 in 100) rabbit polyclonal anti-histone H3 phospho S10 (Abcam; ab5168, 1 in 500). The following secondary antibodies were used: anti-mouse Alexa 568 (A-11004, Molecular Probes, Eugene, OR); anti-rabbit Alexa 568 (A-11011, Molecular Probes). All secondary antibodies were used at a 1 in 200 dilution. The nuclear stain, DAPI (Sigma, D9542, 1 mg/mL) was used at 1 in 1000 dilution. Stained sections were mounted in Vectasheild (Vector Labroratories, Burlingame, CA) and imaged on a Zeiss LSM META confocal microscope with a 63X Plan-Apo/1.4 NA oil lense with DIC capability (Thornwood, NY). GFP fluorescence was visualised directly without the use of antibody staining. All fluorescencent images were captured in the linear range of the confocal to allow quantification with extra care was taken to avoid pixel saturation. To achieve this all images were collected using the range indicator, which is found within the Palette filter. Saturated pixels would appear red and pixels below zero blue, the absence of such pixels confirmed the images were collected in the linear range. Each pixel in the image has a dynamic range grey scale value ranging from zero to a maximum of 256. The background was kept close to zero and the intensity adjustments done to create and image with grey levels within the dynamic range of 256, settings were then kept constant for all images collected for an experiment.

2.2.1.11 Quantification and statistics

Quantification of cells expressing GFP was carried out by identifying GFP positive cells (GFP positive cells were identified qualitatively, as those which had significantly above background levels of GFP fluorescence) with a centrosome(s) in the section being analysed (clear γ-tubulin staining adjacent to the nucleus). GFP shows a pattern of localisation when expressed in early Xenopus cells, it is enriched in the nucleus, perinuclear region and cell cortex. This is due to large amounts of yolk excluding GFP from other regions of the cell. The nuclear localisation explains what can appear as apparent heterogeneity in expression, some cells will have been sectioned through the nucleus (appearing to have strong staining) and some cells will not have their nucleus in the section and so appear to have weaker levels of staining. However, the levels across several sections were fairly even as expected for such injections. The perinuclear region does overlap with where the centrosomes sometimes localises, so GFP cells can have some signal in this area. For this reason, and to allow rigorous analysis of the mutations, very careful quantification was carried out. All cells with clear centrosomes (defined as clear spot of gamma-tubulin staining in close proximity to the nucleus) in the sections being analysed were quantified. For each mutant/control data from three independent experiments were analysed and a large number of individual cells were used (>100). Example of images used for this quantification are illustrated with four figures (Appendix 1-2) and in a table of quantification is included (Appendix-3).

The area and intensity of the centrosomal GFP was then measured by using the LSM510 Image Browser software (ZEISS) and the integrated density was calculated by multiplying the area by the average intensity across the region of interest. The area, intensity and integrated density of the γ-tubulin, DAPI and nuclear GFP staining was measured in the same way. The centrosome number in GFP positive cells was quantified based on the number of clear γ-tubulin spots, each cell was classified as containing 1, 2 or ≥3 centrosomes and each group was displayed as a percentage of the total GFP positive cells. Quantification of mitotic cells (Phospho-H3 positive) or apoptotic cells (active caspase-3) was carried out by calculating the % of GFP positive cells that were also positive for the marker of interest.

Means and standard deviations were calculated and plotted using GraphPad Prism 6 (San Diego, CA). Statistical analysis was carried out using One-way Anova tests with Bonferroni post-test corrections, $p < 0.05$ was considered significant. Statistical analysis was based on data from at least three independent experiments and with a minimum sample size as described in the figure legends.

2.2.2 Cell culture

HEK293 (human embryonic kidney 293) cells (kindly provided by Chris Bryant, University of Bath PhD student) were maintained between passages 30 and 40 at 37°C, 5% CO_2 in DMEM (Invitrogen) supplemented with 10% (v/v) FBS. Cells were passaged twice weekly by briefly washing in PBS and incubating with trypsin-EDTA for 5 minutes at 37°C, 5% CO_2. Cells were resuspended in 12ml of complete DMEM and passaged at a dilution of 1/12. HEK293 cells were frozen for storage and thawed as outlined above. All cell lines were routinely

tested for mycoplasma using the MycoAlert detection kit (Lonza), according to the manufacturer's instructions.

MDCKII cells (Madin-Darby canine kidney cells #00062107, European Collection of Cell Cultures, Salisbury, UK) were maintained at 37°C and 5% CO_2 in Dulbecco's modified Eagle's medium (DMEM) without phenol red (Lonza, Slough, UK) supplemented with 10% (v/v) fetal bovine serum (FBS) (Invitrogen) and 2mM L-glutamine (Invitrogen). Cells were passaged twice weekly at a dilution of 1/10 and maintained in culture for a maximum of 15 passages (approximately 2 months). Cells were washed once in PBS and once quickly with trypsin-EDTA (Invitrogen), prior to incubation in fresh trypsin-EDTA for 10 minutes at 37°C, 5% CO_2. Trypsin was neutralised by re-suspending cells in DMEM containing serum and pelleting at 200 x g for 2 minutes. The pellet was re-suspended in 10ml of complete DMEM and passaged at a 1/10 dilution. For freezing MDCKII cell stocks, one T75 tissue culture flask was trypsinised and pelleted as outlined above. The resulting pellet was re-suspended in 2ml of 10% (v/v) DMSO in FBS and split into four 0.5ml aliquots in sterile cryogenic storage vials (Invitrogen). Vials were frozen at a controlled rate by placing in an isopropanol chamber at -80°C overnight before transferring to liquid nitrogen. To thaw cells, a single vial was thawed at room temperature, re-suspended in 20ml of complete DMEM in a T75 tissue culture flask and incubated at 37°C overnight. Media was refreshed after 24 hours to remove excess cell debris and DMSO.

Prior to plating cells for experiments, a sample of re-suspended cells was counterstained with trypan blue to assess viability. Cells were counted using a haemocytometer and diluted to a plating concentration of $2x10^5$cells/ml. MDCKII

cells were grown until fully confluent, for a minimum of 8 days, with media changes every 2 days prior to experimental use.

2.2.3 IF Staining of MDCKII cells

MDCKII cells were plated at a density of $2x10^5$cells/ml on 8-well µ-slides (Ibidi, Glasgow, UK). Cells were fixed and permeabilised in ice-cold methanol at -20°C for 10 minutes and rinsed three times in PBS. Non-specific binding sites were blocked in 10% (v/v) normal goat serum (NGS) in PBS for 30 minutes. Primary antibodies were diluted in 2% (v/v) NGS/PBS. Appropriate species-specific secondary antibodies were also diluted in 2% (v/v) NGS/PBS. Primary antibody incubations were performed overnight at 4°C and secondary antibody incubations at room temperature for 2 hours. Cells were washed five times in PBS between antibody incubations. Nuclei were counterstained with 300nM DAPI in PBS and stored at 4°C until required. Slides were imaged using a Zeiss LSM510META laser-scanning confocal microscope (Plan-ApoChromat 63x/1.4 Oil Phase objective). Confocal images are presented as overhead composite projections of multiple 1µM Z-slices through the MDCKII monolayer. All images were processed using ImageJ software (National Institutes of Health). Images from different experimental conditions were processed in an identical fashion. Presented images are representative of three independent experiments.

2.2.4 Adenoviral production for Human RASSF7

2.2.4.1 Restriction digest and PCR

GFP-RASSF7 (internal plasmid no: 343) was generated previously by Asha Recino (PhD 2011, University of Bath). Restriction enzymes KpnI (Fisher ER0521) and EcoRI (Fisher ER0271) were used to digest GFP-RASSF7 for sub-cloning. Primers were designed with KpnI and EcoRI restriction sites (restriction sites are underlined): GFP-RASSF7 forward 5'-GAATTAGGTACCCACCATGGCCAGCAAAGGAGAAGAAC-3' and GFP-RASSF7 reverse 5'-GATTAAGAATTCACCACTTTGTACAAGAAAGCTGGGTC-3' and used in the polymerase chain reaction (PCR). PCR was carried out using Phusion® High-Fidelity DNA Polymerase (New England Biolabs) and Techne Genius PCR Thermal Cycler. PCR conditions are presented in Tables 2.7 and 2.8. Digests were performed according to the manufacturers' instructions; to achieve more complete digestion, they kept overnight at 37°C.

Table 2.7: PCR reaction setup**.** Reaction conditions are summarised in Table 2.8

Reagent	Stock Concentration	Final concentration	Volume (µl)
5x HiFi buffer	5X	1X	5
Forward primer	10µM	0.3µM	0.75
Reverse primer	10µM	0.3µM	0.75
dNTPs	10mM	0.3mM each	0.75
Template DNA (GFP-RASSF7)	10ng/µl	10 - 100ng	1 - 10
ddH_2O	N/A	N/A	16.25
HiFi DNA polymerase	1U/µl	1U	0.5
Total	N/A	N/A	25

Table 2.8: PCR conditions. An elongation time of 2 minutes was used for the predicted PCR product of ~2kb.

Cycles	Stages	Temperature (°C)	Time
1	Initial denaturation	95	3 minutes
30	Denaturation	98	20 seconds
	Annealing	67	15 seconds
	Extension	72	2 minutes (15 - 60seconds/kb)
1	Final extension	72	5 minutes
∞	Hold	10	Hold

2.2.4.2 DNA agarose gel electrophoresis

Digested DNA was combined with bromophenol blue loading buffer and loaded onto 0.6 – 1 % (w/v) agarose TBE gels containing SYBR® Safe DNA Gel Stain (Thermo Fisher) alongside 5µl of 1kB DNA Ladder (Promega, Southampton, UK). DNA gels were run at approximately 10V/cm of gel until the gel front approached the end of the gel. DNA was visualised using a non-UV Dark Reader Transilluminator (Clare Chemical Research, CO, US). Where necessary, gel extraction was performed using the Wizard SV Gel and PCR Clean-Up System (Promega) according to the manufacturer's instructions. Digested and purified GFP-RASSF7 was initially ligated into pJET1.2 intermediate vector (kindly provided by Chris Bryant, University of Bath, PhD student, Jim Caunt's lab).

2.2.4.3 Blunt ligation into the intermediate vector

Clonejet PCR cloning kit (Fermentas Life Sciences, K1232) was used for the ligation of GFP-RASSF7 into the intermediate vector. Ligation conditions are shown in Table 2.9. The ligation mixture was incubated at room temperature for 5 minutes and the intermediate vector and insert (GFP-RASSF7) were separated by DNA agarose gel electrophoresis. GFP-RASSF7 was then purified with Wizard SV Gel and PCR Clean-Up System (Promega) according to the manufacturer's instructions. GFP-RASSF7 plasmid was then used for transformation. The experimental steps are summarized in Figure 2.1.

Table 2.9 Blunt ligation reaction conditions

Reagent	Final concentration	Volume (µl)
2x Reaction buffer	1X	10
PCR product (GFP-RASSF7)	10 ng	1
pJET1.2 cloning vector	0.05pmol	1
ddH_2O	N/A	7
T4 DNA ligase	1U	1
Total	N/A	20

DH-5-alpha competent *E. coli* (High Efficiency) cells (New England Biolabs) were thawed on ice and dispensed into 25µl aliquots. 2.5µl of plasmid solution was added to each aliquot and incubated on ice for 30 minutes. Negative "no DNA" and positive pUC19 vector control transformations were included according to the manufacturer's instructions. Samples were heat-shocked at 42°C for 30s and placed on ice for 2 minutes. 250µl of prewarmed SOC

medium (New England Biolabs) was added and samples were incubated at 37°C for 1 hour with vigorous shaking. Bacteria were pelleted by brief centrifugation at 10,000 x g and resuspended in 100µl SOC medium. The bacterial solution was then spread onto LB agar plates containing 50µg/ml ampicillin. Spread plates were incubated at 37°C overnight to allow colony formation.

2.2.4.5 Bacterial culture

Successful transformation was indicated by successful colony formation of pUC19 positive control, vector-transformed samples. Colonies corresponding to the desired plasmid product were expanded by picking a single colony with a pipette tip and adding to prewarmed LB containing 50µg/ml ampicillin (5ml for miniprep, and 250ml for maxiprep cultures). Cultures were grown overnight at 37°C with vigorous shaking.

2.2.4.6 Plasmid purification

Plasmids were purified from overnight cultures using either the Wizard *Plus* SV Minipreps DNA Purification System (Promega) or the GenElute™ HP Maxiprep Kit (Sigma-Aldrich) according to the manufacturers' instructions.

2.2.4.7 Adenoviral shuttle vector production

In order to generate recombinant adenoviruses, desired transgenes were initially subcloned into the pAd5CMV K-NpA adenoviral shuttle vector (from the University of Iowa GTVC). Successful subcloning was confirmed by sequencing, provided by Source Biosciences (Nottingham, UK).

Previously generated GFP-RASSF7 was digested with KpnI and EcoRI and cloned into the multiple cloning site of pAd5CMV K-NpA. The KpnI/EcoRI-digested pAd5CMV K-NpA vector was treated with Antarctic Phosphatase (New England Biolabs) according to the manufacturer's instructions to remove 5' phosphates and minimise recircularisation by self-ligation. Antarctic Phosphatase was heat inactivated at 70°C for 5 minutes. Digested vector and insert was ligated using T4 DNA ligase (Promega) according to the manufacturer's instructions. A "no insert" reaction was included to control for the efficiency of target vector digestion and self-ligation. A vector:insert molar ratio of 1:3 was used to optimise ligation efficiency, and was calculated using the following equation:

$$\text{Insert mass (ng)} = 3 \times \left[\frac{\text{Insert length (bp)}}{\text{Vector length (bp)}}\right] \times \text{Vector mass (ng)}$$

Ligation reactions were used to transform competent *E. coli* and spread onto plates as previously described. Successful ligation was indicated by colony growth on the LB plates containing ampicillin.

2.2.4.8 Calcium phosphate transfection

HEK293 cells were transfected using a calcium phosphate based method for generating recombinant adenovirus. HEK293 cells were plated at a density of $2x10^5$ cells/ml in a T25 tissue culture flask and incubated at 37°C, 5% CO_2 for two days, until 50 – 80% confluent. A total of 6µg of plasmid DNA was diluted to a final volume of 140µl in DNase/RNase-free ddH_2O. 19.8µl of 2M $CaCl_2$ was added dropwise to the DNA solution. 159.8µl of 2x HBSS was added dropwise

to form a precipitate. The solution was incubated at room temperature for 20 minutes, mixed thoroughly by pipetting and added dropwise to the cell culture medium. Cells were incubated at 37°C, 5% CO_2 for 4 hours. The media was removed and cells were rinsed with PBS. Cells were then incubated in fresh culture medium at 37°C, 5% CO_2.

2.2.4.9 Generation of recombinant adenovirus

pAd5CMV+GFP-RASSF7 was cotransfected with the pacAd5 9.2 – 100 sub360 backbone vector into a HEK293 helper cell line (Anderson et al., 2000). Homologous recombination of PacI-digested vectors generates a continuous sequence for viral particle production. Individual shuttle vectors and the pacAd5 9.2 – 100 sub360 backbone vector were digested with PacI (New England Biolabs, Hitchin, UK), mixed and cotransfected into HEK293 cells by calcium phosphate transfection (4.5µg of pacAd5 9.2 – 100 sub360 backbone vector combined with 1.5µg of pAd5 shuttle vector). Transfected cells were incubated at 37°C to allow recombination and for a visible cytopathic effect to become evident. Cytopathic plaques were expected to localised areas of cell death with rounded cells at the periphery but the plaques were not evident.

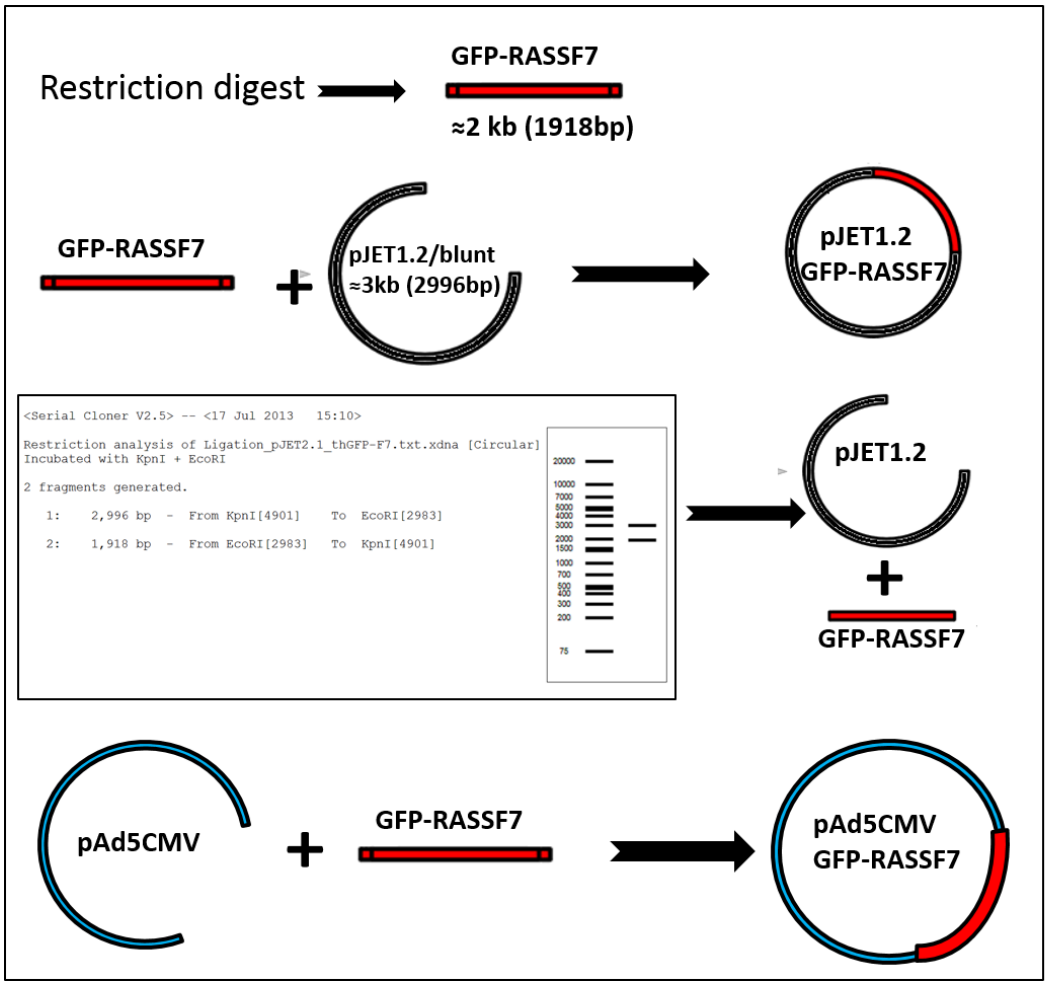

Figure 2.1: Sub-cloning prep diagram. GFP-RASSF7 first digested with restriction sites and then ligated into intermediate vector (pJET1.2) for better ligation with viral vector (pAd5cmv).

3 Analysis of the subcellular localisation of rassf7

3.1 Introduction

Many cell-cycle regulatory proteins or tumour suppressors are localized within specific cellular compartments and their subcellular localization may influence their functions. This introduction will focus on subcellular localisation of RASSF family proteins.

3.1.1 Subcellular localisation of classical RASSFs

RASSF1 is the best-studied RASSF protein among classical family members and its subcellular localisation is well documented. RASSF1 has eight isoforms (A-H) (Volodko et al., 2014); among these isoforms RASSF1A and RASSF1C are the most extensively studied members. RASSF1A is localised to the cytoplasm and cytoskeleton depending upon the cellular environment. It has been shown in different mammalian cell lines, including A549, LNCaP, HeLa and NIH-3T3, that both tagged or endogenous RASSF1A localises to cytoplasmic microtubules during interphase, to bipolar centrosomes associated with microtubules during prophase, and at metaphase and anaphase localise to spindle fibers and spindle poles (Liu et al., 2003; Song et al., 2004). During early telophase localisation is to the midzone and at late telophase and during cytokinesis to the midbody (Liu et al., 2003; Song and Lim, 2004; Song et al., 2004). Intriguingly, a later study in HeLa cells showed that endogenous RASSF1A localises to the centrosome throughout the cell cycle (Guo et al., 2007a) but the reason behind the difference in localisation is not very clear. It is also now established that RASSF1A is a microtubule-associated protein as assessed by both yeast-two-hybrid and immunoprecipitation experiments and it

co-localises to tubulin as shown with immunofluorescence staining in several cell lines (Dallol et al., 2004; Vos et al., 2004) and associates with microtubule binding proteins (Dallol et al., 2007; Liu et al., 2005). Over-expression of RASSF1A resulted in both re-arrangement (Dallol et al., 2004) and preventing microtubules from depolymerisation (Dallol et al., 2004; Liu et al., 2003; Vos et al., 2004). More recently El-Kalla et al (2010) studied the importance of RASSF1A microtubule association and showed that loss of RASSF1A microtubule association resulted in nuclear localisation of RASSF1A, loss of tubulin stability via the loss of tubulin acetylation and complete loss of tumour suppressor properties of RASSF1A. Furthermore, loss of RASSF1A microtubule localisation by a δMT mutant RASSF1A resulted in enhanced tumour promotion when expressed in mice (El-Kalla et al., 2010).

Endogenous studies indicate that RASSF1C primarily localises to the nucleus (Kitagawa et al., 2006; Song et al., 2004), binds to the apoptotic protein Daxx, before translocating to the cytoplasmic microtubules and regulating SAPK/JNK activation (Kitagawa et al., 2006). Overexpressed RASSF1C was localized primarily to the nucleus (Rong et al., 2004) and also associated with tubulin to provide a potential stabilization role for microtubules (Rong et al., 2004; Vos et al., 2004) similar to RASSF1A. Thus, subcellular localisation of RASSF1A and RASSF1C differ and their physiological functions seem to be antagonistic, at least in some contexts (see Introduction for a wider comparison of RASSF1A and RASSF1C).

Endogenous RASSF2 showed nuclear localisation within the both H417 and H720 lung cancer cell lines (Cooper et al., 2008). The same nuclear subcellular localisation for ectopic RASSF2 was observed in COS-7, HeLa, HEK293 and

the breast tumour cell lines MCF7 and HTB19 (Cooper et al., 2008). Nonetheless, RASSF2 was both cytoplasmic and nuclear in gastric cancer JRST cells when epitope tagged (Maruyama et al., 2008). RASSF2 regulates cell cycle and cell growth in a nuclear localisation dependent manner (Kumari and Mahalingam, 2009) and it has a nucleo-cytoplasmic shuttling property (Kumari and Mahalingam, 2009). It has been also reported that in intestinal metaplasia RASSF2 localizes both to the cytoplasm and nucleus (Luo et al., 2012). Finally in intraepithelial neoplasia, RASSF2 is diffuse in cytoplasm and relocates to the nucleus to perform its functions (Guerrero-Setas et al., 2013). Therefore it is possible to describe RASSF2 as a shuttling protein that localises to both cytoplasm and nucleus but it seems to mediate its functions in the nucleus.

RASSF3, the smallest member of RASSF family proteins, has not been extensively studied. There is one study showing that GFP tagged RASSF3 localizes to microtubules in vascular endothelial cells (Fujita et al., 2005). The subcellular localisation of RASSF4 has not been reported.

RASSF5 (also known as NORE1) has four isoforms (A-D). RASSF5A is reportedly centrosomally-localised when both endogenously expressed and GFP tagged in human lung epithelial cells (Moshnikova et al., 2006). In cancerous and normal A549 cell lines, overexpressed RASSF5A localises to the microtubules (Moshnikova et al., 2006). However, in Cos-7 cells, GFP-RASSF5A was present in both cytoplasm and nucleus whereas GFP-RASSF5B was localised only to the cytoplasm (Park et al., 2008). The same study also demonstrated that RASSF5A is a nucleo-cytoplasmic shuttling protein (Park et al., 2008). A further study indicated that RASSF5 is a nucleocytoplasmic

shuttling protein using a heterokaryon assay in HeLa cells (Kumari et al., 2010). Finally, there is evidence that RASSF5 and RASSF1A co-localise in the nucleus in Cos-7 cell lines (Donninger et al., 2014). There is no evidence for subcellular localisation of the shortest isoform, RASSF5C (also known as NORE1B or RAPL).

The literature describing the subcellular localisation of RASSF6 is limited. It has been shown in HeLa cells that FLAG-RASSF6 localises to both cytosol and the nucleus (Ikeda et al., 2007). In another report, GFP-RASSF6 localised to cytoplasm and to the basal portion of primary cilia in HK-2 cells (Withanage et al., 2012). More recently, RASSF6 was detected in both the cytoplasm and nucleus (Huang et al., 2014).

In summary, the subcellular localisation of classical RASSF family members is mainly observed in centrosomes, microtubules, cytoplasm and nucleus and in several cases with a nucleo-cytoplasmic shuttling property.

3.1.2 Subcellular localisation of N-terminal RASSFs

The literature concerning N-terminal RASSF members is much less extensive than for the classical family members and therefore these proteins warrant further investigation. Evidence for the subcellular localisation of RASSF8 first came from *Drosophila* studies: endogenous RASSF8 co-localised with adherens junctions, especially with E-cadherin in wing epithelial cells (Langton et al., 2009). Lock and colleagues continued localisation studies in human and showed that endogenous RASSF8 was present within the nucleus and at the cell membrane, especially at sites of cell-cell contact in both parental A549 and H1792 lung cancer cells (Lock et al., 2010). This report supported *Drosophila*

data of RASSF8 co-localisation with E-cadherin (Langton et al., 2009). RASSF8 immunostaining co-localised with the adherens junction components, β-catenin and E-cadherin, to regulate cell-cell adhesion (Lock et al., 2010).

The only report concerning the subcellular localisation of RASSF9 (also known as PCIP-1) showed that when CHO and AtT-20 cells (fibroblast and endocrine cell lines) were transfected with EGFP-RASSF9, RASSF9 associated with vesicles adjacent to the nucleus which appeared to be the recycling endosomes (Chen et al., 1998). These data have not been followed up and the subcellular localisation of endogenous RASSF9 remains to be elucidated.

The latest member of the RASSF family to be identified, RASSF10, is co-localised with tubulin at developing centrosomes during prophase and displays persistent localisation within centrosomally radiating microtubule bundles until late telophase (Hill et al., 2011). The study also revealed putative nuclear localisation and export sequences on RASSF10, making it a potential nucleo-cytoplasmic shuttling protein, similar to classical members, RASSF2 and RASSF5 (Hill et al., 2011; Richter et al., 2012). In KYSE150 cell lines, RASSF10 was localised to the nucleus (Lu et al., 2014). Finally in SPCA-1 cells, RASSF10 localised at the cell membrane (Wang et al., 2014).

In summary, there is less literature about the subcellular localisation of N-terminal RASSF members. RASSF8 localised to junctions, RASSF9 may be nuclear and RASSF10 seemed to have a nucleo-cytoplasmic shuttling property, similar to classical members.

3.1.3 Subcellular localisation of RASSF7

The first evidence showing RASSF7 localisation came from *Xenopus* studies. Embryos injected either with an N-terminal GFP tagged RASSF7 or a C-terminal HA tagged RASSF7 showed co-localisation with centrosomes (Sherwood et al., 2008). This was shown by co-immunolabelling with the centrosomal protein, γ-tubulin.

Subsequent work showed that the localisation of human RASSF7 protein was consistent with the *Xenopus* studies: RASSF7 co-localised with the centrosome (Recino et al., 2010). This was shown for both endogenous and tagged RASSF7 in HeLa cells (Recino et al., 2010).

3.1.4 Aims

Although it has been shown that RASSF7 localises to the centrosome both in human and *Xenopus*, the mechanism underlying the subcellular localisation of RASSF7 remains elusive. This chapter will focus on:

1. Investigating the domains responsible for centrosomal RASSF7 localisation by using an N-terminal GFP-tag.
2. Potential roles of phosphorylation sites within the RASSF7 for its subcellular localisation.

3.2 Results

3.2.1 Domain analysis of rassf7 and constructs

To begin to understand the functional domains within RASSF7, experiments focused on the domain that is responsible for centrosomal rassf7 localisation. Rassf7 is predicted to have an RA and a coiled-coil domain by the domain prediction programme, SMART (see Materials and Methods) (Figure 31A). In addition, there are two stretches of amino acids that are not predicted to form an identifiable domain by SMART, which have been called the A domain (region between the RA and the coiled-coil domains) and the B domain (C-terminal end of rassf7) (Figure 3.1A). Protein alignments were applied to reveal the similarity in domain architecture with human, mouse and *Xenopus* rassf7 proteins (Figure 3.1B). RASSF7 amino acid sequences were obtained for the following species; *Homo sapiens* (NP_003466, NP_001137465, NP_001137466; 3 splice variants), *Mus musculus* (NP_080162) and *Xenopus laevis* (NP_001086630, ABR21988). Amino acid sequences were obtained from the respective sources (See Materials and Methods), denoted here as NCBI accession numbers.

A series of constructs were generated with site-directed mutagenesis, which coded for truncated versions of rassf7 fused to GFP (Figure 3.2) to study the role of rassf7 domains in rassf7 centrosomal localisation and RNA synthesised from these plasmids was injected into two cell stage embryos. Successful injections were confirmed by examining GFP expression in whole amount stage 10 embryos (Figure 3.3). The amount of centrosomal localisation shown by each truncated protein was then analysed in cells from stage 10 embryos and is described in the following sections.

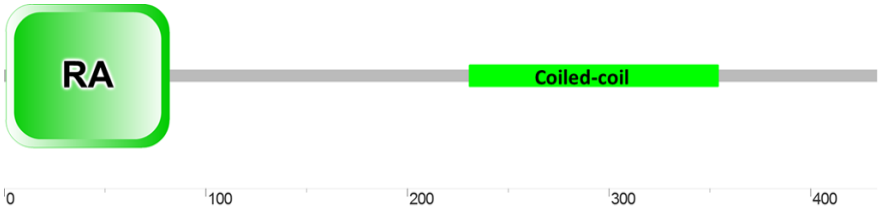

MELKVWVDGVQRVVCGVSEQTSCQDVVIALAQAIGQTGRYVLIQTLRDKERQLLPH
ERPLEFLSKSGQYANDVHFILRRTGPSLAERPSSDTGPVPPERTFVRSSLPLNTRT
AGTEVTKSKEPKKSLTFNLGPIGSTDILSKHRQKQVNGTPVKDGSSPRPPSKEEIFK
MVLRQQDQLKSLEMQNVSLGKDIQTWERGRAGRPMDQDEDEIAYLERLIQCNEAE
LGEEMFWEDELQRERAEEQGRQEKMRKLRATMEEYTVKIQELTERTEALELEIQKE
TSKRLASGPSLTDLEEMVIKMRKELETKIGQQGRQLESNLSNVERACEEARRNLQAR
NQELDEVNKDLRQCNLQQFILQTGSTVTSAQLRPDEDPSLAEPHDVQWQNQQRN
RGPMDSPPRPSSNHLMGHPRNLQNPMVSGLSPEVLSSREASWT

```
Human     1    MLLGLAAMELKVWVDGIQRVVCGVSEQTTCQEVVIALAQAIGQTGRFVLV  50
Mouse          MVLELVAMELKVWVDGIQRVVCGVSEQTTCQEVVIALAQAIGQTGRFVLV  50
Xenopus   1    -------MELKVWVDGVQRVVCGVSEQTSCQDVVIALAQAIGQTGRYVLI  43
                      *********:**********:**:**************:**:

Human     1    QRLREKERQLLPQECPVGAQATCGQFASDVQFVLRRTGPSLAGRPSSDSC 100
Mouse          QRLREKERQLLPQECPVGAQATCGQFANDVQFVLRRTGPSLSGRPSSDNC 100
Xenopus   1    QTLRDKERQLLPHERPLEFLSKSGQYANDVHFILRRTGPSLAERPSSDTG  93
               * **:*******:* *:   :..**:*.**:*:********: *****.

Human     1    P-PPERCLIRASLPVKPRAAL-----GCEPRKTLT--------------- 129
Mouse          P-PPERCPVRASLPPKPSAIP-----GREPRKALTFNL----------R 133
Xenopus   1    PVPPERTFVRSSLPLNTRTAGTEVTKSKEPKKSLTFNLGPIGSTDILSKH 143
               * ****  :*:*** :. :       . **:*:**

Human     1    -PEPAPSLSRPGPAAPVTPTPG--------CCTDLRGLELR--------- 161
Mouse          CPKLVPSPSIPEPAALVGPIPD--------GFADLQDLELR--------- 166
Xenopus   1    RQKQVNGTPVKDGSSPRPPSKEEIFKMVLRQQDQLKSLEMQNVSLGKDIQ 193
                 : . . .    ::   *             :*:.**::

Human     1    ------------------------VQRNAEELGHEAFWEQELRREQARER 187
Mouse          ------------------------IQRNTEELGHEAFWEQELQREQARER 192
Xenopus   1    TWERGRAGRPMDQDEDEIAYLERLIQCNEAELGEEMFWEDELQRERAEEQ 243
                                      :* *  ***.* ***:**:**:*.*:

Human     1    EGQARLQALSAATAEHAARLQALDAQARALEAELQLAA---EAPGP-PSP 233
Mouse          EGQARLQALSAATAEHAARLEALDAQACALEAELRLAA---EAPGP-PSA 238
Xenopus   1    GRQEKMRKLRATMEEYTVKIQELTERTEALELEIQKETSKRLASGPSLTD 293
                 * ::: * *:  *::.::: *  :: *** *::  :    *.**  :

Human     1     MASATERLHQDLAVQERQSAEVQGSLALVSRALEAAERALQAQAQELEEL 283
Mouse           TASAAERLRQDLATQERHSLEMQGTLALVSQALEAAEHALQAQAQELEEL 288
Xenopus   1     LEEMVIKMRKELETKIGQGRQLESNLSNVERACEEARRNLQARNQELDEV 343
                  . . :::::* .:  :. :::..*: *.:* * *.: ***: ***:*:

Human     1     NRELRQCNLQQFIQQTGAALPPPP-RPDRGP----PGTQGPLPPAREESL 328
Mouse           NRELRQCNLQQFIQQTGAALPPPPPQLDRTI----PSTQDLLSPNRGE-L 333
Xenopus   1     NKDLRQCNLQQFILQTGSTVTSAQLRPDEDPSLAEPHDVQWQNQQRNRGP 393
                *::********** ***:::...  : *.     *         * .

Human     1     LGAPS---ESHAGAQPRPRGGPHDAELL-EVAAAPAPEWCPLAAQPQAL 373
Mouse           QGVPQ---SHILVSSLSP----------EVPPMRQSSWR--------- 359
Xenopus   1     MDSPPRPSSNHLMGHPRNLQNPMVSGLSPEVLSSREASWT--------- 433
```

Figure 3.1: RASSF7 domain architecture and protein alignments (A) *Xenopus* rassf7 domains and sequences. The RA and the coiled-coil domain are highlighted in green. **(B)** Protein alignments for human, mouse and *Xenopus* RASSF7s. Underlined residues indicate the RA and the coiled coil domains. Human and mouse have two separate predicted regions of coiled-coil, where Xenopus has one big predicted coiled-coil region. * indicates positions which have a single, fully conserved residue, : indicates conservation between groups of strongly similar properties - scoring > 0.5 in the Gonnet PAM 250 matrix and . indicates conservation between groups of weakly similar properties - scoring =< 0.5 in the Gonnet PAM 250 matrix.

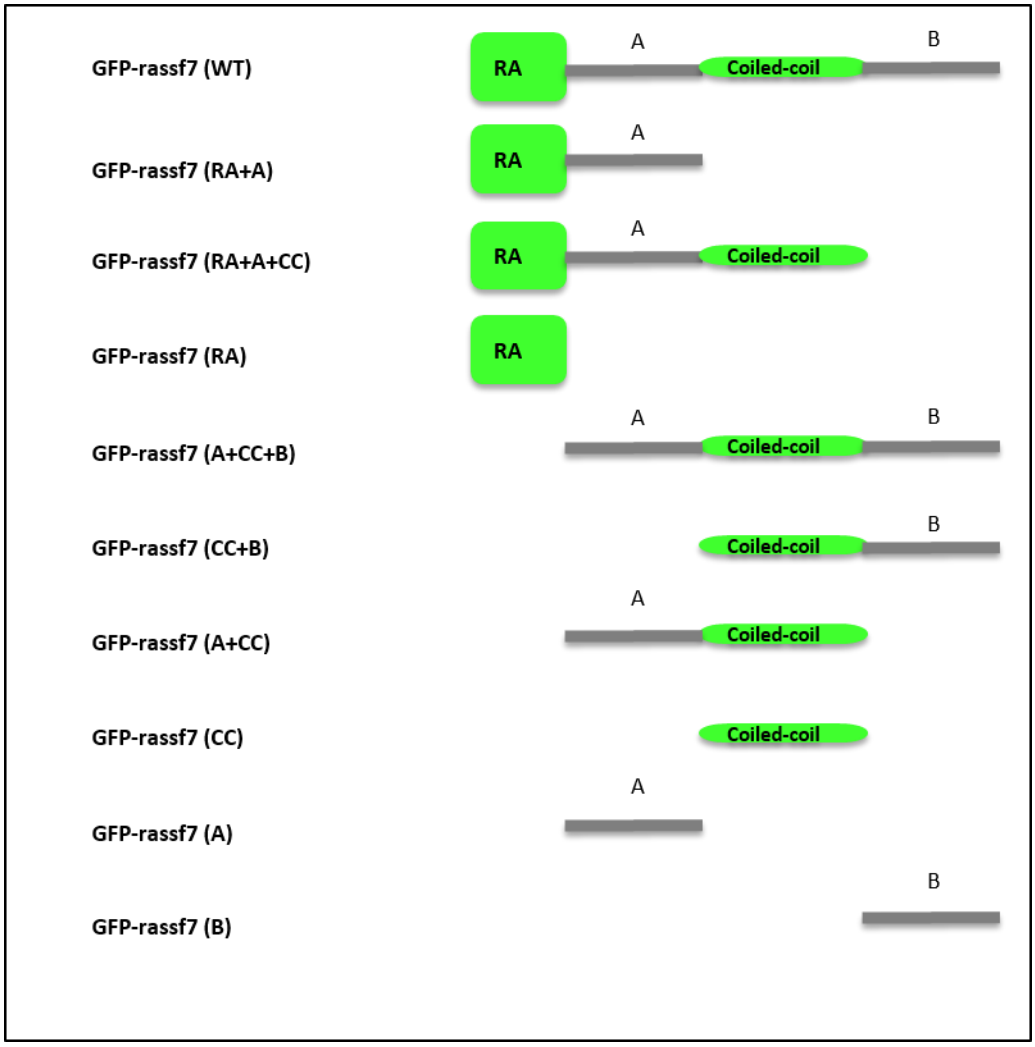

Figure 3.2: GFP-rassf7 constructs. The series of constructs produced by site directed mutagenesis to allow expression of truncated versions of rassf7 fused to GFP. The RA and the coiled-coil domains are shown in green. The A and the B domains are shown in grey. The domain architecture of the following constructs: GFP-rassf7 (WT), GFP-rassf7 (RA+A+), GFP-rassf7 (RA+A+CC), GFP-rassf7 (RA), GFP-rassf7 (A+CC+B), GFP-rassf7 (CC+B), GFP-rassf7 (A+CC), GFP-rassf7 (CC), GFP-rassf7 (A), GFP-rassf7 (B) are represented in the figure.

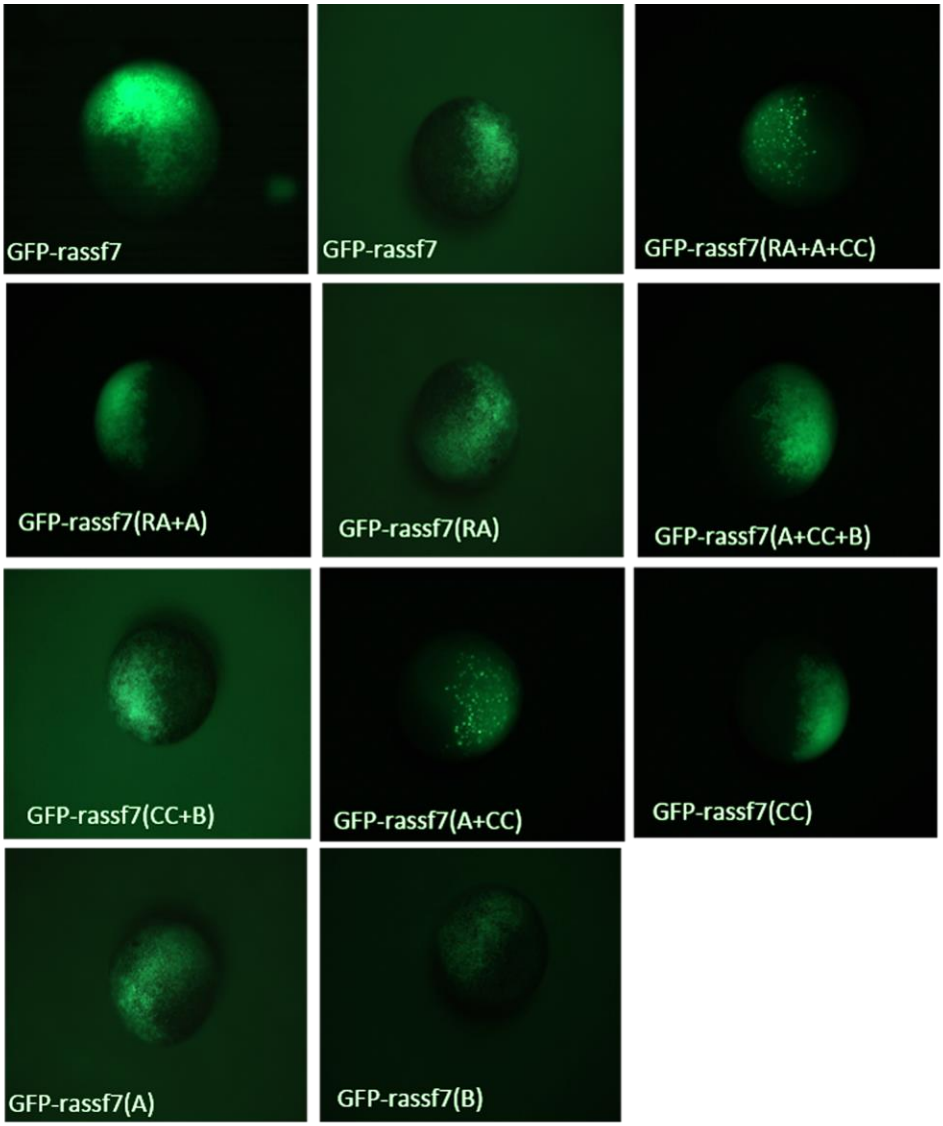

Figure 3.3: Whole-mount images of stage 10 embryos expressing GFP-rassf7, GFP and truncated GFP-rassf7 proteins. Embryos were microinjected with RNA into the one cell at the two-cell stage, cultured until stage 10 and imaged as whole-mounts. GFP fluorescence is shown in green.GFP-rassf7 (RA+A+CC) and GFP-rassf7 (A+CC) showed more punctate GFP fluorescence when compared to other constructs and positive (GFP-rassf7) and negative controls (GFP).

3.2.2 Analysis of the domains required for centrosomal localisation rassf7

3.2.2.1 The coiled coil domain, but not the RA domain, is required for centrosomal rassf7 localisation

The localisation of full-length rassf7 was shown with GFP-rassf7 expressing cells, GFP-rassf7 co-localized with the centrosomal protein γ-tubulin (Figure 3.4A) and was used as a positive control. A GFP control, which did not show enrichment at the γ-tubulin spot was used as a negative control. GFP-rassf7 also showed some nuclear localisation and sometimes some perinuclear or cortical enrichment. However, this staining is also seen in cells expressing the GFP control and so is not specific to the rassf7 protein. Data were quantified by intensity, size and integrated density (size x intensity) measurements (Figure 3.4B).

The domain analysis studies were initially performed with truncations at the N-terminal end of rassf7. The GFP fusion protein which lacked the RA domain, GFP-rassf7 (A+CC+B), showed a very similar pattern of localisation to full length GFP-rassf7, with clear localisation to γ-tubulin containing structures (Figure 3.4C). There was no significant difference between GFP-rassf7 and GFP-rassf7 (A+CC+B) localisation in terms of size, intensity and integrated density of the GFP-rassf7 at the γ-tubulin spot (Figure 3.5A, C and E).

When both the A and the RA domain were removed, GFP-rassf7 (CC+B), a similar distribution was observed. GFP-rassf7 (CC+B) was able to localise to the centrosome with no significant difference to wild type (Figure 3.4D). Quantification of size, intensity and integrated density of GFP-rassf7 at the γ-

tubulin spot showed that localisation did not change in GFP-rassf7 (CC+B) expressing cells.

Further truncation of rassf7 to remove the coiled-coil domain as well as the RA and the A domains, GFP-rassf7 (B), resulted in a loss of the centrosomal localisation of rassf7 (Figure 3.4E) and a distribution resembling that of the GFP control, data quantification was consistent with confocal images (Figure 3.5A-F). The nuclear localisation, seen with the GFP control and full length GFP-rassf7, was not lost and the ratio between centrosomal GFP and nuclear GFP was reduced (appendix 4). This shows that the reduction in centrosomal GFP, seen with GFP-rassf7 (B), cannot be explained by a reduction in RASSF7 levels. These results suggest that the coiled coil domain is required for centrosomal rassf7 localisation whereas the RA and the A domains are not required for centrosomal rassf7 localisation.

The amount of γ-tubulin staining was also measured following expression of the GFP, GFP-rassf7, GFP-rassf7 (A+CC+B), GFP-rassf7 (CC+B) and GFP-rassf7 (B) and there was no significant difference between cells expressing positive control, negative control and three GFP-rassf7 domain constructs. This shows that expression of these constructs did not lead to significant changes in γ-tubulin staining.

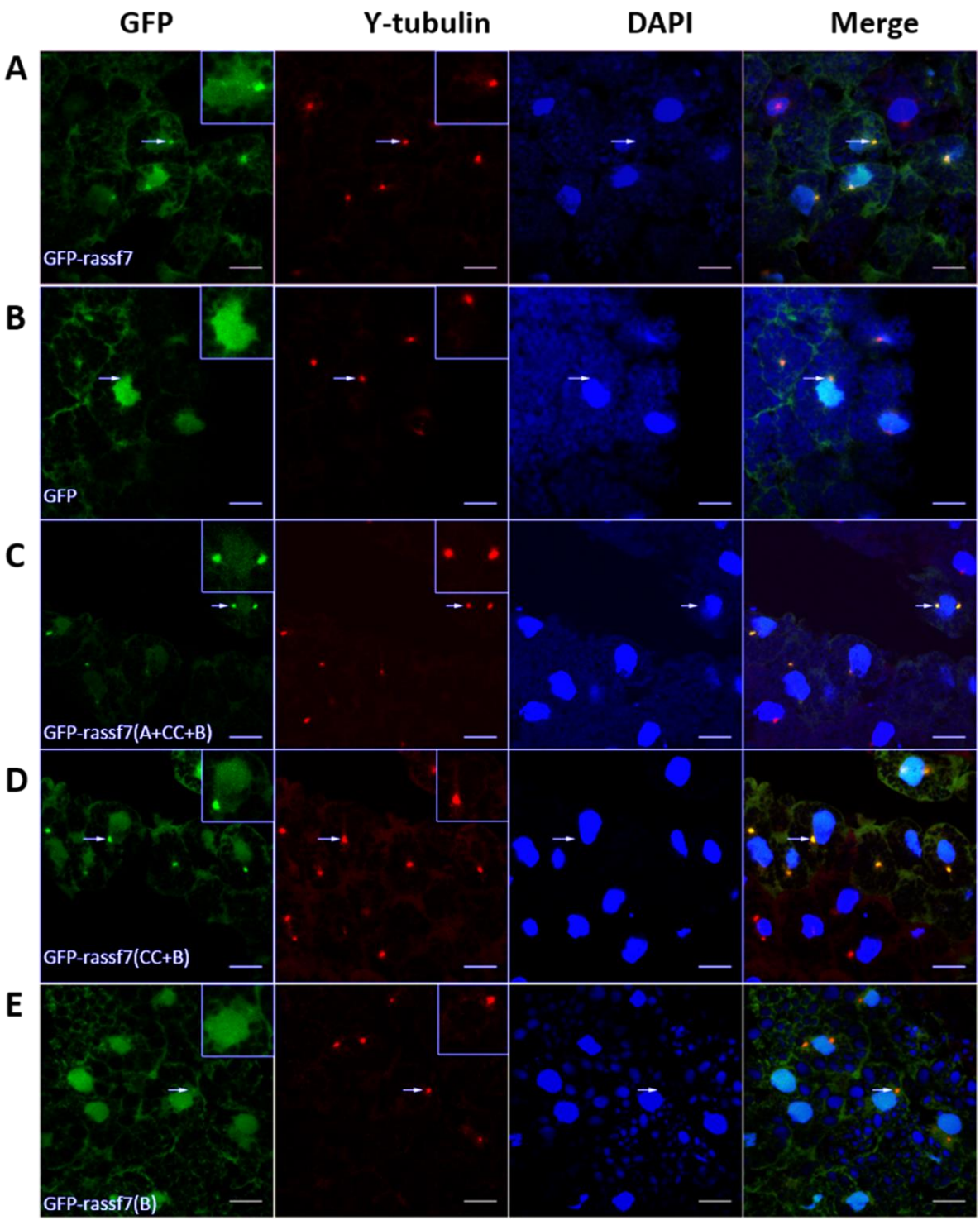
GFP
Y-tubulin
DAPI
Merge
A
GFP-rassf7
B
GFP
C
GFP-rassf7(A+CC+B)
D
GFP-rassf7(CC+B)
E
GFP-rassf7(B)

Figure 3.4: The coiled-coil, but not the RA domain, is required for centrosomal rassf7 localisation. Embryos were microinjected with RNA at the two-cell stage, cultured until stage 10, fixed, sectioned and stained with a centrosomal marker (γ-tubulin/red) and a nuclear marker (DAPI/blue). GFP fluorescence is shown in green. **(A)** GFP-rassf7 (green) co-localised with γ-tubulin (red) (arrows) as previously shown (Sherwood *et al.,* 2008). **(B)** GFP negative control, GFP (green) and γ-tubulin (red, arrows). **(C)** GFP-rassf7 (A+CC+B) (green) co-localised with γ-tubulin (red). **(D)** GFP-rassf7 (CC+B) (green) co-localised with γ-tubulin (red). **(E)** GFP-rassf7 (B) (green) did not show significant co-localisation with γ-tubulin (red). Arrows highlight potential area for co-localisation and scale bars=10μm.

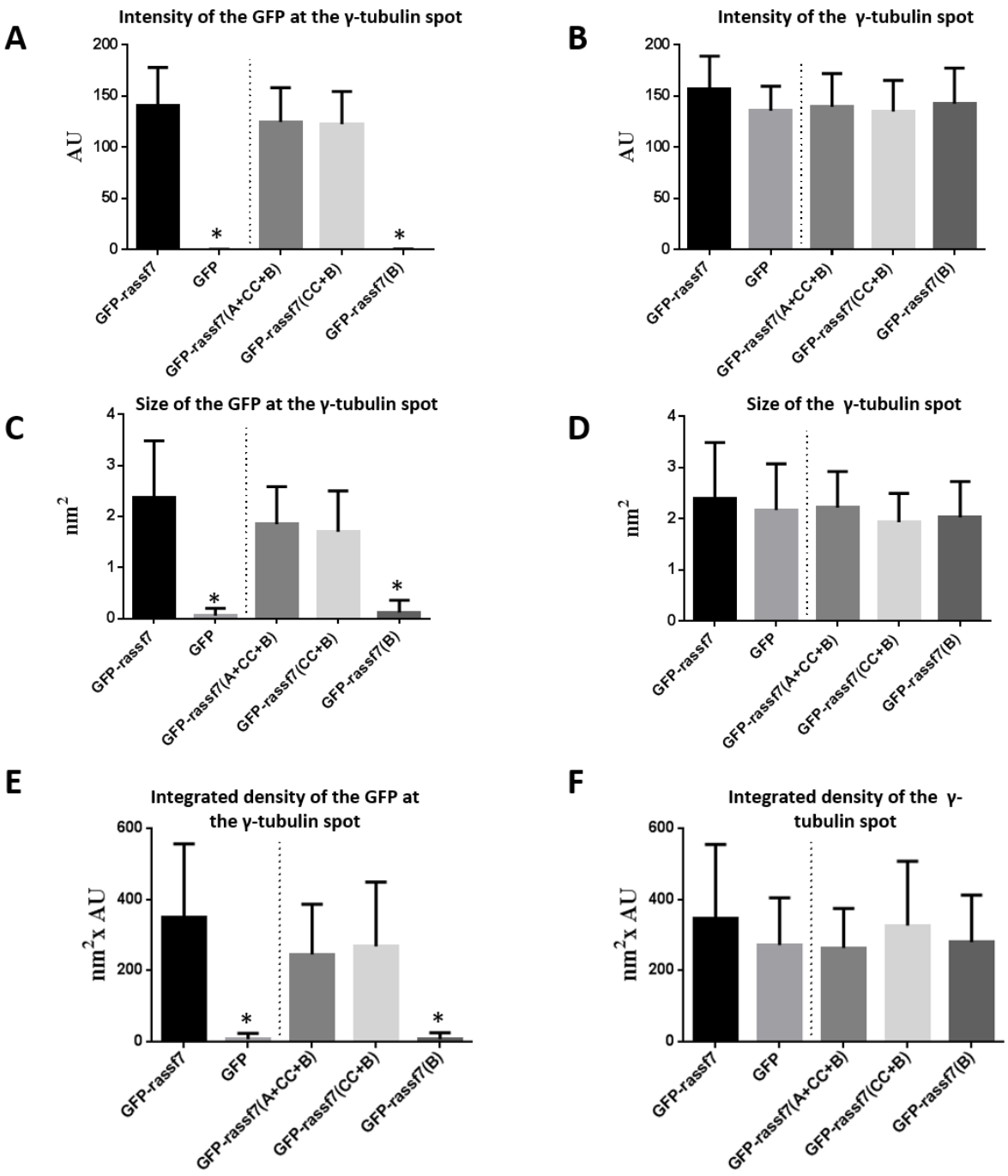
A
Intensity of the GFP at the γ-tubulin spot
AU
200
150
100
50
0
*
*
GFP-rassf7
GFP
GFP-rassf7(A+CC+B)
GFP-rassf7(CC+B)
GFP-rassf7(B)
B
Intensity of the γ-tubulin spot
AU
200
150
100
50
0
GFP-rassf7
GFP
GFP-rassf7(A+CC+B)
GFP-rassf7(CC+B)
GFP-rassf7(B)
C
Size of the GFP at the γ-tubulin spot
nm2
4
3
2
1
0
*
*
GFP-rassf7
GFP
GFP-rassf7(A+CC+B)
GFP-rassf7(CC+B)
GFP-rassf7(B)
D
Size of the γ-tubulin spot
nm2
4
3
2
1
0
GFP-rassf7
GFP
GFP-rassf7(A+CC+B)
GFP-rassf7(CC+B)
GFP-rassf7(B)
E
Integrated density of the GFP at the γ-tubulin spot
nm2x AU
600
400
200
0
*
*
GFP-rassf7
GFP
GFP-rassf7(A+CC+B)
GFP-rassf7(CC+B)
GFP-rassf7(B)
F
Integrated density of the γ-tubulin spot
nm2x AU
600
400
200
0
GFP-rassf7
GFP
GFP-rassf7(A+CC+B)
GFP-rassf7(CC+B)
GFP-rassf7(B)

Figure 3.5: Quantification of the localisation of GFP-rassf7 domain constructs. Embryos were microinjected with RNA at the two-cell stage, cultured until stage 10, fixed, sectioned and images of the GFP fluorescence and γ-tubulin staining were collected by confocal microscopy. Example images are shown in the previous figure**.** The fluorescent area and intensity of the γ-tubulin staining and GFP was measured by using the LSM510 Image Browser software (ZEISS) and the integrated density was calculated by multiplying the area by the average intensity across the region of interest. **(A)** Intensity of GFP fluorescence at the γ-tubulin spot for the GFP-rassf7 fusion proteins and the positive and negative controls (GFP-rassf7 and GFP). Intensity of GFP-rassf7 (B) was similar to the negative control. **(B)** Intensity of γ-tubulin staining. Expression of truncated GFP-rassf7 proteins did not affect the intensity of the γ-tubulin staining. **(C)** Size of the GFP at the γ-tubulin spot. Size of GFP-rassf7 (B) was similar to negative control. **(D)** Size of the γ-tubulin spot. Expression of truncated GFP-rassf7 proteins did not affect the size of the γ-tubulin spot. **(E)** Integrated density of GFP fluorescence at the γ-tubulin spot for the GFP-rassf7 fusion proteins and the positive and negative controls (GFP-rassf7 and GFP). Integrated density of GFP-rassf7 (B) was similar to negative control **(F)** Integrated density of γ-tubulin. Expression of truncated GFP-rassf7 proteins did not affect the integrated density of the γ-tubulin staining. Based on at least three independent experiments, bars represent standard error and were calculated and plotted using GraphPad Prism 6. Statistical analysis was carried out using One-way Anova tests with Bonferroni post-test corrections. >100 cells were measured in total, *$p<0.05$

3.2.2.2 Removal of the B domain caused accumulation of rassf7 at the centrosomes and increased levels of γ-tubulin staining

Having studied the N-terminal truncations, the next sets of truncations were performed from the C-terminal end of rassf7. Removal of the B domain, GFP-rassf7 (RA+A+CC), did not disrupt the ability of the protein to localise at the centrosome (Figure 3.6A). In fact, there was a striking increase in GFP signal that overlapped with the γ-tubulin spot (Figure 3.6A). Quantification revealed that there was a greater than fivefold increase in the amount of GFP (in size and integrated density but not in intensity) that overlapped with the γ-tubulin spot (Figure 3.7A, C and E). This effect was so dramatic that it was possible to observe GFP containing punctae in whole amount embryos (Figure 3.3).

In addition, cells expressing GFP-rassf7 (RA+A+CC) had a fourfold increase in the amount of γ-tubulin staining in comparison to controls (Figure 3.7B, D and F). This suggests that expression of this truncated version of rassf7 can affect centrosomal morphology.

Removal of the coiled-coil and the B domain, GFP-rassf7 (RA+A), caused a loss of co-localisation with γ-tubulin (Figure 3.6B), consistent with the coiled-coil domain being required for centrosomal rassf7 localisation. Quantification of the size, intensity and the integrated density of GFP-rassf7 at the γ-tubulin spot showed the significant decrease in three measurements for GFP-rassf7 (RA+A) expressing cells (Figure 3.7A, C and E) whereas there was no significant change in γ-tubulin staining (Figure 3.7B, D and F).

The RA domain on its own, GFP-rassf7 (RA), also failed to co-localise with γ-tubulin (Figure 3.6C) which suggests the RA domain is not sufficient for centrosomal rassf7 localisation. Following expression of GFP-rassf7 (RA), there was no effect on γ-tubulin staining levels (Figure 3.7B, D and F).

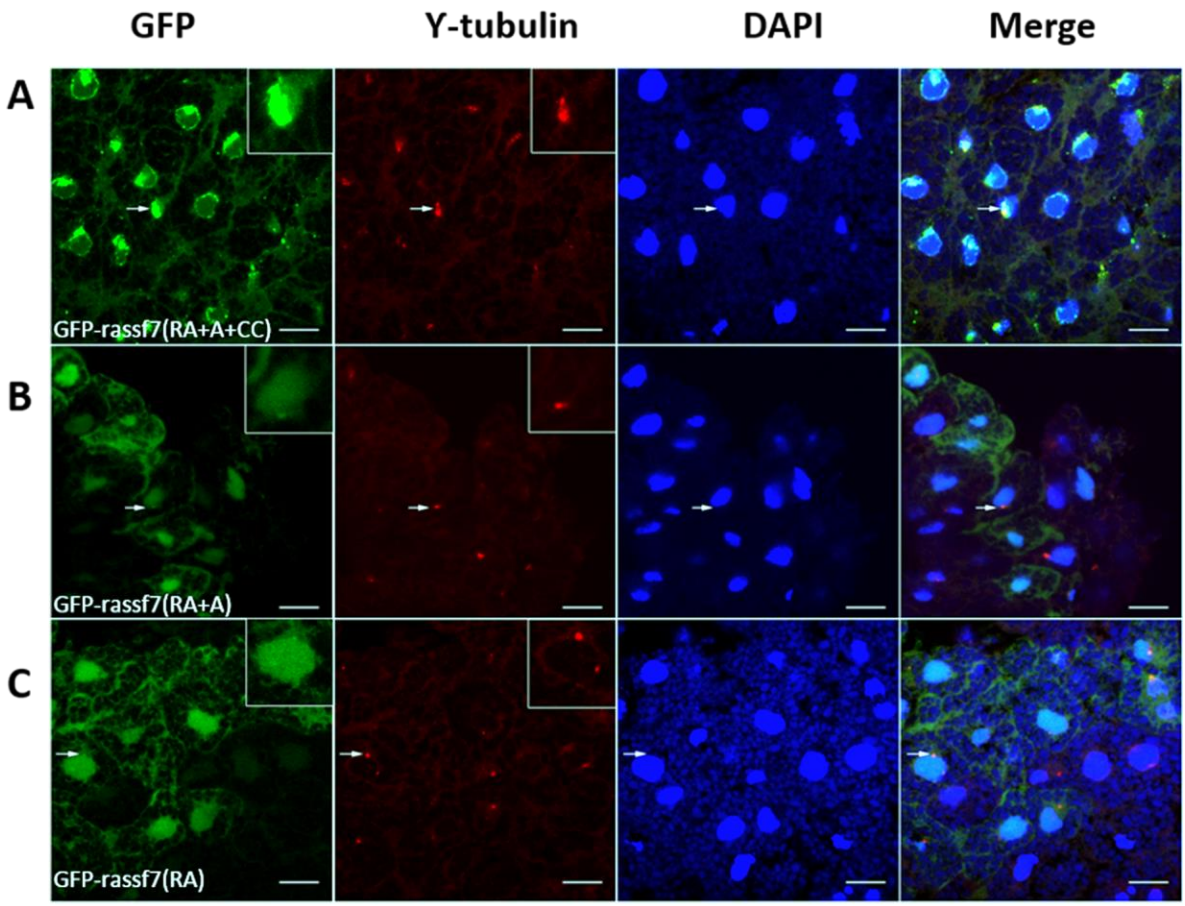

Figure 3.6: Removal of the B domain led to accumulation of truncated rassf7 at γ-tubulin spot and increased γ-tubulin staining. Embryos were microinjected with RNA at the two-cell stage, cultured until stage 10, fixed, sectioned and stained with a centrosomal marker (γ-tubulin/red) and a nuclear marker (DAPI/blue). GFP fluorescence is shown in green. **(A)** GFP-rassf7 (RA+A+CC) (green) co-localised with γ-tubulin (red). There appeared to be increased localisation and also enlargement of the γ-tubulin staining. **(B)** GFP-rassf7 (RA+A) did not show co-localisation with γ-tubulin (red) **(C)** GFP-rassf7 (RA) (green) did not show co-localisation with γ-tubulin (red). Arrows highlight potential area for co-localisation and scale bars=10μm.

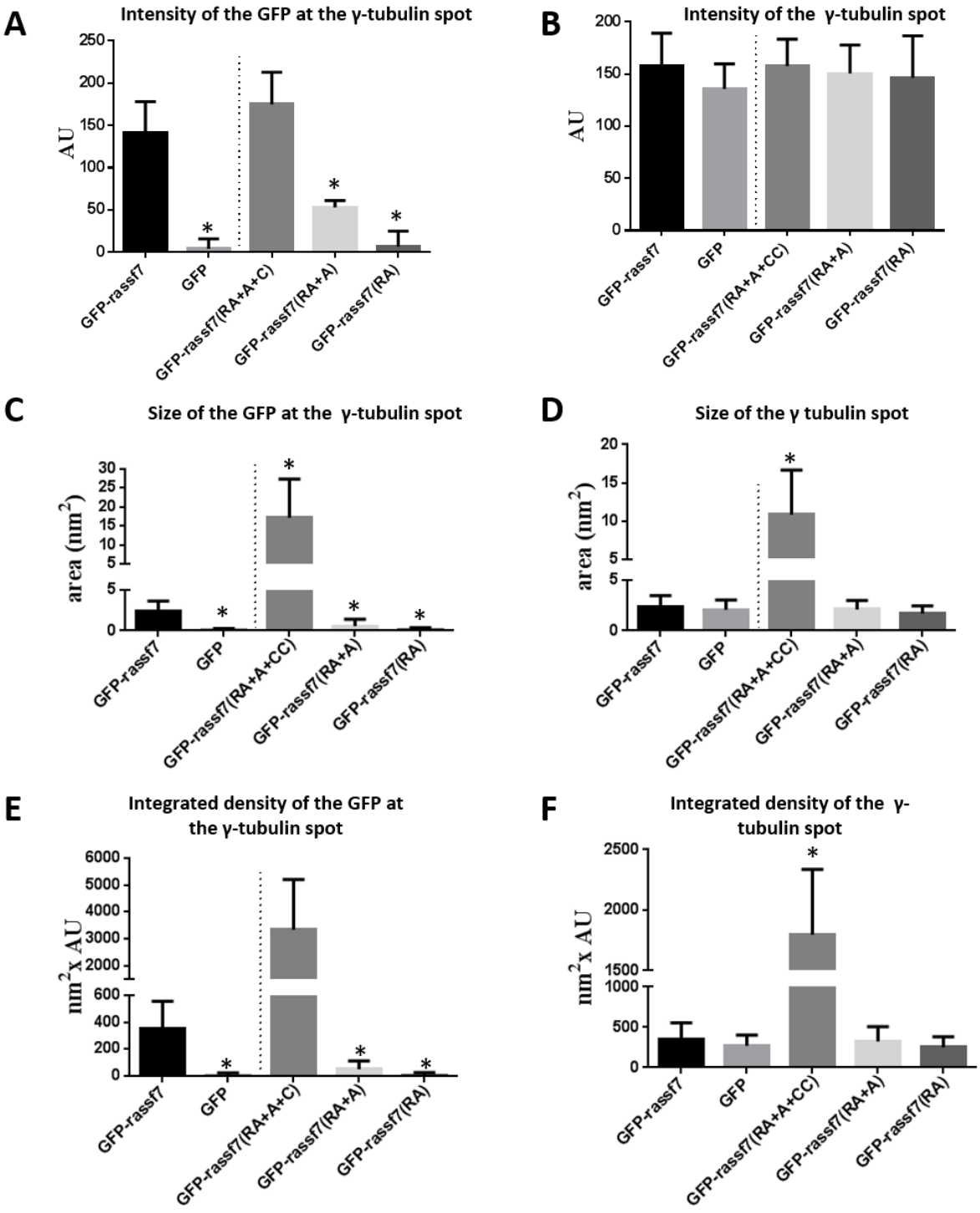
A
Intensity of the GFP at the γ-tubulin spot
AU
250
200
150
100
50
0
GFP-rassf7
GFP
GFP-rassf7(RA+A+C)
GFP-rassf7(RA+A)
GFP-rassf7(RA)
B
Intensity of the γ-tubulin spot
AU
200
150
100
50
0
GFP-rassf7
GFP
GFP-rassf7(RA+A+CC)
GFP-rassf7(RA+A)
GFP-rassf7(RA)
C
Size of the GFP at the γ-tubulin spot
area (nm2)
30
25
20
15
10
5
5
0
GFP-rassf7
GFP
GFP-rassf7(RA+A+CC)
GFP-rassf7(RA+A)
GFP-rassf7(RA)
D
Size of the γ tubulin spot
area (nm2)
20
15
10
5
5
0
GFP-rassf7
GFP
GFP-rassf7(RA+A+CC)
GFP-rassf7(RA+A)
GFP-rassf7(RA)
E
Integrated density of the GFP at the γ-tubulin spot
nm2x AU
6000
5000
4000
3000
2000
600
400
200
0
GFP-rassf7
GFP
GFP-rassf7(RA+A+C)
GFP-rassf7(RA+A)
GFP-rassf7(RA)
F
Integrated density of the γ-tubulin spot
nm2x AU
2500
2000
1500
1000
500
0
GFP-rassf7
GFP
GFP-rassf7(RA+A+CC)
GFP-rassf7(RA+A)
GFP-rassf7(RA)

Figure 3.7: Quantification of the localisation of GFP-rassf7 domain constructs. Embryos were microinjected with RNA at the two-cell stage, cultured until stage 10, fixed, sectioned and images of the GFP fluorescence and γ-tubulin staining were collected by confocal microscopy. Example images are shown in the previous figure**.** The fluorescent area and intensity of the γ-tubulin staining and GFP was measured by using the LSM510 Image Browser software (ZEISS) and the integrated density was calculated by multiplying the area by the average intensity across the region of interest. **(A)** Intensity of GFP fluorescence at the γ-tubulin spot. GFP-rassf7 (RA+A+CC) showed a similar intensity to wild type with a non-significant increase whereas GFP-rassf7 (RA+A) and GFP-rassf7 (RA) showed significant decrease **(B)** Intensity of the γ-tubulin spot did not change among the constructs or controls. **(C)** Size of the GFP at the γ-tubulin spot. GFP-rassf7 (RA+A+CC) size was increased at least four fold. **(D)** Size of the γ-tubulin spot. In GFP-rassf7 (RA+A+CC) injected cells size of the γ-tubulin spot was significantly increased (more than fourfold). **(E)** Integrated density of GFP fluorescence at the γ-tubulin spot. GFP-rassf7 (RA+A+CC) showed an increased integrated density when compared to wild type. **(F)** Integrated density of the γ-tubulin spot. GFP-rassf7 (RA+A+CC) showed an increased integrated density when compared to wild type. Based on at least three independent experiments, bars represent standard error and were calculated and plotted using GraphPad Prism 6. Statistical analysis was carried out using One-way Anova tests with Bonferroni post-test corrections. >100 cells were measured in total, *$p<0.05$.

3.2.2.3 The coiled-coil domain is sufficient for centrosomal rassf7 localisation

The final set of constructs investigated allowed expression of the internal domains of rassf7. GFP-rassf7 (A+CC) lacks the N-terminal RA domain and the C-terminal B domain, but was still able to co-localise with γ-tubulin (Figure 3.8A). Similar to rassf7 which lacked just the B domain, there was also greater than a five-fold increase in GFP that overlapped with the γ-tubulin and a four-fold increase in γ-tubulin staining (Figure 3.9).

The coiled-coil of rassf7 on its own, GFP-rassf7 (CC), was able to localise to centrosomes (Figure 3.8B) at a level comparable to full length GFP-rassf7 (Figure 3.9). This suggests that the coiled-coil domain is sufficient for centrosomal rassf7 localisation, building on observations described above showing the requirement of the coiled-coil domain for centrosomal rassf7 localisation. Expression of GFP-rassf7 (CC) did not result in increased γ-tubulin staining (Figure 3.9B, D and F). This suggests that the combination of the coiled-coil and the A domain are required for aberrant accumulation at centrosomes of both rassf7 and γ-tubulin. The final truncated protein expressed was GFP-rassf7 (A), which failed to co-localise with γ-tubulin (Figure 3.8C and Figure 3.9A, C and E) and did not have any effect on centrosomal morphology (Figure 3.9B, D and F). The results from all the constructs are summarised in Table 3.1.

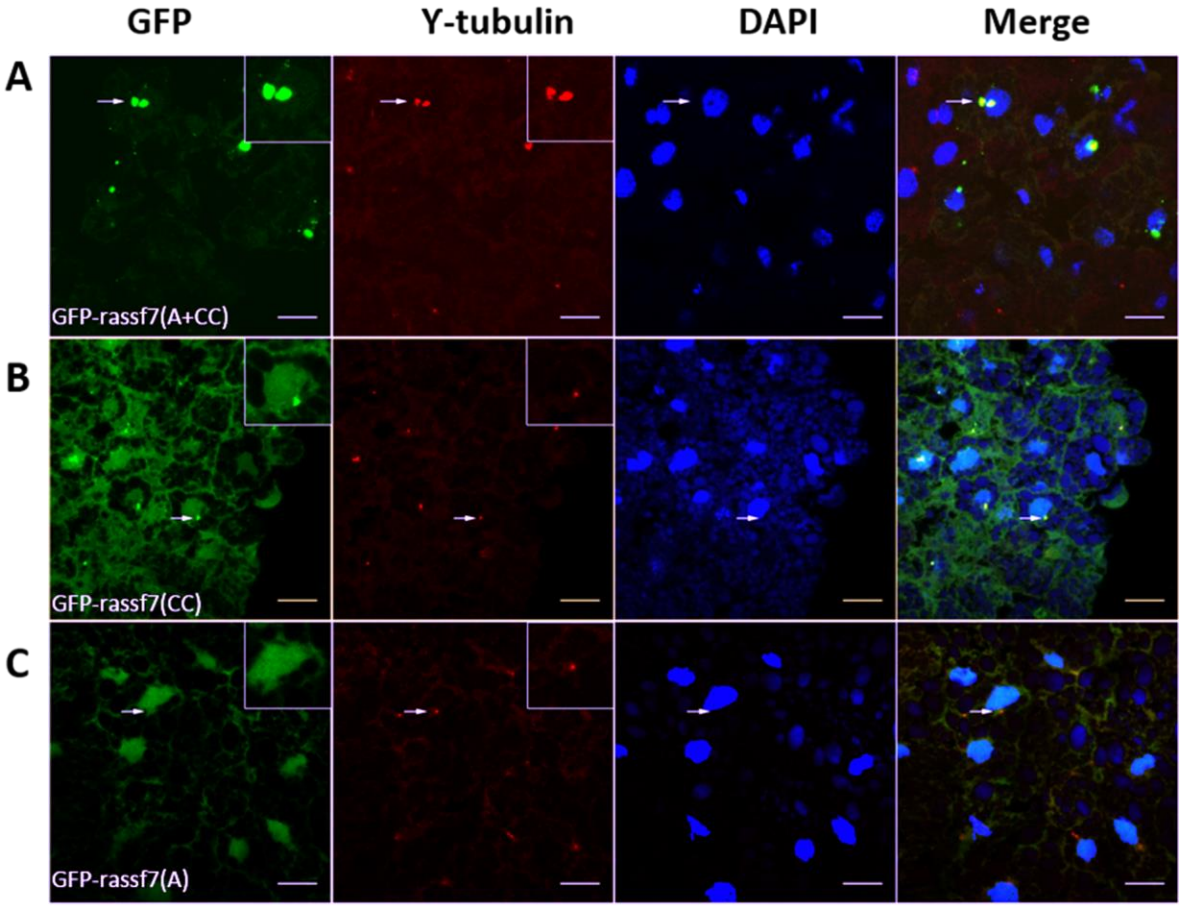

Figure 3.8: **The coiled-coil domain is sufficient for the centrosomal localisation of rassf7.** Embryos were microinjected with RNA at the two-cell stage, cultured until stage 10, fixed, sectioned and stained with a centrosomal marker (γ-tubulin/red) and a nuclear marker (DAPI/blue). GFP fluorescence is shown in green. **(A)** GFP-rassf7 (A+CC) (green) co-localised with γ-tubulin (red). Accumulation at the centrosome and enlargement of γ-tubulin staining was also seen. **(B)** GFP-rassf7 (CC) (green) co-localised with γ-tubulin (red). **(C)** GFP-rassf7 (A) (green) did not show co-localisation with γ-tubulin (red). Arrows highlight the potential area for co-localisation and scale bars=10μm.

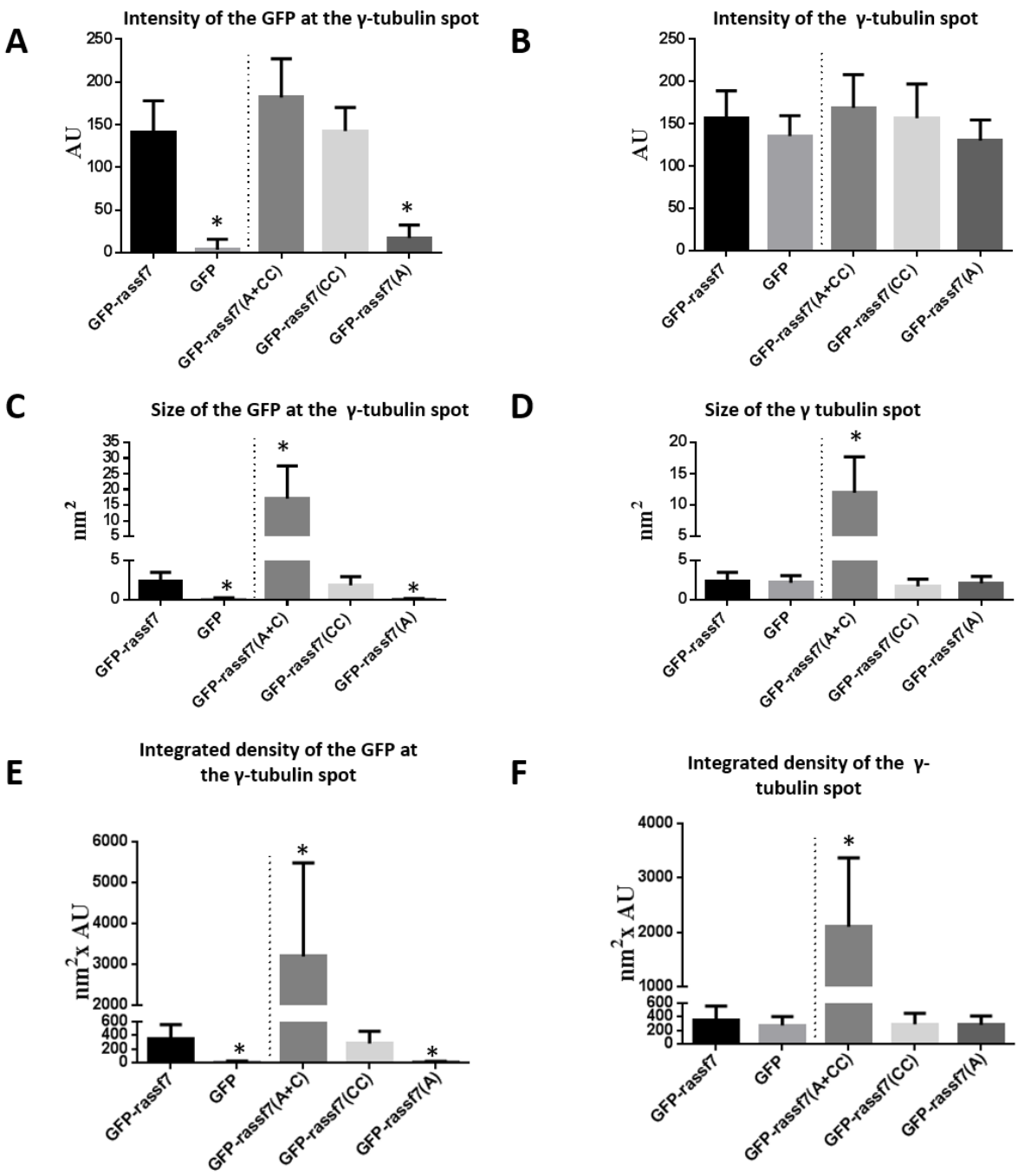
A
Intensity of the GFP at the γ-tubulin spot
AU
250
200
150
100
50
0
*
*
GFP-rassf7
GFP
GFP-rassf7(A+CC)
GFP-rassf7(CC)
GFP-rassf7(A)
B
Intensity of the γ-tubulin spot
AU
250
200
150
100
50
0
GFP-rassf7
GFP
GFP-rassf7(A+CC)
GFP-rassf7(CC)
GFP-rassf7(A)
C
Size of the GFP at the γ-tubulin spot
nm2
35
30
25
20
15
10
5
5
0
*
*
*
GFP-rassf7
GFP
GFP-rassf7(A+C)
GFP-rassf7(CC)
GFP-rassf7(A)
D
Size of the γ tubulin spot
nm2
20
15
10
5
5
0
*
GFP-rassf7
GFP
GFP-rassf7(A+C)
GFP-rassf7(CC)
GFP-rassf7(A)
E
Integrated density of the GFP at the γ-tubulin spot
nm2x AU
6000
5000
4000
3000
2000
600
400
200
0
*
*
*
GFP-rassf7
GFP
GFP-rassf7(A+C)
GFP-rassf7(CC)
GFP-rassf7(A)
F
Integrated density of the γ-tubulin spot
nm2x AU
4000
3000
2000
1000
600
400
200
0
*
GFP-rassf7
GFP
GFP-rassf7(A+CC)
GFP-rassf7(CC)
GFP-rassf7(A)

Figure 3.9: Quantification of the localisation of GFP-rassf7 domain constructs. Embryos were microinjected with RNA at the two-cell stage, cultured until stage 10, fixed, sectioned and images of the GFP fluorescence and γ-tubulin staining were collected by confocal microscopy. Example images are shown in the previous figure**.** The fluorescent area and intensity of the γ-tubulin staining and GFP was measured by using the LSM510 Image Browser software (ZEISS) and the integrated density was calculated by multiplying the area by the average intensity across the region of interest. **(A)** Intensity of the GFP at the γ-tubulin spot. GFP-rassf7 (A) showed a significantly decreased intensity compared to wild type rassf7, GFP-rassf7 (CC) was similar to wild type rassf7 and GFP-rassf7 (A) was similar to the GFP negative control. **(B)** Intensity of the γ-tubulin spot did not change among the constructs or controls. **(C)** Size of the GFP at the γ-tubulin spot. GFP-rassf7 (A+CC) size was significantly increased, GFP-rassf7 (CC) was similar to wild type rassf7 and GFP-rassf7 (A) was similar to the GFP negative control. **(D)** Size of the γ-tubulin spot. In GFP-rassf7 (A+CC) injected cells size of the γ-tubulin spot was significantly increased**. (E)** Integrated density of the GFP at the γ-tubulin spot. GFP-rassf7 (A+CC) showed a significantly increased integrated density compared to wild type rassf7, GFP-rassf7 (CC) was similar to wild type rassf7 and GFP-rassf7 (A) was similar to the GFP negative control. **(F)** Integrated density of the γ-tubulin spot. GFP-rassf7 (A+CC) showed an increase in the integrated density of γ-tubulin when compared to the wild type rassf7. GFP-rassf7 (CC) and GFP-rassf7 (A) did not affect the integrated density of γ-tubulin. Based on at least three independent experiments, bars represent standard error and were calculated and plotted using GraphPad Prism 6. Statistical analysis was carried out using One-way Anova tests with Bonferroni post-test corrections. >100 cells were measured in total, *$p<0.05$.

Table 3.1: The ability of truncated rassf7 proteins to localise at the centrosome and promote increased γ-tubulin staining.

GFP domain construct	Centrosomal localization	Increased γ-tubulin staining
GFP-rassf7 (WT)	✓	×
GFP-rassf7 (RA+A+CC)	✓	✓
GFP-rassf7 (RA+A)	×	×
GFP-rassf7 (RA)	×	×
GFP-rassf7 (A+CC+B)	✓	×
GFP-rassf7 (CC+B)	✓	×
GFP-rassf (A+CC)	✓	✓
GFP-rassf7 (CC)	✓	×
GFP-rassf7 (A)	×	×
GFP-rassf7 (B)	×	×

3.2.2.4 Identification of hydrophobic residues critical for coiled-coil structure

Having shown that the coiled-coil domain is necessary and sufficient for rassf7 to localise to centrosomes; further investigations were performed. To determine whether the coiled-coil structure of rassf7 is required for centrosomal localisation, mutations designed to disrupt the helical nature of the coiled coil sequence were introduced and localisation of the mutants analysed.

Coiled-coils are protein structural motifs that have been the subject of intense research due to their predicted prevalence in proteins and interesting potential applications (Grigoryan and Keating, 2008). The name and structure of the coiled-coil domain were suggested for the first time in 1953 by Crick, after studying the structure of α-keratin (Crick, 1953). In fact, more than 5% open reading frames in eukaryotes are predicted to encode coiled-coils (Schnell et al., 2005).

In a typical coiled-coil, bundles of α-helices are wrapped around each other to form a left-handed super helical structure to form bundles (Mason and Arndt, 2004). Coiled-coils made of two, three or four helices are most commonly observed (Figure 3.10); however, coiled-coils that consist of five or more helices also exist (Lupas and Gruber, 2005). Characteristically, the amino acid side chains are packed in a 'knobs-into-holes' manner, as the helices are wrapped around each other (Crick, 1953). This requires the characteristic feature of all coiled-coils: each helix is encoded by a seven-residue repeat, known as a heptad repeat (Grigoryan and Keating, 2008). The number of heptad repeats in each helix varies largely, from two to two hundred repeats. Each heptad repeat is denoted as **a-b-c-d-e-f-g** (Figure 3.10) (Mason and Arndt, 2004).

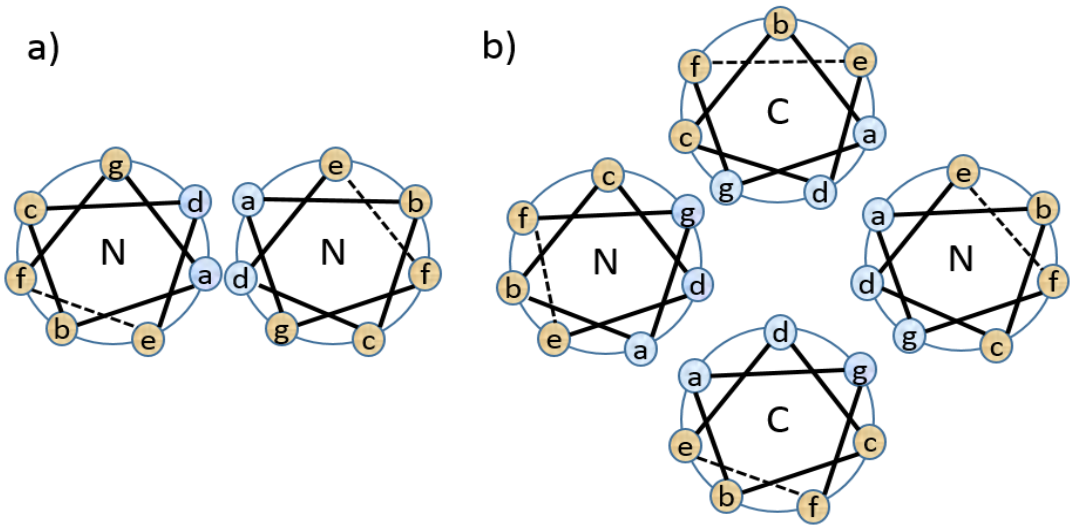

Figure 3.10: The heptad repeats of a coiled-coil. The coiled coils illustrated are a dimer, made up of two helices **(a)** and a tetramer, made up of four helices **(b)**. The heptad repeats are denoted by the letters **abcdefg,** shown with blue and yellow circles. Blue circles are indicating the hydrophobic residues and yellow circles are indicating polar/charged residies. Adapted from (Grigoryan and Keating, 2008).

Although the heptad repeats imply simplicity at the sequence level, coiled-coils have complex and diverse structures (Grigoryan and Keating, 2008).. Hydrophobic-polar patterning is what determines the orientation and specificity of each coiled-coil. Therefore, each individual amino acid plays an important role in maintaining the structure and interactions of a coiled-coil. In general hydrophobic residues (e.g. leucine or valine) are found in positions **a** and **d** on the same side of the helix, and form the interface between two helices with a polar/charged residues (e.g. lysine or glutamate) found in positions **e** and **g** (Mason and Arndt, 2004).

The dimerization of helices is largely facilitated by the non-polar nature of the **a** and **d** residues. This is evident by the fact that coiled-coils with a high

percentage of hydrophobic residues at positions **a** and **d** are more stable than coiled coils with a lower percentage (Mason and Arndt, 2004). Studies examining the important role of the **a** and **d** residues in the stability of coiled coils have provided a better understanding of coiled coil structure; mutating these residues changes the dimerization interface and may even disrupt the coiled-coil structure completely. Indeed, a number of studies have mutated hydrophobic residues to investigate the role of coiled coil domain in the function or localisation of a protein of interest. One example is a study by Cheng et al. (2001), who introduced leucine-to-proline substitutions into coiled coil homology domain of the protein kinase c-Fes (Cheng et al., 2001). Wild type, single and double point mutant *Fes* proteins, tagged with GFP, were expressed in Rat-2 fibroblasts. The results showed that one point mutation (L145P) caused a dramatic increase in the tyrosine kinase activity of *Fes*, while a different point mutation (L334P) had no effect. Of note, the combination of both mutations (L145P+L334P) caused a reduction in the kinase activity by almost 50%. This study emphasizes the importance of selecting appropriate mutations, since different point mutations have different effects on protein function and possibly localisation.

Importantly, it needs to be taken under consideration that sometimes polar residues can be found at positions a and d; these polar residues confer specificity, as hydrophobic interactions are often non-specific, although many times this compromises the stability of the coiled coil (Mason and Arndt, 2004). In a large study by Tripet and colleagues, 20 different amino acid residues were substituted at position d of a model coiled coil protein to examine their effects on stability (Tripet et al., 2000). As expected, the results revealed that the

stability of the coiled coil was correlated with the hydrophobicity of the side chain. Interestingly, the results showed that, when proline was incorporated at position **d**, the formation of coiled coil was prevented. The same result was also observed in a similar study, in which 20 different amino acid residues were substituted at position a of a model coiled coil protein (Wagschal et al., 1999). In conclusion, these results suggest that disruption of coiled coil conformation can be best achieved when hydrophobic residues at positions **a** and **d** are substituted with proline. Proline is a helix breaker because being an imino acid (not an amino acid) it disrupts the hydrogen bonding pattern in alpha helices.

In this study the RASSF protein alignments of human, mouse and *Xenopus* were compared for identification of conserved hydrophobic leucine, isoleucine and valine residues (Figure 3.11) as these hydrophobic residues were mutated in the previous studies. *Xenopus* rassf7 (isoform ABR21988.1) was marked with conserved hydrophobic residues within the coiled-coil domain and fourteen conserved residues were shown (Figure 3.12). The conserved residues, which would disturb the coiled coil conformation to the greatest extent, were assessed using the The simple Modular Architecture Research Tool (SMART) prediction program and these residues were substituted for proline. This approach allowed the identification of key residues and was an alternative to trying to identify and mutate all residues in A and D positions, which may have been difficult due to a lack of structural studies on RASSF7. The mutants would help to further assess the requirement of the coiled-coil domain for rassf7 localisation.

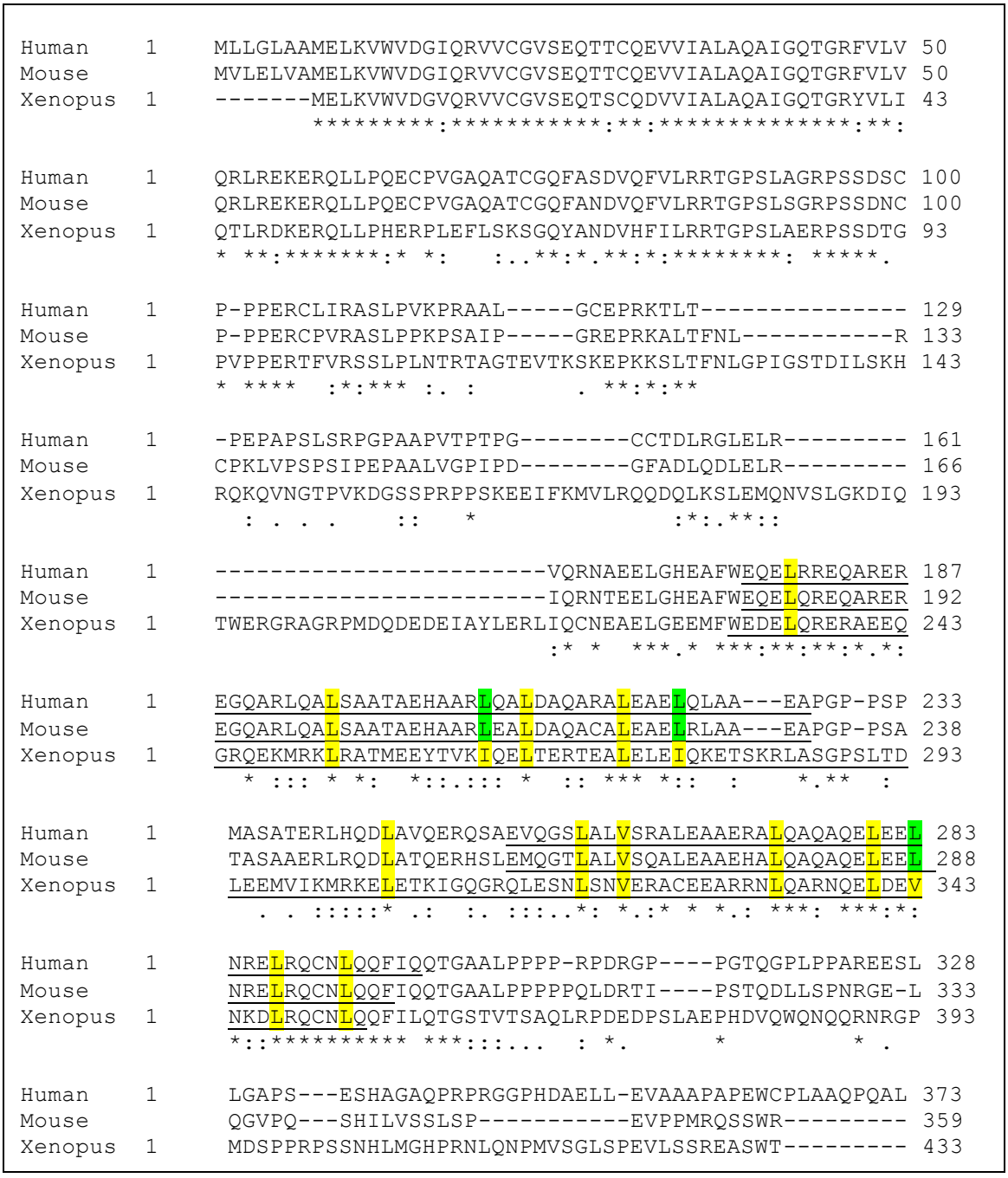

Figure 3.11: Conserved hydrophobic (leucine, isoleucine and valine) residues of RASSF7 coiled coil domain in human, mouse and Xenopus. The proposed coiled-coil domain of *Xenopus* rassf7 is underlined. Conserved residues are highlighted. Yellow highlighted residues indicate conservation in human, mouse and *Xenopus* and green highlighted residues are conserved in human and mouse but are different in *Xenopus.*

3.2.2.5 Point mutations in the coiled-coil domain reduced the centrosomal localisation of GFP-rassf7

Once identified, hydrophobic amino acids were substituted individually for the helix disrupting amino acid proline. As discussed previously, studies have shown that proline disrupts the coiled-coil conformation when introduced at a and d positions. The simple Modular Architecture Research Tool (SMART) was used to predict the effects of each mutation on the coiled-coil structure. Mutations predicted to disturb the coiled-coil structure to a significant extent, were selected to further assessment of the requirement of the coiled-coil domain for localisation. Three point mutations (leucine 235 to proline, leucine 235 and isoleucine 263 to proline, leucine 235, isoleucine 263 and leucine 350 to proline) (Figure 3.13A) were made which replace hydrophobic amino acids (leucine or isoleucine) with prolines according to their predicted effect on coiled-coil structure. These are predicted to disrupt the three dimensional structure of the coiled-coil according to SMART prediction_(Figure 3.13). The single point mutation predicted not to affect significantly the structure of the coiled-coil (Figure 3.11 GFP-rassf7 (RA+A+CC'+B)), also did not affect the centrosomal localisation of GFP-rassf7 (Figure 3.14A + Figure 3.15). The double point mutation predicted to disrupt the structure of the coiled-coil (Figure 3.13 GFP-rassf7 (RA+A+CC"+B)), had only a small measurable effect on the centrosomal localisation of GFP-rassf7 (Figure 3.14B + Figure 3.15). The triple mutation, which was predicted to cause almost complete loss of the coiled-coil structure (Figure 3.13 GFP-rassf7 (RA+A+CC"'+B)), showed significantly less centrosomal localisation than wild type rassf7 (Figure 3.14C + Figure 3.15), consistent with the coiled-coil domain being required for the localisation of

rassf7. Statistical analysis showed that the effect of triple mutation was significant (Figure 3.13). In conclusion, point mutations in the coiled-coil, GFP-rassf7 (RA+A+CC"+B), predicted to disrupt the coiled-coil conformation significantly, reduced the centrosomal rassf7 localisation, which supports the previous finding that the coiled-coil domain is responsible for centrosomal rassf7 localisation.

MELKVWVDGVQRVVCGVSEQTSCQDVVIALAQAIGQTGRYVLIQTLRDKERQLLPHERPL
EFLSKSGQYANDVHFILRRTGPSLAERPSSDTGPVPPERTFVRSSLPLNTRTAGTEVTKSK
EPKKSLTFNLGPIGSTDILSKHRQKQVNGTPVKDGSSPRPPSKEEIFKMVLRQQDQLKSLE
MQNVSLGKDIQTWERGRAGRPMDQDEDEIAYLERLIQCNEAELGEEMFWEDLQRERAE
EQGRQEKMRKLRATMEEYTVKIQELTERTEALELEIQKETSKRLASGPSLTDLEEMVIKM
RKELETKIGQGRQLESNLSNVERACEEARRNLQARNQELDEVNKDLRQCNLQQFILQTG
STVTSAQLRPDEDPSLAEPHDVQWQNQQRNRGPMDSPPRPSSNHLMGHPRNLQNPMV
SGLSPEVLSSREASWT

Figure 3.12: Identification of conserved hydrophobic residues in rassf7 coiled-coil domain in Xenopus. Conserved hydrophobic residues in the coiled-coil domain of rassf7 (*Xenopus* isoform ABR21988.1) are highlighted in yellow. The underlined residues indicate the coiled-coil domain. Due to lack of structural studies on rassf7 coiled-coil, exact positions of the a and d residues were not clear. Therefore mutations were based on SMART predictions of the most important conserved hydrophobic residues, the ones that caused the biggest disruption when mutated (see figure 3.13).

MELKVWVDGVQRVVCGVSEQTSCQDVVIALAQAIGQTGRYVLIQTLRDKERQLLPHERPL
EFLSKSGQYANDVHFILRRTGPSLAERPSSDTGPVPPERTFVRSSLPLNTRTAGTEVTKSK
EPKKSLTFNLGPIGSTDILSKHRQKQVNGTPVKDGSSPRPPSKEEIFKMVLRQQDQLKSLE
MQNVSLGKDIQTWERGRAGRPMDQDEDEIAYLERLIQCNEAELGEEMFWEDLQRERAE
EQGRQEKMRKLRATMEEYTVKIQELTERTEALELEIQKETSKRLASGPSLTDLEEMVIKM
RKELETKIGQGRQLESNLSNVERACEEARRNLQARNQELDEVNKDLRQCNLQQFILQTG
STVTSAQLRPDEDPSLAEPHDVQWQNQQRNRGPMDSPPRPSSNHLMGHPRNLQNPMV
SGLSPEVLSSREASWT

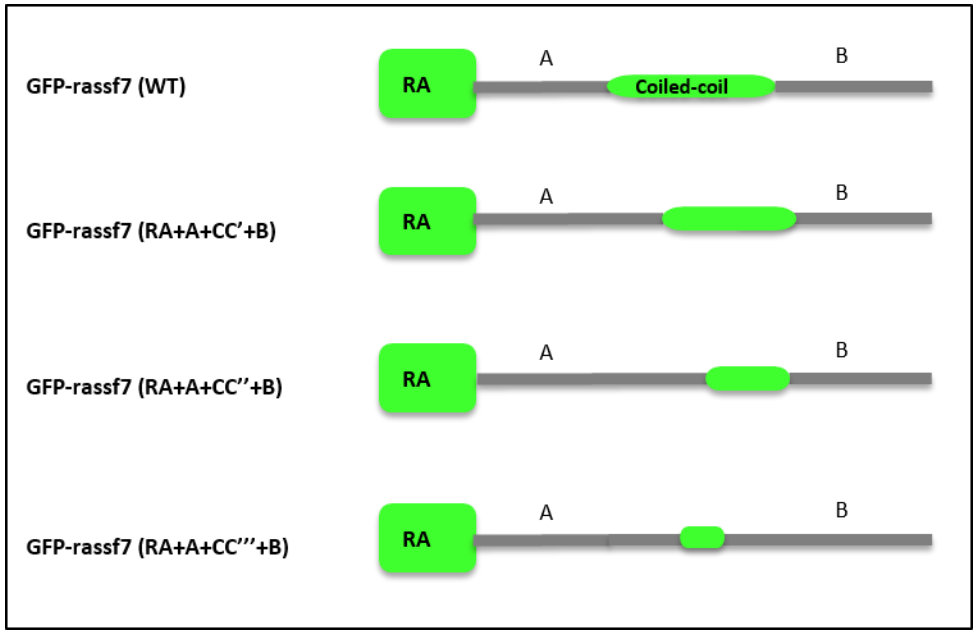

Figure 3.13: The predicted domain architecture of the coiled-coil domain point mutations. Constructs were made that contained mutations in the coiled coil region. Three mutations were made using site directed mutagenesis; GFP-rassf7 (RA+A+CC'+B) with one point mutation (leucine 235 to proline), GFP-rassf7 (RA+A+CC''+B) with two point mutations (leucine 235 and isoleucine 263 to proline) and GFP-rassf7 (RA+A+CC'''+B) with three point mutations (leucine 235, isoleucine 263 and leucine 350 to proline).

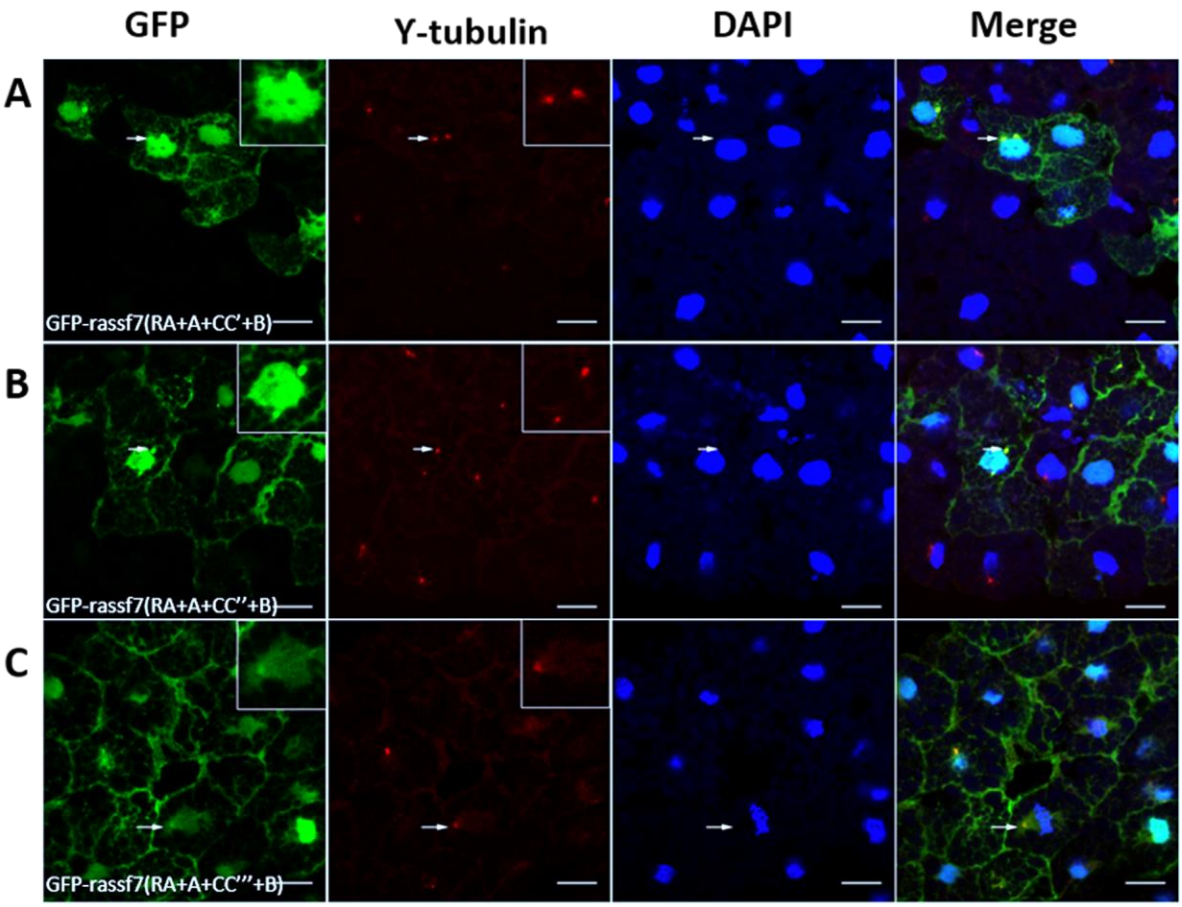

Figure 3.14: Mutations in the coiled coil domain reduced the centrosomal localisation of GFP-rassf7. Embryos were microinjected with RNA at the two-cell stage, cultured until (stage 10), fixed, sectioned and stained with a centrosome marker (γ-tubulin /red) and a nuclear marker (DAPI/blue). GFP fluorescence is shown in green. **(A)** GFP-rassf7 (RA+A+CC'+B) (green) co-localised with γ-tubulin (red). **(B)** GFP-rassf7 (RA+A+CC''+B) (green) co-localised with γ-tubulin (red). **(C)** GFP-rassf7 (RA+A+CC'''+B) (green) showed decreased co-localisation with γ-tubulin (red). In panels A-C arrows highlight the potential area for co-localisation. Scale bars=10μm.

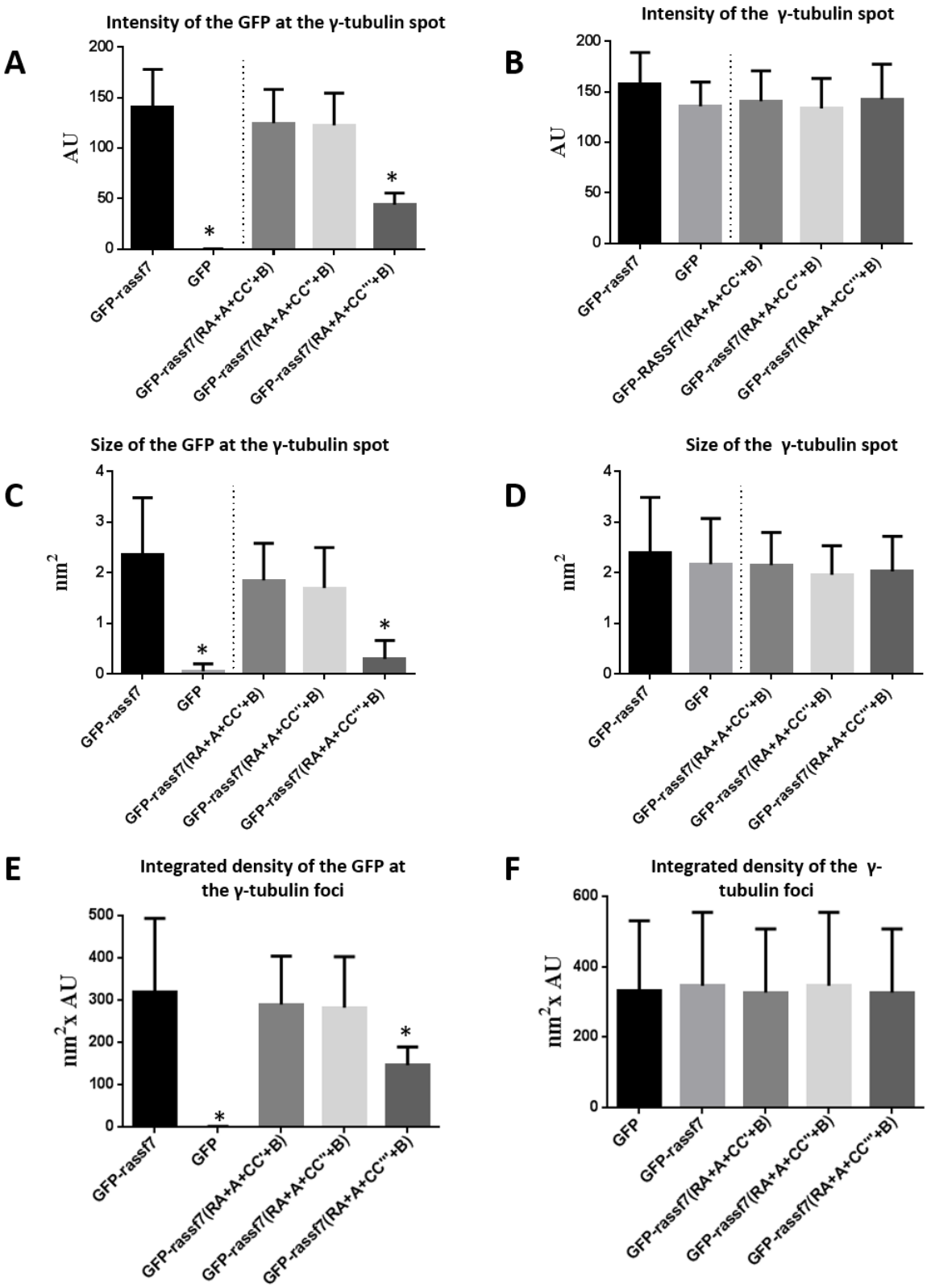
A
Intensity of the GFP at the γ-tubulin spot
AU
200
150
100
50
0
*
*
GFP-rassf7
GFP
GFP-rassf7(RA+A+CC'+B)
GFP-rassf7(RA+A+CC"+B)
GFP-rassf7(RA+A+CC"'+B)
B
Intensity of the γ-tubulin spot
AU
200
150
100
50
0
GFP-rassf7
GFP
GFP-RASSF7(RA+A+CC'+B)
GFP-rassf7(RA+A+CC"+B)
GFP-rassf7(RA+A+CC"'+B)
C
Size of the GFP at the γ-tubulin spot
nm2
4
3
2
1
0
*
*
GFP-rassf7
GFP
GFP-rassf7(RA+A+CC'+B)
GFP-rassf7(RA+A+CC"+B)
GFP-rassf7(RA+A+CC"'+B)
D
Size of the γ-tubulin spot
nm2
4
3
2
1
0
GFP-rassf7
GFP
GFP-rassf7(RA+A+CC'+B)
GFP-rassf7(RA+A+CC"+B)
GFP-rassf7(RA+A+CC"'+B)
E
Integrated density of the GFP at the γ-tubulin foci
nm2x AU
500
400
300
200
100
0
*
*
GFP-rassf7
GFP
GFP-rassf7(RA+A+CC'+B)
GFP-rassf7(RA+A+CC"+B)
GFP-rassf7(RA+A+CC"'+B)
F
Integrated density of the γ-tubulin foci
nm2x AU
600
400
200
0
GFP
GFP-rassf7
GFP-rassf7(RA+A+CC'+B)
GFP-rassf7(RA+A+CC"+B)
GFP-rassf7(RA+A+CC"'+B)

Figure 3.15: Quantification of the localisation of point mutations on the coiled-coil domain. Embryos were microinjected with RNA at the two-cell stage, cultured until stage 10, fixed, sectioned and images of the GFP fluorescence and γ-tubulin staining were collected by confocal microscopy. Example images are shown in the previous figure. The fluorescent area and intensity of the γ-tubulin staining and GFP was measured by using the LSM510 Image Browser software (ZEISS) and the integrated density was calculated by multiplying the area by the average intensity across the region of interest. **A)** Intensity of the GFP fluorescence at the γ-tubulin spot was significantly decreased but not lost in GFP-rassf7 (RA+A+CC'''+B) injected cells. **(B)**Intensity of γ-tubulin. Expression of truncated GFP-rassf7 proteins did not affect the intensity of the γ-tubulin staining. **(C)** Size of the GFP fluorescence at the γ-tubulin spot**. (D)** Size of the γ-tubulin spot was not affected from the injections. **E)** Integrated density of the GFP fluorescence at the γ-tubulin spot. GFP-rassf7 (RA+A+CC'''+B) showed reduced centrosomal localisation when compared to the wild type protein. **(F)** Integrated density of the γ-tubulin spot. Mutations did not affect the integrated density of the γ-tubulin staining. Based on at least three independent experiments, bars represent standard error and were calculated and plotted using GraphPad Prism 6. Statistical analysis was carried out using One-way Anova tests with Bonferroni post-test corrections. >100 cells were measured in total, *$p<0.05$.

.

3.2.3 Identification of Potential Phosphorylation sites on rassf7

Further investigations focused on identification of potential phosphorylation sites within RASSF7 in order to understand the effects of potential phosphorylation sites on centrosomal rassf7 localisation. As discussed in Chapter 1, most centrosomal proteins have their localisation and/ function regulated through phosphorylation. Mutating potential phosphorylation sites (based on the hypothesis that predicted phosphorylation sites are phosphorylated in rassf7) would provide a first step in indicating if phosphorylation is important for correct rassf7 localisation.

Human, mouse and *Xenopus* RASSF7 amino acid sequences were screened with a post-translational modification prediction site, ELM (see Materials and Methods) to identify predicted phosphorylation sites, especially sites that may be modified by kinases implicated in regulating cell division/mitosis. Four interesting groups of potential phosphorylation sites were predicted by ELM at first glance: PKA, PLK, CDK1 and PIKK (Figure 3.16). A predicted PLK phosphorylation site was seen in each of the three species, with differences in sequence position but all were located within the B domains, which made it a possible candidate to mutate. Absence of this predicted phosphorylation site could be responsible for the accumulation seen when the B domain GFP-rassf7 (RA+A+CC) is not present (Figure 3.6A). The other three predicted phosphorylation sites were not seen in the three species therefore experiments focused on the predicted phosphorylation site, PLK, Plk as a mitotic kinase, potentially has a role related to RASSF7's mitotic function.

Another group of potential sites to search for were Aurora A kinase sites, given RASSF7's role in mitosis and its centrosomal localisation. RASSF7 exhibits

strong parallels with Aurora A in its prominent overexpression in cancers and its role at the centrosome and MT dynamics in mitosis, thus raising the question of whether Aurora A phosphorylates and interacts and/or regulates RASSF7 localization. However, no obvious Aurora A phosphorylation sites were predicted with ELM. Thus, to identify potential Aurora A kinase phosphorylation sites, the broad Aurora A phosphorylation consensus, K/R-X-T/S (where X is any amino acid) (Alexander et al., 2011; Kettenbach et al., 2011) was used to select and identify candidate motifs. Furthermore, RASSF1A, which has also been shown to play a significant role on MTs in mitosis, is phosphorylated and regulated by Aurora A (Rong et al., 2007). In addition, RASSF1A is phosphorylated by additional kinases (PKA and PKC) at the same site as Aurora A (Richter et al., 2010). Thus, predicted phosphorylation sites identified (particularly for PKA) were also screened for Aurora A's consensus phosphorylation sequence (Figure 3.16, presented in red). Four motifs apparently satisfied the consensus on RASSF7. Of these, two motifs (R-R-T-G, R-P-S-S-D) exhibited very high conservation between three species, while the other two (R-A/S-S-L, K/R-R-T/A/S-L) were not conserved.

Because of the known importance of phosphorylation by mitotic kinases, experiments were focused on mutating the predicted PLK phosphorylation site and predicted Aurora A consensus phosphorylation sites.

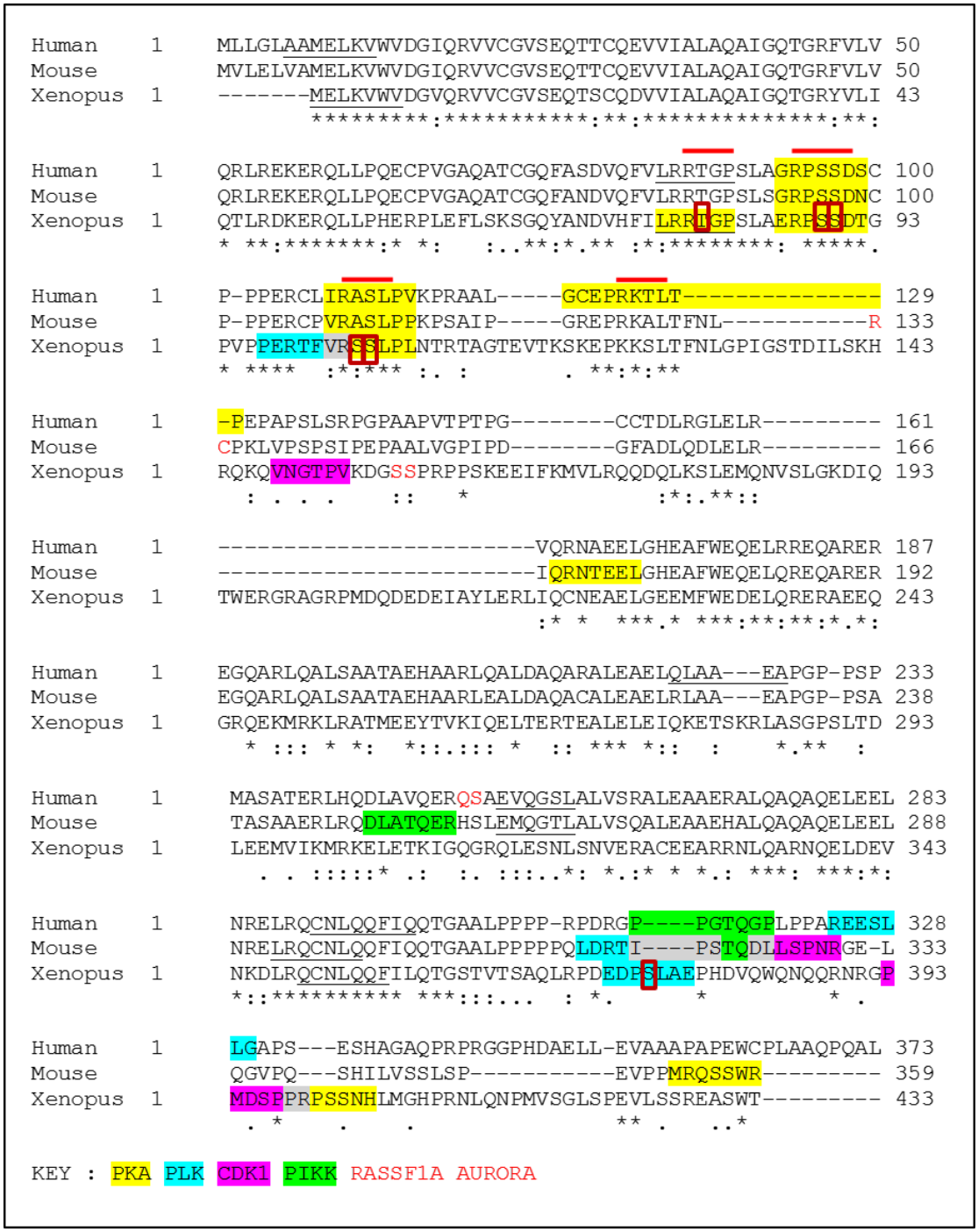
Human 1 MLLGLAAMELKVWVDGIQRVVCGVSEQTTCQEVVIALAQAIGQTGRFVLV 50
Mouse MVLELVAMELKVWVDGIQRVVCGVSEQTTCQEVVIALAQAIGQTGRFVLV 50
Xenopus 1 -------MELKVWVDGVQRVVCGVSEQTSCQDVVIALAQAIGQTGRYVLI 43
Human 1 QRLREKERQLLPQECPVGAQATCGQFASDVQFVLRRTGPSLAGRPSSDSC 100
Mouse QRLREKERQLLPQECPVGAQATCGQFANDVQFVLRRTGPSLSGRPSSDNC 100
Xenopus 1 QTLRDKERQLLPHERPLEFLSKSGQYANDVHFILRRTGPSLAERPSSDTG 93
Human 1 P-PPERCLIRASLPVKPRAAL-----GCEPRKTLT---------- 129
Mouse P-PPERCPVRASLPPKPSAIP-----GREPRKALTFNL----------R 133
Xenopus 1 PVPPERTFVRSSLPLNTRTAGTEVTKSKEPKKSLTFNLGPIGSTDILSKH 143
Human 1 -PEPAPSLSRPGPAAPVTPTPG--------CCTDLRGLELR--------- 161
Mouse CPKLVPSPSIPEPAALVGPIPD--------GFADLQDLELR--------- 166
Xenopus 1 RQKQVNGTPVKDGSSPRPPSKEEIFKMVLRQQDQLKSLEMQNVSLGKDIQ 193
Human 1 ----------VQRNAEELGHEAFWEQELRREQARER 187
Mouse ----------IQRNTEELGHEAFWEQELQREQARER 192
Xenopus 1 TWERGRAGRPMDQDEDEIAYLERLIQCNEAELGEEMFWEDELQRERAEEQ 243
Human 1 EGQARLQALSAATAEHAARLQALDAQARALEAELQLAA---EAPGP-PSP 233
Mouse EGQARLQALSAATAEHAARLEALDAQACALEAELRLAA---EAPGP-PSA 238
Xenopus 1 GRQEKMRKLRATMEEYTVKIQELTERTEALELEIQKETSKRLASGPSLTD 293
Human 1 MASATERLHQDLAVQERQSAEVQGSLALVSRALEAAERALQAQAQELEEL 283
Mouse TASAAERLRQDLATQERHSLEMQGTLALVSQALEAAEHALQAQAQELEEL 288
Xenopus 1 LEEMVIKMRKELETKIGQGRQLESNLSNVERACEEARRNLQARNQELDEV 343
Human 1 NRELRQCNLQQFIQQTGAALPPPP-RPDRGP----PGTQGPLPPAREESL 328
Mouse NRELRQCNLQQFIQQTGAALPPPPPQLDRTI----PSTQDLLSPNRGE-L 333
Xenopus 1 NKDLRQCNLQQFILQTGSTVTSAQLRPDEDPSLAEPHDVQWQNQQRNRGP 393
Human 1 LGAPS---ESHAGAQPRPRGGPHDAELL-EVAAAPAPEWCPLAAQPQAL 373
Mouse QGVPQ---SHILVSSLSP----------EVPPMRQSSWR--------- 359
Xenopus 1 MDSPPRPSSNHLMGHPRNLQNPMVSGLSPEVLSSREASWT--------- 433
KEY : PKA PLK CDK1 PIKK RASSF1A AURORA

Figure 3.16: Predicted phosphorylation sites on RASSF7. Human, mouse and *Xenopus* RASSF7 proteins were aligned via CLUSTAL. Potential protein kinase A (PKA), polo-like kinase (Plk), cyclin-dependant kinase 1 (Cdk1) and Phosphatidylinositol 3-kinase-related kinase (PIKK) phosphorylation sites were predicted with ELM. Overlaps in predicted phosphorylation sites are highlighted in grey. Four highly conserved, potential Aurora A phosphorylation sites (highlighted by red lines) were identified by scanning predicted PKA phosphorylation sites for similarity with the broad Aurora A phosphorylation consensus, K/R-X-T/S (where X is any amino acid). In addition, amino acid residues of RASSF7 corresponding to the identified phosphorylated Ser/Thr motif on RASSF1A (via alignment) are represented in red. The serine/threonine residues that were used for alanine and aspartic acid substitution are shown in the red boxes.

3.2.3.1 Mutating the potential PLK site on rassf7 did not change the centrosomal localisation of rassf7

In order to investigate the importance of phosphorylation in rassf7 centrosomal localisation, the predicted PLK phosphorylation site was mutated. The amino acids that are phosphorylated include serine, threonine and tyrosine because they contain a -OH group substitutable by a phosphate group. Serine 374 (Figure 3.16) within the PLK site was mutated using site-directed mutagenesis in two alternative forms; a serine to alanine (S374-A) substitution (alanine contains an inert alkyl side-group) that is a non-phosphorylatable residue and a serine to aspartic acid (S374-D) substitution (aspartic acid retains a negatively charged carboxy side group), which mimics phosphorylation of serine (see Materials and Methods). Two substitutions; GFP-rassf7 (S374-A) and GFP-rassf7 (S374-D) were applied to further study the centrosomal localisation of rassf7.

GFP-rassf7 (S374-A) and GFP-rassf7 (S374-D) expressing cells showed a similar localisation of rassf7 to the centrosome as the wild type (Figure 3.17A and B). Preventing phosphorylation of the predicted PLK site via an alanine substitution and mimicking the phosphorylation by an aspartic acid substitution appeared to have no effect on centrosomal rassf7 localisation (Figure 3.18A, C and E) and no effect on γ-tubulin staining (Figure 3.18B, D and F).

This result suggests that phosphorylation of the predicted PLK site within rassf7 does not play a direct role in centrosomal rassf7 localisation.

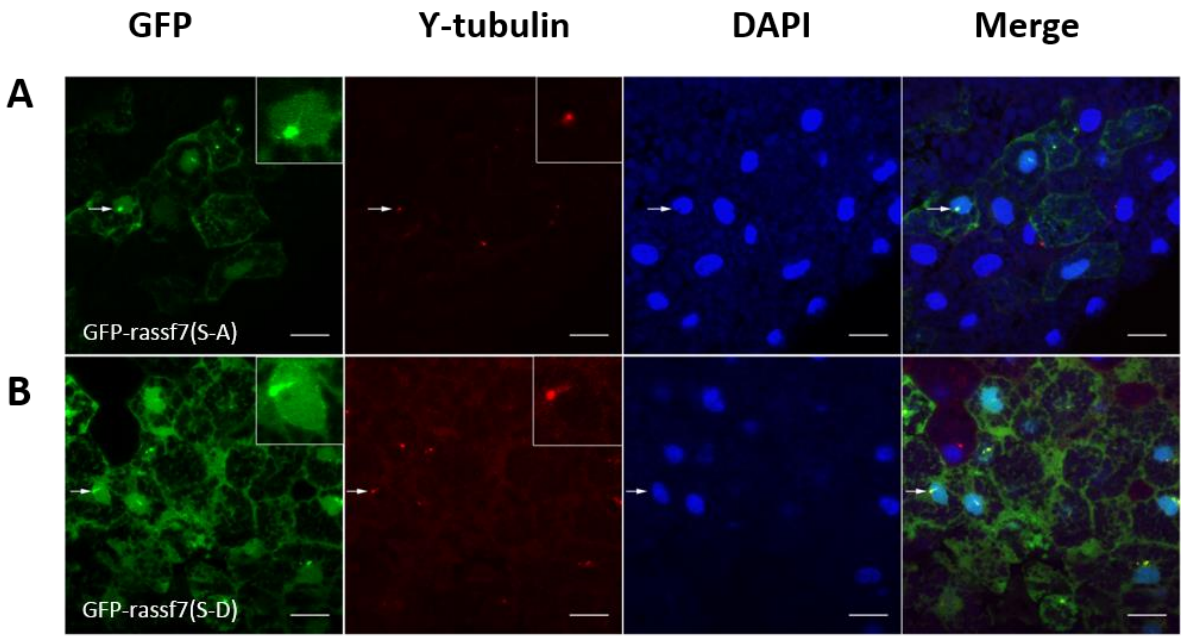

Figure 3.17: Mutating the predicted PLK site does not change the centrosomal rassf7 localisation. Embryos were microinjected with RNA at the two-cell stage, cultured until (stage 10), fixed, sectioned and stained with a centrosome marker (γ-tubulin /red) and a nuclear marker (DAPI/blue). GFP fluorescence is shown in green. **(A)** GFP-rassf7 (S374-A) (green) co-localised with γ-tubulin (red). **(B)** GFP-rassf7 (S374-D) (green) co-localised with γ-tubulin (red). Arrows highlight the potential area for co-localisation. Scale bars=10μm.

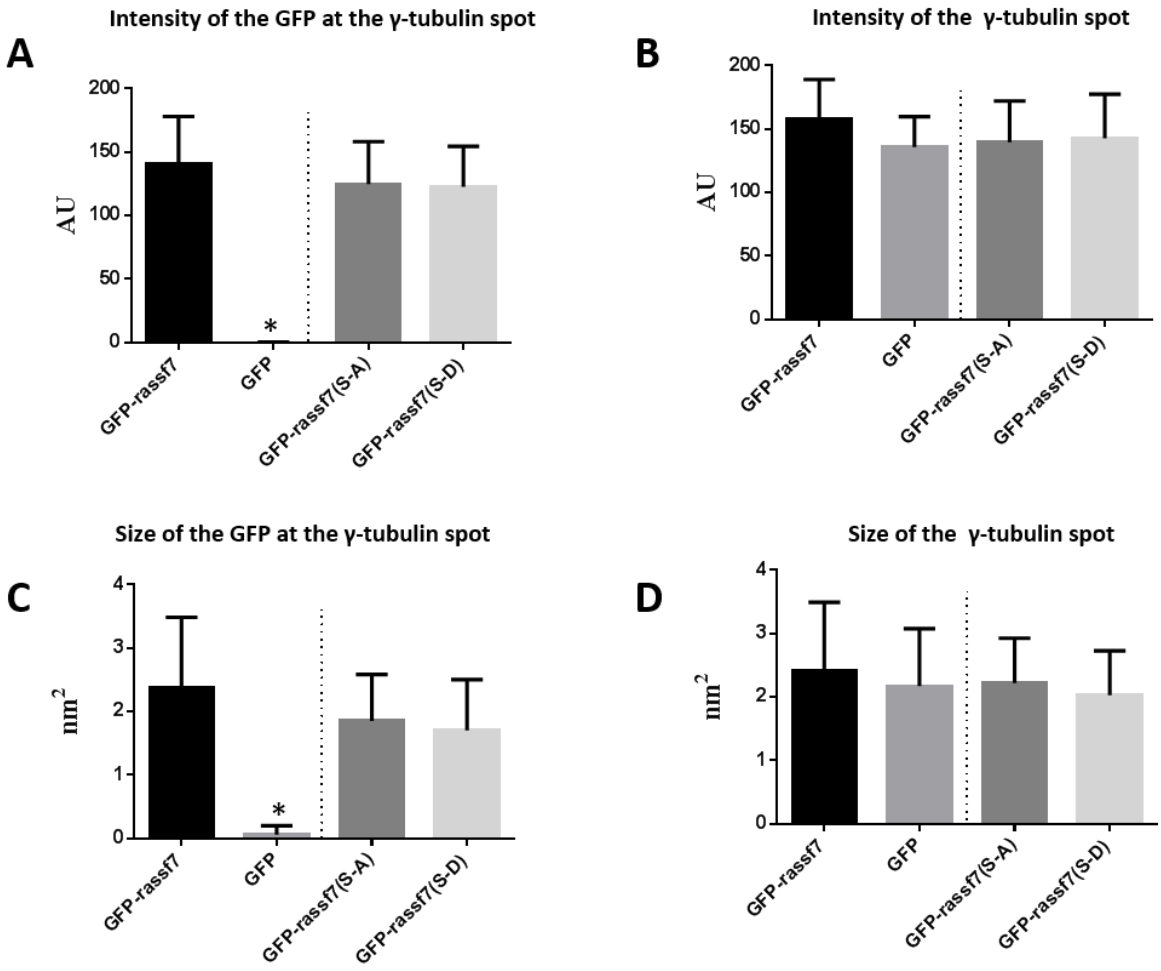
A
Intensity of the GFP at the γ-tubulin spot
AU
200
150
100
50
0
*
GFP-rassf7
GFP
GFP-rassf7(S-A)
GFP-rassf7(S-D)
B
Intensity of the γ-tubulin spot
AU
200
150
100
50
0
GFP-rassf7
GFP
GFP-rassf7(S-A)
GFP-rassf7(S-D)
C
Size of the GFP at the γ-tubulin spot
nm2
4
3
2
1
0
*
GFP-rassf7
GFP
GFP-rassf7(S-A)
GFP-rassf7(S-D)
D
Size of the γ-tubulin spot
nm2
4
3
2
1
0
GFP-rassf7
GFP
GFP-rassf7(S-A)
GFP-rassf7(S-D)

Figure 3.18: Quantification of the localisation of mutated predicted PLK site on rassf7. Embryos were microinjected with RNA at the two-cell stage, cultured until stage 10, fixed, sectioned and images of the GFP fluorescence and γ-tubulin staining were collected by confocal microscopy. Example images are shown in the previous figure**.** The fluorescent area and intensity of the γ-tubulin staining and GFP was measured by using the LSM510 Image Browser software (ZEISS). **(A)** Intensity of the GFP at the γ-tubulin spot. **(B)** Intensity of the γ-tubulin spot. **(C)** Size of the GFP at the γ-tubulin spot. **(D)** Size of the γ-tubulin spot. No significant changes were observed. Based on at least three independent experiments, bars represent standard error and were calculated and plotted using GraphPad Prism 6. Statistical analysis was carried out using One-way Anova tests with Bonferroni post-test corrections. >100 cells were measured in total, *$p<0.05$.

3.2.3.2 Mutating the potential Aurora A phosphorylation sites on rassf7 did not change centrosomal localisation of rassf7

Having studied the effect of mutating the predicted PLK phosphorylation site on rassf7 centrosomal localisation, the effects of Aurora A's consensus phosphorylation sites were then examined. Of the potential Aurora A phosphorylation sites identified as described above, the RSSL motif, matching best with a more stringent predicted Aurora A phosphorylation consensus, K/R-X-S/T-ϕ (where X and ϕ represent any amino acid and hydrophobic residue, respectively) (Alexander et al., 2011; Dephoure et al., 2008; Kettenbach et al., 2011) was selected for substitution with alanine and aspartic acid. Serine 104 and 105 were coding for one predicted Aurora a phosphorylation site (Figure 3.16) so mutation of single predicted Aurora A phosphorylation site was applied by substitution of two serine residues to alanine (S/104,105-A) and to aspartic acid (S/104,105-D). See figure 3.16 (boxes) for the serine residues that are used for substitution.

GFP-rassf7 (S/104,105-A) expressing cells showed a similar localisation of rassf7 to the centrosome as the wild type (Figure 3.19A). Preventing the phosphorylation of one predicted Aurora A phosphorylation site by alanine substitution appeared to have no effect on centrosomal rassf7 localisation (Figure 3.20A, C and E) and no effect on γ-tubulin staining (Figure 3.20B, D and F).

GFP-rassf7 (S/104,105-D) expressing cells also showed a similar localisation of rassf7 to the centrosome as the wild type (Figure 3.19B). Mimicking the phosphorylation of one predicted Aurora A phosphorylation site by an aspartic

acid substitution did not affect the centrosomal localisation of rassf7 (Figure 3.20A, C and E) and did not affect γ-tubulin staining (Figure 3.20B, D and F).

No change was observed in centrosomal localisation of rassf7 and γ-tubulin staining with mutating one predicted Aurora A phosphorylation site either with alanine or aspartic acid substitution. In addition, the three most conserved motifs (RRTG, RPSSD, RSSL) were also selected for combined mutation to give a mutation of three different predicted Aurora A phosphorylation sites (triple mutant; a total of five Ser/Thr residues: T80, S89, 90,104,105 were substituted and annotated as S/T5-A and S/T5-D in Figure 3.19).

Remarkably, GFP-rassf7 (S/T5-A) and GFP-rassf7 (S/T5-D) triple mutants yielded similar results to single mutants. They were both able to co-localise with γ-tubulin (Figure 3.19C and D) with no significant difference than wild type rassf7 levels (Figure 3.20A, C and E). Mutating the triple predicted Aurora A phosphorylation sites also did not change the γ-tubulin staining (Figure 3.20B, D and F).

This result suggests that, similar to predicted PLK site, phosphorylation of the predicted Aurora A sites within rassf7 does not play a direct role in centrosomal localisation of rassf7.

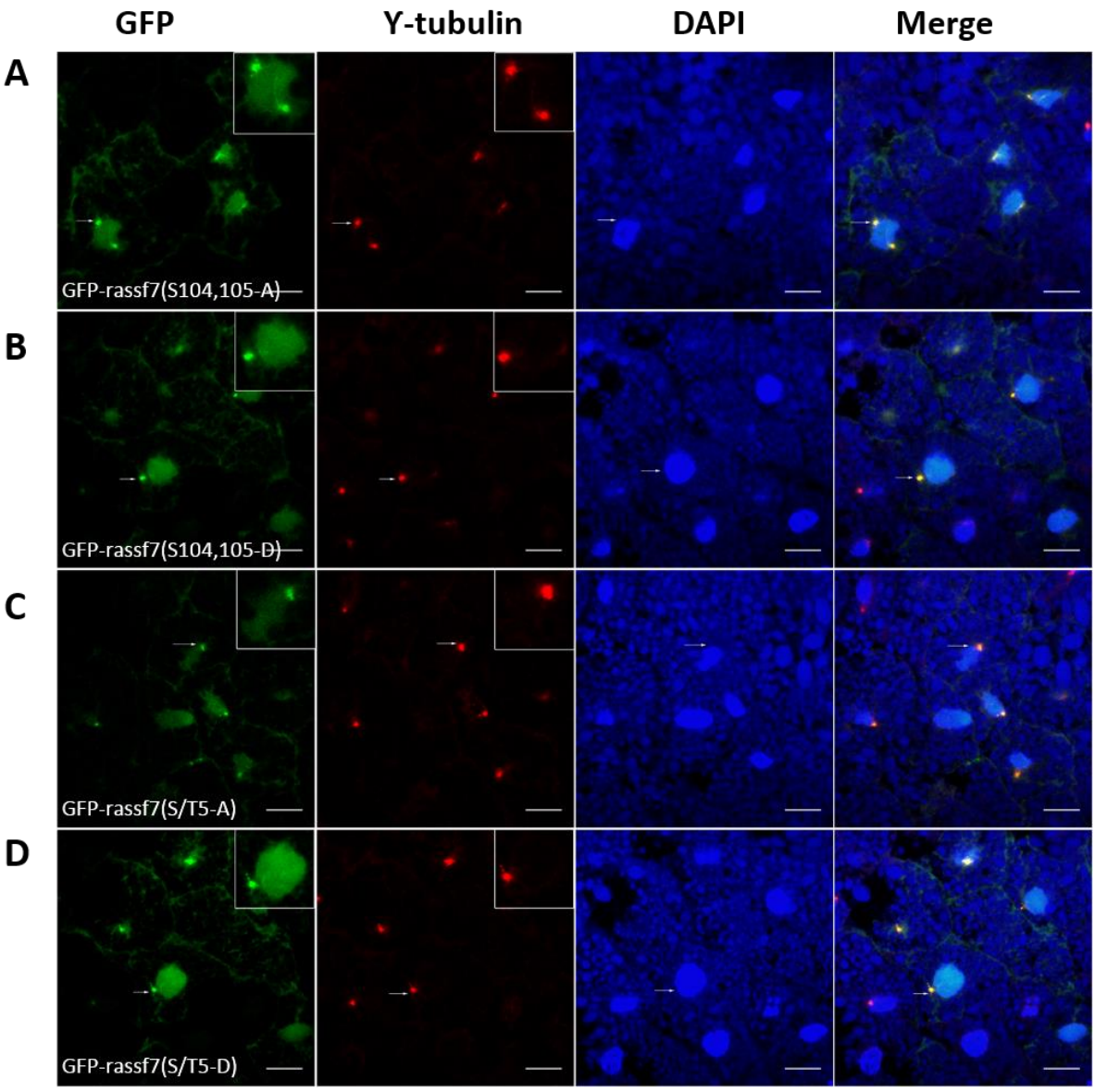

Figure 3.19: Mutating the predicted PKA sites did not change the centrosomal rassf7 localisation. Embryos were microinjected with RNA at the two-cell stage, cultured until (stage 10), fixed, sectioned and stained with a centrosome marker (γ-tubulin /red) and a nuclear marker (DAPI/blue). GFP fluorescence is shown in green. **A)** GFP-rassf7 (S104,105-A) (green) co-localised with γ-tubulin (red). **(B)** GFP-rassf7 (S104,105-D) (green) co-localised with γ-tubulin (red). **(C)** GFP-rassf7 (S/T5-A) (green) co-localised with γ-tubulin (red). **(D)** GFP-rassf7 (S/T5-D) (green) co-localised with γ-tubulin (red). Arrows highlight the potential area for co-localisation. Scale bars=10μm.

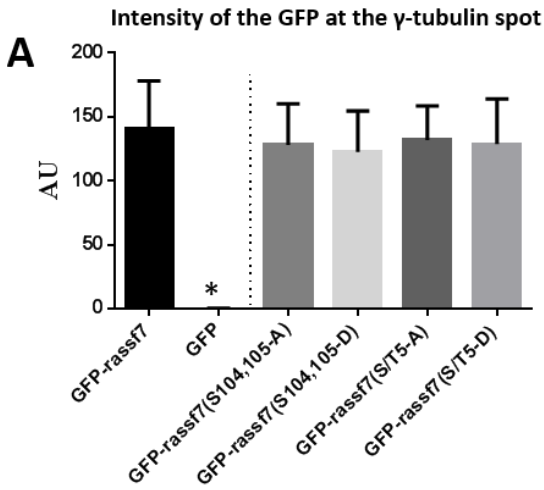
A
Intensity of the GFP at the γ-tubulin spot
AU
200
150
100
50
0
*
GFP-rassf7
GFP
GFP-rassf7(S104,105-A)
GFP-rassf7(S104,105-D)
GFP-rassf7(S/T5-A)
GFP-rassf7(S/T5-D)

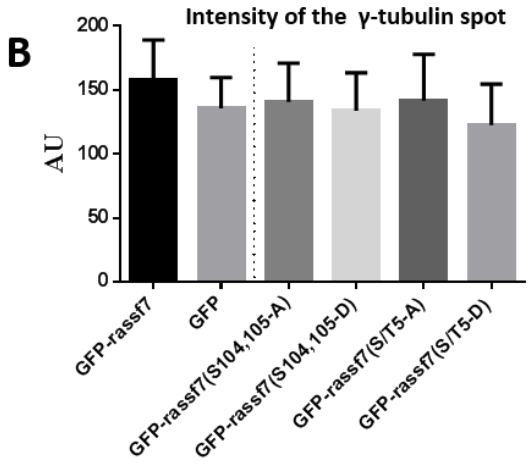
B
Intensity of the γ-tubulin spot
AU
200
150
100
50
0
GFP-rassf7
GFP
GFP-rassf7(S104,105-A)
GFP-rassf7(S104,105-D)
GFP-rassf7(S/T5-A)
GFP-rassf7(S/T5-D)

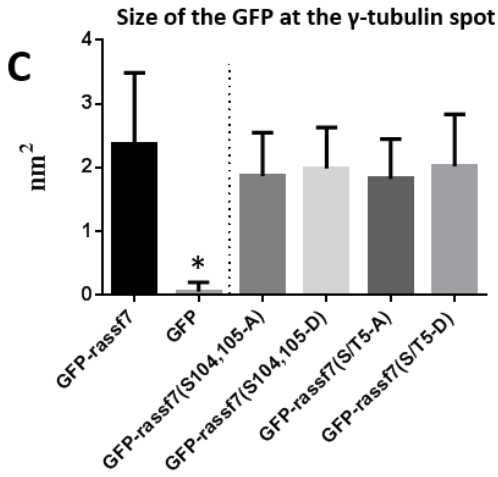
C
Size of the GFP at the γ-tubulin spot
nm2
4
3
2
1
0
*
GFP-rassf7
GFP
GFP-rassf7(S104,105-A)
GFP-rassf7(S104,105-D)
GFP-rassf7(S/T5-A)
GFP-rassf7(S/T5-D)

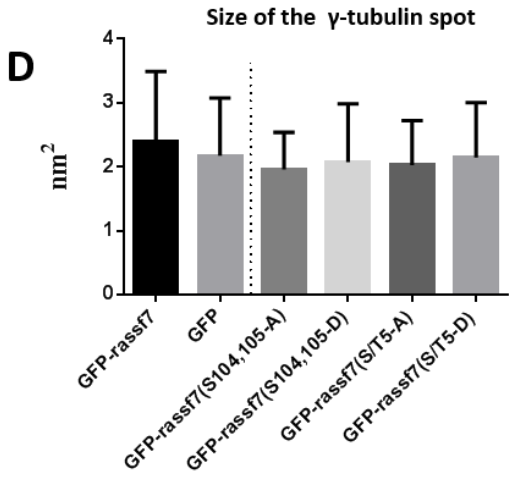
D
Size of the γ-tubulin spot
nm2
4
3
2
1
0
GFP-rassf7
GFP
GFP-rassf7(S104,105-A)
GFP-rassf7(S104,105-D)
GFP-rassf7(S/T5-A)
GFP-rassf7(S/T5-D)

Figure 3.20: Quantification of the localisation of mutated predicted PKA sites on rassf7. Embryos were microinjected with RNA at the two-cell stage, cultured until stage 10, fixed, sectioned and images of the GFP fluorescence and γ-tubulin staining were collected by confocal microscopy. Example images are shown in the previous figure**.** The fluorescent area and intensity of the γ-tubulin staining and GFP was measured by using the LSM510 Image Browser software (ZEISS). **(A)** Intensity of the GFP at the γ-tubulin spot. **(B)** Intensity of the γ-tubulin spot. **(C)** Size of the GFP at the γ-tubulin spot. **(D)** Size of the γ-tubulin spot. No significant changes were observed. Based on at least three independent experiments, bars represent standard error and were calculated and plotted using GraphPad Prism 6. Statistical analysis was carried out using One-way Anova tests with Bonferroni post-test corrections. >100 cells were measured in total, *$p<0.05$.

3.3 Discussion

In the present chapter, the domain responsible for centrosomal RASSF7 localisation has been investigated in *Xenopus laevis*. The key findings are that the coiled-coil domain is sufficient and required for centrosomal rassf7 localisation. In contrast, the RA domain does not seem to be responsible for centrosomal localisation of rassf7. Constructs which lacked the B domain, but contained the A domain and the coiled-coil domain, showed aberrant accumulation at the centrosomes and resulted in an abnormal increase of γ-tubulin staining at centrosomal punctae. Finally, mutating the predicted PLK and Aurora A phosphorylation sites did not have any significant effects on centrosomal rassf7 localisation.

3.3.1 The coiled-coil domain is key in driving centrosomal rassf7 localisation

Data presented here shows that the coiled-coil domain is key in driving the localisation of rassf7 to the centrosome. Previous proteomic characterisation of centrosomes found that a high percentage of centrosomal proteins contain a coiled-coil (Andersen et al., 2003) and many centrosome proteins with coiled-coils have been studied. These include, pericentrin (Doxsey et al., 1994), Ninein (BouckSonCastaing et al., 1996), Hice1 (Wu et al., 2008), TASS (Gergely et al., 2000a; Gergely et al., 2000b) centriolin (Gromley et al., 2003), Cep135 (Gromley et al., 2003), C-Nap1 (Fry et al., 1998a) and Pix1/2 (Hames et al., 2008). Previous studies have also shown that coiled coil domains can mediate centrosome localisation. For example, TACC proteins have a C-terminal coiled-coil domain which is required for interactions with the centrosomes (Gergely et al., 2000a). Therefore, showing that the coiled-coil of rassf7 is sufficient and

required for centrosomal localisation, it supports the idea that coiled-coils play a key role in mediating centrosome localisation of the proteins.

A coiled-coil is a protein-protein interaction domain and it may be regulating centrosomal localization of RASSF7 by interacting with mitotic regulatory proteins. For example, Pascreau et al have identified a centrosomal localization signal which localizes cyclin A to the centrosome independent of Cdk binding, and contributes to targeting and recognition of centrosomal Cdk substrates (Pascreau et al., 2010). Therefore, searching for motifs within the RASSF7 coiled-coil region that may play a role in centrosome localization came next: first a single point mutation, predicted to disrupt the coiled-coil domain was introduced to rassf7. The centrosomal rassf7 localisation did not change with the single point mutation. A previous study showed that a single mutation is not sufficient to effect the localisation: the localisation of HIP1 with a single point mutation in its coiled-coil domain was similar to the localisation of the wild type HIP1 (Fontaine et al., 2012). Importantly, when two or more mutations were introduced into the coiled-coil domain of HIP1, protein aggregates were observed in a proportion of cells and HIP1 lost its normal localisation pattern (Fontaine et al., 2012). Similarly, when more than two mutations were introduced to rassf7, the centrosomal localisation was significantly reduced. It would be very useful in future to find out what coiled-coils bind to at the centrosomes.

3.3.2 The RA domain and the A domain did not appear essential for centrosomal localisation of rassf7

The other domains of rassf7 did not appear necessary for its centrosomal localisation. These included the RA domain, making it likely that the role of this domain is to interact with effector molecules, potentially recruiting them to the centrosome where they may regulate mitosis. RASSF7 has been shown to bind NRas (Takahashi et al., 2011), HRas and KRas via the RA domain (Chan et al., 2013) in pull down experiments with tagged proteins, although it remains to be confirmed that RASSF7 is binding endogenous Ras family members. Recent proteomic studies have shown that RASSF7 can interact with a number of other cellular proteins, including ASPP and PP1 family members (Hauri et al., 2013). dRASSF8, the *Drosophila* homologue of RASSF7 and RASSF8, can also bind dASPP; although dRASSF8 protein localises at epithelial junctions rather than the centrosomes (Langton et al., 2009). Future work is needed to establish whether the RA and A domains, either in concert or independently, bring these or other potential effectors to the centrosomes to regulate mitosis.

3.3.3 Removal of the B domain led to accumulation of rassf7 at the centrosomes and increased levels of γ-tubulin staining

Removing the B domain of rassf7 had a striking effect on its localisation, with a far greater amount of rassf7 co-localising with γ-tubulin. There are a number of possible models to explain this result. The B domain might act as an auto-inhibitory domain that binds to the coiled coil of rassf7 in a regulated way and while in a closed conformation blocks the coiled coil from binding centrosomal proteins. Removing the B domain could then cause unregulated accumulation of rassf7 at the centrosome. This will be investigated with the functional studies of the rassf7 B domain in next chapter.

Another possible explanation for the increased RASSF7 localization to the centrosome when the B domain was removed can be caused by a mechanism such as ubiquitination in the B domain. Ubiquitins regulate protein degradation via the proteasome. Takahashi et al., suggested a ubiquitin proteasome pathway for RASSF7 by showing a reduction in RASSF7 expression in cells which are treated by a proteasome inhibitor (Takahashi et al., 2011). Zhao et al showed the accumulation of parkin (a protein linked to Parkinson disease) to the centrosome when cells were treated with a proteasome inhibitor (Zhao et al., 2003). If there is such a ubiquitination mechanism in the B domain; it may be possible that loss of the B domain prevents ubiquitination. Therefore excess RASSF7 does not become targeted to the proteasome and instead accumulates at the centrosome. Thus no RASSF7 is available for transport to the nucleus. This could be tested by measuring the ubiquitination in the GFP-RASSF7 domain construct lacking a B domain to determine whether the

increased RASSF7 centrosomal accumulation phenotype occurs or not. Examining protein levels of RASSF7 would also be informative.

A related model is that the B domain acts to control the turnover of rassf7 at centrosomes by an unknown mechanism. Consistent with this proposal, there are predicted phosphorylation sites for a number of mitotic kinases in the B domain that could potentially regulate rassf7 turnover. Phosphorylation can alter the structure, function, interaction and subcellular localisation of proteins and it is vital for regulating the cell cycle (Cohen, 2000). ELM identified potential phosphorylation sites within the RASSF7 protein and the predicted PLK phosphorylation site was first chosen for mutation. Although this site is not conserved between species, its presence in human, *Xenopus* and mouse suggests that it may have an important role. The PLKs are a group of serine/threonine kinases localised to the centrosome which play an important role in spindle assembly, cytokinesis and centrosome separation (Nigg, 1998). RASSF7 knockdown causes severe defects in spindle formation (Recino et al., 2010; Sherwood et al., 2008) and associations of PLKs with the centrosome led to interest in this predicted phosphorylation site. Biochemical and genetic analysis has shown the importance of PLKs in regulating centrosome behaviour (Lee et al., 1998). Moreover, overexpression of PLKs in tumour cell lines causes early centrosome maturation resulting in mitotic defects and leads to apoptosis (Takai et al., 2005). The authors further suggest that overexpression of PLK causes early centrosome maturation, increase in centrosome size leading to chromosome instability (Takai et al., 2005). However, mutating the predicted PLK phosphorylation site in rassf7 with either an alanine or aspartic acid mutation did not affect the ability of rassf7 to localise to the centrosome.

Significantly, mutating the predicted PLK site in the B domain did not result in a similar phenotype (accumulation of rassf7 at the centrosome and increased γ-tubulin staining) to truncating the entire B domain.

Another potentially important phosphorylation site to mutate was the PKA phosphorylation site. Interestingly, PKA has also been shown to associate with the centrosome and MTs, whose kinase activity is thought to regulate several aspects of mitosis (Matyakhina et al., 2002; Searle and Sanchez, 2004) and indeed, PKA-phosphorylation was seen to negatively regulate RASSF1A (Richter et al., 2010). Thus, it can be speculated that PKA itself might phosphorylate RASSF7 to regulate its localization and/or function. Furthermore, the consensus for PKA phosphorylation highly resembles that of Aurora A, confirming that Aurora A phosphorylation sites might overlay those of PKA (Kettenbach et al., 2011; Neuberger et al., 2007). Thus, upon identification of potential Aurora A phosphorylation sites (within predicted PKA phosphorylation sites), mutations were introduced to the sites to observe their possible effects on centrosomal rassf7 localisation. Intriguingly, neither single nor triple mutation of the potential Aurora A phosphorylation sites had any effect on the centrosomal rassf7 localisation. Thus, it appears that predicted Aurora A phosphorylation at these motifs does not regulate RASSF7 localization. However, both the PLK and Aurora mutation studies should be considered as preliminary as the sites studied are only predicted sites and localisation was the only aspect of RASSF7 function that was investigated. Future work is required to fully examine a potential role of phosphorylation in the regulation of RASSF7.

3.3.4 Conclusion

In conclusion, the coiled-coil of *Xenopus* rassf7 is responsible for driving its centrosomal localisation. The RA domain and the A domain did not seem to have any role in this process. The removal of the B domain caused an accumulation of GFP at the centrosomes and an enlargement of centrosomes that will be investigated in more detail within the next chapter. Finally, mutation of the predicted phosphorylation sites on rassf7 did not affect the centrosomal rassf7 localisation.

4 Truncated rassf7 causes centrosome and mitotic defects and ultimately cell death

4.1 Introduction

Having showed in the previous chapter that C-terminal truncation of rassf7 causes an accumulation of GFP at the centrosomes and enlargement of centrosomes; this chapter will focus on the possible causes/consequences of these findings.

4.1.1 RASSF7 and cancer

The expression of RASSF7 was shown to be increased in a number of tumour types (Friess et al., 2003; Li et al., 2013c; Logsdon et al., 2003; Lowe et al., 2007; Tan et al., 2009), but it is not clear if RASSF7 can promote tumour formation. The previous work on RASSF7 showed that overexpression of wild type RASSF7, carried out for localisation and rescue experiments, did not have a clear effect on HeLa cells or *Xenopus* embryos (Recino et al., 2010; Sherwood et al., 2008). In the previous chapter (Chapter 3) it has been shown that the wild type full length GFP-rassf7 did not have any strong effect on centrosomes or on the localisation pattern of the protein but when truncated, GFP-rassf7 (RA+A+CC), caused an accumulation of GFP at the centrosomes and centrosome enlargements (see Chapter 3 results).

As discussed in the main introduction, centrosome amplifications/abnormalities are linked to mitotic defects and they were also shown to be a biomarker of cancer cells (see Chapter 1). Furthermore, enlarged centrosome phenotype was shown in some particular cell types, such as breast cancer (Guo et al., 2007b) and bladder cancer (Jiang et al., 2003). Therefore, investigating the

effects of the C-terminal truncation will be informative to explore role of RASSF7 in cancer.

4.1.2 An auto-inhibitory model for the C-terminal B domain

Although it has been shown in the previous chapter that C-terminal truncation causes accumulation of GFP at the centrosomes, the key question is why truncation causes accumulation? One possible explanation for this finding could be an auto-inhibitory role for the B domain. The C-terminal B domain could be an auto-inhibitory domain that interacts with another domain/domains of the protein and stabilizes its localisation within the cell.

Auto-inhibitory domains are regions of proteins that negatively regulate the function of other domains via intra-molecular interactions (Pufall and Graves, 2002) (Figure 4.1). Plk-4 tandem polo box domain (PB1) is a good example for auto inhibitory domains those regulate protein function/activation (Klebba et al., 2015). Regarding to findings reported in this thesis, an autoinhibitory role will be tested in this chapter.

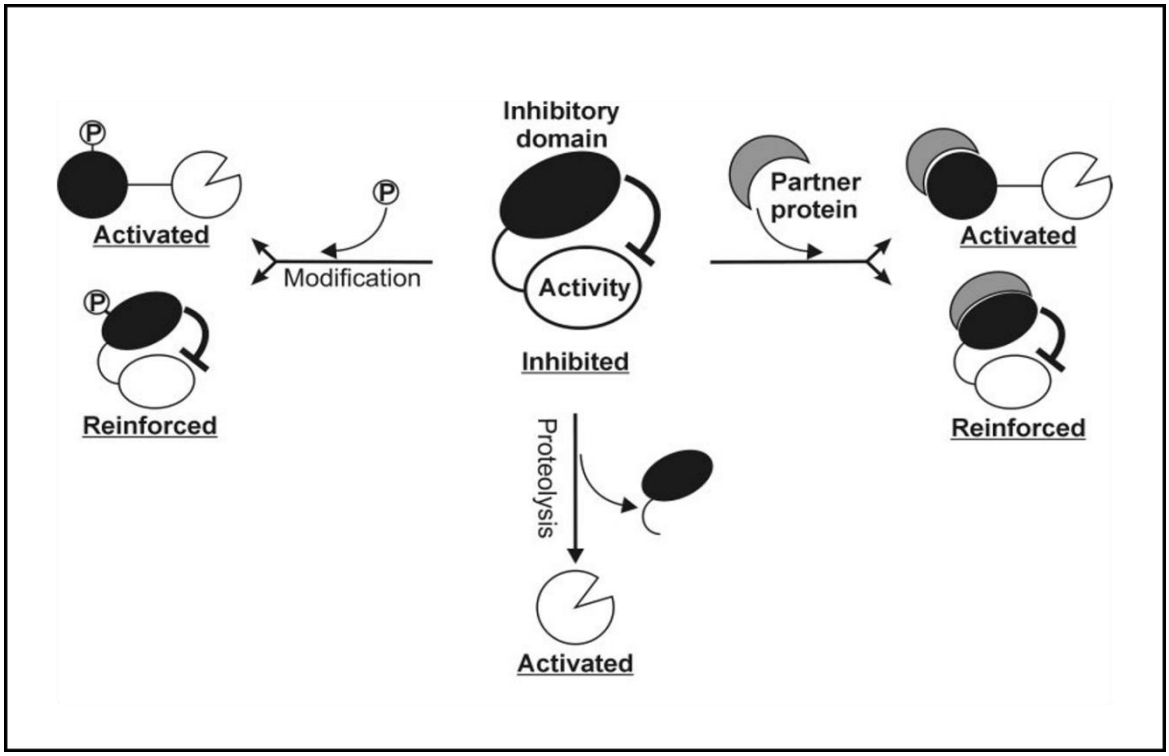

Figure 4.1: Autoinhibition as a regulatory mechanism. An autoinhibitory domain modulates the activity of a second, separable domain (*centre*). Autoinhibition can be counteracted and reinforced by modification (*left*) or by association with a second molecule, partner protein (*right*). Autoinhibition is often identified experimentally by deletion of the autoinhibitory domain. Proteolysis is also a regulatory strategy in vivo (*lower*). Figure adapted from (Pufall and Graves, 2002).

4.1.3 Aims

This chapter will investigate if GFP-rassf7 (RA+A+CC) causes mitotic defects and its role/link, if there is any, in/with cancer cells and will test an auto-inhibitory role for the B domain with the aims listed below:

1) Establish if truncated rassf7 causes mitotic defects.
2) Investigate the mechanism of why accumulation occurs.
3) Find out if similar truncations occur in human tumours.

4.2 Results

4.2.1 GFP-rassf7 (RA+A+CC) promoted amplification of the Υ-tubulin spot

To begin to investigate the aberrant centrosomal morphology observed in cells expressing C-terminally truncated rassf7 in more detail, an analysis of the number of Υ-tubulin spot per cell was carried out. This would show if C-terminal truncation would cause supernumerary centrosomes, which is common in cancer cells.

Cells expressing GFP or wild type GFP-rassf7 had one or two Υ-tubulin spots depending on their cell cycle stage (Figure 4.2A and B). However, in cells expressing GFP-rassf7 (RA+A+CC) there were often three or more Υ-tubulin spots (Figure 4.2C). Quantification of centrosome number (Υ-tubulin spot) showed that unlike controls, GFP-rassf7 (RA+A+CC) injected cells frequently have more than two Υ-tubulin spot (Figure 4.3). In summary, C-terminal truncation of rassf7 caused an increased number of Υ-tubulin spot as well as an increase in the size of the Υ-tubulin spot, suggesting an increase in the number of centrosomes per cell.

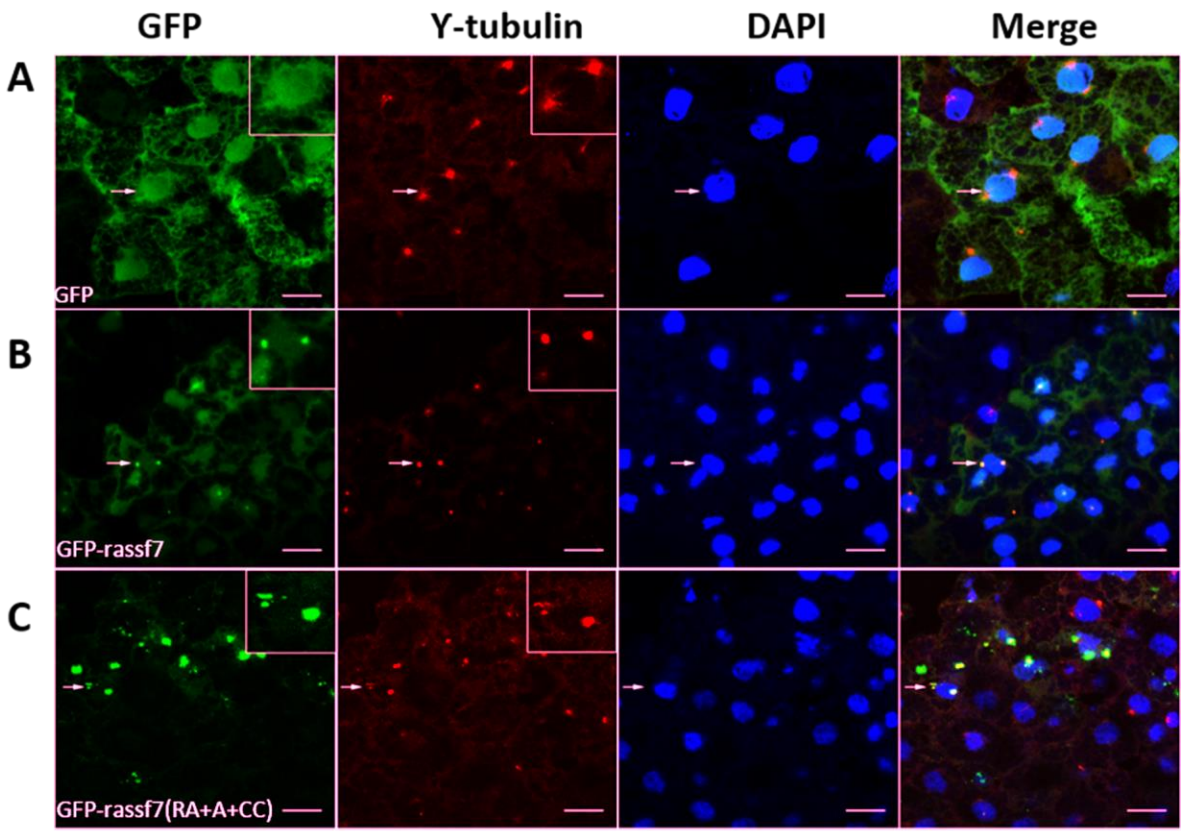

Figure 4.2: Expression of GFP-rassf7 (RA+A+CC) caused increased numbers of γ-tubulin spot. Embryos were microinjected with RNA at the two-cell stage, cultured until stage 10, fixed, sectioned and stained with a centrosomal marker (γ-tubulin/red) and a nuclear marker (DAPI/blue). GFP fluorescence is shown in green. **(A)** GFP (green) and γ-tubulin (red). **(B)** GFP-rassf7 (green) and γ-tubulin (red). **(C)** GFP-rassf7 (RA+A+CC) (green) and γ-tubulin (red). Cells expressing GFP-rassf7 (RA+A+CC) showed increased numbers of γ-tubulin spot. Arrows highlight example cells and scale bars=10μm.

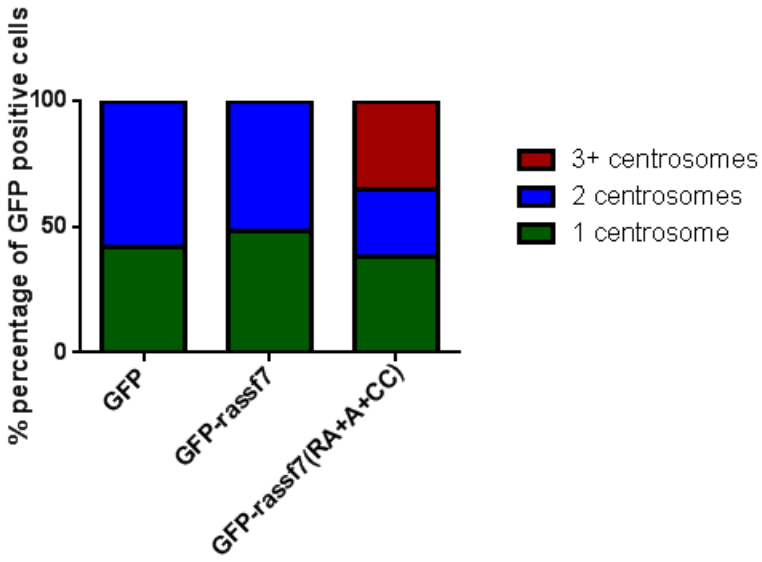

Figure 4.3: Quantification of centrosome numbers. Embryos were microinjected with RNA at the two-cell stage, cultured until stage 10, fixed, sectioned and images of the GFP fluorescence and γ-tubulin staining were collected by confocal microscopy. Centrosome number for GFP, GFP-rassf7 and GFP-rassf7 (RA+C+CC) injected cells were counted. Unlike controls, GFP-rassf7 (RA+A+CC) injected cells frequently have more than two γ-tubulin spot. Based on at least three independent experiments.>100 cells were measured in total, *$p<0.05$.

4.2.2 GFP-rassf7 (RA+A+CC) endorsed increased number of mitotic cells

Given the apparent abnormalities in the centrosomes (increased size and number of Ɣ-tubulin spot), the functional consequences of these defects were then investigated by analysing the proportion of cells in mitosis. This was achieved by staining for Phospho-H3 (Figure 4.4). GFP-rassf7 (RA+A+CC) (Figure 4.4C) expressing cells had more Phospho-H3 positive cells than GFP (Figure 4.4A) and GFP-rassf7 (Figure 4.4B) injected cells (Figure 4.5). Therefore, it is possible to hypothesise that the centrosomal abnormalities caused by expression of GFP-rassf7 (RA+A+CC) lead to a delay in progression through mitosis and an accumulation of mitotic cells (see discussion).

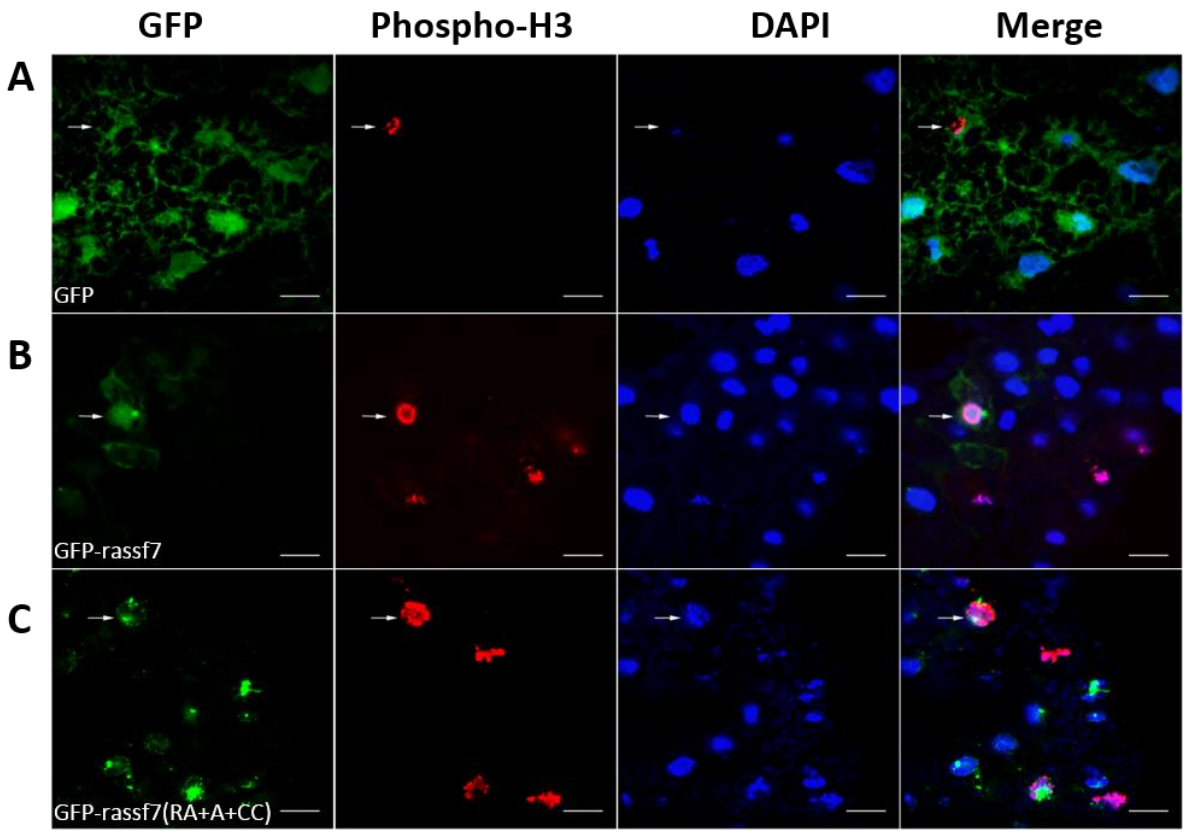

Figure 4.4: GFP-rassf7 (RA+A+CC) injected cells accumulate in mitosis. Embryos were microinjected with RNA at the two-cell stage, cultured until stage 10, fixed, sectioned and stained with a mitosis marker (Phospho-H3/red) and a nuclear marker (DAPI/blue). GFP fluorescence is shown in green. (A) GFP (green) injected cells were stained for Phospho-H3 (red). (B) GFP-rassf7 (green) injected cells were stained for Phospho-H3 (red). (C) GFP-rassf7 (RA+A+CC) (green) injected cells were stained for Phospho-H3 (red). The number of Phospho-H3 positive cells increased when compared to GFP and GFP-rassf7. In panels A-C arrows highlight example nuclear regions and all bars=10μm.

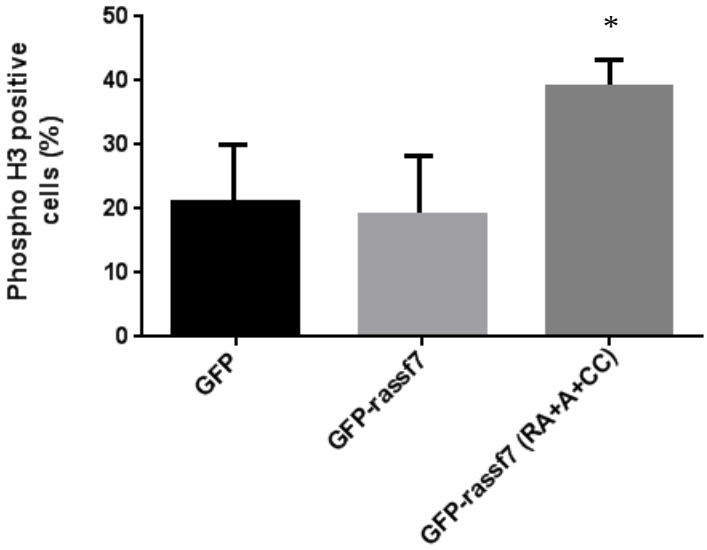

Figure 4.5: Quantification of Phospho-H3 positive cells. Embryos were microinjected with RNA at the two-cell stage, cultured until stage 10, fixed, sectioned and images of the GFP fluorescence and phospho-H3 staining were collected by confocal microscopy. The percentage of GFP positive cells that are Phospho-H3 positive was calculated. Based on at least three independent experiments, bars represent standard error and were calculated and plotted using GraphPad Prism 6. Statistical analysis was carried out using One-way Anova tests with Bonferroni post-test corrections. >100 cells were measured in total, *$p<0.05$.

4.2.3 GFP-rassf7 (RA+A+CC) injected embryos showed increased embryo death and lost the centrosomal localisation at later stages in development

Having shown that GFP-rassf7 (RA+A+CC) caused centrosomal defects, following experiments focused on investigating the long-term consequences of expressing this construct. GFP-rassf7 (RA+A+CC) injected embryos were cultured and rates of embryo death monitored. Uninjected, GFP injected and GFP-rassf7 injected embryos showed some death during development (Figure 4.6A). However, the rate of embryo death was significantly increased in embryos injected with GFP-rassf7 (RA+A+CC) (Figure 4.6A).

Some stage 30 embryos, expressing GFP-rassf7 (RA+A+CC) did however survive (Figure 4.6B), allowing the study of the subcellular localisation of wild type rassf7 and C-terminally truncated rassf7 at this stage. GFP and GFP-rassf7 in stage 30 embryos showed similar subcellular distributions to stage 10, with cytoplasmic and centrosomal localisation respectively (Figure 4.7A and B). However, unexpectedly GFP-rassf7 (RA+A+CC) did not co-localise with Ɣ-tubulin in stage 30 embryos (Figure 4.7C). Where the GFP-rassf7 (RA+A+CC) was expressed, the cells did not appear to have clear Ɣ-tubulin spot. This led the question of whether there was increased programmed cell death, associated with this apparent loss of Ɣ-tubulin spot.

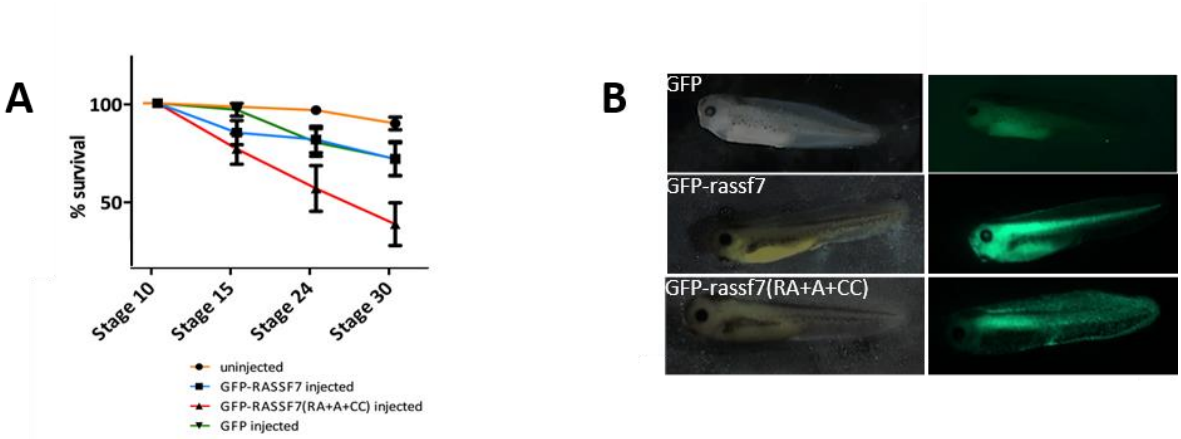

Figure 4.6: GFP-rassf7 injected embryos at tadpole stages. Embryos were microinjected with RNA at the two-cell stage, cultured until tadpole stages (stage 30), fixed, sectioned and stained with a centrosomal marker (γ-tubulin/red) and a nuclear marker (DAPI/blue). GFP fluorescence is shown in green. **(A)** Embryo survival for uninjected, GFP injected, GFP-rassf7 injected and GFP-rassf7 (RA+A+CC) injected embryos. Based on at least three independent experiments, >60 embryos were counted in total. **(B)** Wholemount stage 30 embryos expressing GFP, GFP-rassf7 and GFP-rassf7 (RA+A+CC).

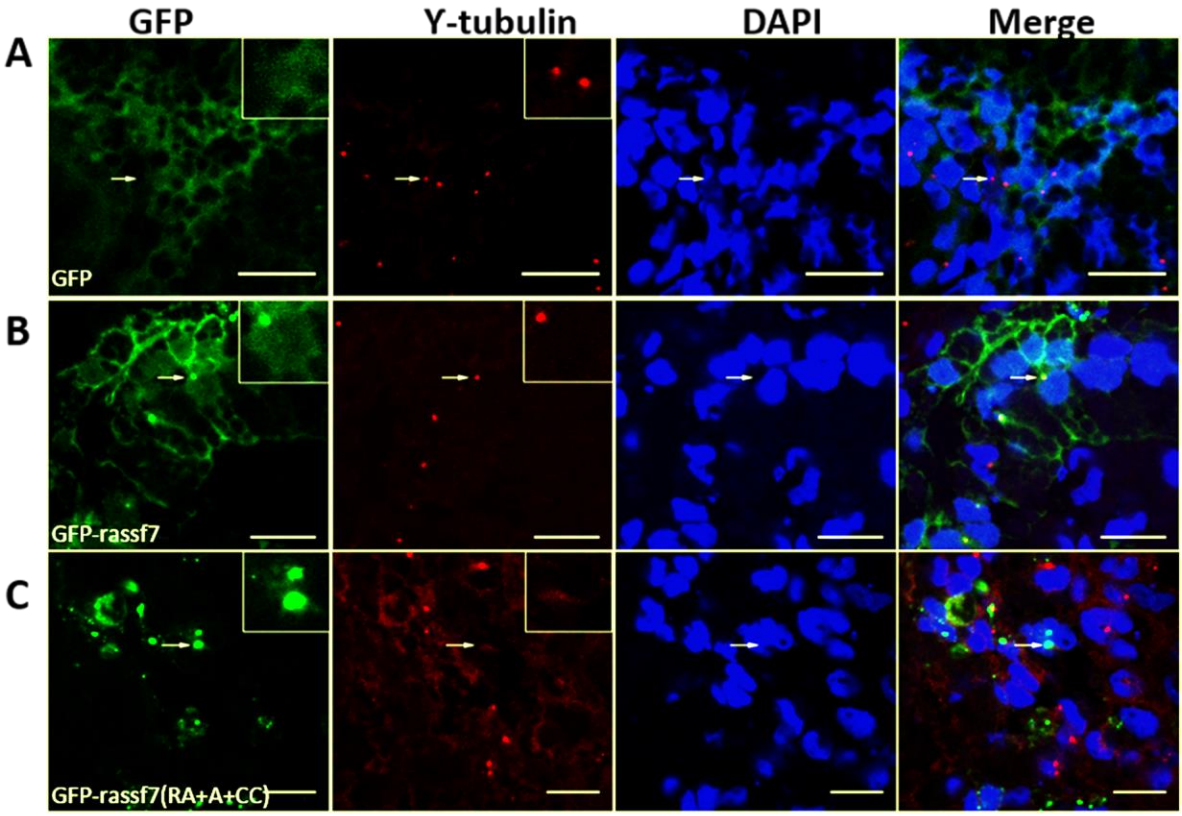

Figure 4.7: Stage 30 embryos lost the centrosomal localisation of GFP-rassf7 (RA+A+CC). Embryos were microinjected with RNA at the two-cell stage, cultured until stage 30, fixed, sectioned and images of the GFP fluorescence and γ-tubulin staining were collected by confocal microscopy **(A)** GFP (green) expressing cells stained with γ-tubulin (red) from stage 30 embryos. **(B)** GFP-rassf7 (green) expressing cells stained with γ-tubulin (red) from stage 30 embryos. **(C)** GFP-rassf7 (RA+A+CC) (green) expressing cells stained with γ-tubulin (red) at stage 30. Unlike the situation at stage 10, the GFP-rassf7 (RA+A+CC) fluorescence (green) did not co-localise with γ-tubulin (red). Arrows highlight possible regions where co-localisation might occur and all scale bars=10μm.

4.2.4 GFP-rassf7 (RA+A+CC) injected cells showed cell death at stage 30

To determine whether the loss of centrosomal localisation in GFP-rassf7 (RA+A+CC) expressing cells was due to the programmed cell death, cells were stained for the apoptosis marker, active caspase-3 (Figure 4.8). GFP (Figure 4.8A) and GFP-rassf7 (Figure 4.8B) expressing control cells showed low levels of active caspase-3 staining. In contrast, a high percentage of GFP-rassf7 (RA+A+CC) (Figure 4.8C) expressing cells were positive for active caspase-3 (Figure 4.9). These data suggest that early centrosome defects may lead to later centrosome loss and apoptosis.

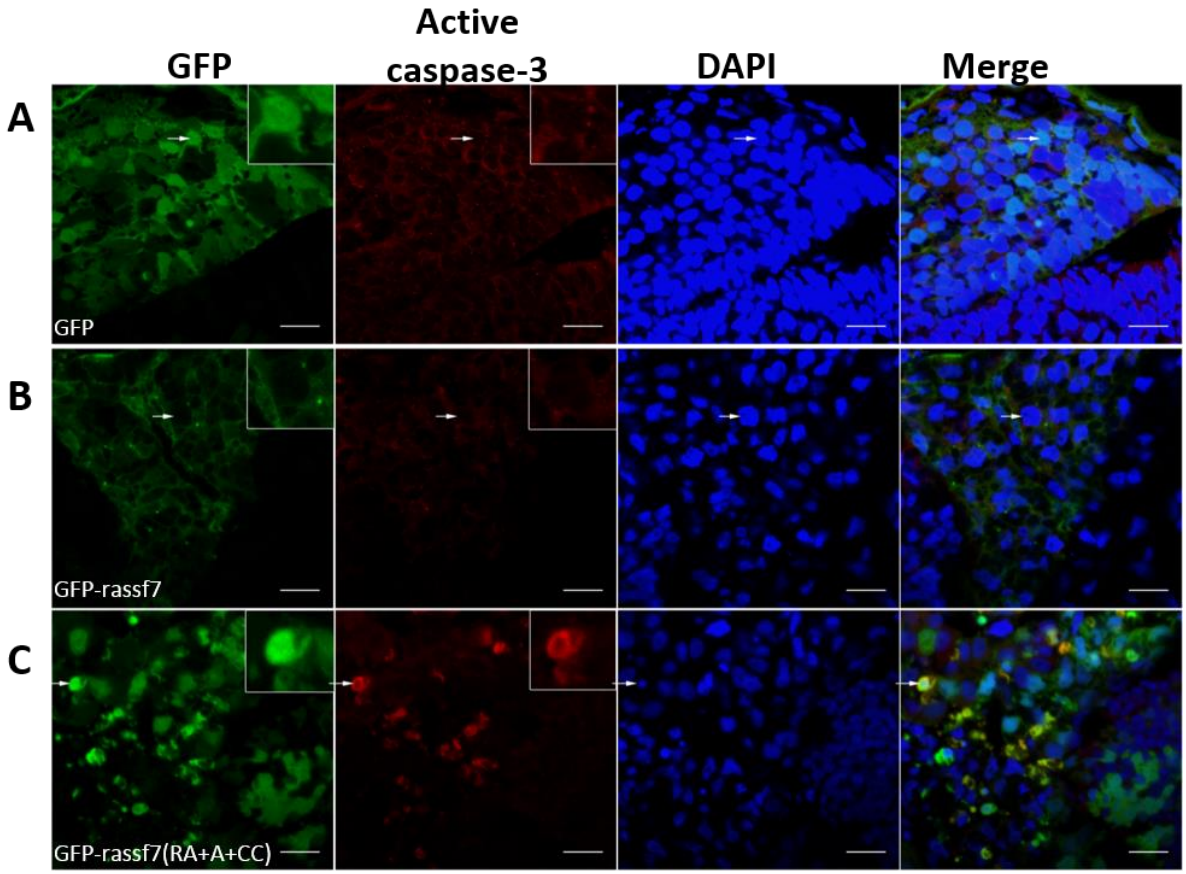

Figure 4.8: GFP-rassf7 injected cells undergo increased rates of apoptosis. Embryos were microinjected with RNA at the two-cell stage, cultured until tadpole stages (stage 30), fixed, sectioned and stained with an apoptosis marker (Active caspase-3/red) and a nuclear marker (DAPI/blue). GFP fluorescence is shown in green. **(A)** GFP injected cells (green) were stained with an antibody against active caspase-3 (red). **(B)** GFP-rassf7 injected cells (green) were stained with an antibody against active caspase-3 (red). **(C)** GFP-rassf7 (RA+A+CC) injected cells (green) were stained an antibody against active caspase-3 (red). GFP-rassf7 (RA+A+CC) expressing cells showed increased levels of active caspase-3 (red) positive nuclei compared to controls. DAPI staining is blue and arrows highlight GFP positive cells. All bars=10μm.

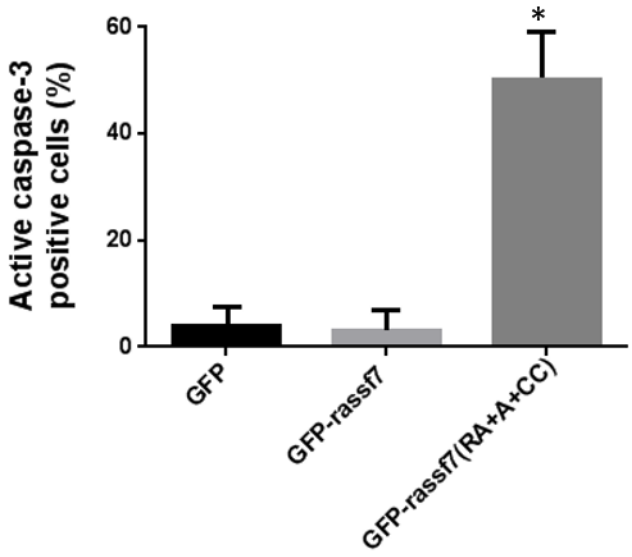

Figure 4.9: Quantification of active caspase positive cells. Embryos were microinjected with RNA at the two-cell stage, cultured until stage 30, fixed, sectioned and images of the GFP fluorescence and active caspase-3 staining were collected by confocal microscopy. The % percentage of GFP positive cells which were active caspase-3 positive was calculated. Based on at least three independent experiments, bars represent standard error and were calculated and plotted using GraphPad Prism 6. Statistical analysis was carried out using One-way Anova tests with Bonferroni post-test corrections. >100 cells were measured in total, *$p<0.05$.

4.2.5 Does the B domain have an auto-inhibitory role?

The accumulation of GFP at the centrosomes and enlargement of the centrosomes were observed in GFP-rassf7 (RA+A+CC) injected cells (see chapter 3) and led to the question: why does removing the B domain cause this effect? One possible explanation for this finding could be an auto-inhibitory role for the B domain (see chapter 4 introduction).

To test this hypothesis, injection of GFP-rassf7 (B) and GFP-rassf7 (RA+A+CC) was carried out at the same time. If the C-terminal B domain is an auto-inhibitory domain, rescue of the phenotype (accumulation of GFP at the centrosome and enlargement of centrosomes) would be expected (Figure 4.10). Figure 4.11 shows the centrosomal localisation of the rescue experiments. When GFP-rassf7 (B) and GFP-rassf7 (RA+A+CC) were injected together, some of the GFP expressing cells showed similar GFP expression and γ-tubulin staining to the wild type whereas some other cells still showed GFP accumulation and enlargement of γ-tubulin (Figure 4.11C). Quantification of the results indicated that GFP-rassf7 (RA+A+CC) + GFP-rassf7 (B) showed reduced GFP accumulation and less enlarged centrosomes compared to wild type GFP-rassf7 (RA+A+CC) (Figure 4.12).

This indicates that addition of the GFP-rassf7 (B) partially rescues the effect of GFP-rassf7 (RA+A+CC) and this is consistent with the auto-inhibitory model for the B domain but more investigation is needed (see discussion).

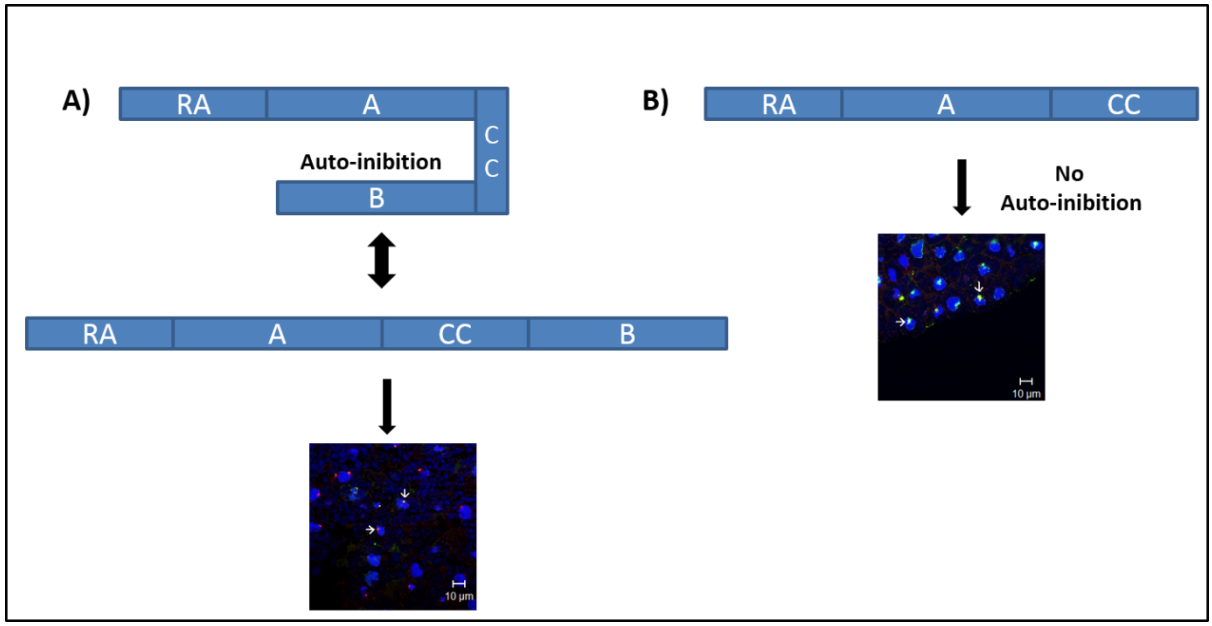

Figure 4.10: Schematic diagram of predicted auto-inhibitory role for the C-terminal B domain. (A) In the presence of the B domain, autoinhibition occurs and centrosomal localisation of rassf7 is regulated. **(B)** In the absence of the B domain, there is no inhibition, which leads to accumulation of rassf7 and an enlargement of the centrosomes.

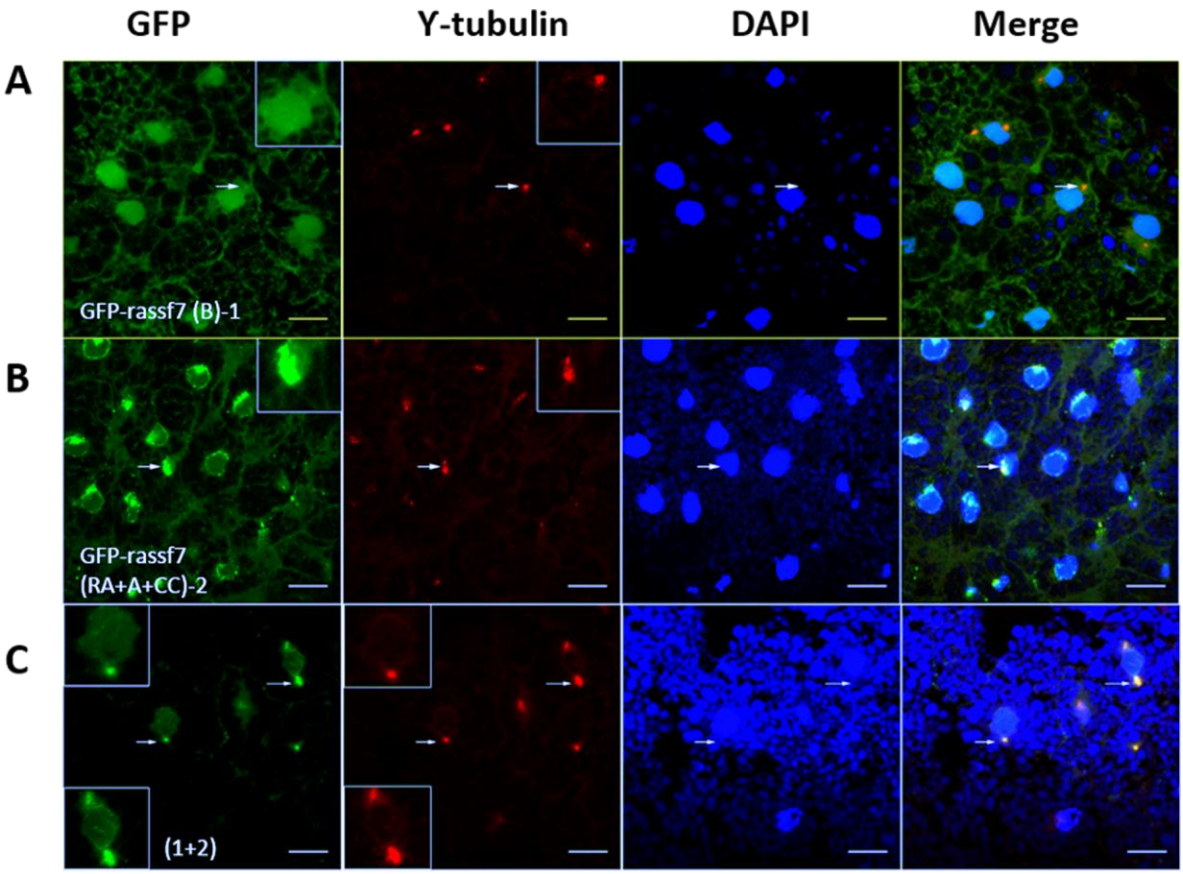

Figure 4.11: Effects of the rescue experiment on the centrosomal localisation of rassf7. Embryos were microinjected with RNA at the two-cell stage, cultured until stage 10, fixed, sectioned and images of the GFP fluorescence and γ-tubulin staining were collected by confocal microscopy.**(A)** GFP-rassf7 (B) expressing cells (green) did not show co-localisation with γ-tubulin (red) (arrows). **(B)** GFP-rassf7 (RA+A+CC) (green) co-localised with γ-tubulin (red) (arrows) and also showed accumulation of GFP at the centrosomes and an enlargement of centrosomes (see chapter 3). **(C)** When GFP-rassf7 (B) was expressed with GFP-rassf7 (RA+A+CC), cells showed co-localisation with γ-tubulin (red) (arrows). Some cells were similar to GFP-rassf7 (RA+A+CC), while others were similar to the wild type GFP-rassf7. Arrows highlight potential area for co-localisation and scale bars=10μm.

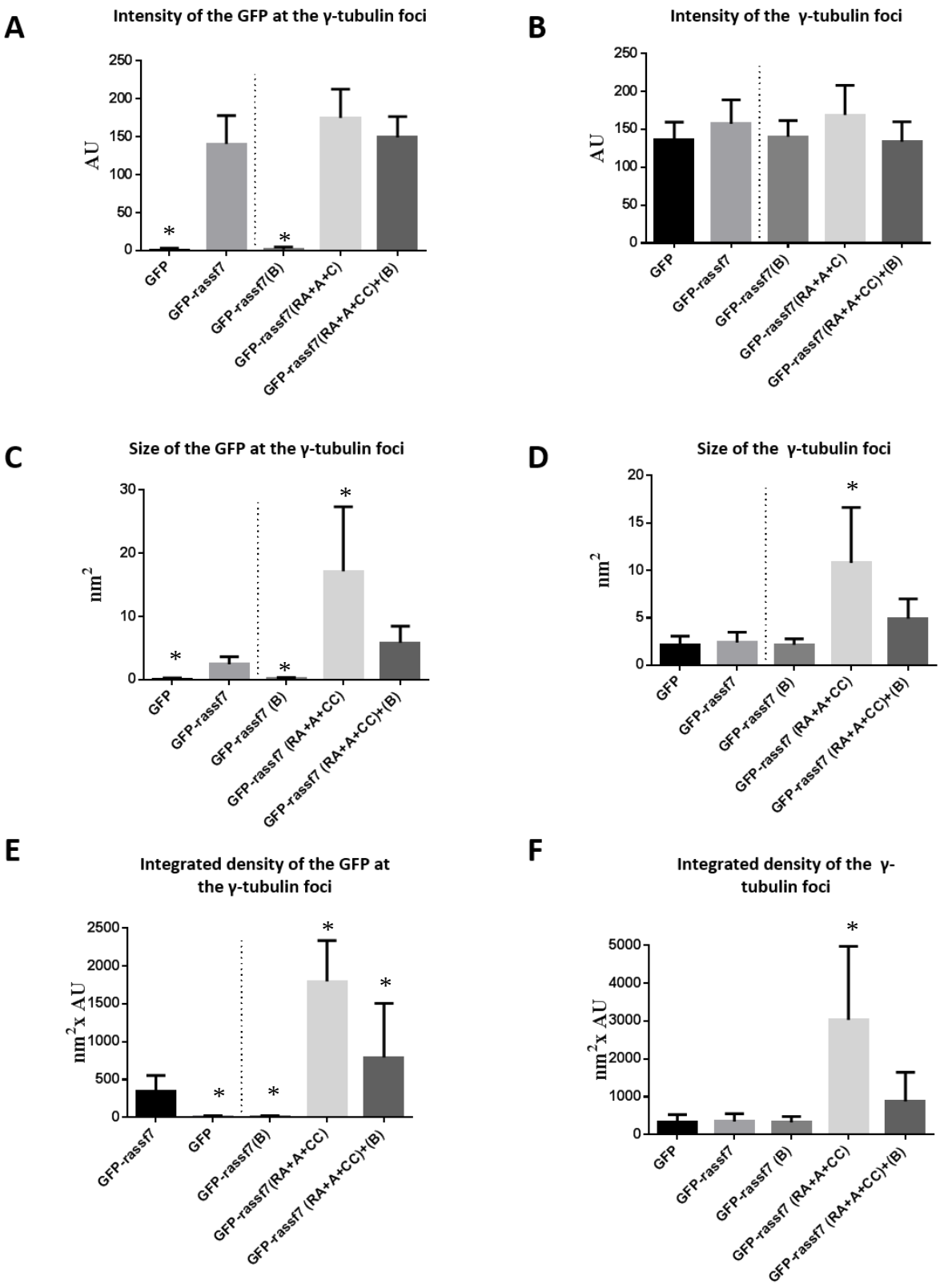
A
Intensity of the GFP at the γ-tubulin foci
AU
250
200
150
100
50
0
GFP
GFP-rassf7
GFP-rassf7(B)
GFP-rassf7(RA+A+C)
GFP-rassf7(RA+A+CC)+(B)
B
Intensity of the γ-tubulin foci
AU
250
200
150
100
50
0
GFP
GFP-rassf7
GFP-rassf7(B)
GFP-rassf7(RA+A+C)
GFP-rassf7(RA+A+CC)+(B)
C
Size of the GFP at the γ-tubulin foci
nm2
30
20
10
0
GFP
GFP-rassf7
GFP-rassf7 (B)
GFP-rassf7 (RA+A+CC)
GFP-rassf7 (RA+A+CC)+(B)
D
Size of the γ-tubulin foci
nm2
20
15
10
5
0
GFP
GFP-rassf7
GFP-rassf7 (B)
GFP-rassf7 (RA+A+CC)
GFP-rassf7 (RA+A+CC)+(B)
E
Integrated density of the GFP at the γ-tubulin foci
nm2x AU
2500
2000
1500
1000
500
0
GFP-rassf7
GFP
GFP-rassf7(B)
GFP-rassf7(RA+A+CC)
GFP-rassf7 (RA+A+CC)+(B)
F
Integrated density of the γ-tubulin foci
nm2x AU
5000
4000
3000
2000
1000
0
GFP
GFP-rassf7
GFP-rassf7 (B)
GFP-rassf7 (RA+A+CC)
GFP-rassf7 (RA+A+CC)+(B)

Figure 4.12: Quantification of the effects of the rescue experiment on centrosomal localisation of rassf7. Embryos were microinjected with RNA at the two-cell stage, cultured until stage 10, fixed, sectioned and images of the GFP fluorescence and γ-tubulin staining were collected by confocal microscopy. Example images are shown in the previous figure**.** The fluorescent area and intensity of the γ-tubulin staining and GFP was measured by using the LSM510 Image Browser software (ZEISS) and the integrated density was calculated by multiplying the area by the average intensity across the region of interest. **(A)** The intensity of GFP signal for GFP-rassf7 (RA+A+CC) + (B) was similar to full length GFP-rassf7 protein. **(B)** The intensity of γ-tubulin did not change after expressing the constructs. **(C, D, E, F)** The size of the GFP, size of the γ-tubulin spot, integrated density of GFP and integrated density of the γ-tubulin spot was significantly increased in GFP-rassf7 (RA+A+CC)+(B) expressing cells when compared to GFP-rassf7, but showed a significant decrease compared to GFP-rassf7 (RA+A+CC). Based on at least three independent experiments, bars represent standard error and were calculated and plotted using GraphPad Prism 6. Statistical analysis was carried out using One-way Anova tests with Bonferroni post-test corrections. >100 cells were measured in total, *$p<0.05$.

4.2.6 Analysis of RASSF7 mutations in human cancers

Truncated rass7, which lacks its C-terminal B domain, can drive centrosomal abnormalities (enlarged and increased numbers of Ɣ-tubulin spot), something that is often seen in cancer cells. This led to the question if there are any mutations of RASSF7 in human cancer samples similar to C-terminal truncation. To establish if similar truncations might occur, a database of mutations in human cancers has been searched.

The cBioPortal database was used to search sequence data from eighty different cancer studies for alterations in RASSF7 (Figure 4.13). RASSF7 was found to be amplified in a number of tumours, consistent with previous reports of increased RASSF7 expression (see introduction to the chapter). Twenty-three cancers, which had mutations in RASSF7, were also identified (Figure 4.14). The mutations were mainly missense mutations, but there were two nonsense mutations and one deletion that would be predicted to truncate RASSF7 (Figure 4.14). One of the nonsense mutations and the deletion were predicted to produce protein that would be truncated in or near the RA domain (Figure 4.14A and B). My data suggests that these are unlikely to localise to the centrosome and may be hypomorphs. The nonsense mutation, from a renal clear cell carcinoma, which is at R285 would be predicted to be truncated at the end of the coiled coil (Figure 4.14C). This resembles GFP-rassf7 (RA+A+CC) (Figure 3.2), and raises the possibility that in this cancer truncated RASSF7 might have accumulated at the centrosome and driven centrosome defects.

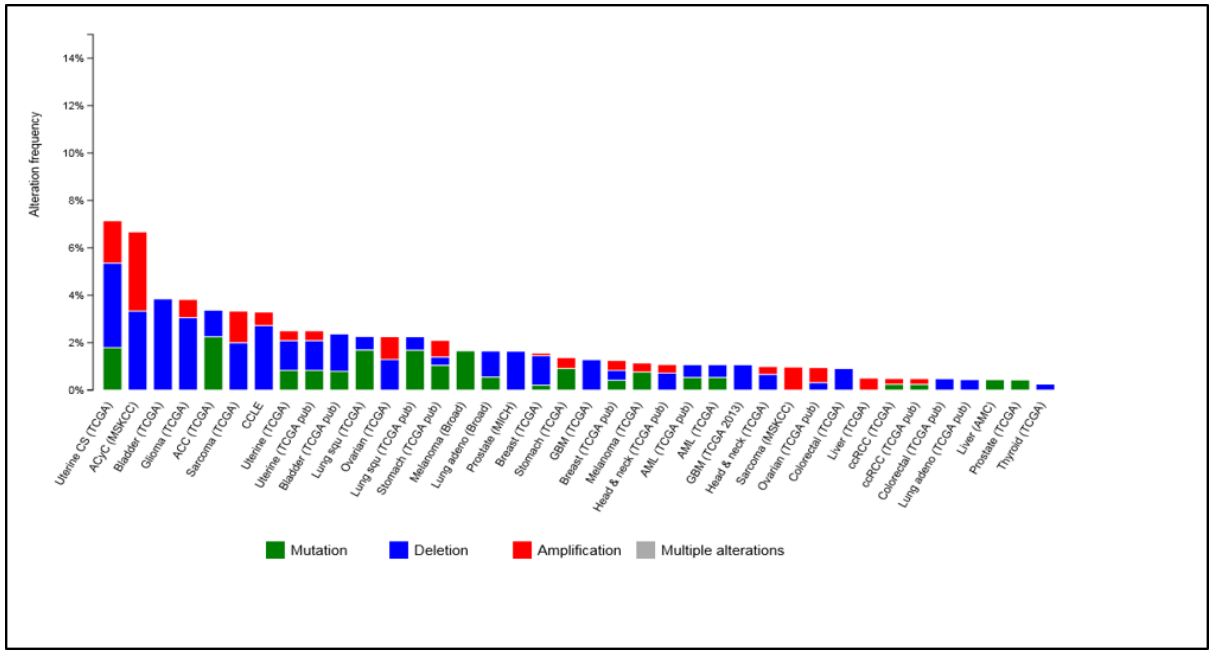

Figure 4.13: RASSF7 alterations in human cancer samples. Alterations in RASSF7 were identified in cancer studies using the cBioPortal for cancer genomics website. There are various alterations in the RASSF7 gene including, mutations (shown in green), deletions (shown in blue) and amplifications (shown in red). Multiple alterations are shown in grey.

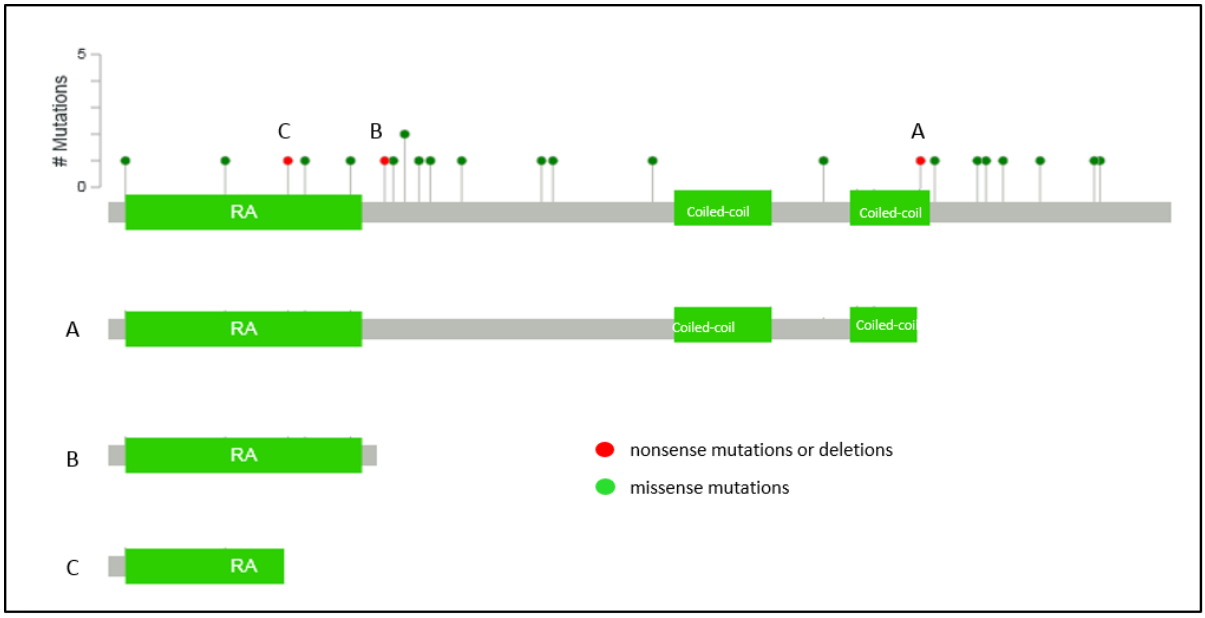

Figure 4.14: RASSF7 mutations in human cancers (red: nonsense mutations or deletions, green: missense mutations). Three nonsense mutations were applied to human RASSF7 protein sequence and domain architectures were predicted using SMART. The predicted domain architecture of RASSF7 for the three nonsense mutations represented as A, B and C. Mutation A, R285* Mutation B, S97*. Mutation C, Q63fs. The predicted structure of the R285* mutation (mutation A) reassembles that of GFP-rassf7 (RA+A+CC).

4.3 Discussion

In the current chapter, the effects of the C-terminal truncation on rassf7 function have been investigated. Experiments focused on the effect of the C-terminal truncation and data showed that C-terminal truncation of rassf7 causes supernumerary γ-tubulin spot, consistent with supernumerary centrosomes, increased number of mitotic cells and cell death later on development. The proposed auto-inhibitory role for the C terminal B domain was tested by a rescue approach and the data showed that adding GFP-rassf7 (B) as well as the GFP-rassf7 (RA+A+CC) partially rescues the accumulation of GFP at the centrosomes and the enlargement of centrosomes. Finally, a similar truncation has been identified in a human tumour samples. This data proposes that RASSF7 might act as an oncogene in a small subset of tumours when truncated C-terminally.

4.3.1 The C-terminal truncation, centrosomal amplifications, increased mitotic levels and cell death

In this current chapter expressing a tagged full length rassf7 did not drive alterations in centrosome size, number, mitotic cells or cell death. This suggests that increased levels of wild type RASSF7 when expressed in wild type cells may not act in an oncogenic role, although RASSF7 can also protect against stress induced cell death, an aspect that I have not investigated here (Takahashi et al., 2011). In contrast to the wild type protein, expression of truncated rassf7, which lacked the B domain, caused elevated amounts of γ-tubulin staining at γ-tubulin spot and an increased number of γ-tubulin spot per cell. This phenotype resemble the enlargement and amplification of

centrosomes that can occur in cancer cells (Godinho and Pellman, 2014; Godinho et al., 2014; Nigg, 2006) and recent evidence suggests that centrosome amplification can drive cellular invasion (Godinho et al., 2014). However, the mechanism/mechanisms that drive the centrosome amplifications still remain elusive. One possibility could be that the GFP-rassf7 (RA+A+CC) expressing cells may have errors during the centrosome cycle. The results reported in this thesis referred to centrosomes and centrosomal amplifications by looking at γ-tubulin spot, however other centrosomal markers are needed for further confirmation and understanding of the mechanism causing the defects discussed above. For this purpose, a centriole marker antibody (centrin) that is predicted to work in *Xenopus*, was tried but didn't work. Future work will need to look at other centrosomal markers. Furthermore, it would be interesting to see the GFP-rassf7 (RA+A+CC) expressing cells' centrosomes with electron microscopy. This would help to identify if the C-terminal truncation causes centrosome structural defects.

In GFP-rassf7 (RA+A+CC) expressing cells increased levels of mitosis were detected by Phospho-H3 staining, this is consistent with the finding that extra centrosomes prolong mitosis in human cells (Yang et al., 2008). Later in development GFP-rassf7 (RA+A+CC) expressing cells did not appear to have a clear γ-tubulin spot, however the cells showed increased programmed cell death. This could be associated with the apparent loss of γ-tubulin spot or it may be possible that the cells undergo apoptosis and therefore lose their γ-tubulin spot. Further investigations would be needed to confirm which comes first.

4.3.2 An auto-inhibitory role for the C-terminal B domain

As seen in the chapter 3 the coiled coil domain was sufficient and required for centrosomal localisation of rassf7, whereas an accumulation of rassf7 at the centrosome and an enlargement of centrosomes was seen when the B domain was removed. This raises the possibility that the B domain might act as an auto-inhibitory domain and stabilizes centrosomal localisation of rassf7. Auto-inhibitory domains are regions of proteins that negatively regulate the function of other domains via molecular interactions (see chapter introduction and Figure 4.1).

The results and the model proposed here suggested that removing the B domain could cause unregulated accumulation of rassf7 at the centrosome. Therefore, adding the B domain back to rassf7 might rescue the effects. Results showed that the rescue was partial. The partial rescue seen in the results might be due to lack of modifications or interactions when the autoinhibitory domain is added separately. A variety of protein-protein interaction assays can demonstrate intermolecular binding of an inhibitory domain to the targeted functional domain. As a future work, one assay to demonstrate auto-inhibitory role would be the FRET (Förster Resonance Energy Transfer) (Shrestha et al., 2015; Tyagi and Lemke, 2015). Well-defined structural domains of a protein retain their folded state as a protein fragment and can function in isolation from other regions. A simpler idea is that a full structure of wild type RASSF7 would show if it is folded like the proposed model. Thus, biochemical and structural approaches should be applied to test an auto-inhibitory function, along with an investigation of regulatory pathways that causes auto-inhibition. Another future direction for the rescue experiment would be to tag the B domain with another

tag (for example with an HA tag) to determine how its position and if there is any interaction with other domains. In summary, to confirm an autoinhibitory role for the B domain further experiments are required including Western Blotting. Western blotting would be a first step and would show if expression of the two protein fragments is altering their stability. The loss of phenotype could also be caused by a reduction in truncated rassf7 protein levels. Although Western Blotting was tried, it was not successful after several tries and due to time limit and requirement of many injections Western Blotting could not be processed any further.

4.3.3 The C-terminal truncation and cancer

The data presented in this chapter suggested that C-terminally truncated rassf7, GFP-rassf7 (RA+A+CC), could act as an oncogene. Interestingly, a mutation was found in RASSF7 from a renal clear cell carcinoma that would produce a similar truncation to GFP-rassf7 (RA+A+CC). My data suggests that the protein produced following this mutation could drive centrosome defects, which would be consistent with RASSF7 acting as an oncogene in this tumour. This oncogenic role would require the cancer cells to also have defects in apoptosis as the truncated protein also promoted cell death that could counter a role in promoting tumour formation. Another possibility is that other changes in tumour cells could promote more wild type RASSF7 to centrosomes, which then causes centrosome defects and promote tumour formation.

I have currently found one tumour with this type of mutation, from a database containing sequences from 80 studies and over 20,000 patient samples, suggesting that it may only be a small subset if tumours where RASSF7

functions in this way. However, as sequences from more and more tumours become available it will be interesting to see whether additional tumours with C-terminal RASSF7 truncations are discovered.

4.3.4 Conclusion

This chapter showed that the C-terminal truncation of rassf7 in Xenopus causes an amplification of the number of centrosome (γ-tubulin spot) and increased number of mitotic cells. These cells lost the centrosomal localisation and went through apoptosis later in development. Lastly, a database of tumour sequences identified a mutation in RASSF7, which would cause a similar C-terminal truncation of the protein suggesting that truncated RASSF7 could act as an oncogene.

5 Evidence for junctional rassf7 localisation

5.1 Introduction

Determining the subcellular localisation of a protein is a key step towards understanding the cellular function of that protein. However, the same protein can have different subcellular localisations within the cell and therefore could be involved in various different processes. Also, proteins may have different subcellular localisations within different species if their function is not evolutionary conserved. This chapter will focus on the possibility of rassf7 localisation in different cellular compartments, especially at the cellular junctions of epithelial cells.

5.1.1 Introduction to junctional complexes

The junctional complexes in epithelial and endothelial cells helps to create a tissue homeostasis (sometimes referred as 'barrier function') that is very important for the formation of tissue and organs (Farquhar and Palade, 1963). Epithelial cells organise into tissues that compartmentalise and line our bodies, providing the primary barrier against chemical, physical and pathogenic insults (Wang et al., 2012). However, rather than being strictly impermeable barriers, these tissues are specialised structures that must also be capable of finely regulating vectorial transport of nutrients, waste and ions (Martin-Belmonte and Perez-Moreno, 2012). As epithelial cells constitute a large percentage of the cells in the human body, and as they are constantly exposed to damaging stimuli, epithelial tumours, or carcinomas, constitute approximately 90% of all human cancers.

A common feature of carcinoma is the loss of epithelial architecture and associated functions (Martin-Belmonte and Perez-Moreno, 2012). Epithelial

tissues have an apical plasma membrane, which faces the central lumen, and a basal plasma membrane, which interacts with the underlying extracellular matrix (ECM) (Figure 5.1). As they face very different environments, the apical and baso-lateral plasma membranes require specific properties and this is achieved through asymmetric lipid and protein compositions (Martin-Belmonte and Perez-Moreno, 2012). Individual epithelial cells are joined together by various junction proteins. The apical junction complex defines the boundary between the apical and basal plasma membrane domains and consists of tight junctions, also known as the zonula occludens, and adherens junctions, or the zonula adherens (Martin-Belmonte and Perez-Moreno, 2012).

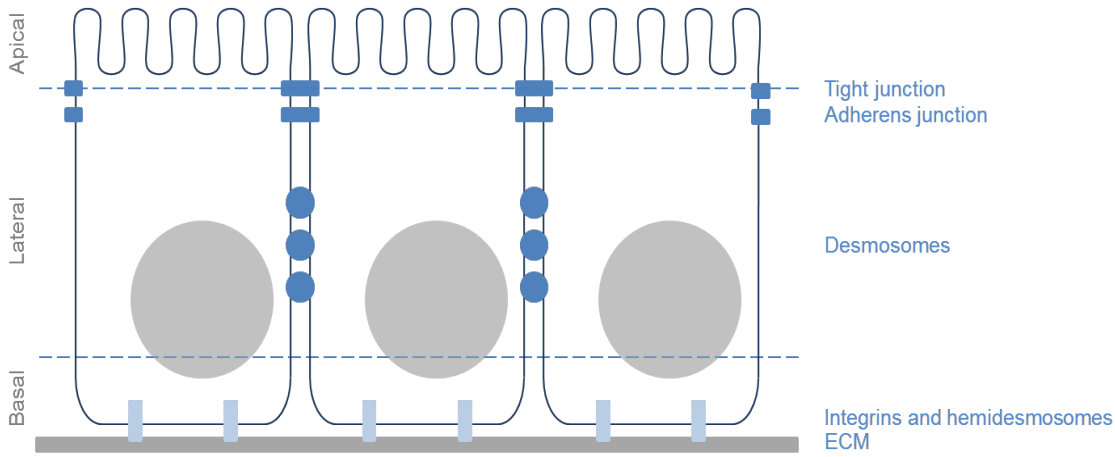

Figure 5.1: A simplified 2D schematic of an epithelium. Epithelia have a polarised structure with specialised apical and basal plasma membranes, which are composed of distinct lipids and proteins. The apical surface faces the central lumen and the basal side interacts with the underlying extracellular matrix (ECM). They are separated by the apical junction complex, which consists of the tight junction and adherens junction.

The tight junctions restrict the movement of fluids and solutes as small as ions (Aijaz et al., 2006; Farquhar and Palade, 1963). Tight junctions are composed of over forty proteins including the transmembrane proteins occludin and claudins along with peripheral membrane-associated proteins zonula occludens (ZO)-1, 2 and 3 which link the transmembrane tight junction proteins to the cytoskeleton (Aijaz et al., 2006; Matter and Balda, 2003). The contribution of tight junction proteins to barrier function is well established and modulation of expression of tight junction molecules resulted in key changes in tight junction barrier function leading to the successful metastasis of a number of different cancer types (Martin and Jiang, 2009), whereas their contribution to cell cycle is only beginning to be understood. However there is an increasing amount of studies showing the involvement of junctional proteins in cell cycle regulation (Chow et al., 2004; Huang et al., 2007; Kaplan et al., 2004; Phillips et al., 2008; Runkle et al., 2011).

5.1.2 Different cellular localisation of RASSF protein

As discussed in previous chapters (chapter 1 and 3), RASSF family members can act as shuttling proteins (such as RASSF2 and RASSF5), translocate between many different cellular compartments and have different biological roles. RASSF family mostly have tumour suppressor properties and they are involved in regulation of cell cycle and microtubules (Clark et al., 2012; Donninger et al., 2007; Richter et al., 2009; Volodko et al., 2014).

Among the N-terminal RASSF members, RASSF8 is shown to co-localise with adherens junctions both in *Drosophila* and Human (Langton et al., 2009; Lock

et al., 2010). Intriguingly, *Drosophila* has one homologue, dmRASSF7/RASSF8, which is very closely related to vertebrate RASSF7 and RASSF8 (Sherwood et al., 2010). Therefore, it is possible to speculate that RASSF7 might have a junctional localisation, but this has not seen previously in our laboratory.

5.1.3 Aims

Although it is now well established that RASSF7 localises to the centrosomes and required for completing mitosis (Recino et al., 2010; Sherwood et al., 2008), it may also have junctional localisation. This chapter will focus on:

1. Establish if rassf7 localises at the junctions in *Xenopus* embryos.
2. If it localises, investigate the responsible domain for the junctional rassf7 localisation.
3. Study the localisation of RASSF7 in human epithelial cells.

5.2 Results

5.2.1 Investigating junctional rassf7 localisation

While studying the localisation of rassf7 in *Xenopus* embryos, a striking GFP-rassf7 localisation at the junctions in the outer layer of the embryo was observed, which raised the possibility that rassf7 may localise to the junctions. In order to investigate this possibility, stage 10 embryos were examined for co-localisation with junctional marker, ZO-1.

5.2.1.1 Investigating junctional rassf7 localisation in stage 10 embryos

To establish whether rassf7 localises to the junctions, embryos were injected with GFP and GFP-rassf7. The vitelline membranes of embryos at stage 10 were removed (see Materials and Methods, vitelline membrane tends to give non-specific background staining). After sectioning, sections were stained with the tight junction marker, ZO-1 to establish any co-localisation with GFP-rassf7 (Figure 5.2). In Xenopus the outer cells are polarised epithelial cells, therefore I looked in the outer cells, which were positive for ZO-1.

It was difficult to interpret the data from early stage embryos. Although it looked like GFP-rassf7 may show some co-localisation with ZO-1 in some embryos (Figure 5.2A), the difference between negative control (GFP) expressing cells (Figure 5.2B) at the junctions was not always clear. However, clear centrosome staining in outer and inner cells was seen as previously.

Quantification of the data was also difficult as the ZO-1 staining was clear only in a few junctions. Therefore, with no clear evidence of junctional rassf7 localisation at stage 10, experiments focused on stage 30 embryos.

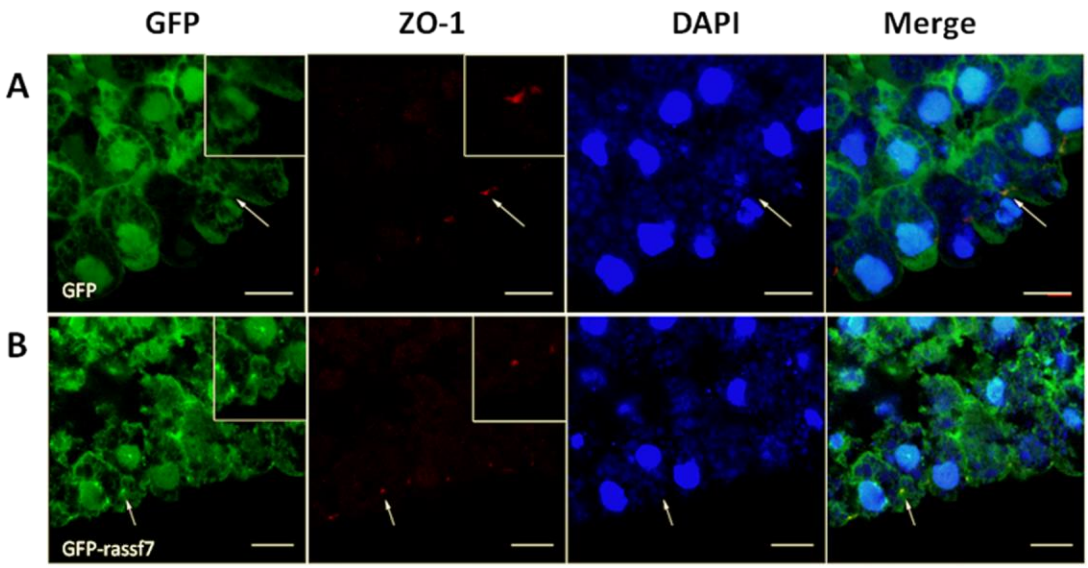

Figure 5.2: Junctional localisation of rassf7 at stage 10 embryos. Embryos were microinjected with RNA at the two-cell stage, cultured until stage 10, fixed, sectioned and stained with a tight junction marker (ZO-1/red) and a nuclear marker (DAPI/blue). GFP fluorescence is shown in green. **(A)** GFP (green) expressing cells did not seem to strongly co-localise with ZO-1 (red) **(B)** GFP-rassf7 (green) expressing cells may have a slightly stronger co-localisation with ZO-1 (red) compared to GFP expressing cells but not clear. Arrows highlight potential area for co-localisation and scale bars=10μm.

5.2.1.2 Evidence for junctional rassf7 localisation at stage 30 embryos

Having seen no obvious co-localisation with ZO-1 at stage 10, embryos were grown until stage 30, when they have a clearer outer layer for junctional staining. GFP and GFP-rassf7 expressing cells at stage 30 were stained with ZO-1 (Figure 5.3).

GFP-rassf7 expressing cells at stage 30 showed clear co-localisation with ZO-1 staining (Figure 5.3A). A GFP control, which showed some enrichment at the junctions but was much less than the full length GFP-rassf7, was used as a negative control (Figure 5.3B). This data provides the first evidence for rassf7 localisation at the tight junctions. In outer cells, GFP-rassf7 localised to junctions, whereas in inner cells, which do not have tight junctions, GFP-rassf7 still localised to the centrosomes.

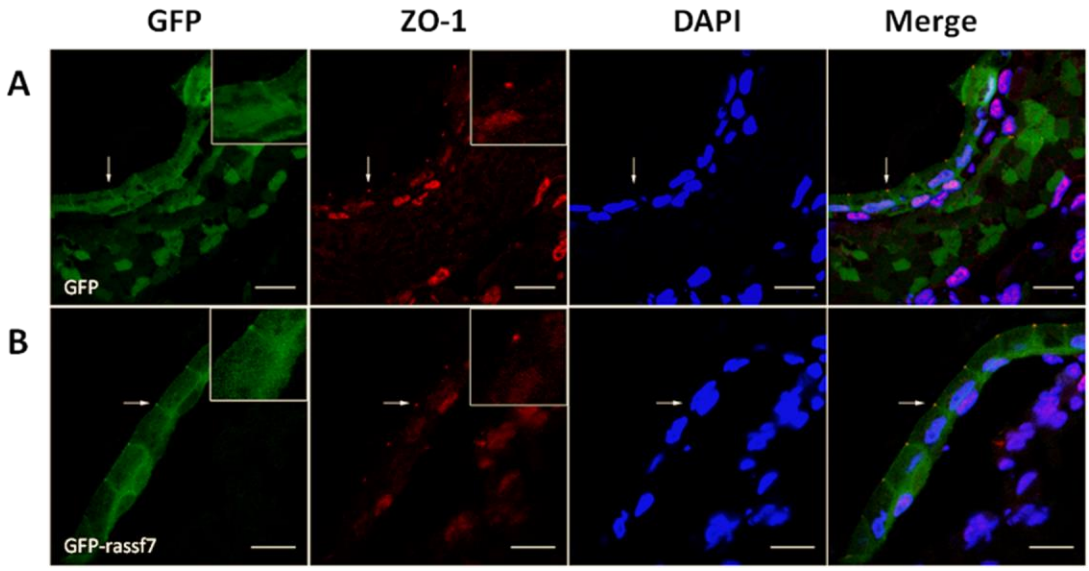

Figure 5.3: Junctional localisation of rassf7 at stage 30 embryos. Embryos were microinjected with RNA at the two-cell stage, cultured until tadpole stages (stage 30), fixed, sectioned and stained with a tight junction marker (ZO-1/red) and a nuclear marker (DAPI/blue). GFP fluorescence is shown in green. **(A)** GFP (green) expressing cells showed less co-localisation with ZO-1 (red), when compared to wild type GFP-rassf7. **(B)** GFP-rassf7 (green) expressing cells showed clear co-localisation with ZO-1 (red). Arrows highlight potential area for co-localisation and scale bars=10μm.

5.2.2 Analysis of the domains required for tight junctional rassf7 localisation

To identify the domains responsible for junctional rassf7 localisation, the GFP-domain constructs described previously were used to make the RNA injected to embryos and grown until stage 30 to study rassf7 localisation at the junctions.

5.2.2.1 The RA and A domains are not required or sufficient for tight junctional rassf7 localisation, but the coiled coil domain is sufficient and required

The GFP fusion protein that lacked the RA domain, GFP-rassf7 (A+CC+B), showed a very similar pattern of junctional localisation to full length GFP-rassf7 with clear co-localisation with ZO-1 (Figure 5.4A), whereas the GFP domain construct, which only had the RA domain, GFP-rassf7 (RA) did not co-localise with the junctions (Figure 5.4B). This suggests that the RA domain is not required or sufficient for junctional rassf7 localisation.

When both the RA and the A domains were removed, GFP-rassf7 (CC+B), a similar junctional localisation pattern was observed and GFP-rassf7 (CC+B) was able to co-localise with ZO-1 (Figure 5.4C). Thus, removing the A domain as well as the RA did not seem to affect rassf7 localisation at the junctions. Further analysis of rassf7 domains was consistent with the idea that the RA and the A domains were not required or sufficient for junctional rassf7 localisation: neither GFP-rassf7 (RA+A) nor GFP-rassf7 (A) showed co-localisation with ZO-1 (Figure 5.5A and C). However, GFP-rassf7 (CC) co-localised with ZO-1 (Figure 5.5B) indicating that the coiled coil domain is sufficient and required for junctional rassf7 localisation.

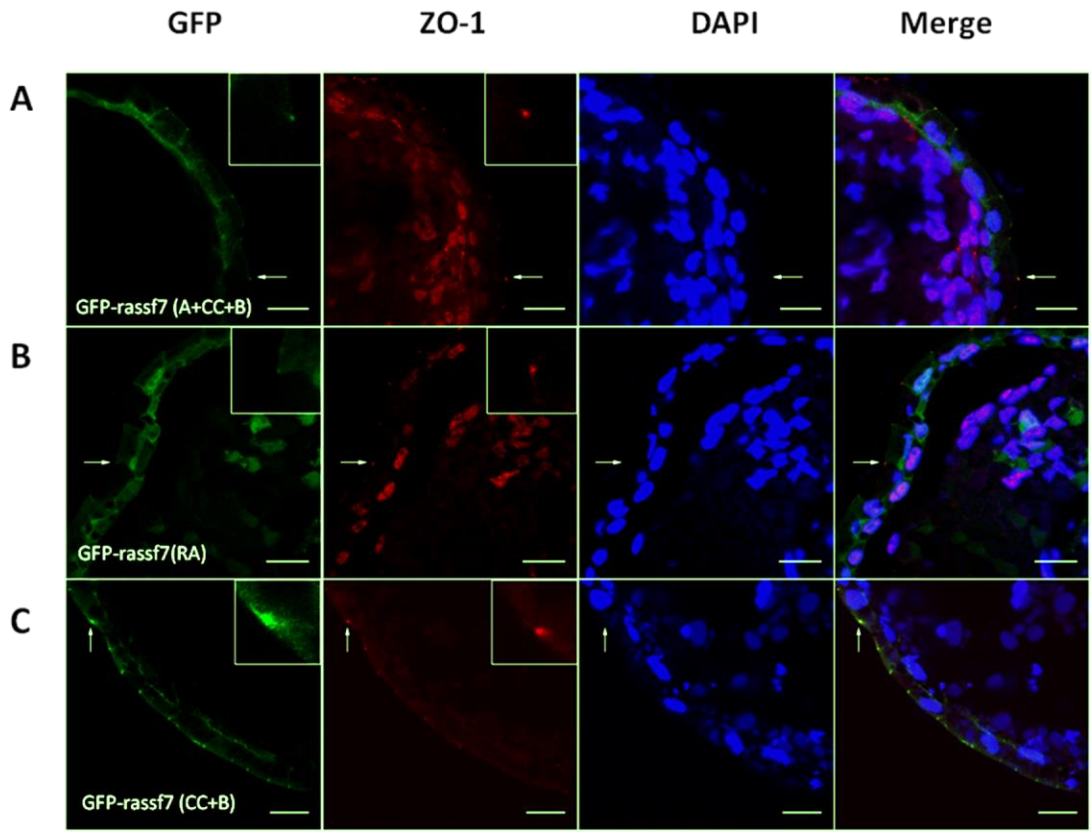

Figure 5.4: The RA and the A domains are not required for tight junctional rassf7 localisation. Embryos were microinjected with RNA at the two-cell stage, cultured until tadpole stages (stage 30), fixed, sectioned and stained with a tight junction marker (ZO-1/red) and a nuclear marker (DAPI/blue). GFP fluorescence is shown in green. **(A)** GFP-rassf7 (A+CC+B) (green) expressing cells co-localised with ZO-1 (red) **(B)** GFP-rassf7 (RA) (green) expressing cells did not co-localise with ZO-1 (red). **(C)** GFP-rassf7 (CC+B) (green) expressing cells showed co-localisation with ZO-1 (red). Arrows highlight potential area for co-localisation and scale bars=10μm.

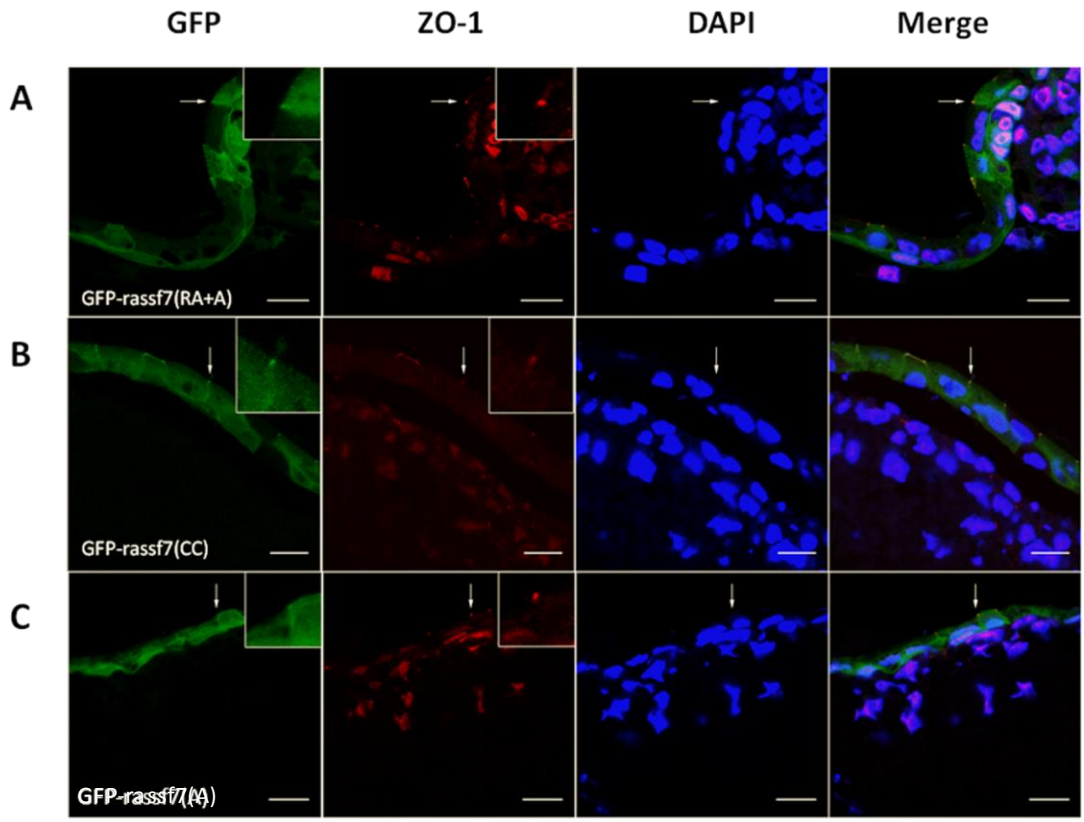

Figure 5.5: The coiled coil domain is sufficient for tight junctional rassf7 localisation. Embryos were microinjected with RNA at the two-cell stage, cultured until tadpole stages (stage 30), fixed, sectioned and stained with a tight junction marker (ZO-1/red) and a nuclear marker (DAPI/blue). GFP fluorescence is shown in green. **(A)** GFP-rassf7 (RA+A) (green) cells showed less co-localisation with ZO-1 (red), when compared to wild type rassf7. **(B)** GFP-rassf7 (CC) (green) showed co-localisation with ZO-1 (red). **(C)** GFP-rassf7 (A) (green) did not co-localise with ZO-1 (red). Arrows highlight potential area for co-localisation and scale bars=10μm.

5.2.2.2 The B domain may contribute to the tight junctional rassf7 localisation, as well as the coiled coil domain

The last set of truncations showed that the B domain may be involved in the junctional rassf7 localisation. The GFP fusion protein, GFP-rassf7 (B), which only has the B domain, also showed co-localisation with ZO-1 (Figure 5.6A).

Removing the B domain, GFP-RASSF7 (RA+A+CC) did not cause any obvious amplification of the junctions and there was no specific localisation of rassf7. Mostly cytoplasmic distribution of GFP-rassf7 (RA+A+CC) bulks was observed at stage 30 embryos (Figure 5.6B) and because of the non-specific distribution, it was difficult to study co-localisation at the junctions. Therefore, quantification was limited to the measurement of the fluorescence intensity at the ZO-1 spot. The size and therefore the integrated density of GFP at the ZO-1 spot or of the ZO-1 spot could not be measured due to the limitations.

The effect of GFP-rassf7 (A+CC) was very similar to GFP-rassf7 (RA+A+CC) (Figure 5.6C).

The quantification of the localisation of GFP-rassf7 domain constructs was consistent with the confocal images (Figure 5.7).

Domain analysis suggests that the RA and the A domains are not required for junctional rassf7 localisation whereas the coiled coil and the B domains are sufficient to drive the junctional rassf7 localisation. Additionally, removal of the B domain did not cause any obvious junctional amplification as seen with the centrosomes.

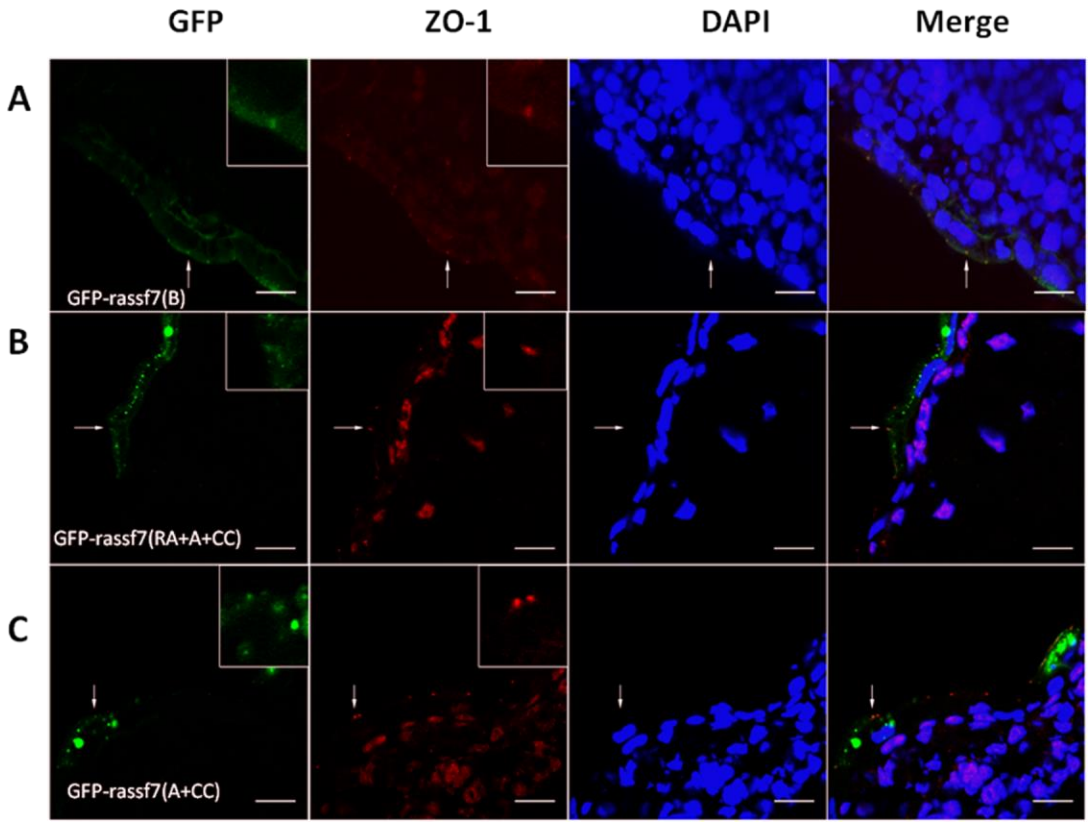

Figure 5.6: The B domain is also sufficient to drive junctional rassf7 localisation. Embryos were microinjected with RNA at the two-cell stage, cultured until tadpole stages (stage 30), fixed, sectioned and stained with a tight junction marker (ZO-1/red) and a nuclear marker (DAPI/blue). GFP fluorescence is shown in green. **(A)** GFP-rassf7 (B) (green) showed co-localisation with ZO-1 (red). **(B)** GFP-rassf7 (RA+A+CC) (green) did not co-localise with ZO-1 (red). **(C)** GFP-rassf7 (A+CC) (red) did not co-localise with ZO-1 (red). Arrows highlight potential area for co-localisation and scale bars=10μm.

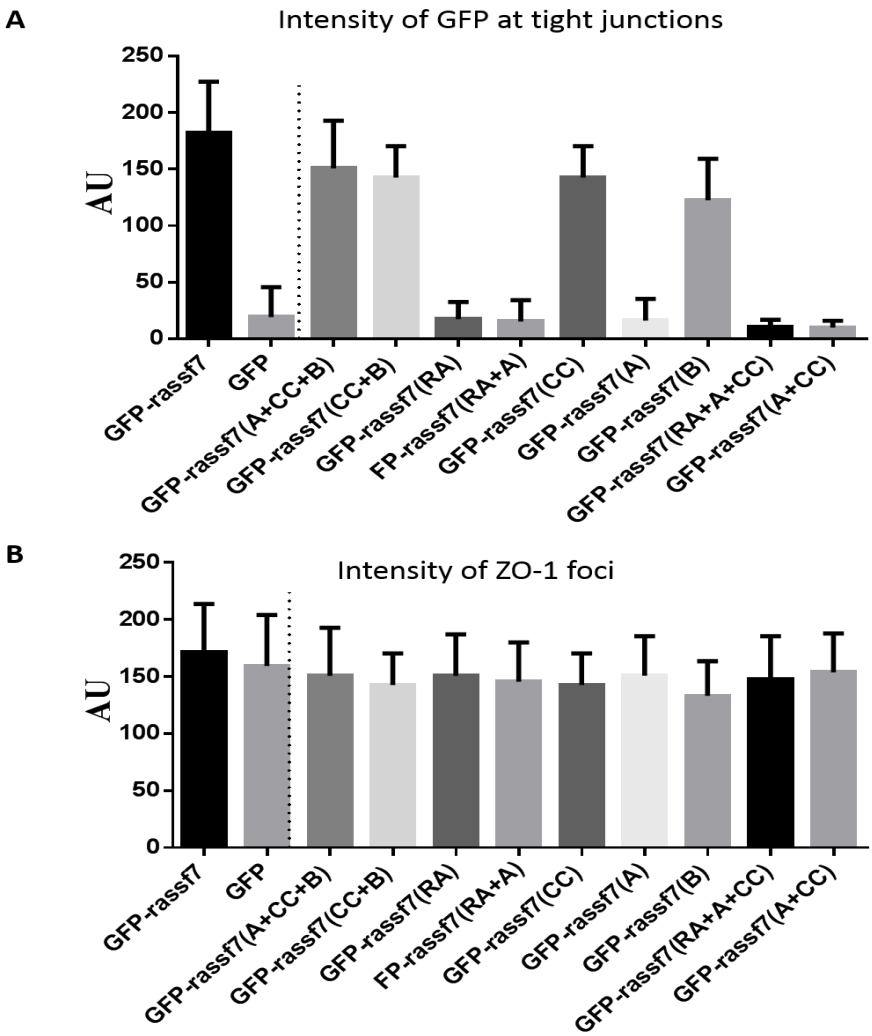

Figure 5.7: Quantification of the localisation of GFP-rassf7 domain constructs at stage 30. Embryos were microinjected with RNA at the two-cell stage, cultured until stage 30, fixed, sectioned and images of the GFP fluorescence and ZO-1 staining were collected by confocal microscopy. Example images are shown in the previous figures**.** The fluorescent intensity of the ZO-1 staining and GFP was measured by using the LSM510 Image Browser software (ZEISS). **(A)** Intensity of GFP fluorescence at the junctions for the GFP-rassf7 fusion proteins and the positive and negative controls (GFP-rassf7 and GFP). **(B)** Intensity of ZO-1 spot. Expression of truncated GFP-rassf7 proteins did not affect the intensity of the ZO-1 staining. Based on at least three independent experiments, bars represent standard error and were calculated and plotted using GraphPad Prism 6. Statistical analysis was carried out using One-way Anova tests with Bonferroni post-test corrections. >50 cells were measured in total.

5.2.3 Sub-cloning of human RASSF7 to establish junctional RASSF7 localisation in mammalian cell lines

In order to establish if RASSF7 is junctional and to study the effects of RASSF7 domains on its localisation in mammalian cell lines, the human RASSF7 was sub-cloned into a viral vector (pAd5cmv-GFP-RASSF7) for adenoviral transduction of the mammalian cell lines (see materials and methods) as viruses are easy to drive expression by infecting epithelial cells such as MDCKII which, are hard to transfect. This would help to establish if RASSF7 localises to junctions as well as the centrosomes in human epithelial cell lines. It would also make it possible to see if the C-terminal truncation of RASSF7 causes the same effect (enlargement of centrosomes, increased centrosome numbers, increased mitotic cells and cell death) on mammalian cells as well as the *Xenopus.*

Firstly the full-length GFP-RASSF7 and the C-terminally truncated GFP-RASSF7 (RA+A+CC) were sub-cloned into the viral vector. The sub-cloning process was successful, the transfection of HEK293 cells showed GFP expression when transfected with pAd5cmv-GFP-RASSF7 and pAd5cmv-GFP-RASSF7 (RA+A+CC) (Figure 5.8). However upon several repeats with different DNA concentrations of RASSF7, the production of virus was not successful, the plaque formation that is necessary for virus production did not occur. Chris Bryant's (University of Bath, PhD student) plasmid (pAd5cmv+EGFPBRAF) that has been successfully sub-cloned into same viral vector and produced virus previously, was transfected to the cells and this plasmid produced the plaque and the virus, whereas cells transfected with pAd5cmv-GFP-RASSF7 and pAd5cmv-GFP-RASSF7 (RA+A+CC) failed to produce any plaques.

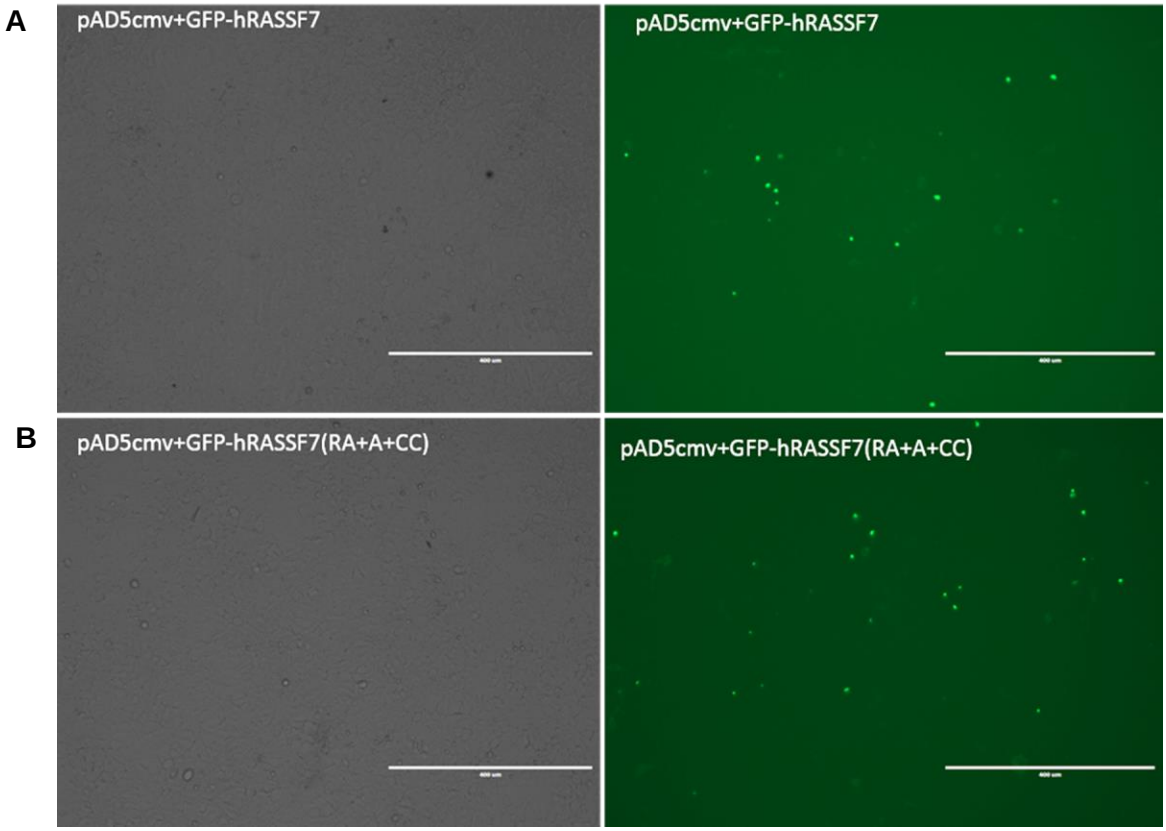

Figure 5.8: HEK293 cells expressing sub-cloned plasmids. HEK293 cells were maintained between passages 30 and 40 at 37° in DMEM supplemented with FBS. Cells were passaged twice weekly at a dilution of 1/12. **(A)** pAd5cmv+GFP-RASSF7 expressing HEK293. **(B)** pAd5cmv+GFP-RASSF7 (RA+A+CC) expressing HEK293 cells.

5.2.4 Endogenous RASSF7 staining of MDCKII cells to establish junctional RASSF7 localisation

Having failed to produce adenovirus for viral transfection of human cell lines, experiments focused on staining MDCKII cells for endogenous RASSF7 to establish if it localises to tight junctions in mammalian epithelial cells.

MDCKII cells were initially stained with RASSF7, ZO-1 and γ-tubulin antibodies individually to establish the best fixation protocol for the cells and the antibodies. Cells were fixed in MeOH (Figure 5.9A) and PFA (Figure 5.9B), MeoH gave the better antibody staining, especially for the γ-tubulin antibody. To establish if RASSF7 shows co-localisation with γ-tubulin and ZO-1 cells were fixed in MeOH; double stained with RASSF7 and γ-tubulin (Figure 5.10A) and with RASSF7 and ZO-1 antibodies (Figure 5.10B).

As it is well known from *Xenopus* (Sherwood et al., 2008) and Human (HeLa cells) (Recino et al., 2010) studies that RASSF7 localises to centrosome, co-localisation with γ-tubulin in MDCKII cells was expected. However, RASSF7 did not show co-localisation with γ-tubulin (Figure 5.10A). The double staining with ZO-1 and RASSF7 also did not indicate any co-localisations (Figure 5.10B).

Endogenous RASSF7 staining showed that RASSF7 is not junctional or centrosomal in MDCKII cells. There was not any co-localisation between RASSF7 and γ-tubulin (Figure 5.10A) and between RASSF7 and ZO-1 (Figure 5.10B). This suggests the antibody that stained HeLa cells did not work in MDCKII cells, perhaps due to species difference. Therefore it remains to be established if RASSF7 localises to junctions in mammalian cells.

To further investigate the rassf7 localisation pattern, the plasmids that were generated for the virus production (pAd5cmv+GFP-RASSF7 and

pAd5cmv+GFP-RASSF7 (RA+A+CC)) were used to transfect the MDCKII cells to look for the exogenous (GFP-RASSF7) localisation. However, the transfection of the MDCKII cells was not successful upon several trials with different DNA concentrations.

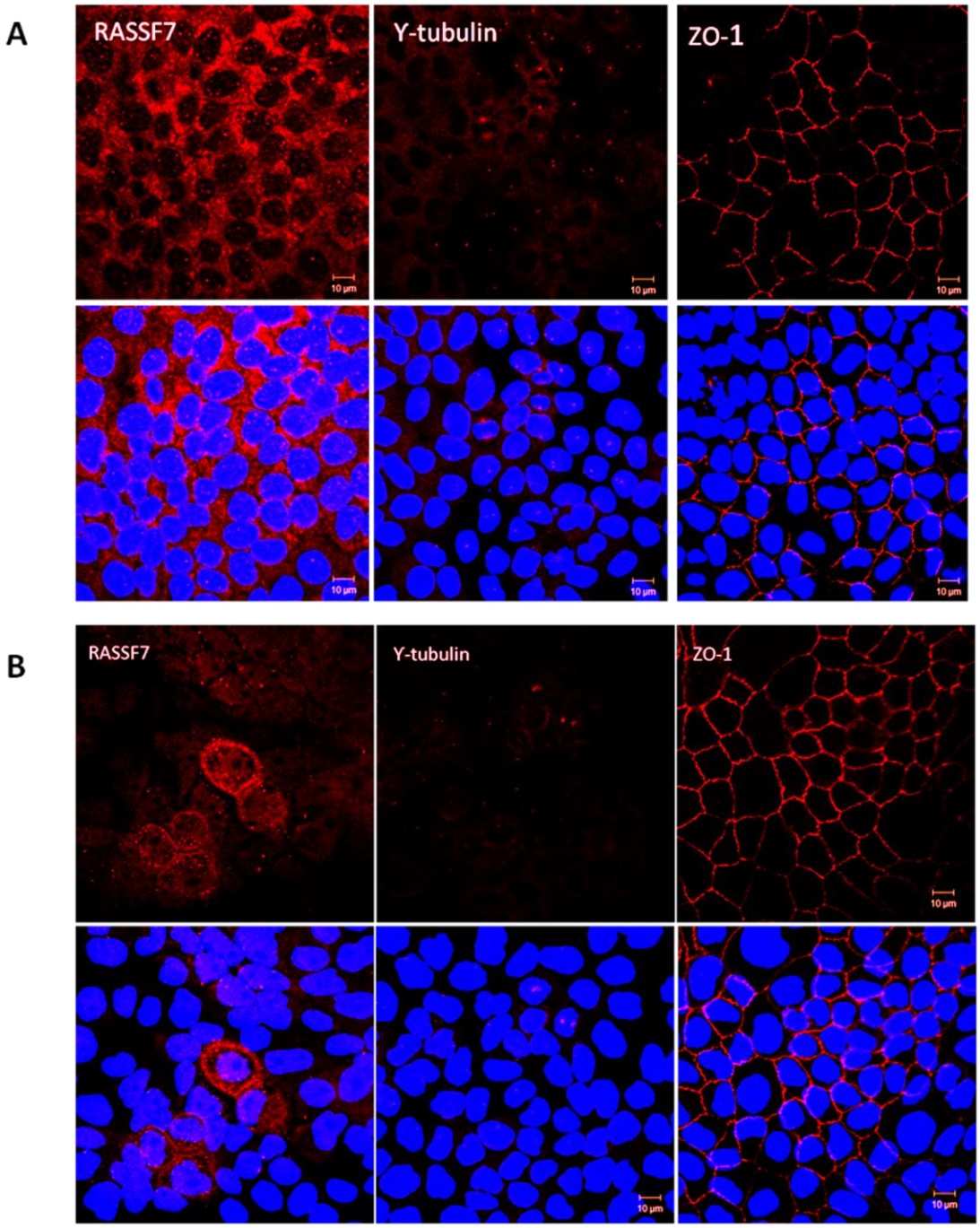
A
RASSF7
Y-tubulin
ZO-1
10 μm
B
RASSF7
Y-tubulin
ZO-1
10 μm

Figure 5.9: MDCKII cells with RASSF7, γ-tubulin and ZO-1 antibody stainings. MDCKII cells were plated at a density of 2x10^{5}cells/ml on 8-well µ-slides. Cells were fixed and permeabilised in ice-cold methanol at -20°C or in PFA at room temperature and rinsed in PBS. Non-specific binding sites were blocked in normal goat serum and cells incubated with primary and then secondary. Nuclei were counterstained with DAPI and slides were imaged using a Zeiss LSM510META laser-scanning confocal microscope. Confocal images are presented as overhead composite projections of multiple 1µM Z-slices through the MDCKII monolayer. All images were processed using ImageJ software. Images from different experimental conditions were processed in an identical fashion. Presented images are representative of three independent experiments **(A)** MDCKII cells fixed in MeOH and stained with RASSF7, γ-tubulin and ZO-1 antibodies individually. **(B)** MDCKII cells fixed in PFA and stained with RASSF7, γ-tubulin and ZO-1 antibodies individually. Lower panels show the merge images with DNA marker DAPI.

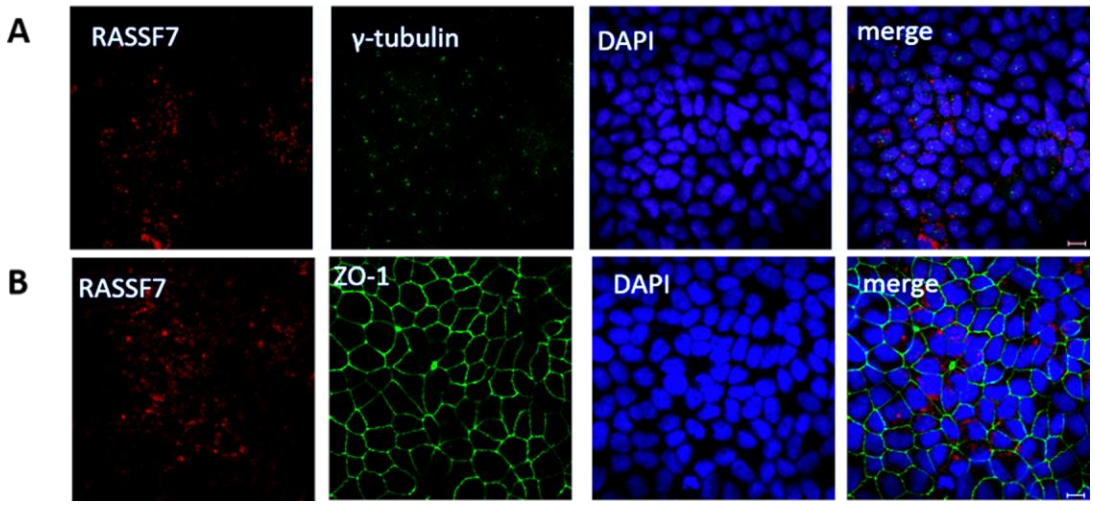

Figure 5.10: MDCKII cells with double staining. MDCKII cells were plated at a density of 2x10^{5}cells/ml on 8-well µ-slides. Cells were fixed and permeabilised in ice-cold methanol at -20°C rinsed in PBS. Non-specific binding sites were blocked in normal goat serum and cells incubated with primary and then secondary. Nuclei were counterstained with DAPI and slides were imaged using a Zeiss LSM510META laser-scanning confocal microscope. Confocal images are presented as overhead composite projections of multiple 1µM Z-slices through the MDCKII monolayer. All images were processed using ImageJ software. Images from different experimental conditions were processed in an identical fashion. Presented images are representative of three independent experiments. **(A)** MDCKII cells double stained with RASSF and γ-tubulin antibodies **(B)** MDCKII cells double stained with RASSF7 and ZO-1 antibodies. A nuclear marker (DAPI) is used for the nuclear staining (blue). No co-localisation was observed.

5.3 Discussion

In the present chapter, the junctional localisation of RASSF7 has been investigated in both *Xenopus laevis* and mammalian cell lines. This data indicates the first evidence for RASSF7 at the junctions and shows that in *Xenopus* the coiled coil and the B domains are sufficient to drive the junctional localisation on their own whereas the RA and A domain do not seem to affect the junctional rassf7 localisation. Localisation in mammalian cells needs further investigation.

5.3.1 GFP-rassf7 shows co-localisation with ZO-1 at stage 30 embryos

Data presented in this chapter showed that GFP-rassf7 co-localises with ZO-1 in outer cells of stage 30 *Xenopus* embryos, which provides the first evidence for junctional rassf7 localisation. The striking junctional GFP-rassf7 localisation was initially observed in GFP-rassf7 expressing stage 30 embryos while studying the effect of GFP-rassf7 (RA+A+CC) at later stage. This localisation was tested with negative control (GFP) to see if the GFP was going to junctions instead of rassf7 but as discussed in the results and shown by the confocal images as well as the intensity measurements, this junctional localisation was specific to rassf7.

Previous studies showed the involvement of junctional proteins in cell cycle regulation and their link with centrosomes and microtubules (Huang et al., 2007; Kaplan et al., 2004; Phillips et al., 2008; Runkle et al., 2011). For instance, a recent study showed that the junctional protein, occludin localises to the centrosomes and modifies mitotic entry (Runkle et al., 2011). Although this is the first and only study showing the centrosomal localisation of occludin;

another study shows that occludin regulates the cell division in retinal pigment epithelial cells (Phillips et al., 2008). Beta-catenin is an adherens junction protein that also localises to the centrosome (Huang et al., 2007) and regulates centrosomal separation in a Nek-2 dependent manner (Bahmanyar et al., 2008). Therefore, it is possible that centrosomal proteins may also have a role at the epithelial junctions.

Recent proteomic studies have shown that RASSF7 can interact with a number of cellular proteins, including ASPP and PP1 family members (Hauri et al., 2013). The *Drosophila* homologue of RASSF7 and RASSF8, also localises to the epithelial junctions and can also bind to dASPP (Langton et al., 2009). My data suggests that rassf7 localises to the tight junctions in *Xenopus* and the future work would need to establish the role of rassf7 at the junctions and if it involves ASPP and PP1.

5.3.2 The coiled coil and the B domains are sufficient on their own to drive junctional rassf7 localisation

The coiled coil (GFP-rassf7 CC)) and the B domains (GFP-rassf7 (B)) drove the junctional rassf7 localisation when expressed individually. A coiled coil is a protein-protein interaction domain and it may be regulating RASSF7's junctional localisation by interacting with the junctional complex. For example, the tight junction protein, occludin, discussed above, contains a coiled coil domain, whichcan act to organize the functional elements of the epithelial tight junction (Walter et al., 2009). Occludin and the adherens junctions protein, α-catenin, also interacts with another junctional protein ZO-1 via their coiled coil domains (Muller et al., 2005). Cingulin is another example of a junctional protein with a

coiled coil domain that interacts to ZO-1 via this domain (Cordenonsi et al., 1999). Thus, it is not surprising that the coiled coil of rassf7 drives the junctional localisation and as seen in chapter3 it also drives the centrosomal localisation of rassf7.

Intriguingly, the B domain was also able to drive the junctional rassf7 localisation on its own (GFP-rassf7 (B)). From the domain prediction programmes, the B domain did not come up as any known domains; it was an unknown protein region. Therefore, it is not possible to give/find example proteins that localises to junctions via this domain. However, phosphorylation prediction programmes revealed potential phosphorylation sites within the B domain (chapter 3). It may be possible that the phosphorylation of the B domain may mediate its localisation at the junctions, as it is well-known phosphorylation can mediate/control intracellular localisation of proteins (Diaz-Moreno et al., 2009; Esmenjaud-Mailhat et al., 2007). It would be interesting to see if mutating the phosphorylation site within the B domain would affect the junctional rassf7 localisation. Future work will need a blast search of the B domain, to see if any other proteins have similar domains.

Altering the other two domains of rassf7 did not affect the junctional localisation; upon removal of the RA, the A and the both domains, junctional localisation still observed. As discussed in the chapter 3, future work will need to establish any possible interaction mechanisms (such as binding partners, see final discussion) of these domains.

5.3.3 Sub-cloning of human RASSF7 to establish junctional RASSF7 localisation in human cell lines

Junctional localisation is observed in in later stage Xenopus embryos. The next section aimed to analyse the junctional localisation of rassf7 in human cell lines. However, although the sub-cloning process was successful, the virus production failed. This may be due to the RASSF7 plasmid used for sub-cloning was blocking the virus formation. Virus production has been tested with a positive control; under the same experimental conditions and it was successful. Future work will need to try an alternative system to express RASSF7 in human cell lines.

5.3.4 Endogenous RASSF7 staining in MDCKII cells

Staining MDCKII cells by using a RASSF7 antibody did not show any co-localisation with γ-tubulin and ZO-1 antibodies. It may be possible that RASSF7 has a different localisation pattern in MDCKII cells although this was unexpected especially as it has been shown in different species that RASSF7 localises to the centrosomes (Recino et al., 2010; Sherwood et al., 2008). Thus, it raised the possibility that the antibody might have not worked in this cell line, as RASSF7 antibody was a human antibody and MDCKII cells are canine in origin. Future work would be staining the other epithelial human cell lines (such as Caco2) with the RASSF7 antibody to establish junctional localisation or to raise an antibody against canine RASSF7.

The next experiments aimed to transfect the MDCKII cells with the plasmids that are generated for the virus production, pAd5cmv+GFP-RASSF7 and pAd5cmv+GFP-RASSF7 (RA+A+CC), however transfections were not

successful. Future work will need to repeat the transfections using the HeLa cells, although they don't have tight junctions and this wouldn't establish the junctional rassf7 localisation, it would be interesting to see if the centrosome defects would occur in the GFP-RASSF7 (RA+A+CC) expressing HeLa cells. Due to time limitations, RASSF7 localisation studies in human cells and further establishment of junctional RASSF7 localisation was not investigated any further.

5.3.5 Conclusion

In the current chapter, *Xenopus* rassf7 is shown to co-localise with the tight junctional marker ZO-1. These data reveal the first evidence for junctional rassf7 localisationin *Xenopus* Domain analysis studies showed that the coiled coil and the B domains were sufficient to drive the junctional rassf7 localisation on their own, whereas the RA and the A domains did not affect the localisation pattern of rassf7 at the junctions. Establishment of junctional rassf7 localisation in human cell lines could not be completed due to failure in virus production and time limitations.

6 Final Discussion

RASSF7 is a key regulator of mitosis and possible oncogene, but the molecular basis of its function remains to be elucidated. The current project aimed to understand the molecular basis of RASSF7 function with emphasis on the RASSF7 domains driving its localisation.

6.1 Main Conclusions

The key findings from this thesis demonstrated that:

- The coiled coil domain is sufficient and required for centrosomal rassf7 localisation.
- The RA domain of rassf7 does not appear to play a key role in mediating its centrosomal localisation.
- Removing the B domain of rassf7 caused it to accumulate at the γ-tubulin spot and cause accumulation of abnormally high levels of γ-tubulin.
- Expression of C-terminally truncated rassf7 also increased the number of γ-tubulin spot per cell, elevated the number of cells in mitosis and ultimately resulted in cell and embryo death.
- Analysis of sequences from human tumours identified a similar truncated version of RASSF7 from a clear renal cell carcinoma, suggesting that RASSF7 may promote centrosome defects and act as an oncogene in a small subset of tumours with such mutations.
- Localisation studies provided the first evidence for RASSF7 at the junctions and shows that in *Xenopus* the coiled coil and the B domains are sufficient to drive junctional localisation on their own.

6.2 Understanding the coiled coil driven localisation

Although it has been shown in the chapter 3 and 5 that rassf7 localises to the centrosomes and tight junctions via its coiled coil domain, due to the lack of structural studies and interaction partners, the mechanism behind the coiled coil driven rassf7 localisation remains elusive.

Previous proteomic characterisation of centrosomes found that a high percentage of centrosomal proteins contain a coiled coil (Andersen et al., 2003) and many centrosome proteins with coiled coils have been studied, however it is not clear for many centrosomal proteins if they localise to the centrosome via their coiled coil domains and if so how is this localisation driven by the coiled coil. Recently, structural studies of SAS-6 shed light on how coiled coils can drive localisation of centrosomal proteins, and provided a major advance in our molecular understanding of centriole assembly (Cottee et al., 2011; Kitagawa et al., 2011; van Breugel et al., 2011). SAS-6 is a centrosomal coiled coil protein and required for centriole duplication (Avidor-Reiss and Gopalakrishnan, 2013; Hirono, 2014; Leidel et al., 2005; Strnad et al., 2007) and the dimerization of SAS-6 coiled coil domain is required for its interaction with other centriole proteins (SAS-5), thus regulating centriole assembly (Qiao et al., 2012). These studies demonstrated that dimerization/oligomerization of coiled coil domains is necessary for other regulatory domains to interact with centriole proteins. In terms of RASSF7, the results represented in this thesis, propose a direct role for rassf7's coiled coil to interact with centrosome proteins as the GFP domain construct that had only the coiled coil domain of rassf7, GFP-rassf7 (CC), showed clear co-localisation with γ-tubulin (see chapter 3). However, the structure of RASSF7 and the binding partners has not been solved/identified.

Therefore, the exact mechanism of the rassf7 coiled coil domain driven localisation remains to be established. Future work would need to study the rassf7 structure and interaction/binding partners.

6.3 Identifying RASSF7 interaction partners are crucial to understand RASSF7 function

The identification of RASSF7 binding partners is required to fully explain the molecular mechanisms of RASSF7 function. RASSF7 could interact with other centrosomal proteins by direct or indirect binding to localise to centrosomes, and also to function in mitosis. RASSF7 interaction partners at the tight junctions would also explain the new junctional localisation pattern that was shown in chapter 5.

Potential binding partners for human RASSF7 have been identified via a number of large-scale yeast two-hybrid studies. Proteins with a possible interaction with RASSF7 include CHMP1B (charged multivesicular body protein 1B), which is associated with endosomal membrane trafficking and forms part of CHMP protein-interaction network, homologous to the yeast ESCRT III. This complex is a group of proteins involved in the formation of multivescular bodies and degradation of internalized transmembrane receptor proteins (Tsang et al., 2006). Secondly, RASSF7 interacts with a centrosome associated protein DISC1 (disrupted in schizophrenia 1), associated with schizophrenia (Morris et al., 2003). DISC1 interacts with cytoskeletal and centrosome proteins and co-localises with the centrosomal complex (Morris et al., 2003). DISC1 interaction is a good example to explain the centrosomal localisation of RASSF7 as DISC1 is shown to be required for recruiting other centrosomal proteins to the

centrosome (Fukuda et al., 2010; Kamiya et al., 2008) and is also shown to interact with microtubules (Morris et al., 2003). Lastly an interaction partner from yeast two-hybrid studies was TSC1 (tuberous sclerosis protein 1) gene product, hamartin, a peripheral membrane protein potentially involved in vesicular transport and docking (Yasui et al., 2007).

In addition to yeast two hybrid studies, a recent proteomic study has shown that RASSF7 can interact with a number of other cellular proteins, including ASPP and PP1 family members (Hauri et al., 2013). The analysis of ASPP2 and ASPP1, and the PP1G catalytic subunit interactions resulted in an network which includes RASSF7 and all three PP1 catalytic subunits (PP1A, B and G) and multiple regulatory subunits (Hauri et al., 2013). Both ASPP1 and ASPP2 can interact with three PP1 catalytic subunits, the coiled coil proteins CC85B and CC85C and RASSF7, RASSF8 and RASSF9; interaction data refined the ASPP/RASSF/PP1 sub network (Hauri et al., 2013). ASPP1 and ASSP2 do not interact with each other; therefore authors suggested a mutually exclusive ASPP/RASSF/PP1 complex (Hauri et al., 2013). ASPP localises to the junctions (Langton et al., 2009; Lock et al., 2010) and ASPP knock out mouse loses its junctions (Sullivan and Lu, 2007). dRASSF8, the Drosophila homologue of RASSF7 and RASSF8, can also bind dASPP and dRASSF8 protein localises at epithelial junctions (Langton et al., 2009). This ASPP/RASSF/PP1 complex can explain the findings from Drosophila and also a junctional role for RASSF7 as suggested by this study.

Another recent study showed that ASPP1 and ASPP2 interact with C-Nap1 (centrosome linker protein 1) and PP1 and regulates centrosome assembly (Zhang et al., 2015). RASSF7 might be involved in this interaction, however it is

crucial to verify these RASSF7 protein-protein interactions by immunoprecipitation, mass spectrometry and Western blotting techniques. Once this is done, it will be interesting to test if the constitutively active/inactive forms of the binding partners, which are capable of attenuating or reversing the mitotic aberrations observed in RASSF7 deficient cells and/or to see if these inactive forms are able to drive centrosomal localization, if there is any centrosomal amplification when interaction is blocked. Another approach would be to overexpress or knockdown of interaction partners to see if these would change RASSF7 localisation. Finally, it would also improve our understanding of rassf7 junctional localisation and what functions the protein has at the junctions.

6.4 RASSF7 and cancer

Although gene and protein studies have identified a correlation between abundant expression of RASSF7 and cancer progression (Friess et al., 2003; Logsdon et al., 2003; Lowe et al., 2007; Mutter et al., 2001; Tan et al., 2009), the lack of molecular and functional data has led to incomplete understanding of what role, if any, RASSF7 could have in cancer progression.

The results reported in this thesis, especially the existence of the C-terminal truncation of RASSF7 in a human cancer, as well as the previous work from Recino et al., (2010) and the work of Takashi and colleagues (2011) suggest an association of elevated RASSF7 levels with tumourigenesis. In addition, the new localisation pattern of rassf7 that was seen at tight junctions may suggest a new role for the protein, which could be related with cancer as the tight junction has a vital role in maintaining cell to cell integrity and that the loss of cohesion

of the structure can lead to invasion and thus metastasis of cancer cells (Martin and Jiang, 2009). Unlike other RASSF proteins with tumour suppressor properties, RASSF7 could exert an anti-apoptotic function and increased levels could be responsible for incorrect completion of mitosis if work from this thesis and previous studies are combined.

As a future work, the production of RASSF7 transgenic mice overexpressing RASSF7 could elucidate whether RASSF7 wild type or mutants have the ability to promote cancer. However, overexpressing RASSF7 on its own is not likely to be enough to promote tumour formation in a mouse model, established oncogenes may also need to be expressed.

In summary, more investigation is needed on the molecular basis of RASSF7 including its binding partners as well as the mouse knockout system to improve our understanding of RASSF7 function and its role in cancer cells.

7 References

Adams, R. R., M. Carmena, A. Carvalho, C. J. Chang, D. F. Hudson, H. Maiato, P. Vagnarelli, S. P. Wheatley, and W. C. Earnshaw, 2001a, Genetic analysis of chromosomal passenger protein function in vertebrates: Molecular Biology of the Cell, v. 12, p. 180A-180A.

Adams, R. R., M. Carmena, and W. C. Earnshaw, 2001b, Chromosomal passengers and the (aurora) ABCs of mitosis: Trends in Cell Biology, v. 11, p. 49-54.

Adams, R. R., S. P. Wheatley, A. M. Gouldsworthy, S. E. Kandels-Lewis, M. Carmena, C. Smythe, D. L. Gerloff, and W. D. Earnshaw, 2000, INCENP binds the Aurora-related kinase AIRK2 and is required to target it to chromosomes, the central spindle and cleavage furrow: Current Biology, v. 10, p. 1075-1078.

Aijaz, S., M. S. Balda, and K. Matter, 2006, Tight junctions: Molecular architecture and function: International Review of Cytology - a Survey of Cell Biology, Vol 248, v. 248, p. 261-298.

Alam, M. R., B. D. Caldwell, R. C. Johnson, D. N. Darlington, R. E. Mains, and B. A. Eipper, 1996, Novel proteins that interact with the COOH-terminal cytosolic routing determinants of an integral membrane peptide-processing enzyme: Journal of Biological Chemistry, v. 271, p. 28636-28640.

Alexander, J., D. Lim, B. A. Joughin, B. Hegemann, J. R. A. Hutchins, T. Ehrenberger, F. Ivins, F. Sessa, O. Hudecz, E. A. Nigg, A. M. Fry, A. Musacchio, P. T. Stukenberg, K. Mechtler, J.-M. Peters, S. J. Smerdon, and M. B. Yaffe, 2011, Spatial Exclusivity Combined with Positive and Negative Selection of Phosphorylation Motifs Is the Basis for Context-Dependent Mitotic Signaling: Science Signaling, v. 4.

Allen, N. P. C., H. Donninger, M. D. Vos, K. Eckfeld, L. Hesson, L. Gordon, M. J. Birrer, F. Latif, and G. J. Clark, 2007, RASSF6 is a novel member of the RASSF family of tumor suppressors: Oncogene, v. 26, p. 6203-6211.

Amaar, Y. G., M. G. Minera, L. K. Hatran, D. D. Strong, S. Mohan, and M. E. Reeves, 2006, Ras association domain family 1C protein stimulates human lung cancer cell proliferation: American Journal of Physiology-Lung Cellular and Molecular Physiology, v. 291, p. L1185-L1190.

Andersen, J. S., C. J. Wilkinson, T. Mayor, P. Mortensen, E. A. Nigg, and M. Mann, 2003, Proteomic characterization of the human centrosome by protein correlation profiling: Nature, v. 426, p. 570-574.

Anderson, R. D., R. E. Haskell, H. Xia, B. J. Roessler, and B. L. Davidson, 2000, A simple method for the rapid generation of recombinant adenovirus vectors: Gene Therapy, v. 7, p. 1034-1038.

Aoyama, Y., J. Avruch, and X. F. Zhang, 2004, Norel inhibits tumor cell growth independent of Ras or the MST1/2 kinases: Oncogene, v. 23, p. 3426-3433.

Archambault, V., and M. Carmena, 2012, Polo-like kinase-activating kinases: Cell Cycle, v. 11, p. 1490-1495.

Archambault, V., P. P. D'Avino, M. J. Deery, K. S. Lilley, and D. M. Glover, 2008, Sequestration of Polo kinase to microtubules by phosphopriming-independent binding to Map205 is relieved by phosphorylation at a CDK site in mitosis: Genes & Development, v. 22, p. 2707-2720.

Archambault, V., G. Lepine, and D. Kachaner, 2015, Understanding the Polo Kinase machine, Oncogene.

Arion, D., L. Meijer, L. Brizuela, and D. Beach, 1988, CDC2 IS A COMPONENT OF THE M-PHASE SPECIFIC HISTONE-H1 KINASE - EVIDENCE FOR IDENTITY WITH MPF: Cell, v. 55, p. 371-378.

Artimo, P., M. Jonnalagedda, K. Arnold, D. Baratin, G. Csardi, E. de Castro, S. Duvaud, V. Flegel, A. Fortier, E. Gasteiger, A. Grosdidier, C. Hernandez, V. Ioannidis, D. Kuznetsov, R. Liechti, S. Moretti, K. Mostaguir, N. Redaschi, G. Rossier, I. Xenarios, and H. Stockinger, 2012, ExPASy: SIB bioinformatics resource portal: Nucleic Acids Research, v. 40, p. W597-W603.

Ault, J. G., and C. L. Rieder, 1994, CENTROSOME AND KINETOCHORE MOVEMENT DURING MITOSIS: Current Opinion in Cell Biology, v. 6, p. 41-49.

Avidor-Reiss, T., and J. Gopalakrishnan, 2013, Building a centriole: Current Opinion in Cell Biology, v. 25, p. 72-77.

Avruch, J., M. Praskova, S. Ortiz-Vega, M.-R. Liu, and X.-F. Zhang, 2006, Nore1 and RASSF1 regulation of cell proliferation and of the MST1/2 kinases: Regulators and Effectors of Small Gtpases: Ras Family, v. 407, p. 290-310.

Avruch, J., R. Xavier, N. Bardeesy, X.-F. Zhang, M. Praskova, D. Zhou, and F. Xia, 2009, Rassf Family of Tumor Suppressor Polypeptides: Journal of Biological Chemistry, v. 284, p. 11001-11005.

Bahe, S., Y. D. Stierhof, C. J. Wilkinson, F. Leiss, and E. A. Nigg, 2005, Rootletin forms centriole-associated filaments and functions in centrosome cohesion: Journal of Cell Biology, v. 171, p. 27-33.

Bahmanyar, S., D. D. Kaplan, J. G. DeLuca, T. H. Giddings, Jr., E. T. O'Toole, M. Winey, E. D. Salmon, P. J. Casey, W. J. Nelson, and A. I. M. Barth, 2008, beta-Catenin is a Nek2 substrate involved in centrosome separation: Genes & Development, v. 22, p. 91-105.

Baksh, S., S. Tommasi, S. Fenton, V. C. Yu, L. M. Martins, G. P. Pfeifer, F. Latif, J. Downward, and B. G. Neel, 2005, The tumor suppressor RASSF1A and MAP-1 link death receptor signaling to bax conformational change and cell death: Molecular Cell, v. 18, p. 637-650.

Balczon, R., 2001, Overexpression of cyclin A in human HeLa cells induces detachment of kinetochores and spindle pole/centrosome overproduction: Chromosoma, v. 110, p. 381-392.

Barr, A. R., and F. Gergely, 2007, Aurora-A: the maker and breaker of spindle poles: Journal of Cell Science, v. 120, p. 2987-2996.

Barr, F. A., P. R. Elliott, and U. Gruneberg, 2011, Protein phosphatases and the regulation of mitosis: Journal of Cell Science, v. 124, p. 2323-2334.

Barr, F. A., and U. Gruneberg, 2007, Cytokinesis: Placing and making the final cut: Cell, v. 131, p. 847-860.

Barr, F. A., H. H. W. Sillje, and E. A. Nigg, 2004, Polo-like kinases and the orchestration of cell division: Nature Reviews Molecular Cell Biology, v. 5, p. 429-440.

Barros, T. P., K. Kinoshita, A. A. Hyman, and J. W. Raff, 2005, Aurora A activates D-TACC-Msps complexes exclusively at centrosomes to stabilize centrosomal microtubules: Journal of Cell Biology, v. 170, p. 1039-1046.

Basto, R., K. Brunk, T. Vinadogrova, N. Peel, A. Franz, A. Khodjakov, and J. W. Raff, 2008, Centrosome amplification can initiate tumorigenesis in flies: Cell, v. 133, p. 1032-1042.

Basto, R., J. Lau, T. Vinogradova, A. Gardiol, C. G. Woods, A. Khodjakov, and J. W. Raff, 2006, Flies without centrioles: Cell, v. 125, p. 1375-1386.

Belham, C., J. Roig, J. A. Caldwell, Y. Aoyama, B. E. Kemp, M. Comb, and J. Avruch, 2003, A mitotic cascade of NIMA family kinases - Nercc1/Nek9 activates the Nek6 and Nek7 kinases: Journal of Biological Chemistry, v. 278, p. 34897-34909.

Belmont, A. S., 2006, Mitotic chromosome structure and condensation: Current Opinion in Cell Biology, v. 18, p. 632-638.

Berdnik, D., and J. A. Knoblich, 2002, Drosophila aurora-A is required for centrosome maturation and actin-dependent asymmetric protein localization during mitosis: Current Biology, v. 12, p. 640-647.

Bettencourt-Dias, M., R. Giet, R. Sinka, A. Mazumdar, W. G. Lock, F. Balloux, P. J. Zafiropoulos, S. Yamaguchi, S. Winter, R. W. Carthew, M. Cooper, D. Jones, L. Frenz, and D. M. Glover, 2004, Genome-wide survey of protein kinases required for cell cycle progression: Nature, v. 432, p. 980-987.

Bettencourt-Dias, M., A. Rodrigues-Martins, L. Carpenter, M. Riparbelli, L. Lehmann, M. K. Gatt, N. Carmo, F. Balloux, G. Callaini, and D. M. Glover, 2005, SAK/PLK4 is required for centriole duplication and flagella development: Current Biology, v. 15, p. 2199-2207.

Bischoff, J. R., L. Anderson, Y. F. Zhu, K. Mossie, L. Ng, B. Souza, B. Schryver, P. Flanagan, F. Clairvoyant, C. Ginther, C. S. M. Chan, M. Novotny, D. J. Slamon, and G. D. Plowman, 1998, A homologue of Drosophila aurora kinase is oncogenic and amplified in human colorectal cancers: Embo Journal, v. 17, p. 3052-3065.

Bitko, V., N. E. Garmon, T. Cao, B. Estrada, J. E. Oakes, R. N. Lausch, and S. Barik, 2004, Activation of cytokines and NF-kappa B in corneal epithelial cells infected by respiratory syncytial virus: potential relevance in ocular inflammation and respiratory infection: Bmc Microbiology, v. 4.

Blachon, S., J. Gopalakrishnan, Y. Omori, A. Polyanovsky, A. Church, D. Nicastro, J. Malicki, and T. Avidor-Reiss, 2008, Drosophila asterless and Vertebrate Cep152 Are Orthologs Essential for Centriole Duplication: Genetics, v. 180, p. 2081-2094.

Blagden, S. P., and D. M. Glover, 2003, Polar expeditions - provisioning the centrosome for mitosis: Nature Cell Biology, v. 5, p. 505-511.

Bornens, M., 2012, The Centrosome in Cells and Organisms: Science, v. 335, p. 422-426.

BoucksonCastaing, V., M. Moudjou, D. J. P. Ferguson, S. Mucklow, Y. Belkaid, G. Milon, and P. R. Crocker, 1996, Molecular characterisation of ninein, a new coiled-coil protein of the centrosome: Journal of Cell Science, v. 109, p. 179-190.

Brait, M., M. Loyo, E. Rosenbaum, K. L. Ostrow, A. Markova, S. Papagerakis, M. Zahurak, S. N. Goodman, M. Zeiger, D. Sidransky, C. B. Umbricht, and M. O. Hoque, 2012, Correlation between BRAF mutation and promoter methylation of TIMP3, RAR beta 2 and RASSF1A in thyroid cancer: Epigenetics, v. 7, p. 710-719.

Brembeck, F. H., M. Rosario, and W. Birchmeier, 2006, Balancing cell adhesion and Wnt signaling, the key role of beta-catenin: Current Opinion in Genetics & Development, v. 16, p. 51-59.

Brinkley, B. R., 2001, Managing the centrosome numbers game: from chaos to stability in cancer cell division: Trends in Cell Biology, v. 11, p. 18-21.

Brownlee, C. W., and G. C. Rogers, 2013, Show me your license, please: deregulation of centriole duplication mechanisms that promote amplification: Cellular and Molecular Life Sciences, v. 70, p. 1021-1034.

Bruinsma, W., J. A. Raaijmakers, and R. H. Medema, 2012, Switching Polo-like kinase-1 on and off in time and space: Trends in Biochemical Sciences, v. 37, p. 534-542.

Camps, C., F. M. Buffa, S. Colella, J. Moore, C. Sotiriou, H. Sheldon, A. L. Harris, J. M. Gleadle, and J. Ragoussis, 2008, hsa-miR-210 is induced by hypoxia and is an independent prognostic factor in breast cancer: Clinical Cancer Research, v. 14, p. 1340-1348.

Carmena, M., and W. C. Earnshaw, 2003, The cellular geography of aurora kinases: Nature Reviews Molecular Cell Biology, v. 4, p. 842-854.

Castro, A., Y. Arlot-Bonnemains, S. Vigneron, J. C. Labbe, C. Prigent, and T. Lorca, 2002a, APC/Fizzy-Related targets Aurora-A kinase for proteolysis: Embo Reports, v. 3, p. 457-462.

Castro, A., S. Vigneron, C. Bernis, J. C. Labbe, C. Prigent, and T. Lorca, 2002b, The D-Box-activating domain (DAD) is a new proteolysis signal that stimulates the silent D-Box sequence of Aurora-A: Embo Reports, v. 3, p. 1209-1214.

Chalmers, A. D., K. Lacham, Y. Shin, V. Sherwood, K. W. Y. Cho, and N. Papalopulu, 2006, Grainyhead-like 3, a transcription factor identified in a microarray screen, promotes the specification of the superficial layer of the embryonic epidermis: Mechanisms of Development, v. 123, p. 702-718.

Chalmers, A. D., M. Pambos, J. Mason, S. Lang, C. Wylie, and N. Papalopulu, 2005, aPKC, Crumbs3 and Lgl2 control apicobasal polarity in early vertebrate development: Development, v. 132, p. 977-986.

Chalmers, A. D., B. Strauss, and N. Papalopulu, 2003, Oriented cell divisions asymmetrically segregate aPKC and generate cell fate diversity in the early Xenopus embryo: Development, v. 130, p. 2657-2668.

Chan, C. S. M., and D. Botstein, 1993, ISOLATION AND CHARACTERIZATION OF CHROMOSOME-GAIN AND INCREASE-IN-PLOIDY MUTANTS IN YEAST: Genetics, v. 135, p. 677-691.

Chan, J. J., D. Flatters, F. Rodrigues-Lima, J. Yan, K. Thalassinos, and M. Katan, 2013, Comparative analysis of interactions of RASSF1-10: Advances in biological regulation, v. 53, p. 190-201.

Chan, J. Y., 2011, A Clinical Overview of Centrosome Amplification in Human Cancers: International Journal of Biological Sciences, v. 7, p. 1122-1144.

Chee, M. K., and S. B. Haase, 2010, B-Cyclin/CDKs Regulate Mitotic Spindle Assembly by Phosphorylating Kinesins-5 in Budding Yeast: Plos Genetics, v. 6.

Cheeseman, I. M., S. Anderson, M. Jwa, E. M. Green, J.-s. Kang, J. R. Yates, III, C. S. M. Chan, D. G. Drubin, and G. Barnes, 2002, Phospho-regulation of kinetochore-microtubule attachments by the Aurora kinase IpI1p: Cell, v. 111, p. 163-172.

Chen, F., V. Archambault, A. Kar, P. Lio, P. P. D'Avino, R. Sinka, K. Lilley, E. D. Laue, P. Deak, L. Capalbo, and D. M. Glover, 2007, Multiple protein phosphatases are required for mitosis in Drosophila: Current Biology, v. 17, p. 293-303.

Chen, L. H., R. C. Johnson, and S. L. Milgram, 1998, P-CIP1, a novel protein that interacts with the cytosolic domain of peptidylglycine alpha-amidating monooxygenase, is associated with endosomes: Journal of Biological Chemistry, v. 273, p. 33524-33532.

Chen, X., Z. Li, J. Zhang, Z. Mao, D. Ma, and H. Wang, 2012, Tissue factor pathway inhibitor-2 may interact with nuclear protein RASSF1C: Acta Biochimica Et Biophysica Sinica, v. 44, p. 183-185.

Chen, Z. H., V. B. Indjeian, M. McManus, L. Y. Wang, and B. D. Dynlacht, 2002, CP110, a cell cycle-dependent CDK substrate, regulates centrosome duplication in human cells: Developmental Cell, v. 3, p. 339-350.

Cheng, H. Y., A. P. Schiavone, and T. E. Smithgall, 2001, A point mutation in the N-terminal coiled-coil domain releases c-Fes tyrosine kinase activity and survival signaling in myeloid leukemia cells: Molecular and Cellular Biology, v. 21, p. 6170-6180.

Chieffi, P., L. Cozzolino, A. Kisslinger, S. Libertini, S. Staibano, G. Mansueto, G. De Rosa, A. Villacci, M. Vitale, S. Linardopoulos, G. Portella, and D. Tramontano, 2006, Aurora B expression directly correlates with prostate cancer malignancy and influence prostate cell proliferation: Prostate, v. 66, p. 326-333.

Choi, M., W. Kim, M. G. Cheon, C.-W. Lee, and J.-E. Kim, 2015, Polo-like kinase 1 inhibitor BI2536 causes mitotic catastrophe following activation of the spindle assembly checkpoint in non-small cell lung cancer cells: Cancer Letters, v. 357, p. 591-601.

Chow, L. S. N., K. W. Lo, J. Kwong, A. Y. H. Wong, and D. P. Huang, 2004, Aberrant methylation of RASSF4/AD037 in nasopharyngeal carcinoma: Oncology Reports, v. 12, p. 781-787.

Cizmecioglu, O., M. Arnold, R. Bahtz, F. Settele, L. Ehret, U. Haselmann-Weiss, C. Antony, and I. Hoffmann, 2010, Cep152 acts as a scaffold for recruitment of Plk4 and CPAP to the centrosome: Journal of Cell Biology, v. 191, p. 731-739.

Clark, G. J., S. Baksh, F. Latif, and D.-S. Lim, 2012, RASSF Family Proteins: Molecular biology international, v. 2012, p. 938916-938916.

Clarke, P. R., and C. M. Zhang, 2001, Ran GTPase: a master regulator of nuclear structure and function during the eukaryotic cell division cycle?: Trends in Cell Biology, v. 11, p. 366-371.

Cohen, C., and D. A. D. Parry, 1990, ALPHA-HELICAL COILED COILS AND BUNDLES - HOW TO DESIGN AN ALPHA-HELICAL PROTEIN: Proteins-Structure Function and Genetics, v. 7, p. 1-15.

Cohen, P., 2000, The regulation of protein function by multisite phosphorylation - a 25 year update: Trends in Biochemical Sciences, v. 25, p. 596-601.

Conduit, P. T., J. H. Richens, A. Wainman, J. Holder, C. C. Vicente, M. B. Pratt, C. I. Dix, Z. A. Novak, I. M. Dobbie, L. Schermelleh, and J. W. Raff, 2014, A molecular mechanism of mitotic centrosome assembly in Drosophila: Elife, v. 3.

Cooke, C. A., M. M. S. Heck, and W. C. Earnshaw, 1987, THE INNER CENTROMERE PROTEIN (INCENP) ANTIGENS - MOVEMENT FROM INNER CENTROMERE TO MIDBODY DURING MITOSIS: Journal of Cell Biology, v. 105, p. 2053-2067.

Cooper, W. N., R. E. Dickinson, A. Dallol, E. V. Grigorieva, T. V. Pavlova, L. B. Hesson, I. Bieche, M. Broggini, E. R. Maher, E. R. Zabarovsky, G. J. Clark, and F. Latif,

2008, Epigenetic regulation of the ras effector/tumour suppressor RASSF2 in breast and lung cancer: Oncogene, v. 27, p. 1805-1811.
Cordenonsi, M., F. D'Atri, E. Hammar, D. A. D. Parry, J. Kendrick-Jones, D. Shore, and S. Citi, 1999, Cingulin contains globular and coiled-coil domains and interacts with ZO-1, ZO-2, ZO-3, and myosin: Journal of Cell Biology, v. 147, p. 1569-1581.
Cottee, M. A., J. W. Raff, S. M. Lea, and H. Roque, 2011, SAS-6 oligomerization: the key to the centriole?: Nature Chemical Biology, v. 7, p. 650-653.
Crick, F. H. C., 1953, THE FOURIER TRANSFORM OF A COILED-COIL: Acta Crystallographica, v. 6, p. 685-689.
Crose, L. E. S., K. A. Galindo, J. G. Kephart, C. Chen, J. Fitamant, N. Bardeesy, R. C. Bentley, R. L. Galindo, J.-T. A. Chi, and C. M. Linardic, 2014, Alveolar rhabdomyosarcoma-associated PAX3-FOXO1 promotes tumorigenesis via Hippo pathway suppression: Journal of Clinical Investigation, v. 124, p. 285-296.
Cunha-Ferreira, I., A. Rodrigues-Martins, I. Bento, M. Riparbelli, W. Zhang, E. Laue, G. Callaini, D. M. Glover, and M. Bettencourt-Dias, 2009, The SCF/Slimb Ubiquitin Ligase Limits Centrosome Amplification through Degradation of SAK/PLK4: Current Biology, v. 19, p. 43-49.
D'Assoro, A. B., W. L. Lingle, and J. L. Salisbury, 2002a, Centrosome amplification and the development of cancer: Oncogene, v. 21, p. 6146-6153.
D'Assoro, A. B., W. L. Lingle, and J. L. Salisbury, 2002b, Centrosome amplification and the development of cancer: Oncogene, v. 21, p. 6146-6153.
Dallol, A., A. Agathanggelou, S. L. Fenton, J. Ahmed-Choudhury, L. Hesson, M. D. Vos, G. J. Clark, J. Downward, E. R. Maher, and F. Latif, 2004, RASSFIA interacts with microtubule-associated proteins and modulates microtubule dynamics: Cancer Research, v. 64, p. 4112-4116.
Dallol, A., A. Agathanggelou, S. Tommasi, G. P. Pfeifer, E. R. Maher, and F. Latif, 2005, Involvement of the RASSF1A tumor suppressor gene in controlling cell migration: Cancer Research, v. 65, p. 7653-7659.
Dallol, A., W. N. Cooper, F. Al-Mulla, A. Agathanggelou, E. R. Maher, and F. Latif, 2007, Depletion of the ras association domain family 1, isoform A-associated novel microtubule-associated protein, C190RF5/MAP1S, causes mitotic abnormalities: Cancer Research, v. 67, p. 492-500.
Dammann, R., C. Li, J. H. Yoon, P. L. Chin, S. Bates, and G. P. Pfeifer, 2000, Epigenetic inactivation of a RAS association domain family protein from the lung tumour suppressor locus 3p21.3: Nature Genetics, v. 25, p. 315-319.
Dammermann, A., T. Muller-Reichert, L. Pelletier, B. Habermann, A. Desai, and K. Oegema, 2004, Centriole assembly requires both centriolar and pericentriolar material proteins: Developmental Cell, v. 7, p. 815-829.
Dansranjavin, T., F. Wagenlehner, S. Gattenloehner, K. Steger, W. Weidner, R. Dammann, and U. Schagdarsurengin, 2012, Epigenetic down regulation of RASSF10 and its possible clinical implication in prostate carcinoma: Prostate, v. 72, p. 1550-1558.
de Gramont, A., and O. Cohen-Fix, 2005, The many phases of anaphase: Trends in Biochemical Sciences, v. 30, p. 559-568.
De Luca, M., P. Lavia, and G. Guarguaglini, 2006, A functional interplay between Aurora-A, Plk1 and TPX2 at spindle poles - Plk1 controls centrosomal

localization of Aurora-A and TPX2 spindle association: Cell Cycle, v. 5, p. 296-303.

De Souza, C. P. C., K. A. O. Ellem, and B. G. Gabrielli, 2000, Centrosomal and cytoplasmic cdc2/cyclin B1 activation precedes nuclear mitotic events: Experimental Cell Research, v. 257, p. 11-21.

Dephoure, N., C. Zhou, J. Villen, S. A. Beausoleil, C. E. Bakalarski, S. J. Elledge, and S. P. Gygi, 2008, A quantitative atlas of mitotic phosphorylation: Proceedings of the National Academy of Sciences of the United States of America, v. 105, p. 10762-10767.

Diaz-Moreno, I., D. Hollingworth, T. A. Frenkiel, G. Kelly, S. Martin, S. Howell, M. F. Garcia-Mayoral, R. Gherzi, P. Briata, and A. Ramos, 2009, Phosphorylation-mediated unfolding of a KH domain regulates KSRP localization via 14-3-3 binding: Febs Journal, v. 276, p. 136-136.

Difilippantonio, M. J., B. M. Ghadimi, T. Howard, J. Camps, Q. T. Nguyen, D. K. Ferris, D. L. Sackett, and T. Ried, 2009, Nucleation Capacity and Presence of Centrioles Define a Distinct Category of Centrosome Abnormalities that Induces Multipolar Mitoses in Cancer Cells: Environmental and Molecular Mutagenesis, v. 50, p. 672-696.

Ditchfield, C., V. L. Johnson, A. Tighe, R. Ellston, C. Haworth, T. Johnson, A. Mortlock, N. Keen, and S. S. Taylor, 2003, Aurora B couples chromosome alignment with anaphase by targeting BubR1, Mad2, and Cenp-E to kinetochores: Journal of Cell Biology, v. 161, p. 267-280.

Djos, A., T. Martinsson, P. Kogner, and H. Caren, 2012, The RASSF gene family members RASSF5, RASSF6 and RASSF7 show frequent DNA methylation in neuroblastoma: Molecular Cancer, v. 11.

Donninger, H., N. Allen, A. Henson, J. Pogue, A. Williams, L. Gordon, S. Kassler, T. Dunwell, F. Latif, and G. J. Clark, 2011, Salvador Protein Is a Tumor Suppressor Effector of RASSF1A with Hippo Pathway-independent Functions: Journal of Biological Chemistry, v. 286, p. 18483-18491.

Donninger, H., J. A. Clark, M. K. Monaghan, M. L. Schmidt, M. Vos, and G. J. Clark, 2014, Cell Cycle Restriction Is More Important Than Apoptosis Induction for RASSF1A Protein Tumor Suppression: Journal of Biological Chemistry, v. 289, p. 31287-31295.

Donninger, H., M. D. Vos, and G. J. Clark, 2007, The RASSF1A tumor suppressor: Journal of Cell Science, v. 120, p. 3163-3172.

Doonan, J. H., 1992, CELL-DIVISION IN ASPERGILLUS: Journal of Cell Science, v. 103, p. 599-611.

Doxsey, S. J., P. Stein, L. Evans, P. D. Calarco, and M. Kirschner, 1994, PERICENTRIN, A HIGHLY CONSERVED CENTROSOME PROTEIN INVOLVED IN MICROTUBULE ORGANIZATION: Cell, v. 76, p. 639-650.

Draetta, G., and D. Beach, 1988, ACTIVATION OF CDC2 PROTEIN-KINASE DURING MITOSIS IN HUMAN-CELLS - CELL-CYCLE DEPENDENT PHOSPHORYLATION AND SUBUNIT REARRANGEMENT: Cell, v. 54, p. 17-26.

Draetta, G., F. Luca, J. Westendorf, L. Brizuela, J. Ruderman, and D. Beach, 1989, CDC2 PROTEIN-KINASE IS COMPLEXED WITH BOTH CYCLIN-A AND CYCLIN-B - EVIDENCE FOR PROTEOLYTIC INACTIVATION OF MPF: Cell, v. 56, p. 829-838.

Duelli, D. M., S. Hearn, M. P. Myers, and Y. Lazebnik, 2005, A primate virus generates transformed human cells by fusion: Journal of Cell Biology, v. 171, p. 493-503.

Dunphy, W. G., L. Brizuela, D. Beach, and J. Newport, 1988, THE XENOPUS CDC2 PROTEIN IS A COMPONENT OF MPF, A CYTOPLASMIC REGULATOR OF MITOSIS: Cell, v. 54, p. 423-431.

Durkacz, B., A. Carr, and P. Nurse, 1986, TRANSCRIPTION OF THE CDC2 CELL-CYCLE CONTROL GENE OF THE FISSION YEAST SCHIZOSACCHAROMYCES-POMBE: Embo Journal, v. 5, p. 369-373.

Dutcher, S. K., N. S. Morrissette, A. M. Preble, C. Rackley, and J. Stanga, 2002, epsilon-Tubulin is an essential component of the centriole: Molecular Biology of the Cell, v. 13, p. 3859-3869.

Dutertre, S., M. Cazales, M. Quaranta, C. Froment, V. Trabut, C. Dozier, G. Mirey, J. P. Bouche, N. Theis-Febvre, E. Schmitt, B. Monsarrat, C. Prigent, and B. Ducommun, 2004, Phosphorylation of CDC25B by Aurora-A at the centrosome contributes to the G2-M transition: Journal of Cell Science, v. 117, p. 2523-2531.

Dutertre, S., E. Hamard-Peron, J. Y. Cremet, Y. Thomas, and C. Prigent, 2005, The absence of p53 aggravates polyploidy and centrosome number abnormality induced by Aurora-C overexpression: Cell Cycle, v. 4, p. 1783-1787.

Dzhindzhev, N. S., Q. D. Yu, K. Weiskopf, G. Tzolovsky, I. Cunha-Ferreira, M. Riparbelli, A. Rodrigues-Martins, M. Bettencourt-Dias, G. Callaini, and D. M. Glover, 2010, Asterless is a scaffold for the onset of centriole assembly: Nature, v. 467, p. 714-U104.

Eckerdt, F., J. P. Yuan, and K. Strebhardt, 2005, Polo-like kinases and oncogenesis: Oncogene, v. 24, p. 267-276.

Eckfeld, K., L. Hesson, M. D. Vos, I. Bieche, F. Latif, and G. I. Clark, 2004, RASSF4/AD037 is a potential ras effector/tumor suppressor of the RASSF family: Cancer Research, v. 64, p. 8688-8693.

El-Kalla, M., C. Onyskiw, and S. Baksh, 2010, Functional importance of RASSF1A microtubule localization and polymorphisms: Oncogene, v. 29, p. 5729-5740.

Elledge, S. J., 1996, Cell cycle checkpoints: Preventing an identity crisis: Science, v. 274, p. 1664-1672.

Esmenjaud-Mailhat, C., V. Lobjois, C. Froment, R. M. Golsteyn, B. Monsarrat, and B. Ducommun, 2007, Phosphorylation of CDC25C at S263 controls its intracellular localisation: Febs Letters, v. 581, p. 3979-3985.

Eyers, P. A., E. Erikson, L. G. Chen, and J. L. Maller, 2003, A novel mechanism for activation of the protein kinase aurora A: Current Biology, v. 13, p. 691-697.

Eyers, P. A., and J. L. Maller, 2003, Regulating the regulators: Aurora A activation and mitosis: Cell cycle (Georgetown, Tex.), v. 2, p. 287-9.

Falvella, F. S., G. Manenti, M. Spinola, C. Pignatiello, B. Conti, U. Pastorino, and T. A. Dragani, 2006, Identification of RASSF8 as a candidate lung tumor suppressor gene: Oncogene, v. 25, p. 3934-3938.

Farquhar, M. G., and G. E. Palade, 1963, JUNCTIONAL COMPLEXES IN VARIOUS EPITHELIA: Journal of Cell Biology, v. 17, p. 375-&.

Ferguson, R. L., and J. L. Maller, 2008, Cyclin E-dependent localization of MCM5 regulates centrosome duplication: Journal of Cell Science, v. 121, p. 3224-3232.

Fisher, D., L. Krasinska, D. Coudreuse, and B. Novak, 2012, Phosphorylation network dynamics in the control of cell cycle transitions: Journal of Cell Science, v. 125, p. 4703-4711.

Fisher, D. L., and P. Nurse, 1996, A single fission yeast mitotic cyclin B p34(cdc2) kinase promotes both S-phase and mitosis in the absence of G(1) cyclins: Embo Journal, v. 15, p. 850-860.

Foley, C. J., H. Freedman, S. L. Choo, C. Onyskiw, N. Y. Fu, V. C. Yu, J. Tuszynski, J. C. Pratt, and S. Baksh, 2008, Dynamics of RASSF1A/MOAP-1 association with death receptors: Molecular and Cellular Biology, v. 28, p. 4520-4535.

Fontaine, S. N., S. P. Bauer, X. Lin, S. Poorfarahani, and J. A. Ybe, 2012, Replacement of charged and polar residues in the coiled-coiled interface of huntingtin-interacting protein 1 (HIP1) causes aggregation and cell death: Febs Letters, v. 586, p. 3030-3036.

Freed, E., K. R. Lacey, P. Huie, S. A. Lyapina, R. J. Deshaies, T. Stearns, and P. K. Jackson, 1999, Components of an SCE ubiquitin ligase localize to the centrosome and regulate the centrosome duplication cycle: Genes & Development, v. 13, p. 2242-2257.

Friess, H., J. Ding, J. Kleeff, L. Fenkell, J. A. Rosinski, A. Guweidhi, J. F. Reidhaar-Olson, M. Korc, J. Hammer, and M. W. Buchler, 2003, Microarray-based identification of differentially expressed growth- and metastasis-associated genes in pancreatic cancer: Cellular and Molecular Life Sciences, v. 60, p. 1180-1199.

Fry, A. M., 2002, The Nek2 protein kinase: a novel regulator of centrosome structure: Oncogene, v. 21, p. 6184-6194.

Fry, A. M., P. Descombes, C. Twomey, R. Bacchieri, and E. A. Nigg, 2000, The NIMA-related kinase X-Nek2B is required for efficient assembly of the zygotic centrosome in Xenopus laevis: Journal of Cell Science, v. 113, p. 1973-1984.

Fry, A. M., T. Mayor, P. Meraldi, Y. D. Stierhof, K. Tanaka, and E. A. Nigg, 1998a, C-Nap1, a novel centrosomal coiled-coil protein and candidate substrate of the cell cycle-regulated protein kinase Nek2: Journal of Cell Biology, v. 141, p. 1563-1574.

Fry, A. M., P. Meraldi, and E. A. Nigg, 1998b, A centrosomal function for the human Nek2 protein kinase, a member of the NIMA family of cell cycle regulators: Embo Journal, v. 17, p. 470-481.

Fu, J., M. Bian, Q. Jiang, and C. Zhang, 2007, Roles of aurora kinases in mitosis and tumorigenesis: Molecular Cancer Research, v. 5, p. 1-10.

Fu, J., I. M. Hagan, and D. M. Glover, 2015, The centrosome and its duplication cycle: Cold Spring Harbor perspectives in medicine, v. 5, p. a015800-a015800.

Fujioka, T., Y. Takebayashi, M. Ito, and T. Uchida, 2000, Nek2 expression and localization in porcine oocyte during maturation: Biochemical and Biophysical Research Communications, v. 279, p. 799-802.

Fujita, H., S. Fukuhara, A. Sakurai, A. Yamagishi, Y. Kamioka, Y. Nakaoka, M. Masuda, and N. Mochizuki, 2005, Local activation of Rap1 contributes to directional vascular endothelial cell migration accompanied by extension of microtubules on which RAPL, a Rap1-associating molecule, localizes: Journal of Biological Chemistry, v. 280, p. 5022-5031.

Fukasawa, K., 2011, Aberrant Activation of Cell Cycle Regulators, Centrosome Amplification, and Mitotic Defects: Hormones & Cancer, v. 2, p. 104-112.

.

.
Fukuda, T., S. Sugita, R. Inatome, and S. Yanagi, 2010, CAMDI controls radial migration via centrosome regulation by myosin II-mediated gamma-tubulin dynamics: Neuroscience Research, v. 68, p. E139-E139.

Ganem, N. J., Z. Storchova, and D. Pellman, 2007, Tetraploidy, aneuploidy and cancer: Current Opinion in Genetics & Development, v. 17, p. 157-162.

Gautier, J., C. Norbury, M. Lohka, P. Nurse, and J. Maller, 1988, PURIFIED MATURATION-PROMOTING FACTOR CONTAINS THE PRODUCT OF A XENOPUS HOMOLOG OF THE FISSION YEAST-CELL CYCLE CONTROL GENE CDC2+: Cell, v. 54, p. 433-439.

Geng, Y., Y.-M. Lee, M. Welcker, J. Swanger, A. Zagozdzon, J. D. Winer, J. M. Roberts, P. Kaldis, B. E. Clurman, and P. Sicinski, 2007, Kinase-independent function of cyclin E: Molecular Cell, v. 25, p. 127-139.

Gergely, F., C. Karlsson, I. Still, J. Cowell, J. Kilmartin, and J. W. Raff, 2000a, The TACC domain identifies a family of centrosomal proteins that can interact with microtubules: Proceedings of the National Academy of Sciences of the United States of America, v. 97, p. 14352-14357.

Gergely, F., D. Kidd, K. Jeffers, J. G. Wakefield, and J. W. Raff, 2000b, D-TACC: a novel centrosomal protein required for normal spindle function in the early Drosophila embryo: Embo Journal, v. 19, p. 241-252.

Ghadimi, B. M., D. L. Sackett, M. J. Difilippantonio, E. Schrock, T. Neumann, A. Jauho, G. Auer, and T. Ried, 2000, Centrosome amplification and instability occurs exclusively in aneuploid, but not in diploid colorectal cancer cell lines, and correlates with numerical chromosomal aberrations: Genes Chromosomes & Cancer, v. 27, p. 183-190.

Gharbi-Ayachi, A., J.-C. Labbe, A. Burgess, S. Vigneron, J.-M. Strub, E. Brioudes, A. Van-Dorsselaer, A. Castro, and T. Lorca, 2010, The Substrate of Greatwall Kinase, Arpp19, Controls Mitosis by Inhibiting Protein Phosphatase 2A: Science, v. 330, p. 1673-1677.

Giet, R., and D. M. Glover, 2001, Drosophila Aurora B kinase is required for histone H3 phosphorylation and condensin recruitment during chromosome condensation and to organize the central spindle during cytokinesis: Journal of Cell Biology, v. 152, p. 669-681.

Giet, R., D. McLean, S. Descamps, M. J. Lee, J. W. Raff, C. Prigent, and D. M. Glover, 2002, Drosophila Aurora A kinase is required to localize D-TACC to centrosomes and to regulate astral microtubules: Journal of Cell Biology, v. 156, p. 437-451.

Giet, R., C. Petretti, and C. Prigent, 2005, Aurora kinases, aneuploidy and cancer, a coincidence or a real link?: Trends in Cell Biology, v. 15, p. 241-250.

Giet, R., and C. Prigent, 1999, Aurora/Ipl1p-related kinases, a new oncogenic family of mitotic serine-threonine kinases: Journal of Cell Science, v. 112, p. 3591-3601.

Giet, R., R. Uzbekov, F. Cubizolles, K. Le Guellec, and C. Prigent, 1999, The Xenopus laevis aurora-related protein kinase pEg2 associates with and phosphorylates the kinesin-related protein XlEg5: Journal of Biological Chemistry, v. 274, p. 15005-15013.

.
Glover, D. M., C. Gonzalez, and J. W. Raff, 1993, THE CENTROSOME: Scientific American, v. 268, p. 62-68.

Glover, D. M., M. H. Leibowitz, D. A. McLean, and H. Parry, 1995, MUTATIONS IN AURORA PREVENT CENTROSOME SEPARATION LEADING TO THE FORMATION OF MONOPOLAR SPINDLES: Cell, v. 81, p. 95-105.

Godinho, S. A., and D. Pellman, 2014, Causes and consequences of centrosome abnormalities in cancer: Philosophical transactions of the Royal Society of London. Series B, Biological sciences, v. 369.

Godinho, S. A., R. Picone, M. Burute, R. Dagher, Y. Su, C. T. Leung, K. Polyak, J. S. Brugge, M. Thery, and D. Pellman, 2014, Oncogene-like induction of cellular invasion from centrosome amplification: Nature, v. 510, p. 167-+.

Goenczy, P., 2012, Towards a molecular architecture of centriole assembly: Nature Reviews Molecular Cell Biology, v. 13, p. 425-435.

Golsteyn, R. M., K. E. Mundt, A. M. Fry, and E. A. Nigg, 1995, CELL-CYCLE REGULATION OF THE ACTIVITY AND SUBCELLULAR-LOCALIZATION OF PLK1, A HUMAN PROTEIN-KINASE IMPLICATED IN MITOTIC SPINDLE FUNCTION: Journal of Cell Biology, v. 129, p. 1617-1628.

Gopalan, G., C. S. M. Chan, and P. J. Donovan, 1997, A novel mammalian, mitotic spindle-associated kinase is related to yeast and fly chromosome segregation regulators: Journal of Cell Biology, v. 138, p. 643-656.

Gordon, M., and S. Baksh, 2011, RASSF1A: Not a prototypical Ras effector: Small GTPases, v. 2, p. 148-157.

Goto, H., Y. Tomono, K. Ajiro, H. Kosako, M. Fujita, M. Sakurai, K. Okawa, A. Iwamatsu, T. Okigaki, T. Takahashi, and M. Inagaki, 1999, Identification of a novel phosphorylation site on histone H3 coupled with mitotic chromosome condensation: Journal of Biological Chemistry, v. 274, p. 25543-25549.

Goto, H., Y. Yasui, A. Kawajiri, E. A. Nigg, Y. Terada, M. Tatsuka, K. Nagata, and M. Inagaki, 2003, Aurora-B regulates the cleavage furrow-specific vimentin phosphorylation in the cytokinetic process: Journal of Biological Chemistry, v. 278, p. 8526-8530.

Goto, H., Y. Yasui, E. A. Nigg, and M. Inagaki, 2002, Aurora-B phosphorylates histone H3 at serine28 with regard to the mitotic chromosome condensation: Genes to Cells, v. 7, p. 11-17.

Graf, R., 2002, DdNek2, the first non-vertebrate homologue of human Nek2, is involved in the formation of microtubule-organizing centers: Journal of Cell Science, v. 115, p. 1919-1929.

Graser, S., Y.-D. Stierhof, S. B. Lavoie, O. S. Gassner, S. Lamla, M. Le Clech, and E. A. Nigg, 2007, Cep164, a novel centriole appendage protein required for primary cilium formation: Journal of Cell Biology, v. 179, p. 321-330.

Grigoryan, G., and A. E. Keating, 2008, Structural specificity in coiled-coil interactions: Current Opinion in Structural Biology, v. 18, p. 477-483.

Gromley, A., A. Jurczyk, J. Sillibourne, E. Halilovic, M. Mogensen, I. Groisman, M. Blomberg, and S. Doxsey, 2003, A novel human protein of the maternal centriole is required for the final stages of cytokinesis and entry into S phase: Journal of Cell Biology, v. 161, p. 535-545.

Gruss, O. J., R. E. Carazo-Salas, C. A. Schatz, G. Guarguaglini, J. Kast, M. Wilm, N. Le Bot, I. Vernos, E. Karsenti, and I. W. Mattaj, 2001, Ran induces spindle assembly by reversing the inhibitory effect of importin alpha on TPX2 activity: Cell, v. 104, p. 83-93.

.

Guderian, G., J. Westendorf, A. Uldschmid, and E. A. Nigg, 2010, Plk4 trans-autophosphorylation regulates centriole number by controlling beta TrCP-mediated degradation: Journal of Cell Science, v. 123, p. 2163-2169.

Guerrero-Setas, D., N. Perez-Janices, L. Blanco-Fernandez, A. Ojer, K. Cambra, M. Berdasco, M. Esteller, S. Maria-Ruiz, N. Torrea, and R. Guarch, 2013, RASSF2 hypermethylation is present and related to shorter survival in squamous cervical cancer: Modern Pathology, v. 26, p. 1111-1122.

Guo, C., S. Tommasi, L. Liu, J.-K. Yee, R. Dammann, and G. P. Pfeifer, 2007a, RASSF1A is part of a complex similar to the Drosophila Hippo/Salvador/Lats tumor-suppressor network: Current Biology, v. 17, p. 700-705.

Guo, H.-Q., M. Gao, J. Ma, T. Xiao, L.-L. Zhao, Y. Gao, and Q.-J. Pan, 2007b, Analysis of the cellular centrosome in fine-needle aspirations of the breast: Breast Cancer Research, v. 9.

Guse, A., M. Mishima, and M. Glotzer, 2005, Phosphorylation of ZEN-4/MKLP1 by aurora B regulates completion of cytokinesis: Current Biology, v. 15, p. 778-786.

Ha Kim, Y., J. Yeol Choi, Y. Jeong, D. J. Wolgemuth, and K. Rhee, 2002, Nek2 localizes to multiple sites in mitotic cells, suggesting its involvement in multiple cellular functions during the cell cycle: Biochemical and biophysical research communications, v. 290, p. 730-6.

Habedanck, R., Y. D. Stierhof, C. J. Wilkinson, and E. A. Nigg, 2005, The Polo kinase Plk4 functions in centriole duplication: Nature Cell Biology, v. 7, p. 1140-1146.

Hamanaka, R., M. R. Smith, P. M. Oconnor, S. Maloid, K. Mihalic, J. L. Spivak, D. L. Longo, and D. K. Ferris, 1995, POLO-LIKE KINASE IS A CELL-CYCLE-REGULATED KINASE ACTIVATED DURING MITOSIS: Journal of Biological Chemistry, v. 270, p. 21086-21091.

Hames, R. S., R. E. Crookes, K. R. Straatman, A. Merdes, M. J. Hayes, A. J. Faragher, and A. M. Fry, 2005, Dynamic recruitment of Nek2 kinase to the centrosome involves microtubules, PCM-1, and localized proteasomal degradation: Molecular Biology of the Cell, v. 16, p. 1711-1724.

Hames, R. S., and A. M. Fry, 2002, Alternative splice variants of the human centrosome kinase Nek2 exhibit distinct patterns of expression in mitosis: Biochemical Journal, v. 361, p. 77-85.

Hames, R. S., R. Hames, S. L. Prosser, U. Euteneuer, C. A. M. Lopes, W. Moore, H. R. Woodland, and A. M. Fry, 2008, Pix1 and Pix2 are novel WD40 microtubule-associated proteins that colocalize with mitochondria in Xenopus germ plasm and centrosomes in human cells: Experimental cell research, v. 314, p. 574-89.

Hamilton, G., K. S. Yee, S. Scrace, and E. O'Neill, 2009, ATM Regulates a RASSF1A-Dependent DNA Damage Response: Current Biology, v. 19, p. 2020-2025.

Haren, L., I. Bazin, and M.-H. Remy, 2006a, NEDD1 and microtubule nucleation complexes: to recruit for better organizing: M S-Medecine Sciences, v. 22, p. 804-806.

Haren, L., M. H. Remy, I. Bazin, I. Callebaut, M. Wright, and A. Merdes, 2006b, NEDD1-dependent recruitment of the gamma-tubulin ring complex to the centrosome is necessary for centriole duplication and spindle assembly: Journal of Cell Biology, v. 172, p. 505-515.

Haruta, M., Y. Matsumoto, H. Izumi, N. Watanabe, M. Fukuzawa, S. Matsuura, and Y. Kaneko, 2008, Combined BubR1 protein down-regulation and RASSF1A hypermethylation in Wilms tumors with diverse cytogenetic changes: Molecular Carcinogenesis, v. 47, p. 660-666.

Hatano, T., and G. Sluder, 2012, The interrelationship between APC/C and Plk1 activities in centriole disengagement: Biology Open, v. 1, p. 1153-1160.

Hatch, E. M., A. Kulukian, A. J. Holland, D. W. Cleveland, and T. Stearns, 2010, Cep152 interacts with Plk4 and is required for centriole duplication: Journal of Cell Biology, v. 191, p. 721-729.

Hauf, S., R. W. Cole, S. LaTerra, C. Zimmer, G. Schnapp, R. Walter, A. Heckel, J. van Meel, C. L. Rieder, and J. M. Peters, 2003, The small molecule Hesperadin reveals a role for Aurora B in correcting kinetochore-microtubule attachment and in maintaining the spindle assembly checkpoint: Journal of Cell Biology, v. 161, p. 281-294.

Hauri, S., A. Wepf, A. van Drogen, M. Varjosalo, N. Tapon, R. Aebersold, and M. Gstaiger, 2013, Interaction proteome of human Hippo signaling: modular control of the co-activator YAP1: Molecular Systems Biology, v. 9.

Hayden, J. H., S. S. Bowser, and C. L. Rieder, 1990, KINETOCHORES CAPTURE ASTRAL MICROTUBULES DURING CHROMOSOME ATTACHMENT TO THE MITOTIC SPINDLE - DIRECT VISUALIZATION IN LIVE NEWT LUNG-CELLS: Journal of Cell Biology, v. 111, p. 1039-1045.

Hayward, D. G., and A. M. Fry, 2006, Nek2 kinase in chromosome instability and cancer: Cancer Letters, v. 237, p. 155-166.

Heinrich, R., B. G. Neel, and T. A. Rapoport, 2002, Mathematical models of protein kinase signal transduction: Molecular Cell, v. 9, p. 957-970.

Helps, N. R., X. Luo, H. M. Barker, and P. T. W. Cohen, 2000, NIMA-related kinase 2 (Nek2), a cell-cycle-regulated protein kinase localized to centrosomes, is complexed to protein phosphatase 1: Biochemical Journal, v. 349, p. 509-518.

Hemerly, A. S., S. G. Prasanth, K. Siddiqui, and B. Stillman, 2009, Orc1 Controls Centriole and Centrosome Copy Number in Human Cells: Science, v. 323, p. 789-793.

Herrmann, C., 2003, Ras-effector interactions: after one decade: Current Opinion in Structural Biology, v. 13, p. 122-129.

Hesson, L., A. Dallol, J. D. Minna, E. R. Maher, and F. Latif, 2003, NORE1A, a homologue of RASSF1A tumour suppressor gene is inactivated in human cancers: Oncogene, v. 22, p. 947-954.

Hesson, L. B., T. L. Dunwell, W. N. Cooper, D. Catchpoole, A. T. Brini, R. Chiaramonte, M. Griffiths, A. D. Chalmers, E. R. Maher, and F. Latif, 2009, The novel RASSF6 and RASSF10 candidate tumour suppressor genes are frequently epigenetically inactivated in childhood leukaemias: Molecular Cancer, v. 8.

Hill, V. K., N. Underhill-Day, D. Krex, K. Robel, C. B. Sangan, H. R. Summersgill, M. Morris, D. Gentle, A. D. Chalmers, E. R. Maher, and F. Latif, 2011, Epigenetic inactivation of the RASSF10 candidate tumor suppressor gene is a frequent and an early event in gliomagenesis: Oncogene, v. 30, p. 978-989.

Hinchcliffe, E. H., C. Li, E. A. Thompson, J. L. Maller, and G. Sluder, 1999, Requirement of Cdk2-cyclin E activity for repeated centrosome reproduction in Xenopus egg extracts: Science, v. 283, p. 851-854.

Hinchcliffe, E. H., F. J. Miller, M. Cham, A. Khodjakov, and G. Sluder, 2001, Requirement of a centrosomal activity for cell cycle progression through G(1) into S phase: Science, v. 291, p. 1547-1550.

Hirono, M., 2014, Cartwheel assembly: Philosophical transactions of the Royal Society of London. Series B, Biological sciences, v. 369.

Hochegger, H., N. Hegarat, and J. B. Pereira-Leal, 2013, Aurora at the pole and equator: overlapping functions of Aurora kinases in the mitotic spindle: Open Biology, v. 3.

Holland, A. J., D. Fachinetti, S. Da Cruz, Q. Zhu, B. Vitre, M. Lince-Faria, D. Chen, N. Parish, I. M. Verma, M. Bettencourt-Dias, and D. W. Cleveland, 2012, Polo-like kinase 4 controls centriole duplication but does not directly regulate cytokinesis: Molecular Biology of the Cell, v. 23, p. 1838-1845.

Holland, A. J., W. Lan, S. Niessen, H. Hoover, and D. W. Cleveland, 2010, Polo-like kinase 4 kinase activity limits centrosome overduplication by autoregulating its own stability: Journal of Cell Biology, v. 188, p. 191-198.

Holy, T. E., and S. Leibler, 1994, DYNAMIC INSTABILITY OF MICROTUBULES AS AN EFFICIENT WAY TO SEARCH IN-SPACE: Proceedings of the National Academy of Sciences of the United States of America, v. 91, p. 5682-5685.

Honda, K., H. Mihara, Y. Kato, A. Yamaguchi, H. Tanaka, H. Yasuda, K. Furukawa, and T. Urano, 2000, Degradation of human Aurora2 protein kinase by the anaphase-promoting complex-ubiquitin-proteasome pathway: Oncogene, v. 19, p. 2812-2819.

Hsu, J. Y., Z. W. Sun, X. M. Li, M. Reuben, K. Tatchell, D. K. Bishop, J. M. Grushcow, C. J. Brame, J. A. Caldwell, D. F. Hunt, R. L. Lin, M. M. Smith, and C. D. Allis, 2000, Mitotic phosphorylation of histone H3 is governed by Ipl1/aurora kinase and Glc7/PP1 phosphatase in budding yeast and nematodes: Cell, v. 102, p. 279-291.

Hu, H. M., C. K. Chuang, M. J. Lee, T. C. Tseng, and T. K. Tang, 2000, Genomic organization, expression, and chromosome localization of a third aurora-related kinase gene, Aie1: DNA and Cell Biology, v. 19, p. 679-688.

Huang, P., T. Senga, and M. Hamaguchi, 2007, A novel role of phospho-beta-catenin in microtubule regrowth at centrosome: Oncogene, v. 26, p. 4357-4371.

Huang, Z., W. Li, S. Lin, X. Fang, C. Zhang, and Z. Liao, 2014, Identification of novel tumor suppressor genes down-regulated in recurrent nasopharyngeal cancer by DNA microarray: Indian journal of otolaryngology and head and neck surgery : official publication of the Association of Otolaryngologists of India, v. 66, p. 120-5.

Hutterer, A., D. Berdnik, F. Wirtz-Peitz, M. Zigman, A. Schleiffer, and J. A. Knoblich, 2006, Mitotic activation of the kinase Aurora-A requires its binding partner Bora: Developmental Cell, v. 11, p. 147-157.

Ikeda, M., S. Hirabayashi, N. Fujiwara, H. Mori, A. Kawata, J. Iida, Y. Bao, T. Iida, H. Sugimura, and Y. Hata, 2007, Ras-association domain family protein 6 induces apoptosis via both caspase-dependent and caspase-independent pathways: Experimental Cell Research, v. 313, p. 1484-1495.

Ikeda, M., A. Kawata, M. Nishikawa, Y. Tateishi, M. Yamaguchi, K. Nakagawa, S. Hirabayashi, Y. Bao, S. Hidaka, Y. Hirata, and Y. Hata, 2009, Hippo Pathway-Dependent and -Independent Roles of RASSF6: Science Signaling, v. 2.

Inoue, S., and E. D. Salmon, 1995, FORCE GENERATION BY MICROTUBULE ASSEMBLY DISASSEMBLY IN MITOSIS AND RELATED MOVEMENTS: Molecular Biology of the Cell, v. 6, p. 1619-1640.

Irimia, M., M. F. Fraga, M. Sanchez-Cespedes, and M. Esteller, 2004, CpG island promoter hypermethylation of the Ras-effector gene NORE1A occurs in the context of a wild-type K-ras in lung cancer: Oncogene, v. 23, p. 8695-8699.

Ishikawa, H., A. Kubo, and S. Tsukita, 2005, Odf2-deficient mother centrioles lack distal/subdistal appendages and the ability to generate primary cilia: Nature Cell Biology, v. 7, p. 517-U79.

Iwasa, H., T. Kudo, S. Maimaiti, M. Ikeda, J. Maruyama, K. Nakagawa, and Y. Hata, 2013, The RASSF6 Tumor Suppressor Protein Regulates Apoptosis and the Cell Cycle via MDM2 Protein and p53 Protein: Journal of Biological Chemistry, v. 288, p. 30320-30329.

Jacquemart, I. C., A. E. B. Springs, and W. Y. Chen, 2009, Rassf3 is responsible in part for resistance to mammary tumor development in neu transgenic mice: International Journal of Oncology, v. 34, p. 517-528.

Jakobsen, L., K. Vanselow, M. Skogs, Y. Toyoda, E. Lundberg, I. Poser, L. G. Falkenby, M. Bennetzen, J. Westendorf, E. A. Nigg, M. Uhlen, A. A. Hyman, and J. S. Andersen, 2011, Novel asymmetrically localizing components of human centrosomes identified by complementary proteomics methods: Embo Journal, v. 30, p. 1520-1535.

Jemseena, V., and M. Gopalakrishnan, 2013, Microtubule catastrophe from protofilament dynamics: Physical Review E, v. 88.

Jiang, F., N. P. Caraway, A. L. Sabichi, H. Z. Zhang, A. Ruitrok, H. B. Grossman, J. Gu, S. P. Lerner, S. Lippman, and R. L. Katz, 2003, Centrosomal abnormality is common in and a potential biomarker for bladder cancer: International Journal of Cancer, v. 106, p. 661-665.

Kaitna, S., M. Mendoza, V. Jantsch-Plunger, and M. Glotzer, 2000, Incenp and an Aurora-like kinase form a complex essential for chromosome segregation and efficient completion of cytokinesis: Current Biology, v. 10, p. 1172-1181.

Kalab, P., and R. Heald, 2008, The RanGTP gradient - a GPS for the mitotic spindle: Journal of Cell Science, v. 121, p. 1577-1586.

Kamiya, A., P. L. Tan, K.-i. Kubo, C. Engelhard, K. Ishizuka, A. Kubo, S. Tsukita, A. E. Pulver, K. Nakajima, N. G. Cascella, N. Katsanis, and A. Sawa, 2008, Recruitment of PCM1 to the centrosome by the cooperative action of DISC1 and BBS4 - A candidate for psychiatric illnesses: Archives of General Psychiatry, v. 65, p. 996-1006.

Kang, S., H.-S. Kim, S. S. Seo, S.-Y. Park, D. Sidransky, and S. M. Dong, 2007, Inverse correlation between RASSF1A hypermethylation, KRAS and BRAF mutations in cervical adenocarcinoma: Gynecologic Oncology, v. 105, p. 662-666.

Kapitein, L. C., E. J. G. Peterman, B. H. Kwok, J. H. Kim, T. M. Kapoor, and C. F. Schmidt, 2005, The bipolar mitotic kinesin Eg5 moves on both microtubules that it crosslinks: Nature, v. 435, p. 114-118.

Kaplan, D. D., T. E. Meigs, P. Kelly, and P. J. Casey, 2004, Identification of a role for beta-catenin in the establishment of a bipolar mitotic spindle: Journal of Biological Chemistry, v. 279, p. 10829-10832.

Karaiskou, A., L. H. Perez, I. Ferby, R. Ozon, C. Jessus, and A. R. Nebreda, 2001, Differential regulation of Cdc2 and Cdk2 by RINGO and Cyclins: Journal of Biological Chemistry, v. 276, p. 36028-36034.

Kastan, M. B., and J. Bartek, 2004, Cell-cycle checkpoints and cancer: Nature, v. 432, p. 316-323.

Katagiri, K., A. Maeda, M. Shimonaka, and T. Kinashi, 2003, RAPL, a Rap1-binding molecule that mediates Rap1-induced adhesion through spatial regulation of LFA-1: Nature Immunology, v. 4, p. 741-748.

Katagiri, K., Y. Ueda, T. Tomiyama, K. Yasuda, Y. Toda, S. Ikehara, K. I. Nakayama, and T. Kinashi, 2011, Deficiency of Rap1-Binding Protein RAPL Causes Lymphoproliferative Disorders through Mislocalization of p27kip1: Immunity, v. 34, p. 24-38.

Katayama, H., T. Ota, F. Jisaki, Y. Ueda, T. Tanaka, S. Odashima, F. Suzuki, Y. Terada, and M. Tatsuka, 1999, Mitotic kinase expression and colorectal cancer progression: Journal of the National Cancer Institute, v. 91, p. 1160-1162.

Kettenbach, A. N., D. K. Schweppe, B. K. Faherty, D. Pechenick, A. A. Pletnev, and S. A. Gerber, 2011, Quantitative Phosphoproteomics Identifies Substrates and Functional Modules of Aurora and Polo-Like Kinase Activities in Mitotic Cells: Science Signaling, v. 4.

Khokhlatchev, A., S. Rabizadeh, R. Xavier, M. Nedwidek, T. Chen, X. F. Zhang, B. Seed, and J. Avruch, 2002, Identification of a novel Ras-regulated proapoptotic pathway: Current Biology, v. 12, p. 253-265.

Kimura, M., S. Kotani, T. Hattori, N. Sumi, T. Yoshioka, K. Todokoro, and Y. Okano, 1997, Cell cycle-dependent expression and spindle pole localization of a novel human protein kinase, aik, related to aurora of Drosophila and yeast Ipl1: Journal of Biological Chemistry, v. 272, p. 13766-13771.

Kimura, M., Y. Matsuda, T. Yoshioka, and Y. Okano, 1999, Cell cycle-dependent expression and centrosome localization of a third human Aurora/Ip11-related protein kinase, AIK3: Journal of Biological Chemistry, v. 274, p. 7334-7340.

Kirkham, M., T. Muller-Reichert, K. Oegema, S. Grill, and A. A. Hyman, 2003, SAS-4 is a C-elegans centriolar protein that controls centrosome size: Cell, v. 112, p. 575-587.

Kitagawa, D., H. Kajiho, T. Negishi, S. Ura, T. Watanabe, T. Wada, H. Ichijo, T. Katada, and H. Nishina, 2006, Release of RASSF1C from the nucleus by Daxx degradation links DNA damage and SAPK/JNK activation: Embo Journal, v. 25, p. 3286-3297.

Kitagawa, D., I. Vakonakis, N. Olieric, M. Hilbert, D. Keller, V. Olieric, M. Bortfeld, M. C. Erat, I. Flueckiger, P. Goenczy, and M. O. Steinmetz, 2011, Structural Basis of the 9-Fold Symmetry of Centrioles: Cell, v. 144, p. 364-375.

Kitajima, T. S., T. Sakuno, K. Ishiguro, S. Iemura, T. Natsume, S. A. Kawashima, and Y. Watanabe, 2006, Shugoshin collaborates with protein phosphatase 2A to protect cohesin: Nature, v. 441, p. 46-52.

Klajic, J., T. Fleischer, E. Dejeux, H. Edvardsen, F. Warnberg, I. Bukholm, P. E. Lonning, H. Solvang, A.-L. Borresen-Dale, J. Tost, and V. N. Kristensen, 2013, Quantitative DNA methylation analyses reveal stage dependent DNA methylation and association to clinico-pathological factors in breast tumors: Bmc Cancer, v. 13.

Klebba, J. E., D. W. Buster, T. A. McLamarrah, N. M. Rusan, and G. C. Rogers, 2015, Autoinhibition and relief mechanism for Polo-like kinase 4: Proceedings of the National Academy of Sciences of the United States of America, v. 112, p. E657-E666.

Kleylein-Sohn, J., J. Westendorf, M. Le Clech, R. Habedanck, Y.-D. Stierhof, and E. A. Nigg, 2007, Plk4-induced centriole biogenesis in human cells: Developmental Cell, v. 13, p. 190-202.

Kohlmaier, G., J. Loncarek, X. Meng, B. F. McEwen, M. M. Mogensen, A. Spektor, B. D. Dynlacht, A. Khodjakov, and P. Goenczy, 2009, Overly Lona Centrioles and Defective Cell Division upon Excess of the SAS-4-Related Protein CPAP: Current Biology, v. 19, p. 1012-1018.

Kok, K., S. L. Naylor, and C. Buys, 1997, Deletions of the short arm of chromosome 3 in solid tumors and the search for suppressor genes: Advances in Cancer Research, Vol 71, v. 71, p. 27-92.

Kops, G. J. P. L., 2009, Dividing the goods: co-ordination of chromosome biorientation and mitotic checkpoint signalling by mitotic kinases: Biochemical Society Transactions, v. 37, p. 971-975.

Korah, R., J. M. Healy, J. W. Kunstman, A. L. Fonseca, A. H. Ameri, M. L. Prasad, and T. Carling, 2013, Epigenetic silencing of RASSF1A deregulates cytoskeleton and promotes malignant behavior of adrenocortical carcinoma: Molecular Cancer, v. 12.

Korzeniewski, N., R. Cuevas, A. Duensing, and S. Duensing, 2010, Daughter Centriole Elongation Is Controlled by Proteolysis: Molecular Biology of the Cell, v. 21, p. 3942-3951.

Kramer, A., J. Lukas, and J. Bartek, 2004, Checking out the centrosome: Cell Cycle, v. 3, p. 1390-1393.

Kudo, T., M. Ikeda, M. Nishikawa, Z. Yang, K. Ohno, K. Nakagawa, and Y. Hata, 2012, The RASSF3 Candidate Tumor Suppressor Induces Apoptosis and G(1)-S Cell-Cycle Arrest via p53: Cancer Research, v. 72, p. 2901-2911.

Kufer, T. A., H. H. W. Sillje, R. Korner, O. J. Gruss, P. Meraldi, and E. A. Nigg, 2002, Human TPX2 is required for targeting Aurora-A kinase to the spindle: Journal of Cell Biology, v. 158, p. 617-623.

Kumagai, A., and W. G. Dunphy, 1996, Purification and molecular cloning of Plx1, a Cdc25-regulatory kinase from Xenopus egg extracts: Science, v. 273, p. 1377-1380.

Kumari, G., and S. Mahalingam, 2009, Extracellular signal-regulated kinase 2 (ERK-2) mediated phosphorylation regulates nucleo-cytoplasmic shuttling and cell growth control of Ras-associated tumor suppressor protein, RASSF2: Experimental Cell Research, v. 315, p. 2775-2790.

Kumari, G., P. K. Singhal, R. Suryaraja, and S. Mahalingam, 2010, Functional Interaction of the Ras Effector RASSF5 with the Tyrosine Kinase Lck: Critical Role in Nucleocytoplasmic Transport and Cell Cycle Regulation: Journal of Molecular Biology, v. 397, p. 89-109.

Labbe, J. C., M. G. Lee, P. Nurse, A. Picard, and M. Doree, 1988, ACTIVATION AT M-PHASE OF A PROTEIN-KINASE ENCODED BY A STARFISH HOMOLOG OF THE CELL-CYCLE CONTROL GENE CDC2+: Nature, v. 335, p. 251-254.

Lane, H. A., and E. A. Nigg, 1996, Antibody microinjection reveals an essential role for human polo-like kinase 1 (Plk1) in the functional maturation of mitotic centrosomes: Journal of Cell Biology, v. 135, p. 1701-1713.

Langton, P. F., J. Colombani, E. H. Y. Chan, A. Wepf, M. Gstaiger, and N. Tapon, 2009, The dASPP-dRASSF8 Complex Regulates Cell-Cell Adhesion during Drosophila Retinal Morphogenesis: Current Biology, v. 19, p. 1969-1978.

Lee, C.-M., P. Yang, L.-C. Chen, C.-C. Chen, S.-C. Wu, H.-Y. Cheng, and Y.-S. Chang, 2011, A Novel Role of RASSF9 in Maintaining Epidermal Homeostasis: Plos One, v. 6.

Lee, K. S., T. Z. Grenfell, F. R. Yarm, and R. L. Erikson, 1998, Mutation of the polo-box disrupts localization and mitotic functions of the mammalian polo kinase Plk: Proceedings of the National Academy of Sciences of the United States of America, v. 95, p. 9301-9306.

Lee, K. S., Y. L. O. Yuan, R. Kuriyama, and R. L. Erikson, 1995, PLK IS AN M-PHASE-SPECIFIC PROTEIN-KINASE AND INTERACTS WITH A KINESIN-LIKE PROTEIN, CHO1/MKLP-1: Molecular and Cellular Biology, v. 15, p. 7143-7151.

Leidel, S., M. Delattre, L. Cerutti, K. Baumer, and P. Gonczy, 2005, SAS-6 defines a protein family required for centrosome duplication in C-elegans and in human cells: Nature Cell Biology, v. 7, p. 115-U19.

Lens, S. M. A., E. E. Voest, and R. H. Medema, 2010, Shared and separate functions of polo-like kinases and aurora kinases in cancer: Nature Reviews Cancer, v. 10, p. 825-841.

Lerman, M. I., J. D. Minna, and C. Int Lung Canc, 2000, The 630-kb lung cancer homozygous deletion region on human chromosome 3p21.3: Identification and evaluation of the resident candidate tumor suppressor genes: Cancer Research, v. 60, p. 6116-6133.

Li, J., V. D'Angiolella, E. S. Seeley, S. Kim, T. Kobayashi, W. Fu, E. I. Campos, M. Pagano, and B. D. Dynlacht, 2013a, USP33 regulates centrosome biogenesis via deubiquitination of the centriolar protein CP110: Nature, v. 495, p. 255-259.

Li, X., G. Zhao, Y. Wang, J. Zhang, Z. Duan, and S. Xin, 2013b, RASSF7 and RASSF8 proteins are predictive factors for development and metastasis in malignant thyroid neoplasms: Journal of Cancer Research and Therapeutics, v. 9, p. S173-S177.

Li, X., G. Zhao, Y. H. Wang, J. Zhang, Z. Q. Duan, and S. J. Xin, 2013c, RASSF7 and RASSF8 proteins are predictive factors for development and metastasis in malignant thyroid neoplasms: Journal of Cancer Research and Therapeutics, v. 9, p. S173-S177.

Liang, G.-P., Y.-Y. Su, J. Chen, Z.-C. Yang, Y.-S. Liu, and X.-D. Luo, 2009, Analysis of the early adaptive response of endothelial cells to hypoxia via a long serial analysis of gene expression: Biochemical and Biophysical Research Communications, v. 384, p. 415-419.

Lindqvist, A., M. de Bruijn, L. Macurek, A. Bras, A. Mensinga, W. Bruinsma, O. Voets, O. Kranenburg, and R. H. Medema, 2009, Wip1 confers G2 checkpoint recovery competence by counteracting p53-dependent transcriptional repression: Embo Journal, v. 28, p. 3196-3206.

Lingle, W. L., S. L. Barrett, V. C. Negron, A. B. D'Assoro, K. Boeneman, W. G. Liu, C. M. Whitehead, C. Reynolds, and J. L. Salisbury, 2002, Centrosome amplification drives chromosomal instability in breast tumor development: Proceedings of the National Academy of Sciences of the United States of America, v. 99, p. 1978-1983.

Littlepage, L. E., and J. V. Ruderman, 2002, Identification of a new APC/C recognition domain, the A box, which is required for the Cdh1-dependent destruction of the kinase Aurora-A during mitotic exit: Molecular Biology of the Cell, v. 13, p. 171A-172A.

Littlepage, L. E., H. Wu, T. Andresson, J. K. Deanehan, L. T. Amundadottir, and J. V. Ruderman, 2002, Identification of phosphorylated residues that affect the activity of the mitotic kinase Aurora-A: Proceedings of the National Academy of Sciences of the United States of America, v. 99, p. 15440-15445.

Liu, L. M., S. Tommasi, D. H. Lee, R. Dammann, and G. P. Pfeifer, 2003, Control of microtubule stability by the RASSF1A tumor suppressor: Oncogene, v. 22, p. 8125-8136.

Liu, L. Y., A. Vo, and W. L. McKeehan, 2005, Specificity of the methylation-suppressed A isoform of candidate tumor suppressor RASSF1 for microtubule hyperstabilization is determined by cell death inducer C19ORF5: Cancer Research, v. 65, p. 1830-1838.

Lock, F. E., N. Underhill-Day, T. Dunwell, D. Matallanas, W. Cooper, L. Hesson, A. Recino, A. Ward, T. Pavlova, E. Zabarovsky, M. M. Grant, E. R. Maher, A. D. Chalmers, W. Kolch, and F. Latif, 2010, The RASSF8 candidate tumor suppressor inhibits cell growth and regulates the Wnt and NF-kappa B signaling pathways: Oncogene, v. 29, p. 4307-4316.

Logsdon, C. D., D. M. Simeone, C. Binkley, T. Arumugam, J. K. Greenson, T. J. Giordano, D. E. Misek, R. Kuick, and S. Hanash, 2003, Molecular profiling of pancreatic adenocarcinoma and chronic pancreatitis identifies multiple genes differentially regulated in pancreatic cancer (vol 63, pg 2649, 2003): Cancer Research, v. 63, p. 3445-3445.

Lohka, M. J., M. K. Hayes, and J. L. Maller, 1988, PURIFICATION OF MATURATION-PROMOTING FACTOR, AN INTRACELLULAR REGULATOR OF EARLY MITOTIC EVENTS: Proceedings of the National Academy of Sciences of the United States of America, v. 85, p. 3009-3013.

Loncarek, J., P. Hergert, V. Magidson, and A. Khodjakov, 2008, Control of daughter centriole formation by the pericentriolar material: Nature Cell Biology, v. 10, p. 322-U55.

Lou, Y., W. Xie, D. F. Zhang, J. H. Yao, Z. F. Luo, Y. Z. Wang, Y. Y. Shi, and X. B. Yao, 2004a, Nek2A specifies the centrosomal localization of Erk2: Biochemical and Biophysical Research Communications, v. 321, p. 495-501.

Lou, Y., J. H. Yao, A. Zereshki, Z. Dou, K. Ahmed, H. M. Wang, J. B. Hu, Y. Z. Wang, and X. B. Yao, 2004b, NEK2A interacts with MAD1 and possibly functions as a novel integrator of the spindle checkpoint signaling: Journal of Biological Chemistry, v. 279, p. 20049-20057.

Lowe, A. W., M. Olsen, Y. Hao, S. P. Lee, K. T. Lee, X. Chen, M. van de Rijn, and P. O. Brown, 2007, Gene Expression Patterns in Pancreatic Tumors, Cells and Tissues: Plos One, v. 2.

Lu, D., J. Ma, Q. Zhan, Y. Li, J. Qin, and M. Guo, 2014, Epigenetic Silencing of RASSF10 Promotes Tumor Growth in Esophageal Squamous Cell Carcinoma: Discovery Medicine, v. 94, p. 169-178.

Luders, J., and T. Stearns, 2007, Opinion - Microtubule-organizing centres: a re-evaluation: Nature Reviews Molecular Cell Biology, v. 8, p. 161-167.

Lukas, J., C. Lukas, and J. Bartek, 2004, Mammalian cell cycle checkpoints: signalling pathways and their organization in space and time: DNA Repair, v. 3, p. 997-1007.

Lukasiewicz, K. B., and W. L. Lingle, 2009, Aurora A, Centrosome Structure, and the Centrosome Cycle: Environmental and Molecular Mutagenesis, v. 50, p. 602-619.

Luo, D., T. Ye, T.-Q. Li, P. Tang, S.-D. Min, G.-F. Zhao, H. Huang, J. Chang, Y. Wang, L. Lv, M.-L. Lu, and M.-Y. Zheng, 2012, Ectopic expression of RASSF2 and its prognostic role for gastric adenocarcinoma patients: Experimental and Therapeutic Medicine, v. 3, p. 391-396.

Lupas, A. N., and M. Gruber, 2005, The structure of alpha-helical coiled coils: Fibrous Proteins: Coiled-Coils, Collagen and Elastomers, v. 70, p. 37-+.

Ma, H. T., and R. Y. C. Poon, 2011, How protein kinases co-ordinate mitosis in animal cells: Biochemical Journal, v. 435, p. 17-31.

MacDonald, B. T., K. Tamai, and X. He, 2009, Wnt/beta-Catenin Signaling: Components, Mechanisms, and Diseases: Developmental Cell, v. 17, p. 9-26.

Mahen, R., and A. R. Venkitaraman, 2012, Pattern formation in centrosome assembly: Current Opinion in Cell Biology, v. 24, p. 14-23.

Malumbres, M., 2011, PHYSIOLOGICAL RELEVANCE OF CELL CYCLE KINASES: Physiological Reviews, v. 91, p. 973-1007.

Malumbres, M., 2014, Cyclin-dependent kinases: Genome Biology, v. 15.

Malumbres, M., and M. Barbacid, 2005, Mammalian cyclin-dependent kinases: Trends in Biochemical Sciences, v. 30, p. 630-641.

Malumbres, M., and M. Barbacid, 2007, Cell cycle kinases in cancer: Current Opinion in Genetics & Development, v. 17, p. 60-65.

Martin, T. A., and W. G. Jiang, 2009, Loss of tight junction barrier function and its role in cancer metastasis: Biochimica Et Biophysica Acta-Biomembranes, v. 1788, p. 872-891.

Martin-Belmonte, F., and M. Perez-Moreno, 2012, Epithelial cell polarity, stem cells and cancer, Nat Rev Cancer, v. 12: England, p. 23-38.

Martin-Granados, C., A. Philp, S. K. Oxenham, A. R. Prescott, and P. T. W. Cohen, 2008, Depletion of protein phosphatase 4 in human cells reveals essential roles in centrosome maturation, cell migration and the regulation of Rho GTPases: International Journal of Biochemistry & Cell Biology, v. 40, p. 2315-2332.

Maruyama, R., K. Akino, M. Toyota, H. Suzuki, T. Imai, M. Ohe-Toyota, E. Yamamoto, M. Nojima, T. Fujikane, Y. Sasaki, T. Yamashita, Y. Watanabe, H. Hiratsuka, K. Hirata, F. Itoh, K. Imai, Y. Shinomura, and T. Tokino, 2008, Cytoplasmic RASSF2A is a proapoptotic mediator whose expression is epigenetically silenced in gastric cancer: Carcinogenesis, v. 29, p. 1312-1318.

Mason, J. M., and K. M. Arndt, 2004, Coiled coil domains: Stability, specificity, and biological implications: Chembiochem, v. 5, p. 170-176.

Masui, Y., and C. L. Markert, 1971, CYTOPLASMIC CONTROL OF NUCLEAR BEHAVIOR DURING MEIOTIC MATURATION OF FROG OOCYTES: Journal of Experimental Zoology, v. 177, p. 129-&.

Matsumoto, Y., K. Hayashi, and E. Nishida, 1999, Cyclin-dependent kinase 2 (Cdk2) is required for centrosome duplication in mammalian cells: Current Biology, v. 9, p. 429-432.

Matter, K., and M. S. Balda, 2003, Holey barrier: claudins and the regulation of brain endothelial permeability: Journal of Cell Biology, v. 161, p. 459-460.
Matthies, H. J. G., H. B. McDonald, L. S. B. Goldstein, and W. E. Theurkauf, 1996, Anastral meiotic spindle morphogenesis: Role of the non-claret disjunctional kinesin-like protein: Journal of Cell Biology, v. 134, p. 455-464.
Matyakhina, L. D., S. Lenherr, F. Sandrini, L. S. Kurschner, A. Dutra, E. Pak, and C. A. Stratakis, 2002, Protein kinase A may be involved in chromosomal stability: Induction of cytogenetic abnormalities in mouse embryonic fibroblasts by PRKAR1A down- regulation: American Journal of Human Genetics, v. 71, p. 183-183.
Meraldi, P., R. Honda, and E. A. Nigg, 2002, Aurora-A overexpression reveals tetraploidization as a major route to centrosome amplification in p53(-/-) cells: Embo Journal, v. 21, p. 483-492.
Meraldi, P., J. Lukas, A. M. Fry, J. Bartek, and E. A. Nigg, 1999, Centrosome duplication in mammalian somatic cells requires E2F and Cdk2-cyclin A: Nature Cell Biology, v. 1, p. 88-93.
Michaelis, C., R. Ciosk, and K. Nasmyth, 1997, Cohesins: Chromosomal proteins that prevent premature separation of sister chromatids: Cell, v. 91, p. 35-45.
Michifuri, Y., Y. Hirohashi, T. Torigoe, A. Miyazaki, J. Fujino, Y. Tamura, T. Tsukahara, T. Kanaseki, J. Kobayashi, T. Sasaki, A. Takahashi, K. Nakamori, A. Yamaguchi, H. Hiratsuka, and N. Sato, 2013, Small proline-rich protein-1B is overexpressed in human oral squamous cell cancer stem-like cells and is related to their growth through activation of MAP kinase signal: Biochemical and Biophysical Research Communications, v. 439, p. 96-102.
Mikule, K., B. Delaval, P. Kaldis, A. Jurcyzk, P. Hergert, and S. Doxsey, 2007, Loss of centrosome integrity induces p38-p53-p21dependent G1-S arrest: Nature Cell Biology, v. 9, p. 160-U49.
Minoshima, Y., T. Kawashima, K. Hirose, A. Kawajiri, T. Nosaka, M. Inagaki, and T. Kitamura, 2003, Phosphorylation by Aurora-B converts MgcRacGAP to a RhoGAP during cytokinesis: Cell Structure and Function, v. 28, p. 314-314.
Mochida, S., S. Ikeo, J. Gannon, and T. Hunt, 2009, Regulated activity of PP2A-B55 delta is crucial for controlling entry into and exit from mitosis in Xenopus egg extracts: Embo Journal, v. 28, p. 2777-2785.
Mochida, S., S. L. Maslen, M. Skehel, and T. Hunt, 2010, Greatwall Phosphorylates an Inhibitor of Protein Phosphatase 2A That Is Essential for Mitosis: Science, v. 330, p. 1670-1673.
Morgan, D. O., 1995, PRINCIPLES OF CDK REGULATION: Nature, v. 374, p. 131-134.
Mori, D., Y. Yano, K. Toyo-Oka, N. Yoshida, M. Yamada, M. Muramatsu, D. Zhang, H. Saya, Y. Y. Toyoshima, K. Kinoshita, A. Wynshaw-Boris, and S. Hirotsune, 2007, NDEL1 phosphorylation by aurora-A kinase is essential for centrosomal maturation, separation, and TACC3 recruitment: Molecular and Cellular Biology, v. 27, p. 352-367.
Morris, J. A., G. Kandpal, L. Ma, and C. P. Austin, 2003, DISC1 (Disrupted-In-Schizophrenia 1) is a centrosome-associated protein that interacts with MAP1A, MIPT3, ATF4/5 and NUDEL: regulation and loss of interaction with mutation: Human Molecular Genetics, v. 12, p. 1591-1608.
Morris, N. R., S. A. Osmani, D. B. Engle, and R. T. Pu, 1988, TWO GENES NIMA AND BIME THAT REGULATE MITOSIS IN ASPERGILLUS-NIDULANS: Beach, D., C. Basilico and J. Newport (Ed.). Current Communications in Molecular

Biology: Cell Cycle Control in Eukaryotes; Meeting, Cold Spring Harbor, New York, USA, March 1988. Xi+211p. Cold Spring Harbor Laboratory: Cold Spring Harbor, New York, USA. Illus. Paper, p. 145-150.

Moshnikova, A., J. Frye, J. W. Shay, J. D. Minna, and A. V. Khokhlatchev, 2006, The growth and tumor suppressor NORE1A is a cytoskeletal protein that suppresses growth by inhibition of the ERK pathway: Journal of Biological Chemistry, v. 281, p. 8143-8152.

Muller, S. L., M. Portwich, A. Schmidt, D. I. Utepbergenov, O. Huber, I. E. Blasig, and G. Krause, 2005, The tight junction protein occludin and the adherens junction protein alpha-catenin share a common interaction mechanism with ZO-1: Journal of Biological Chemistry, v. 280, p. 3747-3756.

Mutter, G. L., J. P. A. Baak, J. T. Fitzgerald, R. Gray, D. Neuberg, G. A. Kust, R. Gentleman, S. R. Gullans, L. J. Wei, and M. Wilcox, 2001, Global expression changes of constitutive and hormonally regulated genes during endometrial neoplastic transformation: Gynecologic Oncology, v. 83, p. 177-185.

Nakamura, N., J. A. Carney, L. Jin, S. Kajita, J. Pallares, H. Y. Zhang, X. Qian, T. J. Sebo, L. A. Erickson, and R. V. Lloyd, 2005, RASSF1A and NORE1A methylation and BRAF(V600E) mutations in thyroid tumors: Laboratory Investigation, v. 85, p. 1065-1075.

Neuberger, G., G. Schneider, and F. Eisenhaber, 2007, pkaPS: prediction of protein kinase A phosphorylation sites with the simplified kinase-substrate binding model: Biology Direct, v. 2.

Nezi, L., and A. Musacchio, 2009, Sister chromatid tension and the spindle assembly checkpoint: Current Opinion in Cell Biology, v. 21, p. 785-795.

Nigg, E. A., 1995, CYCLIN-DEPENDENT PROTEIN-KINASES - KEY REGULATORS OF THE EUKARYOTIC CELL-CYCLE: Bioessays, v. 17, p. 471-480.

Nigg, E. A., 1998, Polo-like kinases: positive regulators of cell division from start to finish: Current Opinion in Cell Biology, v. 10, p. 776-783.

Nigg, E. A., 2001, Mitotic kinases as regulators of cell division and its checkpoints: Nature Reviews Molecular Cell Biology, v. 2, p. 21-32.

Nigg, E. A., 2006, Origins and consequences of centrosome aberrations in human cancers: International Journal of Cancer, v. 119, p. 2717-2723.

Nigg, E. A., 2007, Centrosome duplication: of rules and licenses: Trends in Cell Biology, v. 17, p. 215-221.

Nigg, E. A., A. Blangy, and H. A. Lane, 1996, Dynamic changes in nuclear architecture during mitosis: On the role of protein phosphorylation in spindle assembly and chromosome segregation: Experimental Cell Research, v. 229, p. 174-180.

Nigg, E. A., and J. W. Raff, 2009, Centrioles, Centrosomes, and Cilia in Health and Disease: Cell, v. 139, p. 663-678.

Nizard, P., F. Ezan, D. Bonnier, N. Le Meur, S. Langouet, G. Baffet, Y. Arlot-Bonnemains, and N. Theret, 2014, Integrative analysis of high-throughput RNAi screen data identifies the FER and CRKL tyrosine kinases as new regulators of the mitogenic ERK-dependent pathways in transformed cells: Bmc Genomics, v. 15.

Noguchi, K., H. Fukazawa, Y. Murakami, and Y. Uehara, 2004, Nucleolar Nek11 is a novel target of Nek2A in G(1)/S-arrested cells: Journal of Biological Chemistry, v. 279, p. 32716-32727.

Nurse, P., 1975, GENETIC-CONTROL OF CELL-SIZE AT CELL-DIVISION IN YEAST: Nature, v. 256, p. 547-551.

.

O'Connell, K. F., C. Caron, K. R. Kopish, D. D. Hurd, K. J. Kemphues, Y. J. Li, and J. G. White, 2001, The C-elegans zyg-1 gene encodes a regulator of centrosome duplication with distinct maternal and paternal roles in the embryo: Cell, v. 105, p. 547-558.

O'Farrell, P. H., 2001, Triggering the all-or-nothing switch into mitosis: Trends in Cell Biology, v. 11, p. 512-519.

O'Toole, E. T., T. H. Giddings, J. R. McIntosh, and S. K. Dutcher, 2003, Three-dimensional organization of basal bodies from wild-type and delta-tubulin deletion strains of Chlamydomonas reinhardtii: Molecular Biology of the Cell, v. 14, p. 2999-3012.

Oh, H. J., K. K. Lee, S. J. Song, N. S. Jin, M. S. Song, J. H. Lee, C. R. Im, J. O. Lee, S. Yonehara, and D. S. Lim, 2006, Role of the tumor suppressor RASSF1A in Mst1-medated apoptosis: Cancer Research, v. 66, p. 2562-2569.

Ohi, R., T. Sapra, J. Howard, and T. J. Mitchison, 2004, Differentiation of cytoplasmic and meiotic spindle assembly MCAK functions by aurora B-dependent phosphorylation: Molecular Biology of the Cell, v. 15, p. 2895-2906.

Okuda, M., 2002, The role of nucleophosmin in centrosome duplication: Oncogene, v. 21, p. 6170-6174.

Okuda, M., H. F. Horn, P. Tarapore, Y. Tokuyama, A. G. Smulian, P. K. Chan, E. S. Knudsen, I. A. Hofmann, J. D. Snyder, K. E. Bove, and K. Fukasawa, 2000, Nucleophosmin/B23 is a target of CDK2/Cyclin E in centrosome duplication: Cell, v. 103, p. 127-140.

Ortega, S., I. Prieto, J. Odajima, A. Martin, P. Dubus, R. Sotillo, J. L. Barbero, M. Malumbres, and M. Barbacid, 2003, Cyclin-dependent kinase 2 is essential for meiosis but not for mitotic cell division in mice: Nature Genetics, v. 35, p. 25-31.

Ortiz-Vega, S., A. Khokhlatchev, M. Nedwidek, X. F. Zhang, R. Dammann, G. P. Pfeifer, and J. Avruch, 2002, The putative tumor suppressor RASSF1A homodimerizes and heterodimerizes with the Ras-GTP binding protein Nore1 (vol 21, pg 1381, 2002): Oncogene, v. 21, p. 1943-1943.

Osmani, A. H., S. L. McGuire, and S. A. Osmani, 1991, PARALLEL ACTIVATION OF THE NIMA AND P34CDC2 CELL CYCLE-REGULATED PROTEIN-KINASES IS REQUIRED TO INITIATE MITOSIS IN ASPERGILLUS-NIDULANS: Cell, v. 67, p. 283-291.

Park, J., S. I. Kang, S.-Y. Lee, X. F. Zhang, M. S. Kim, L. F. Beers, D.-S. Lim, J. Avruch, H.-S. Kim, and S. B. Lee, 2010a, Tumor Suppressor Ras Association Domain Family 5 (RASSF5/NORE1) Mediates Death Receptor Ligand-induced Apoptosis: Journal of Biological Chemistry, v. 285, p. 35029-35038.

Park, J.-E., N.-K. Soung, Y. Johmura, Y. H. Kang, C. Liao, K. H. Lee, C. H. Park, M. C. Nicklaus, and K. S. Lee, 2010b, Polo-box domain: a versatile mediator of polo-like kinase function: Cellular and Molecular Life Sciences, v. 67, p. 1957-1970.

Park, S.-J., D. Lee, C.-Y. Choi, and S.-Y. Ryu, 2008, Induction of apoptosis by NORE1A in a manner dependent on its nuclear export: Biochemical and Biophysical Research Communications, v. 368, p. 56-61.

Pascreau, G., F. Eckerdt, M. E. A. Churchill, and J. L. Maller, 2010, Discovery of a distinct domain in cyclin A sufficient for centrosomal localization independently of Cdk binding: Proceedings of the National Academy of Sciences of the United States of America, v. 107, p. 2932-2937.

Peel, N., N. R. Stevens, R. Basto, and J. W. Raff, 2007, Overexpressing centriole-replication proteins in vivo induces centriole overduplication and de novo formation: Current Biology, v. 17, p. 834-843.

Petronczki, M., P. Lenart, and J.-M. Peters, 2008, Polo on the rise - from mitotic entry to cytokinesis with Plk1: Developmental Cell, v. 14, p. 646-659.

Phillips, B. E., L. Cancel, J. M. Tarbell, and D. A. Antonetti, 2008, Occludin independently regulates permeability under hydrostatic pressure and cell division in retinal pigment epithelial cells: Investigative Ophthalmology & Visual Science, v. 49, p. 2568-2576.

Picketth.Jd, 1969, EVOLUTION OF MITOTIC APPARATUS - AN ATTEMPT AT COMPARATIVE ULTRASTRUCTURAL CYTOLOGY IN DIVIDING PLANT CELLS: Cytobios, v. 1, p. 257-&.

Pihan, G. A., A. Purohit, J. Wallace, H. Knecht, B. Woda, P. Quesenberry, and S. J. Doxsey, 1998, Centrosome defects and genetic instability in malignant tumors: Cancer Research, v. 58, p. 3974-3985.

Pihan, G. A., A. Purohit, J. Wallace, R. Malhotra, L. Liotta, and S. J. Doxsey, 2001, Centrosome defects can account for cellular and genetic changes that characterize prostate cancer progression: Cancer Research, v. 61, p. 2212-2219.

Pihan, G. A., J. Wallace, Y. N. Zhou, and S. J. Doxsey, 2003, Centrosome abnormalities and chromosome instability occur together in pre-invasive carcinomas: Cancer Research, v. 63, p. 1398-1404.

Ponting, C. P., and D. R. Benjamin, 1996, A novel family of Ras-binding domains: Trends in Biochemical Sciences, v. 21, p. 422-425.

Porteous, D. J., J. K. Millar, N. J. Brandon, and A. Sawa, 2011, DISC1 at 10: connecting psychiatric genetics and neuroscience: Trends in Molecular Medicine, v. 17, p. 699-706.

Praskova, M., A. Khoklatchev, S. Ortiz-Vega, and J. Avruch, 2004, Regulation of the MST1 kinase by autophosphorylation, by the growth inhibitory proteins, RASSF1 and NORE1, and by Ras: Biochemical Journal, v. 381, p. 453-462.

Prigent, C., and S. Dimitrov, 2003, Phosphorylation of serine 10 in histone H3, what for?: Journal of Cell Science, v. 116, p. 3677-3685.

Prigent, C., D. M. Glover, and R. Giet, 2005, Drosophila Nek2 protein kinase knockdown leads to centrosome maturation defects while overexpression causes centrosome fragmentation and cytokinesis failure: Experimental Cell Research, v. 303, p. 1-13.

Pufall, M. A., and B. J. Graves, 2002, Autoinhibitory domains: Modular effectors of cellular regulation: Annual Review of Cell and Developmental Biology, v. 18, p. 421-462.

Pugacheva, E. N., and E. A. Golemis, 2005, The focal adhesion scaffolding protein HEF1 regulates activation of the Aurora-A and Nek2 kinases at the centrosome: Nature Cell Biology, v. 7, p. 937-U18.

Qiao, R., G. Cabral, M. M. Lettman, A. Dammermann, and G. Dong, 2012, SAS-6 coiled-coil structure and interaction with SAS-5 suggest a regulatory

mechanism in C. elegans centriole assembly: Embo Journal, v. 31, p. 4334-4347.
Raff, J. W., 2002, Centrosomes and cancer: lessons from a TACC: Trends in Cell Biology, v. 12, p. 222-225.
Recino, A., V. Sherwood, A. Flaxman, W. N. Cooper, F. Latif, A. Ward, and A. D. Chalmers, 2010, Human RASSF7 regulates the microtubule cytoskeleton and is required for spindle formation, Aurora B activation and chromosomal congression during mitosis: Biochem J, v. 430, p. 207-13.
Reeves, M. E., S. W. Baldwin, M. L. Baldwin, S.-T. Chen, J. M. Moretz, R. J. Aragon, X. Li, D. D. Strong, S. Mohan, and Y. G. Amaar, 2010, Ras-association domain family 1C protein promotes breast cancer cell migration and attenuates apoptosis: Bmc Cancer, v. 10.
Rhee, K., and D. J. Wolgemuth, 1997, The NIMA-related kinase 2, Nek2, is expressed in specific stages of the meiotic cell cycle and associates with meiotic chromosomes: Development, v. 124, p. 2167-2177.
Richter, A. M., G. P. Pfeifer, and R. H. Dammann, 2009, The RASSF proteins in cancer; from epigenetic silencing to functional characterization: Biochimica Et Biophysica Acta-Reviews on Cancer, v. 1796, p. 114-128.
Richter, A. M., U. Schagdarsurengin, M. Rastetter, K. Steinmann, and R. H. Dammann, 2010, Protein kinase A-mediated phosphorylation of the RASSF1A tumour suppressor at Serine 203 and regulation of RASSF1A function: European Journal of Cancer, v. 46, p. 2986-2995.
Richter, A. M., S. K. Walesch, P. Wurl, H. Taubert, and R. H. Dammann, 2012, The tumor suppressor RASSF10 is upregulated upon contact inhibition and frequently epigenetically silenced in cancer: Oncogenesis, v. 1, p. e18-e18.
Riedel, C. G., V. L. Katis, Y. Katou, S. Mori, T. Itoh, W. Helmhart, M. Galova, M. Petronczki, J. Gregan, B. Cetin, I. Mudrak, E. Ogris, K. Mechtler, L. Pelletier, F. Buchholz, K. Shirahige, and K. Nasmyth, 2006, Protein phosphatase 2A protects centromeric sister chromatid cohesion during meiosis I: Nature, v. 441, p. 53-61.
Rodrigues-Martins, A., M. Bettencourt-Dias, M. Riparbelli, C. Ferreira, I. Ferreira, G. Callaini, and D. M. Glover, 2007, DSAS-6 organizes a tube-like centriole precursor, and its absence suggests modularity in centriole assembly: Current Biology, v. 17, p. 1465-1472.
Rodriguez-Viciana, P., C. Sabatier, and F. McCormick, 2004, Signaling specificity by Ras family GTPases is determined by the full spectrum of effectors they regulate: Molecular and Cellular Biology, v. 24, p. 4943-4954.
Rogers, G. C., N. M. Rusan, D. M. Roberts, M. Peifer, and S. L. Rogers, 2009, The SCFSlimb ubiquitin ligase regulates Plk4/Sak levels to block centriole reduplication: Journal of Cell Biology, v. 184, p. 225-239.
Roig, J., A. Groen, J. Caldwell, and J. Avruch, 2005, Active Nercc1 protein kinase concentrates at centrosomes early in mitosis and is necessary for proper spindle assembly: Molecular Biology of the Cell, v. 16, p. 4827-4840.
Rong, W. Jin, J. Zhang, M. S. Sheikh, and Y. Huang, 2004, Tumor suppressor RASSF1A is a microtubule-binding protein that stabilizes microtubules and induces G2/M arrest: Oncogene, v. 23, p. 8216-8230.
Rong, R., L. Y. Jiang, M. S. Sheikh, and Y. Huang, 2007, Mitotic kinase Aurora-A phosphorylates RASSF1A and modulates RASSF1A-mediated microtubule

interaction and M-phase cell cycle regulation: Oncogene, v. 26, p. 7700-7708.

Ruchaud, S., M. Carmena, and W. C. Earnshaw, 2007, Chromosomal passengers: conducting cell division: Nature Reviews Molecular Cell Biology, v. 8, p. 798-812.

Runkle, E. A., J. M. Sundstrom, K. B. Runkle, X. Liu, and D. A. Antonetti, 2011, Occludin Localizes to Centrosomes and Modifies Mitotic Entry: Journal of Biological Chemistry, v. 286, p. 30847-30858.

Rykova, E. Y., T. E. Skvortsova, A. L. Hoffmann, S. N. Tamkovich, A. V. Starikov, O. E. Bryzgunova, V. I. Permjakova, J. M. Warnecke, G. Sczakiel, V. V. Vlassov, and P. P. Laktionov, 2008, Breast cancer diagnostics based on extracellular DNA and RNA circulating in blood: Biomeditsinskaya Khimiya, v. 54, p. 94-103.

Salaun, P., Y. Rannou, and C. Prigent, 2008, Cdk1, Plks, auroras, and Neks: The mitotic bodyguards: Hormonal Carcinogenesis V, v. 617, p. 41-56.

Sankaran, S., L. M. Starita, and J. D. Parvin, 2004, BRCA1 regulates centrosome function by inhibiting microtubule nucleation activity: Molecular Biology of the Cell, v. 15, p. 408A-409A.

Santamaria, D., C. Barriere, A. Cerqueira, S. Hunt, C. Tardy, K. Newton, J. F. Caceres, P. Dubus, M. Malumbres, and M. Barbacid, 2007, Cdk1 is sufficient to drive the mammalian cell cycle: Nature, v. 448, p. 811-U8.

Sasai, K., H. Katayama, D. L. Stenoien, S. Fujii, R. Honda, M. Kimura, Y. Okano, M. Tatsuka, F. Suzuki, E. A. Nigg, W. C. Earnshaw, W. R. Brinkley, and S. Sen, 2004, Aurora-C kinase is a novel chromosomal passenger protein that can complement Aurora-B kinase function in mitotic cells: Cell Motility and the Cytoskeleton, v. 59, p. 249-263.

Saucedo, L. J., and B. A. Edgar, 2007, Filling out the Hippo pathway: Nature Reviews Molecular Cell Biology, v. 8, p. 613-621.

Saunders, W. S., and M. A. Hoyt, 1992, KINESIN-RELATED PROTEINS REQUIRED FOR STRUCTURAL INTEGRITY OF THE MITOTIC SPINDLE: Cell, v. 70, p. 451-458.

Schagdarsurengin, U., A. M. Richter, C. Woehler, and R. H. Dammann, 2009, Frequent epigenetic inactivation of RASSF10 in thyroid cancer: Epigenetics, v. 4, p. 571-576.

Schatten, H., 2008, The mammalian centrosome and its functional significance: Histochemistry and Cell Biology, v. 129, p. 667-686.

Scheel, H., and K. Hofmann, 2003, A novel interaction motif, SARAH, connects three classes of tumor suppressor: Current Biology, v. 13, p. R899-R900.

Schmidt, T. I., J. Kleylein-Sohn, J. Westendorf, M. Le Clech, S. B. Lavoie, Y.-D. Stierhof, and E. A. Nigg, 2009, Control of Centriole Length by CPAP and CP110: Current Biology, v. 19, p. 1005-1011.

Schnell, J. R., G. P. Zhou, M. Zweckstetter, A. C. Rigby, and J. J. Chou, 2005, Rapid and accurate structure determination of coiled-coil domains using NMR dipolar couplings: Application to cGMP-dependent protein kinase I alpha: Protein Science, v. 14, p. 2421-2428.

Schultz, S. J., A. M. Fry, C. Sutterlin, T. Ried, and E. A. Nigg, 1994, CELL CYCLE-DEPENDENT EXPRESSION OF NEK2, A NOVEL HUMAN PROTEIN-KINASE RELATED TO THE NIMA MITOTIC REGULATOR OF ASPERGILLUS-NIDULANS: Cell Growth & Differentiation, v. 5, p. 625-635.

Schumacher, J. M., A. Golden, and P. J. Donovan, 1998, AIR-2: An Aurora/Ip11-related protein kinase associated with chromosomes and midbody microtubules is required for polar body extrusion and cytokinesis in Caenorhabditis elegans embryos: Journal of Cell Biology, v. 143, p. 1635-1646.

Searle, J. S., and Y. Sanchez, 2004, Stopped for repairs - A new role for nutrient sensing pathways?: Cell Cycle, v. 3, p. 865-868.

Sekido, Y., M. Ahmadian, Wistuba, II, F. Latif, S. Bader, M. H. Wei, F. M. Duh, A. F. Gazdar, M. I. Lerman, and J. D. Minna, 1998, Cloning of a breast cancer homozygous deletion junction narrows the region of search for a 3p21.3 tumor suppressor gene: Oncogene, v. 16, p. 3151-3157.

Sen, S., H. Y. Zhou, R. D. Zhang, D. S. Yoon, F. Vakar-Lopez, S. Ito, F. Jiang, D. Johnston, H. B. Grossman, A. C. Ruifrok, R. L. Katz, W. Brinkley, and B. Czerniak, 2002, Amplification/overexpression of a mitotic kinase gene in human bladder cancer: Journal of the National Cancer Institute, v. 94, p. 1320-1329.

Severson, A. F., D. R. Hamill, J. C. Carter, J. Schumacher, and B. Bowerman, 2000, The Aurora-related kinase AIR-2 recruits ZEN-4/CeMKLP1 to the mitotic spindle at metaphase and is required for cytokinesis: Current Biology, v. 10, p. 1162-1171.

.

Shekhar, M. P. V., A. Lyakhovich, D. W. Visscher, H. Heng, and N. Kondrat, 2002, Rad6 overexpression induces multinucleation, centrosome amplification, abnormal mitosis, aneuploidy, and transformation: Cancer Research, v. 62, p. 2115-2124.

Sherwood, V., R. Manbodh, C. Sheppard, and A. D. Chalmers, 2008, RASSF7 is a member of a new family of RAS association domain-containing proteins and is required for completing mitosis: Mol Biol Cell, v. 19, p. 1772-82.

Sherwood, V., A. Recino, A. Jeffries, A. Ward, and A. D. Chalmers, 2010, The N-terminal RASSF family: a new group of Ras-association-domain-containing proteins, with emerging links to cancer formation: Biochemical Journal, v. 425, p. 303-311.

Shivakumar, L., J. Minna, T. Sakamaki, R. Pestell, and M. A. White, 2002, The RASSF1A tumor suppressor blocks cell cycle progression and inhibits cyclin D1 accumulation: Molecular and Cellular Biology, v. 22, p. 4309-4318.

Shrestha, D., A. Jenei, P. Nagy, G. Vereb, and J. Szollosi, 2015, Understanding FRET as a Research Tool for Cellular Studies, Int J Mol Sci, v. 16, p. 6718-6756.

Sievers, F., A. Wilm, D. Dineen, T. J. Gibson, K. Karplus, W. Li, R. Lopez, H. McWilliam, M. Remmert, J. Soeding, J. D. Thompson, and D. G. Higgins, 2011, Fast, scalable generation of high-quality protein multiple sequence alignments using Clustal Omega: Molecular Systems Biology, v. 7.

Sikirzhytski, V., V. Magidson, J. B. Steinman, J. He, M. Le Berre, I. Tikhonenko, J. G. Ault, B. F. McEwen, J. K. Chen, H. Sui, M. Pie, T. M. Kapoor, and A. Khodjakov, 2014, Direct kinetochore-spindle pole connections are not required for chromosome segregation: Journal of Cell Biology, v. 206, p. 231-243.

Smith, L. D., and R. E. Ecker, 1971, INTERACTION OF STEROIDS WITH RANA-PIPIENS OOCYTES IN INDUCTION OF MATURATION: Developmental Biology, v. 25, p. 232-&.

Smith, M. R., M. L. Wilson, R. Hamanaka, D. Chase, H. F. Kung, D. L. Longo, and D. K. Ferris, 1997, Malignant transformation of mammalian cells initiated by constitutive expression of the polo-like kinase: Biochemical and Biophysical Research Communications, v. 234, p. 397-405.

Song, H., S. Oh, H. J. Oh, and D.-S. Lim, 2010, Role of the tumor suppressor RASSF2 in regulation of MST1 kinase activity: Biochemical and Biophysical Research Communications, v. 391, p. 969-973.

Song, M. S., and D. S. Lim, 2004, Control of APC-Cdc20 by the tumor suppressor RASSF1A: Cell Cycle, v. 3, p. 574-576.

Song, M. S., S. J. Song, N. G. Ayad, J. S. Chang, J. H. Lee, H. K. Hong, H. Lee, N. Choi, J. Kim, H. Kim, J. W. Kim, E. J. Choi, M. W. Kirschner, and D. S. Lim, 2004, The tumour suppressor RASSF1A regulates mitosis by inhibiting the APC-Cdc20 complex: Nature Cell Biology, v. 6, p. 129-+.

Song, M. S., S. J. Song, S. Y. Kim, H. J. Oh, and D.-S. Lim, 2008, The tumour suppressor RASSF1A promotes MDM2 self-ubiquitination by disrupting the MDM2-DAXX-HAUSP complex: Embo Journal, v. 27, p. 1863-1874.

Starita, L. M., Y. Machida, S. Sankaran, J. E. Elias, K. Griffin, B. P. Schlegel, S. P. Gygi, and J. D. Parvin, 2004, BRCA1-dependent ubiquitination of gamma-tubulin regulates centrosome number: Molecular and Cellular Biology, v. 24, p. 8457-8466.

Strebhardt, K., and A. Ullrich, 2006, Opinion - Targeting polo-like kinase 1 for cancer therapy: Nature Reviews Cancer, v. 6, p. 321-330.

Strnad, P., S. Leidel, T. Vinogradova, U. Euteneuer, A. Khodjakov, and P. Goenczy, 2007, Regulated HsSAS-6 levels ensure formation of a single procentriole per centriole during the centrosome duplication cycle: Developmental Cell, v. 13, p. 203-213.

Strunnikov, A. V., 2003, Condensin and biological role of chromosome condensation: Progress in cell cycle research, v. 5, p. 361-7.

Sullivan, A., and X. Lu, 2007, ASPP: a new family of oncogenes and tumour suppressor genes: British Journal of Cancer, v. 96, p. 196-200.

Sunkel, C. E., and D. M. Glover, 1988, POLO, A MITOTIC MUTANT OF DROSOPHILA DISPLAYING ABNORMAL SPINDLE POLES: Journal of Cell Science, v. 89, p. 25-38.

Tachibana, K. E. K., M. A. Gonzalez, G. Guarguaglini, E. A. Nigg, and R. A. Laskey, 2005, Depletion of licensing inhibitor geminin causes centrosome overduplication and mitotic defects: Embo Reports, v. 6, p. 1052-1057.

Takahashi, S., A. Ebihara, H. Kajiho, K. Kontani, H. Nishina, and T. Katada, 2011, RASSF7 negatively regulates pro-apoptotic JNK signaling by inhibiting the activity of phosphorylated-MKK7: Cell Death and Differentiation, v. 18, p. 645-655.

Takahashi, T., M. Futamura, N. Yoshimi, J. Sano, M. Katada, Y. Takagi, M. Kimura, T. Yoshioka, Y. Okano, and S. Saji, 2000, Centrosomal kinases, HsAIRK1 and HsAIRK3, are overexpressed in primary colorectal cancers: Japanese Journal of Cancer Research, v. 91, p. 1007-1014.

Takai, N., R. Hamanaka, J. Yoshimatsu, and I. Miyakawa, 2005, Polo-like kinases (Plks) and cancer: Oncogene, v. 24, p. 287-291.

Takaki, T., K. Trenz, V. Costanzo, and M. Petronczkil, 2008, Polo-like kinase 1 reaches beyond mitosis-cytokinesis, DNA damage response, and development: Current Opinion in Cell Biology, v. 20, p. 650-660.

Tan, D. S. P., M. B. K. Lambros, S. Rayter, R. Natrajan, R. Vatcheva, Q. Gao, C. Marchio, F. C. Geyer, K. Savage, S. Parry, K. Fenwick, N. Tamber, A. Mackay, T. Dexter, C. Jameson, W. G. McCluggage, A. Williams, A. Graham, D. Faratian, M. El-Bahrawy, A. J. Paige, H. Gabra, M. E. Gore, M. Zvelebil, C. J. Lord, S. B. Kaye, A. Ashworth, and J. S. Reis-Filho, 2009, PPM1D Is a Potential Therapeutic Target in Ovarian Clear Cell Carcinomas: Clinical Cancer Research, v. 15, p. 2269-2280.

Tanaka, T., M. Kimura, K. Matsunaga, D. Fukada, H. Mori, and Y. Okano, 1999, Centrosomal kinase AIK1 is overexpressed in invasive ductal carcinoma of the breast: Cancer Research, v. 59, p. 2041-2044.

Tang, C.-J. C., R.-H. Fu, K.-S. Wu, W.-B. Hsu, and K. T. Tang, 2009, CPAP is a cell-cycle regulated protein that controls centriole length: Nature Cell Biology, v. 11, p. 825-U103.

Taniguchi, E., F. Toyoshima-Morimoto, and E. Nishida, 2002, Nuclear translocation of Plk1 mediated by its bipartite nuclear localization signal: Journal of Biological Chemistry, v. 277, p. 48884-48888.

Telkoparan, P., S. Erkek, E. Yaman, H. Alotaibi, D. Bayik, and U. H. Tazebay, 2013, Coiled-Coil Domain Containing Protein 124 Is a Novel Centrosome and Midbody Protein That Interacts with the Ras-Guanine Nucleotide Exchange Factor 1B and Is Involved in Cytokinesis: Plos One, v. 8.

Terada, Y., M. Tatsuka, F. Suzuki, Y. Yasuda, S. Fujita, and M. Otsu, 1998, AIM-1: a mammalian midbody-associated protein required for cytokinesis: Embo Journal, v. 17, p. 667-676.

Thrane, S., A. M. Pedersen, M. B. Thomsen, T. Kirkegaard, B. B. Rasmussen, A. K. Duun-Henriksen, A. V. Laenkholm, M. Bak, A. E. Lykkesfeldt, and C. W. Yde, 2014, A kinase inhibitor screen identifies Mcl-1 and Aurora kinase A as novel treatment targets in antiestrogen-resistant breast cancer cells, Oncogene.

Toji, S., N. Yabuta, T. Hosomi, S. Nishihara, T. Kobayashi, S. Suzuki, K. Tamai, and H. Nojima, 2004, The centrosomal protein Lats2 is a phosphorylation target of Aurora-A kinase: Genes to Cells, v. 9, p. 383-397.

Tokuyama, Y., H. F. Horn, K. Kawamura, P. Tarapore, and K. Fukasawa, 2001, Specific phosphorylation of nucleophosmin on Thr(199) by cyclin-dependent kinase 2-cyclin E and its role in centrosome duplication: Journal of Biological Chemistry, v. 276, p. 21529-21537.

Tommasi, S., R. Dammann, S. G. Jin, X. F. Zhang, J. Avruch, and G. P. Pfeifer, 2002, RASSF3 and NORE1: identification and cloning of two human homologues of the putative tumor suppressor gene RASSF1: Oncogene, v. 21, p. 2713-2720.

Tommasi, S., R. Dammann, Z. Q. Zhang, Y. Wang, L. M. Liu, W. M. Tsark, S. P. Wilczynski, J. Li, N. You, and G. P. Pfeifer, 2005, Tumor susceptibility of Rassf1a knockout mice: Cancer Research, v. 65, p. 92-98.

Toyoshima-Morimoto, F., E. Taniguchi, N. Shinya, A. Iwamatsu, and E. Nishida, 2001, Polo-like kinase 1 phosphorylates cyclin B1 and targets it to the nucleus during prophase: Nature, v. 410, p. 215-220.

Tripet, B., K. Wagschal, P. Lavigne, C. T. Mant, and R. S. Hodges, 2000, Effects of side-chain characteristics on stability and oligomerization state of a de novo-designed model coiled-coil: 20 amino acid substitutions in position "d": Journal of Molecular Biology, v. 300, p. 377-402.

Tsai, M. Y., C. Wiese, K. Cao, O. Martin, P. Donovan, J. Ruderman, C. Prigent, and Y. X. Zheng, 2003, A Ran signalling pathway mediated by the mitotic kinase Aurora A in spindle assembly: Nature Cell Biology, v. 5, p. 242-248.

Tsai, M. Y., and Y. X. Zheng, 2005, Aurora A kinase-coated beads function as microtubule-organizing centers and enhance RanGTP-induced spindle assembly: Current Biology, v. 15, p. 2156-2163.

Tsang, H. T. H., J. W. Connell, S. E. Brown, A. Thompson, E. Reid, and C. M. Sanderson, 2006, A systematic analysis of human CHMP protein interactions: Additional MIT domain-containing proteins bind to multiple components of the human ESCRT III complex: Genomics, v. 88, p. 333-346.

Tsou, M.-F. B., and T. Stearns, 2006a, Mechanism limiting centrosome duplication to once per cell cycle: Nature, v. 442, p. 947-951.

Tsou, M. F. B., and T. Stearns, 2006b, Controlling centrosome number: licenses and blocks: Current Opinion in Cell Biology, v. 18, p. 74-78.

Tyagi, S., and E. A. Lemke, 2015, Single-molecule FRET and crosslinking studies in structural biology enabled by noncanonical amino acids: Curr Opin Struct Biol, v. 32, p. 66-73.

Uetake, Y., J. Loncarek, J. J. Nordberg, C. N. English, S. La Terra, A. Khodjakov, and G. Sluder, 2007, Cell cycle progression and de novo centriole assembly after centrosomal removal in untransformed human cells: Journal of Cell Biology, v. 176, p. 173-182.

Ulisse, S., J. G. Delcros, E. Baldini, M. Toller, F. Curcio, L. Giacomelli, C. Prigent, F. S. Ambesi-Impiombato, M. D'Armiento, and Y. Arlot-Bonnemains, 2006, Expression of Aurora kinases in human thyroid carcinoma cell lines and tissues: International Journal of Cancer, v. 119, p. 275-282.

Underhill-Day, N., V. Hill, and F. Latif, 2011, N-terminal RASSF family (RASSF7-RASSF10) A mini review: Epigenetics, v. 6, p. 284-292.

van Breugel, M., M. Hirono, A. Andreeva, H.-a. Yanagisawa, S. Yamaguchi, Y. Nakazawa, N. Morgner, M. Petrovich, I.-O. Ebong, C. V. Robinson, C. M. Johnson, D. Veprintsev, and B. Zuber, 2011, Structures of SAS-6 Suggest Its Organization in Centrioles: Science, v. 331, p. 1196-1199.

van de Weerdt, B. C. M., and R. H. Medema, 2006, Polo-like kinases - A team in control of the division: Cell Cycle, v. 5, p. 853-864.

van der Weyden, L., and D. J. Adams, 2007, The Ras-association domain family (RASSF) members and their role in human tumourigenesis: Biochimica Et Biophysica Acta-Reviews on Cancer, v. 1776, p. 58-85.

van der Weyden, L., K. K. Tachibana, M. A. Gonzalez, D. J. Adams, B. L. Ng, R. Petty, A. R. Venkitaraman, M. J. Arends, and A. Bradley, 2005, The RASSF1A isoform of RASSF1 promotes microtubule stability and suppresses tumorigenesis: Molecular and Cellular Biology, v. 25, p. 8356-8367.

Vavvas, D., X. Li, J. Avruch, and X. F. Zhang, 1998, Identification of Nore1 as a potential Ras effector: Journal of Biological Chemistry, v. 273, p. 5439-5442.

Vermeulen, K., D. R. Van Bockstaele, and Z. N. Berneman, 2003, The cell cycle: a review of regulation, deregulation and therapeutic targets in cancer: Cell Proliferation, v. 36, p. 131-149.

Vidwans, S. J., M. L. Wong, and P. H. O'Farrell, 1999, Mitotic regulators govern progress through steps in the centrosome duplication cycle: Journal of Cell Biology, v. 147, p. 1371-1377.

Volodko, N., M. Gordon, M. Salla, H. Abu Ghazaleh, and S. Baksh, 2014, RASSF tumor suppressor gene family: Biological functions and regulation: Febs Letters, v. 588, p. 2671-2684.
Vos, M. D., A. Dallol, K. Eckfeld, N. P. C. Allen, H. Donninger, L. B. Hesson, D. Calvisi, F. Latif, and G. J. Clark, 2006, The RASSF1A tumor suppressor activates Bax via MOAP-1: Journal of Biological Chemistry, v. 281, p. 4557-4563.
Vos, M. D., C. A. Ellis, A. Bell, M. J. Birrer, and G. J. Clark, 2000, Ras uses the novel tumor suppressor RASSF1 as an effector to mediate apoptosis: Journal of Biological Chemistry, v. 275, p. 35669-35672.
Vos, M. D., C. A. Ellis, C. Elam, A. S. Ulku, B. J. Taylor, and G. J. Clark, 2003, RASSF2 is a novel K-Ras-specific effector and potential tumor suppressor: Journal of Biological Chemistry, v. 278, p. 28045-28051.
Vos, M. D., A. Martinez, C. Elam, A. Dallol, B. J. Taylor, F. Latif, and G. J. Clark, 2004, A role for the RASSF1A tumor suppressor in the regulation of tubulin polymerization and genomic stability: Cancer Research, v. 64, p. 4244-4250.
Wagschal, K., B. Tripet, P. Lavigne, C. Mant, and R. S. Hodges, 1999, The role of position a in determining the stability and oligomerization state of alpha-helical coiled coils: 20 amino acid stability coefficients in the hydrophobic core of proteins: Protein Science, v. 8, p. 2312-2329.
Waizenegger, I. C., S. Hauf, A. Meinke, and J. M. Peters, 2000, Two distinct pathways remove mammalian cohesin from chromosome arms in prophase and from centromeres in anaphase: Cell, v. 103, p. 399-410.
Walter, A. O., W. Seghezzi, W. Korver, J. Sheung, and E. Lees, 2000, The mitotic serine/threonine kinase Aurora2/AIK is regulated by phosphorylation and degradation: Oncogene, v. 19, p. 4906-4916.
Walter, J. K., C. Rueckert, M. Voss, S. L. Mueller, J. Piontek, K. Gast, and I. E. Blasig, 2009, The Oligomerization of the Coiled Coil-domain of Occluddin Is Redox Sensitive: Molecular Structure and Function of the Tight Junction: from Basic Mechanisms to Clinical Manifestations, v. 1165, p. 19-27.
Wang, C.-C., L. Jamal, and K. A. Janes, 2012, Normal morphogenesis of epithelial tissues and progression of epithelial tumors: Wiley Interdisciplinary Reviews-Systems Biology and Medicine, v. 4, p. 51-78.
Wang, W., A. Budhu, M. Forgues, and X. W. Wang, 2005, Temporal and spatial control of nucleophosmin by the Ran-Crm1 complex in centrosome duplication: Nature Cell Biology, v. 7, p. 823-830.
Wang, Y., T. Ma, J. Bi, B. Song, Y. Zhou, C. Zhang, and M. Gao, 2014, RASSF10 is epigenetically inactivated and induces apoptosis in lung cancer cell lines: Biomedicine & Pharmacotherapy, v. 68, p. 321-326.
Wei, Z., X. Chen, J. Chen, W. Wang, X. Xu, and Q. Cai, 2013, RASSF10 is epigenetically silenced and functions as a tumor suppressor in gastric cancer: Biochemical and Biophysical Research Communications, v. 432, p. 632-637.
Weitzel, J. N., A. Kasperczyk, C. Mohan, and T. G. Krontiris, 1992, THE HRAS1 GENE-CLUSTER - 2 UPSTREAM REGIONS RECOGNIZING TRANSCRIPTS AND A 3RD ENCODING A GENE WITH A LEUCINE ZIPPER DOMAIN: Genomics, v. 14, p. 309-319.
Whang, Y. M., Y. H. Kim, J. S. Kim, and D. Y. Yoo, 2005, RASSF1A suppresses the c-Jun-NH2-kinase pathway and inhibits cell cycle progression: Cancer Research, v. 65, p. 3682-3690.

Winey, M., and E. O'Toole, 2014, Centriole structure: Philosophical transactions of the Royal Society of London. Series B, Biological sciences, v. 369.

Winkles, J. A., and G. F. Alberts, 2005, Differential regulation of polo-like kinase 1, 2, 3, and 4 gene expression in mammalian cells and tissues: Oncogene, v. 24, p. 260-266.

Withanage, K., K. Nakagawa, M. Ikeda, H. Kurihara, T. Kudo, Z. Yang, A. Sakane, T. Sasaki, and Y. Hata, 2012, Expression of RASSF6 in kidney and the implication of RASSF6 and the Hippo pathway in the sorbitol-induced apoptosis in renal proximal tubular epithelial cells: Journal of Biochemistry, v. 152, p. 111-119.

Wohlgemuth, S., C. Kiel, A. Kramer, L. Serrano, F. Wittinghofer, and C. Herrmann, 2005, Recognizing and defining true Ras binding domains 1: Biochemical analysis: Journal of Molecular Biology, v. 348, p. 741-758.

Wojcik, E., D. Glover, and T. S. Hays, 2000, The SCF ubiquitin ligase protein Slimb regulates centrosome duplication in Drosophila: Molecular Biology of the Cell, v. 11, p. 92A-92A.

Wong, J., and G. W. Fang, 2006, HURP controls spindle dynamics to promote proper interkinetochore tension and efficient kinetochore capture: Journal of Cell Biology, v. 173, p. 879-891.

Wu, G., Y.-T. Lin, R. Wei, Y. Chen, Z. Shan, and W.-H. Lee, 2008, Hice1, a novel microtubule-associated protein required for maintenance of spindle integrity and chromosomal stability in human cells: Molecular and Cellular Biology, v. 28, p. 3652-3662.

Wurzenberger, C., and D. W. Gerlich, 2011, Phosphatases: providing safe passage through mitotic exit: Nature Reviews Molecular Cell Biology, v. 12, p. 469-482.

Xing, M. Z., Y. Cohen, E. Mambo, G. Tallini, R. Udelsman, P. W. Ladenson, and D. Sidransky, 2004a, Early occurrence of RASSF1A hypermethylation and its mutual exclusion with BRAF mutation in thyroid tumorigenesis: Cancer Research, v. 64, p. 1664-1668.

Xing, X.-S., L.-M. Huang, and X.-D. Ma, 2004b, Progress of RASSF1A gene in neoplasms: Zhonghua bing li xue za zhi Chinese journal of pathology, v. 33, p. 562-4.

Xu, J., C. Shen, T. Wang, and J. Quan, 2013, Structural basis for the inhibition of Polo-like kinase 1: Nature Structural & Molecular Biology, v. 20, p. 1047-+.

Yang, Z., J. Loncarek, A. Khodjakov, and C. L. Rieder, 2008, Extra centrosomes and/or chromosomes prolong mitosis in human cells: Nature Cell Biology, v. 10, p. 748-751.

Yasui, S., K. Tsuzaki, H. Ninomiya, F. Floricel, Y. Asano, H. Maki, A. Takamura, E. Nanba, K. Higaki, and K. Ohno, 2007, The TSC1 gene product hamartin interacts with NADE: Molecular and Cellular Neuroscience, v. 35, p. 100-108.

Yin, M. J., L. H. Shao, D. Voehringer, T. Smeal, and B. Jallal, 2003, The serine/threonine kinase Nek6 is required for cell cycle progression through mitosis: Journal of Biological Chemistry, v. 278, p. 52454-52460.

Zaessinger, S., Y. Zhou, S. J. Bray, N. Tapon, and A. Djiane, 2015, Drosophila MAGI interacts with RASSF8 to regulate E-Cadherinbased adherens junctions in the developing eye: Development, v. 142, p. 1102-1112.

Zeitlin, S. G., R. D. Shelby, and K. F. Sullivan, 2001, CENP-A is phosphorylated by Aurora B kinase and plays an unexpected role in completion of cytokinesis: Journal of Cell Biology, v. 155, p. 1147-1157.

Zeng, K., R. N. Bastos, F. A. Barr, and U. Gruneberg, 2010, Protein phosphatase 6 regulates mitotic spindle formation by controlling the T-loop phosphorylation state of Aurora A bound to its activator TPX2: Journal of Cell Biology, v. 191, p. 1315-1332.

Zhang, Y., Y. Wang, Y. Wei, J. Ma, J. Peng, R. Wumaier, S. Shen, P. Zhang, and L. Yu, 2015, The tumor suppressor proteins ASPP1 and ASPP2 interact with C-Nap1 and regulate centrosome linker reassembly: Biochemical and biophysical research communications, v. 458, p. 494-500.

Zhang, Z., D. Sun, D. N. Van, A. Tang, L. Hu, and G. Huang, 2007, Inactivation of RASSF2A by promoter methylation correlates with lymph node metastasis in nasopharyngeal carcinoma: International Journal of Cancer, v. 120, p. 32-38.

Zhao, J. H., Y. Ren, Q. Jiang, and J. Feng, 2003, Parkin is recruited to the centrosome in response to inhibition of proteasomes: Journal of Cell Science, v. 116, p. 4011-4019.

Zhou, H. Y., J. Kuang, L. Zhong, W. L. Kuo, J. W. Gray, A. Sahin, B. R. Brinkley, and S. Sen, 1998, Tumour amplified kinase STK15/BTAK induces centrosome amplification, aneuploidy and transformation: Nature Genetics, v. 20, p. 189-193.

Zhu, F., S. Lawo, A. Bird, D. Pinchev, A. Ralph, C. Richter, T. Mueller-Reichert, R. Kittler, A. A. Hyman, and L. Pelletier, 2008, The mammalian SPD-2 ortholog Cep192 regulates centrosome biogenesis: Current Biology, v. 18, p. 136-141.

Zitouni, S., C. Nabais, S. C. Jana, A. Guerrero, and M. Bettencourt-Dias, 2014, Polo-like kinases: structural variations lead to multiple functions: Nature Reviews Molecular Cell Biology, v. 15, p. 433-452.

Zucca, E., and E. A. Nigg, 1995, Cell cycle regulation and the function of cancer genes: Annals of Oncology, v. 6, p. 975-978.

8 APPENDIX

Apendix 1: Example of quantification of GFP-rassf7 co-localisation w ith gamma tubulin.

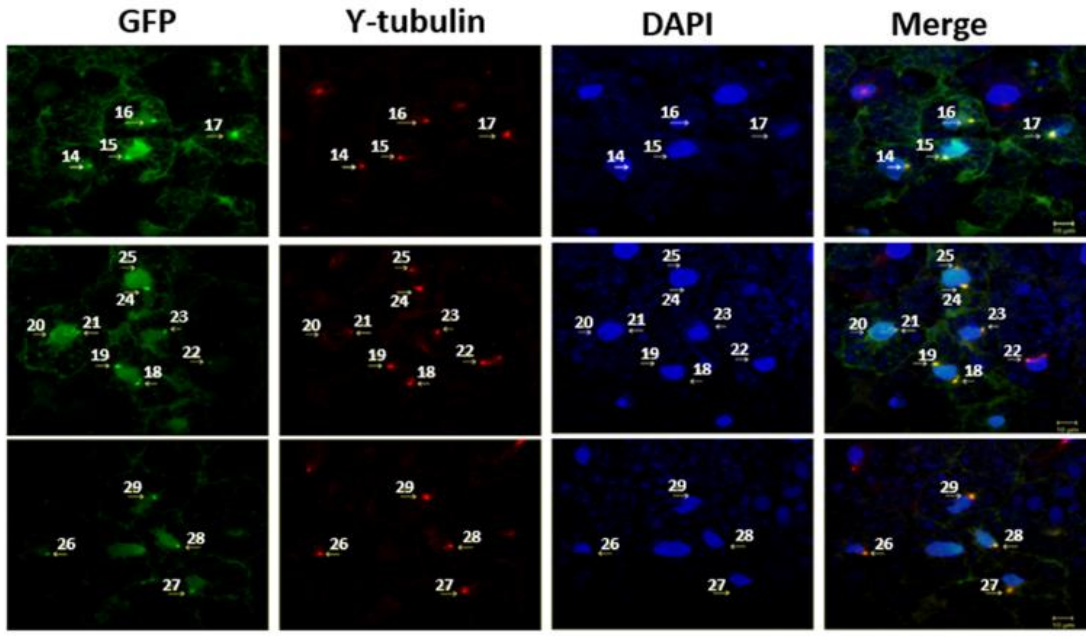

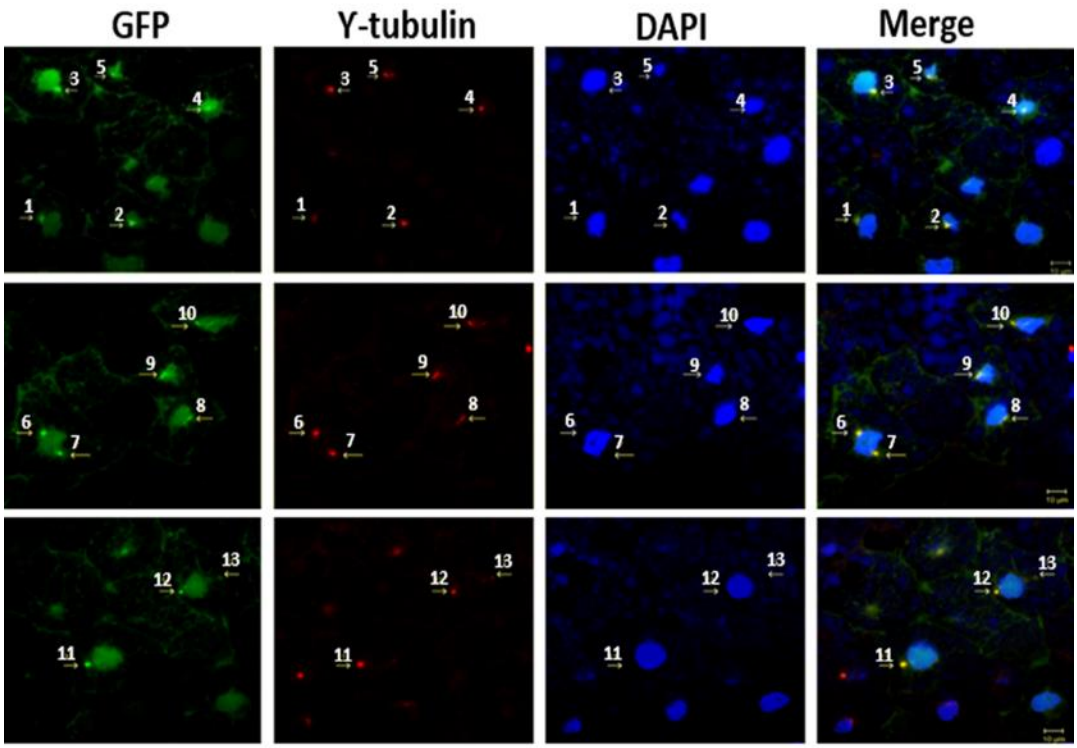

Appendix 2: Example of quantification of lack of co-localisation of GFP and gamma tubulin.

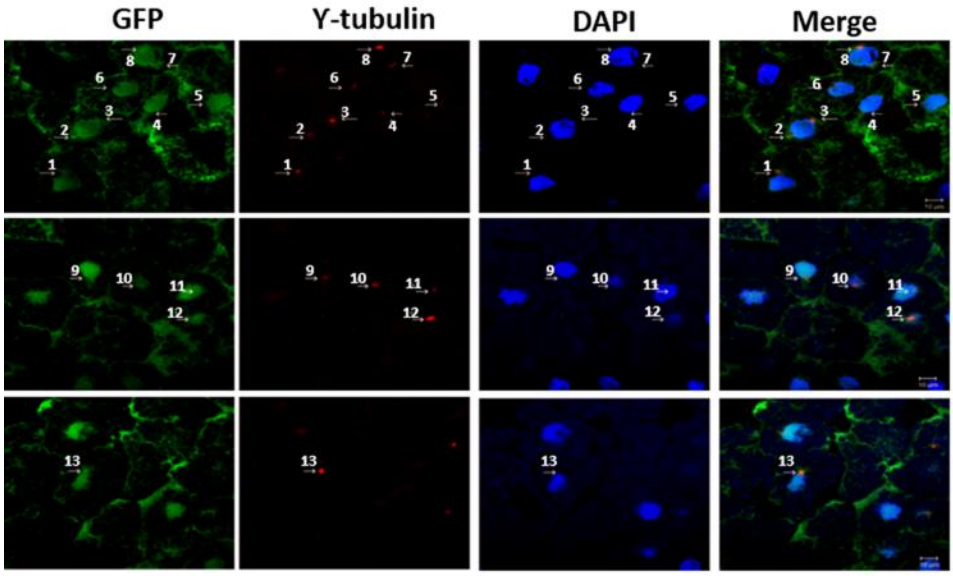

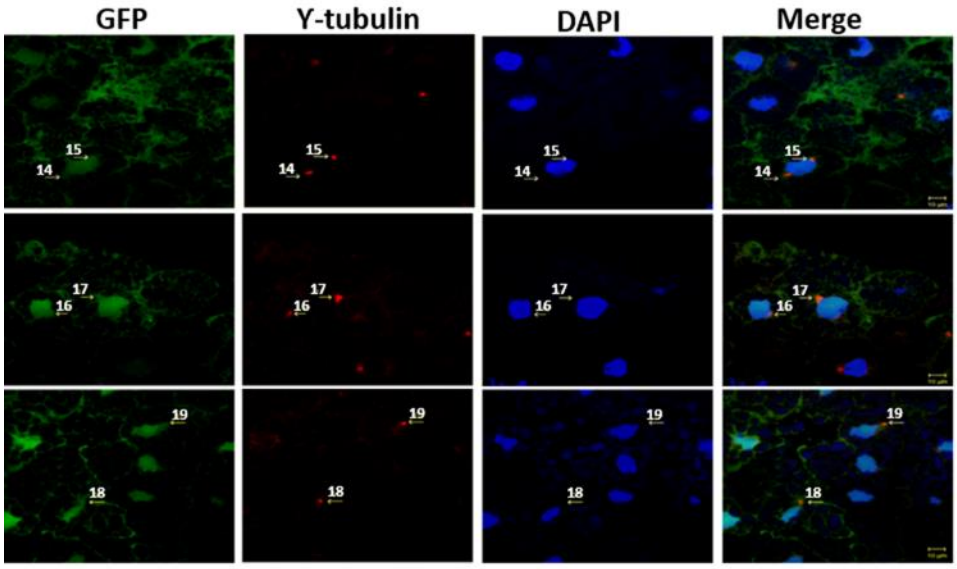

Appendix 3: Table of the example quantifications that w ere shown in appendix 1 and 2.

	GFP-rassf7						GFP					
	GFP at the γ-tubulin foci, size (area nm²)	GFP at the γ-tubulin foci, intensity (AU)	Integrated density	γ-tubulin foci, size (area nm²)	γ-tubulin foci, intensity (AU)	Integrated density	GFP at the γ-tubulin foci, size (area nm²)	GFP at the γ-tubulin foci, intensity (AU)	Integrated density	γ-tubulin foci, size (area nm²)	γ-tubulin foci, intensity (AU)	Integrated density
1	6.67	71	473.57	6.17	82	505.94	0	5	0	7.12	119	847.28
2	4.88	123	600.24	4.88	127	619.76	1.98	70	138.6	7.13	43	306.59
3	4.28	122	522.16	4.28	125	535	0.63	30	18.9	8.1	115	931.5
4	2.63	115	302.45	2.63	123	323.49	0	5	0	2.26	23	51.98
5	3.16	109	344.44	3.21	112	359.52	0	7	0	1.98	21	41.58
6	4.78	93	444.54	4.63	112	518.56	0	8	0	6.98	42	293.16
7	3.28	92	301.76	3.33	113	376.29	1.16	32	37.12	6.49	53	343.97
8	2.88	70	201.6	2.86	72	205.92	0	72	0	5.07	121	613.47
9	3.56	85	302.6	3.57	109	389.13	1.02	54	55.08	1.82	52	94.64
10	3.57	72	257.04	3.67	98	359.66	0	6	0	5.28	88	464.64
11	4.64	132	612.48	4.57	128	584.96	0	23	0	3.01	34	102.34
12	2.21	138	304.98	2.45	112	274.4	0	36	0	6.97	123	857.31
13	1.16	43	49.88	0.97	35	33.95	0	35	0	5.47	125	683.75
14	2.72	80	217.6	3.9	95	370.5	0	6	0	6.2	95	589
15	4.23	116	490.68	4.16	112	465.92	0	17	0	5.06	112	566.72
16	4.85	105	509.25	4.22	117	493.74	0	5	0	5.46	98	535.08
17	5.75	119	684.25	5.36	123	659.28	0	15	0	4.88	111	541.68
18	4.89	117	572.13	4.96	127	629.92	0	13	0	3.62	95	343.9
19	5.06	121	612.26	5.43	132	716.76	0	17	0	4.35	117	508.95
20	1.16	82	95.12	1.08	91	98.28	**0.252**	**24**	**13.14**	**5.118**	**83.52**	**458.8179**
21	1.2	79	94.8	1.16	89	103.24						
22	1.67	71	118.57	3.67	138	506.46						
23	2.79	94	262.26	2.92	123	359.16						
24	5.84	125	730	6.01	136	817.36						
25	2.63	76	199.88	3.78	119	449.82						
26	1.82	95	172.9	4.74	123	583.02						
27	2.36	89	210.04	5.14	133	683.62						
28	2.41	102	245.82	3.07	119	365.33						
29	3.02	98	295.96	5.08	138	701.04						
av	**3.451724**	**97.724**	**352.7331**	**3.858**	**112.5**	**451.334**						

Appendix 4: **Ratio of GFP intensity at the Ɣ-tubulin foci vs GFP intensity in the nuclei.** The ratio of intensity for GFP at the Ɣ-tubulin foci vs GFP intensity at the nuclei was calculated for each construct. Constructs which showed reduced centrosomal staining had reduced Ɣ-tubulin to nuclei ratio. Constructs with increased centrosomal localisation showed increased Ɣ-tubulin to nuclei ratio. The change in ratio shows that the changes in localisation seen with the constructs cannot be explained by changes in protein expression levels of the constructs. Based on at least three independent experiments and n>100 cells.